

UNIVERSITA' DEGLI STUDI DI MILANO-BICOCCA

Facoltà di Scienze Matematiche, Fisiche e Naturali

Dipartimento di Biotecnologie e Bioscienze

Corso di Dottorato di Ricerca in Biologia XXVII ciclo



Systematics, taxonomy and phylogenetic relationships of the
coral family Lobophylliidae (Cnidaria, Scleractinia)

Roberto Arrigoni

Relatore: Dott.ssa Francesca Benzoni

Coordinatore: Prof. Paolo Tortora

Anno Accademico 2013-2014

UNIVERSITA' DEGLI STUDI DI MILANO-BICOCCA

Facoltà di Scienze Matematiche, Fisiche e Naturali

Dipartimento di Biotecnologie e Bioscienze

Corso di Dottorato di Ricerca in Biologia XXVII ciclo



Systematics, taxonomy and phylogenetic relationships of the
coral family Lobophylliidae (Cnidaria, Scleractinia)

Roberto Arrigoni

Relatore: Dott.ssa Francesca Benzoni

Coordinatore: Prof. Paolo Tortora

Anno Accademico 2013-2014

Dottorato di Ricerca In Biologia

Ciclo XXVII

Roberto Arrigoni

Maricola 056356

Tutor: Dott.ssa Francesca Benzoni



Università degli Studi di Milano-Bicocca

Piazza dell'Ateneo Nuovo 1, 20126 Milano



Dipartimento di Biotecnologie e Bioscienze

Piazza della Scienza 2, 20126 Milano

*“Alter any event, ever so slightly and
without apparent importance at the time,
and evolution cascades into radically different channel”*

*(Stephen Jay Gould, Wonderful Life:
The Burgess Shale and the Nature of History)*

- ABSTRACT -

Traditional classification of scleractinian corals (Cnidaria, Anthozoa, Scleractinia) have been conducted on the basis of skeleton macromorphology and arose from detailed studies of skeletal structures of both recent and fossil corals. However, the commonly used skeletal characters are plagued by a host of factors, such as phenotypic plasticity, intraspecific variation, and morphological convergence, that render challenging the definition of taxa boundaries and fail to recognize most natural evolutionary lineages. Recent molecular studies have revolutionized the conventional taxonomic schemes, suggesting remarkably different phylogenetic relationships when compared with those based on macromorphology and providing new reliable characters to establish the evolutionary history of these animals. In the last decade, the integration of this increasing amount of genetic data and new micromorphological and microstructural traits has led to a better understanding of evolutionary relationships between hard corals and opened the way to the new era of coral taxonomy.

In this context, the Indo-Pacific family Lobophylliidae Dai and Horng, 2009 potentially represents an interesting case study of “reciprocal illumination” between genetics and morphology. This taxon has been recently defined on a combination of phylogenetic analyses and micromorphological observations, although it still remains poorly understood. In fact, most lobophylliids are unstudied and the evolutionary relationships within the family unknown as well as detailed micromorphological analyses still have to be conducted. This dissertation aims to fill this gap in knowledge through the investigation of evolutionary relationships of the Lobophylliidae and starting the impending process of taxonomic revision of this family as a result of an integrated molecular and micromorphological approach.

A molecular phylogeny reconstruction of one of the three major groups recovered in the order Scleractinia, the Robusta, to which the Lobophylliidae belong was presented. Based on the partial mitochondrial COI gene and the

ribosomal ITS region, the representatives of this family were recovered in a cohesive lineage for the first time and the phylogenetic relationships with the other closely related families were discussed. The analysis was then expanded analyzing more species and samples and focused exclusively on the Lobophylliidae in order to produce the most comprehensive molecular phylogeny reconstruction of this group to date. A total of 32 species ascribed to nine genera were investigated sequencing one mitochondrial and one nuclear locus. The monophyly of the family was strongly supported and nine main monophyletic genus-level lineages were recovered within the Lobophylliidae. All analyzed polytypic genera, *i.e.* *Acanthastrea*, *Echinophyllia*, *Lobophyllia*, *Micromussa*, *Oxypora*, and *Symphyllia*, were not monophyletic and resulted in need of a formal taxonomic revision.

Subsequently, to further investigate the evolution of the Lobophylliidae, the complete mitochondrial genome of *Acanthastrea maxima* was sequenced. The species based on a combination of data including its restricted geographic distribution, evolutionary distinctiveness, and small population size was revealed be a potential case of priority for future conservation strategies. This mitochondrial genome represented the first sequenced mitogenome of a member of this family and suggested potential informative markers for phylogenetic studies of the other lobophylliid genera. Being 18,278 bp in length, it is the longest sequence among the robust corals sequenced mitogenome to date, while the GC content and the gene arrangement are similar to those of the other scleractinian corals.

Finally, integrating multi-locus molecular phylogenies and detailed gross- and fine-scale morphologic observations three cases analyzed in the family provided examples of how reverse taxonomy can be useful in understanding the evolutionary history of the Lobophylliidae: I) a taxonomic revision for the monotypic genus *Australomussa*, revealed to be a junior synonym of *Parascolymia*, was proposed; II) the long-ignored monospecific genus *Sclerophyllia* was resurrected and the unforeseen sister relationships between *Sclerophyllia margariticola* and *A. maxima* led to the placement of the latter species in *Sclerophyllia*; III) the closely related genera *Homophyllia* and *Micromussa* were revised with the description of two new

species, *Micromussa pacifica* sp. nov. and *Micromussa indiana* sp. nov., and *Symphyllia wilsoni*, a South-western Australian endemism, was placed in *Hydnophyllia* gen. nov. based on an unique combination of molecular and micromorphological data.

Overall, the results stemming from the data provided in the framework of my thesis significantly improve our understanding of evolution of the family Lobophylliidae. Furthermore they represent a solid case for the importance of an integrated morpho-molecular approach in resolving taxonomy and systematics of this ecologically important group of marine animals with notable consequences on their biogeography and conservation strategies.

- CONTENT -

Abstract	2
List of Figures	9
List of Tables	18
List of Appendices	20
<u>Chapter 1: General Introduction</u>	23
1.1 From traditional to reverse taxonomy	23
1.2 The family Lobophylliidae Dai and Horng, 2009	30
1.3 Aims of the dissertation	33
<u>Chapter 2: Molecular phylogeny of the Robust Clade clade (Faviidae, Mussidae, Merulinidae, and Pectiniidae): An Indian Ocean perspective</u>	34
2.1 Abstract	35
2.2 Introduction	36
2.2 Materials and methods	40
2.3.1 Sampling and specimen identification	40
2.3.2 DNA extraction, PCR amplification, and sequencing	43
2.3.3 Phylogenetic analyses	43
2.4 Results	45
2.4.1 Sequence data characteristics	45
2.4.2 Phylogenetic analyses	46
2.5 Discussion	49
2.5.1 New contributions to the phylogeny of Faviidae and Mussida	49
2.5.2 Within species divergences between Indian and Pacific Ocean populations	51
2.5.3 Molecular and phylogenetic implications	56
<u>Chapter 3: Lobophylliidae reshuffled (Cnidaria, Scleractinia): pervasive non-monophyly at genus level</u>	60
3.1 Abstract	61
3.2 Introduction	61
3.3 Materials and Methods	63
3.4 Results and Discussion	66

Chapter 4: The complete mitochondrial genome of <i>Acanthastrea maxima</i> (Cnidaria, Scleractinia, Lobophylliidae)	72
4.1 Abstract	73
4.2 Introduction	73
4.3 Materials and methods	74
4.4 Results and Discussion	75
Chapter 5: Taxonomy and phylogenetic relationships of the coral genera <i>Australomussa</i> and <i>Parascolymia</i> (Scleractinia, Lobophylliidae)	77
5.1 Abstract	78
5.2 Introduction	78
5.3 Materials and methods	83
5.3.1 Sampling	83
5.3.2 Morphological analyses	87
5.3.3 Molecular analyses	88
5.4 Results	90
5.4.1 Macromorphology	90
5.4.2 Micromorphology	94
5.4.3 Molecular analyses	97
5.5 Taxonomic account	101
5.5.1 Examined material	101
5.5.2 Taxonomy	102
5.6 Discussion	104
5.6.1 Morphology of <i>P. rowleyensis</i> and <i>P. vitiensis</i> and consequences for taxonomy	104
5.6.2 Molecular phylogeny of <i>P. rowleyensis</i> and <i>P. vitiensis</i>	107
5.6.3 Utility of the examined molecular markers	108
Chapter 6: Forgotten in the taxonomic literature: resurrection of the scleractinian coral genus <i>Sclerophyllia</i> (Scleractinia, Lobophylliidae) from the Arabian Peninsula and its phylogenetic relationships	111
6.1 Abstract	112
6.2 Introduction	112
6.3 Materials and methods	115
6.3.1 Sampling	115
6.3.2 DNA extraction, amplification, and sequence analyses	120
6.3.3 Morphological analyses	122
6.3.4 Ancestral character state reconstruction	122
6.3.5 Museum collections and other examined specimens	123

6.4 Results	123
6.4.1 Phylogenetic and haplotype network analyses	123
6.4.2 Morphological analyses	129
6.4.2.1 Macromorphology	129
6.4.2.2 Micromorphology	134
6.4.3 Ancestral character state reconstruction	136
6.5 Taxonomic account	137
6.5.1 Examined material	137
6.5.2 Taxonomy	138
6.6 Discussion	140
6.6.1 Morphology of <i>Sclerophyllia</i> vs <i>Acanthastrea</i> and <i>Cynarina</i>	140
6.6.2 Biogeographical patterns revealed by genetic evidence	145
6.6.3 The relevance of being solitary	146
6.7 Conclusions	148
Chapter 7: Integrating genetics and morphology: revision of the reef coral genera <i>Micromussa</i> and <i>Homophyllia</i> (Scleractinia, Lobophylliidae) with description of two new species	149
7.1 Abstract	151
7.2 Introduction	152
7.3 Materials and methods	156
7.3.1 Coral sampling and identification	156
7.3.2 DNA preparation, amplification and sequence analyses	163
7.3.3 Morphological analyses	165
7.4 Results	165
7.4.1 Phylogenetic and haplotype network analyses	165
7.4.2 Morphological analyses	170
7.4.2.1 Macromorphology	170
7.4.2.2 Micromorphology	175
7.5 Taxonomic account	179
7.5.1 Examined material	179
7.5.2 Taxonomy	182
7.6 Discussion	186
7.6.1 Phylogeny, taxonomy, and geographical distribution of <i>Homophyllia</i>	187
7.6.2 Phylogeny and taxonomy of <i>Micromussa</i>	189
7.6.3 The strange case of <i>Hydnophyllia wilsoni</i>	191

Chapter 8: General discussion and conclusions	193
8.1 Discussion	193
8.2 Future perspectives	197
Acknowledgments	200
References	204
Annexes	218
Annex I: List of publications arising from this PhD Thesis	218
Annex II: Publications to which the candidate has contributed during his PhD Candidature	220
Annex III: Grants and Internships during the PhD candidature	222
Annex IV: List of Appendices	224

- LIST OF FIGURES -

Figure 1.1. Illustration of septa of the genera traditionally ascribed to the Mussidae (A-J) and to the Pectiniidae (M-L) as reported in Vaughan and Wells (1943). Modified from Vaughan and Wells (1943). A, B) *Circophyllia truncate*, x3; C) *Mussismilia braziliensis*, x2; D) *Mussismilia harttii*, x2; E) *Syzygophyllia brevis*, x2; F) *Leptomussa variabilis*, x1^{1/2}; G) *Acanthastrea echinata*, x3; H) *Antillia gregorii*, x2; I) *Acanthophyllia dashayesiana*, x1; J) *Mussa angulosa*, x1^{1/2}; M) *Echinophyllia aspera*, x2.2; K) *Oxypora lacera*, x2.2; L) *Mycedium tubifex*, x2.2. Modified from Vaughan and Wells (1943). 25

Figure 1.2. The classification system and evolutionary relationships among stony corals proposed by Wells (1956). Branches represent families, patterns represent superfamilies, and columns represent suborders. Modified from Wells (1956). 26

Figure 1.3. Phylogenetic relationships among scleractinian corals and outgroups. Topology was inferred by Bayesian analysis, based on combined mitochondrial COI and CYTB sequences. Numbers on main branches show percentages of Bayesian probability ($\geq 70\%$) and bootstrap values ($\geq 50\%$) in ML analysis. Dashes mean bootstrap values $< 50\%$ in ML. Numbers in circles show the connection of trees from A to D: A, outgroups; B, complex corals and corallimorpharians; C, the family Pocilloporidae; D, robust corals. Three-letter codes correspond with traditional families; numbers in Roman numerals indicate clades interpreted from the tree. Modified from Fukami et al. (2008). 28

Figure 1.4. An example of micromorphology showing the study of the shape of septal teeth and the granulations on septal faces (Budd and Stolarski, 2009, 2011). Clade XXI *sensu* Fukami et al. (2008) (A-C) is distinguished by regular blocky teeth with pointed tips, and aligned granules. Clade XIX *sensu* Fuami et al. (2008) (D-F) is distinguished by irregular lobate or bulbous teeth with elliptical tooth bases, and rounded granules enveloped by extensive thickening deposits. Clade XVII *sensu* Fuami et al. (2008) (G-I) is distinguished by irregular multiaxial teeth with circular bases, and irregular scattered granules. A) XXI, *Pseudodiploria strigosa*; B) XXI, *Mussismilia braziliensis*; C) XXI, *Isophyllia sinuosa*; D) XIX, *Lobophyllia pachysepta*; E) XIX, *Parascolymia vitiensis*; F) XIX, *Echinophyllia echinoporoides*; G) XVII, *Merulina ampliata*; H) XVII, *Favites halicora*; I) XVII, *Hydnophora exesa*. Modified from Budd et al. (2012). 29

Figure 2.1. Number of “Bigmessidae” species currently known to have an Atlantic Ocean (ATL), Indian Ocean (IO), Pacific Ocean (PO), or Indo-Pacific (IP) distribution based on Veron’s (2000) distribution maps. For each column the white

area represents the number species for which no published molecular phylogeny is available (October 2011), the light grey area the species for which the published phylogeny is currently based on one specimen, the dark grey area the species for which the phylogeny is based on two to five specimens, and the black area the species for which more than five samples have been analyzed (data from Fukami et al., 2007, 2008; Nunes et al., 2008; Kitahara et al., 2010; Huang et al., 2011; Benzoni et al., 2011). Note that for all species with IP distribution only material from P.O. was studied in the examined molecular phylogenies (cf Fig. 2.2).

39

Figure 2.2. Bayesian tree of the combined rDNA and COI datasets. Posterior Bayesian probabilities (>70%), Sh-like support (>70%) and bootstrap values (>50%) are shown at nodes in the following order: BI, ML and MP. Dashes (-) indicate nodes that are statistically unsupported. Clade numbers and sub-clade codes are the same ones reported respectively by Fukami et al. (2008) and Huang et al. (2011). Species included for the first time in a molecular study are indicated in bold. IO samples are evidenced in blue and PO samples in black. Species with divergence between IO and PO populations are indicated with full circles: yellow circles = *Blastomussa merleti*; blue circles = *Echinopora gemmacea*; brown circles = *Favites complanata*; red circles = *Favites halicora*; green circles = *Favia matthaii*; purple circles = *Favia pallida*; orange circles = *Favia rotumana*.

47

Figure 2.3. Within colony plasticity of the skeleton morphology in the genus *Favia*. A) colony of *Favia pallida* (BA050) and B) of *F. rotumana* (BA086) showing a typically plocoid (left) as well as sub-ceroid or ceroid (right) corallite arrangement within the same specimen, respectively. Within clade plasticity of *F. pallida* and *F. matthaii*, and intermediate morphs C) skeleton (above) and *in vivo* morphology (below) of a *F. pallida* colony (BA119), and D) skeleton morphology of a colony (BA067) of the same species and in the same clade (Fig. 2.2) but with more exert septa; E) skeleton (above) and *in vivo* morphology (below) of a *F. matthaii* colony (BA101) showing the typically exert septa in this species; F) *in vivo* morphology of specimen BA082 displaying a *F. pallida* morphology of the left and a *F. matthaii* morphology on the right hand side of the image. This specimen was identified as *F. matthaii*, however, note its intermediate position in the phylogeny in Fig. 2.2.

54

Figure 3.1. Phylogeny of the Lobophylliidae inferred from Bayesian Inference analyses of COI and rDNA. Node values are Posterior Bayesian probabilities (> 70%), ML SH-like support (> 70%) and MP (> 50%) bootstrap values. Dashes (-) indicate nodes that are statistically unsupported. Uppercase letters and colour codes

delineate lineages referred to in Fig. 3.2 and Table 3.1. Type species in bold. * species analyzed for the first time from a molecular point of view. 68

Figure 3.2. *In situ* and corallum photos of species with unexpected phylogenetic relationships: a) *Micromussa amakusensis*; b) *Phymastrea multipunctata*; c) *A. bowerbanki*; d) *A. hillae*; e) *A. maxima*; f) *A. echinata*; g) *Echinophyllia aspera*; h) *Oxypora glabra*; i) *O. lacera*; j) *E. echinata*; k) *Lobophyllia corymbosa*; l) *Symphyllia radians*; m) *Parascolymia vitiensis*; n) *A. ishigakiensis*. Colour codes and uppercase letters in white circles indicate clades in Fig. 3.1. Specimen code on the corallum image. 69

Figure 4.1. In-vivo picture of the analyzed specimen of *Acanthastrea maxima* (SO131). 74

Figure 4.2. Distribution map of *Acanthastrea maxima*. Modified from Veron (2000). 74

Figure 5.1. *Parascolymia vitiensis* (A-D) and *P. rowleyensis* (previously *Australomussa*) (E-G) *in situ*: A) IRD HS2984 (monostomatous); B) UNIMIB PFB056 (bistomatous); C) IRD HS3139 (polystomatous, same as in Figure 2H); D) UNIMIB PFB057 (polystomatous, same as in Figure 2I); E) WAM Z65786; F) WAM Z65785; G) close up of the same colony as in E; H) close up of the same colony as in F. 84

Figure 5.2. Corallum morphology in *Parascolymia vitiensis*: A) IRD HS3255; B) IRD HS2955; C) detail of the same specimen in B showing variability in shape and size of septal teeth; D) UNIMIB PFB031; E) IRD HS2985; F) UNIMIB PFB056; G) UNIMIB PFB055; H) IRD HS3139; I) UNIMIB PFB057. All specimens are in the phylogenetic trees in Figures 5.9, Apps. 5.1, 5.2, 5.33. 92

Figure 5.3. Corallum morphology in *Parascolymia rowleyensis* (previously *Australomussa*): A) WAM Z65785; B) WAM Z65788; C) WAM Z65786; D) lamellar linkage between centres of adjacent corallites in same specimen as in B ; E) corallite polymorphism in the same specimen as in A; F) size and shape of costosepta in specimen WAM Z65787. All specimens are in the phylogenetic trees in Figures 5.9, Apps. 5.1, 5.2, 5.33. 93

Figure 5.4. Comparison of the macromorphology of *Parascolymia vitiensis* (A-C) and *P. rowleyensis* (D-E): A) septa in the monocentric specimen IRD HS2964; B) top view of the costosepta in the polycentric specimen UNIMIB PFB057; C) side view of the same portion of the specimen in B; D) peripheral calices in specimen WAM Z65786; E) top view of the costosepta in the same specimen as D; F) side view of the same portion of the specimen in E. Red arrows indicate the position of the columella in adjacent corallites, red brackets placed perpendicularly

to the costosepta show the number of costosepta intercepted by a 1 cm transect.

94

Figure 5.5. SEM images of radial elements of *Parascolymia rowleyensis* (previously *Australomussa*) (WAM Z65789: A-B) and *P. vitiensis* (UNIMIB PFB151: C-D): A) top view of septa reaching the wall; B) side view of septa of different cycles showing some variability in septal teeth size between cycles but overall homogeneous shape; C) top view of septa reaching the wall; D) side view of septa of different cycles showing high variability in septal teeth size and shape between cycles.

95

Figure 5.6. Vesicular endotheca: A) longitudinal section of the periphery of a calice of *Parascolymia vitiensis* (modified from Chevalier, 1975: Fig. 190); B) SEM image of a longitudinal section along the septa of *P. rowleyensis* (WAM Z65789); C) detail of vesicular endothecal dissepiments in the same specimen as in B. e = epitheca; w = wall; ed = endothecal dissepiments.

96

Figure 5.7. SEM of *Parascolymia vitiensis* (UNIMIB PFB151): A) top view of a S1 showing its thickness and clumped teeth; B) side view of an S2 septum tooth; C) side view of an S2 septum tooth, note the difference in shape of the tooth tip compared to B; D) side view of an S5 septum tooth.

96

Figure 5.8. SEM of *Parascolymia rowleyensis* (previously *Australomussa*) (WAM Z65789): A) side view of septa of different cycles showing homogeneous shape of septum teeth between cycles; B) side view of an S4 septum tooth; C) side view of an S2 septum tooth showing granulation; D) side view of the tip of an S1 septum tooth.

97

Figure 5.9. Phylogenetic position of *Parascolymia vitiensis* and *P. rowleyensis* (previously *Australomussa*) and their relationships within the family Lobophylliidae based on concatenated matrix (COI, histone H3, and ITS region). Bayesian topology is shown. Numbers associated with branches indicate Maximum Likelihood bootstrap (>70%) support (left) and Bayesian posterior probabilities (>0.9) (right). Clades within Lobophylliidae are coloured and labelled A to I according to Arrigoni et al. (2014a).

100

Figure 6.1. Map of the type and sampling localities of *S. margariticola* (green) and *S. maxima* (previously *Acanthastrea*) (yellow) for this study. Squares indicate sampling localities, stars indicate type localities. BA = Bir Ali, Yemen; MU = Al Mukallah, Yemen; SO = Socotra Island; K = Kuwait.

116

Figures 6.2-6.9. *Sclerophyllia margariticola* in situ: **6.2**, encrusting round-shaped corallum, KAUST SA880; **6.3**, round-shaped corallum, KAUST SA932; **6.4**, oval-shaped corallum, KAUST SA1016; **6.5**, triangular-shaped corallum, KAUST SA934; **6.6**, cyathiform oval-shaped corallum with obvious paliform lobes, KAUST SA976; **6.7**, cyathiform oval-shaped corallum, KAUST SA977; **6.8**,

round-shaped corallum, KAUST SA1297; **6.9**, round-shaped corallum with obvious paliform lobes, KAUST SA1298. Scale bars represent 1 cm. 117

Figures 6.10-6.17. *Sclerophyllia maxima* (previously *Acanthastrea*) *in situ*: **6.10**, UNIMIB SO131; **6.11**, colony at Al Mukallah, Yemen; **6.12**, UNIMIB BA136; **6.13**, UNIMIB MU163, Yemen; **6.14**, UNIMIB SO132; **6.15**, colony at Al Mukallah, Yemen; **6.16**, colony at Burum, Yemen; **6.17**, colony at Al Mukallah, Yemen. Scale bars represent 1 cm. 118

Figure 6.18. Phylogeny reconstruction of *Sclerophyllia margariticola* and *Sclerophyllia maxima* (previously *Acanthastrea*) within the family Lobophylliidae, based on Bayesian Inference (BI) analysis of the nuclear gene Histone H3. Bayesian posterior probability (left) higher than 0.95 and ML bootstrap values (right) higher than 70 are displayed on the nodes. Clades within Lobophylliidae are coloured and labelled A to I according to Arrigoni et al. (2014a). 126

Figure 6.19. Phylogeny reconstruction of *Sclerophyllia margariticola* and *Sclerophyllia maxima* (previously *Acanthastrea*) within the family Lobophylliidae, based on Bayesian Inference (BI) analysis of the partial mitochondrial gene COI. Bayesian posterior probability (left) higher than 0.95 and ML bootstrap values (right) higher than 70 are displayed on the nodes. Clades within Lobophylliidae are coloured and labelled A to I according to Arrigoni et al. (2014a). 127

Figures 6.20-6.21. Most-parsimonious median-joining networks of *Sclerophyllia margariticola* (in green) and *Sclerophyllia maxima* (previously *Acanthastrea*) (in yellow): **6.20**, network inferred from the mitochondrial intergenic spacer region (IGR) between COI and 1-rRNA; **6.21**, network inferred from the nuclear internal transcribed spacer 2 (ITS2) region. The size of circles is proportional to the frequencies of specimens sharing the same haplotype. The black solid circles are indicative of mutations that differentiate each haplotype. 128

Figure 6.22. Ancestral state reconstruction of the character “development of multiple mouths” within the family Lobophylliidae obtained using Maximum Parsimony with Mesquite 2.75. Character states as follows: 0, white, polystomatous; 1, grey, monostomatous; 2, black, polystomatous or monostomatous. 136

Figures 6.23–6.30. Coralla of *Sclerophyllia margariticola*: **6.23**, KAUST SA1017; **6.24**, KAUST SA934; **6.25**, top view of KAUST SA1014; **6.26**, side view of KAUST SA1014; **6.27**, top view of KAUST SA976; **6.28**, side view of KAUST SA976; **6.29**, top view of KAUST SA933; **6.30**, side view of KAUST SA933. Arabic numerals at the outer end of the septa in 6.23, 6.25, 6.27, and 6.29 indicate the cycle number (from 1 to 5). Scale bars represent 1 cm. 130

Figures 6.31–6.38. Radial elements (6.31, 6.33, 6.35, 6.37) and columella (6.32, 6.34, 6.36, 6.38) of *Sclerophyllia margariticola*: **6.31**, KAUST SA1017; **6.32**, KAUST SA1017; **6.33**, KAUST SA1014; **6.34**, KAUST SA1014; **6.35**, KAUST SA976; **6.36**, KAUST SA976; **6.37**, well formed crown of paliform lobes in KAUST SA933; **6.38**, relatively small columella in the same specimen as in 6.37. Scale bars represent 5 mm. 131

Figures 6.39–6.44. *Sclerophyllia maxima* (previously *Acanthastrea*): **6.39**, UNIMIB MU163, same specimen as in Fig. 6.11; **6.40**, UNIMIB BA136, same specimen as in Fig. 6.12; **6.41**, view of specimen UNIMIB K001 showing a top view of the central corallite (arrow); **6.42**, view of same specimen as in 6.41 showing a lateral view of the central corallite (arrow); **6.43**, largest calice in the holotype BMNH 1986.11.17.2; **6.44**, largest calice in UNIMIB MU163. Black arrows indicate the central and larger corallite. Arabic numerals at the outer end of the septa in 6.44 indicate the cycle number (from 1 to 5). Scale bars represent 1 cm. 133

Figures 6.45–6.59. Macro and micro-morphology of *S. margariticola* (6.45, 6.48, 6.51, 6.54, 6.57), *S. maxima* (previously *Acanthastrea*) (6.46, 6.49, 6.52, 6.55, 6.58), and *Acanthastrea echinata* (6.47, 6.50, 6.53, 6.56, 6.59): **6.45**, KAUST SA1017; **6.46**, UNIMIB MU161; **6.47**, IRD HS3126; **6.48**, columella of the same corallite as in 6.45; **6.49**, columella of the same corallite as in 6.46; **6.50**, corallite of the same specimen as in 6.47; **6.51**, SEM image of the septa of KAUST SA1175 showing granulated septal sides; **6.52**, SEM image of the septa of UNIMIB MU161 showing granulated septal sides; **6.53**, SEM image of the septa of IRD HS3126 showing smooth septal sides; **6.54**, SEM image of two septa of the same specimen as in 6.51 showing margin and side ornamentation; **6.55**, SEM image of a septum of the same specimen as in 6.52 showing margin and side ornamentation; **6.56**, SEM image of septa of the same specimen as in 6.53 showing septal margin ornamentation; **6.57**, top view of a septal teeth in the same specimen as in 6.51 and 6.54; **6.58**, top view of a septal teeth in the same specimen as in 6.52 and 6.55; **6.59**, septal teeth in the same specimen as in 6.53 and 6.56. Arabic numerals on the septa in 6.46 and 6.50 indicate the cycle number (from 1 to 6). Scale bars represent: Figs. 6.45–6.47, 1 cm; Figs. 6.48–6.50, 5 mm; Figs. 6.51–6.53, 2 mm; Figs. 6.54–6.56, 1 mm; Figs. 6.57–6.59, 500 µm. 135

Figures 6.60–6.63. Morphology and dimensions of septa and septal teeth in *Cynarina lacrymalis* (6.60, 6.62) and *Sclerophyllia margariticola* (6.61, 6.63): **6.60**, top view of the septa; **6.61**, top view of the septa of (KAUST SA934); **6.62**, side view of the septa shown in 6.60; **6.63**, side view of the septa shown in 6.61. Arabic numerals at the end of the septa indicate the cycle number (from 1 to 6).

Black arrows point at the large septal internal lobes in the major septa of *C. lacrymalis*. Scale bars represent 5 mm. 156

Figure 7.1. Skeleton macro-morphology of the Lobophylliidae included in this study: **A)** holotype of *Micromussa amakusensis* MTQ G32485 from Japan; **B)** *Acanthastrea lordhowensis* 1642 from Australia; **C)** *Micromussa amakusensis* MNHN-IK-2012-14232 from the Gulf of Aden; **D)** *Phymastrea multipunctata* RMNH Coel 40090 from Malaysia; **E)** cf *Homophyllia australis* IRD HS3543 from New Caledonia; **F)** *Homophyllia australis* IRD HS3424 from New Caledonia; **G)** *Acanthastrea bowerbanki* MH043 from Australia; **H)** *Acanthastrea hillae* IRD HS3287 from New Caledonia; **I)** *Acanthastrea hemprichii* UNIMIB BA115; **J)** *Symphyllia wilsoni* from Australia. 161

Figure 7.2. In situ morphology of the Lobophylliidae included in this study: **A)** *Micromussa amakusensis* from Japan; **B)** *Acanthastrea lordhowensis* from Lord Howe, Australia; **C)** *Micromussa amakusensis* from the gulf of Aden, same specimen shown in 7.1C; **D)** *Phymastrea multipunctata* RMNH Coel 40090 from Malaysia; **E)** cf *Homophyllia australis*, same specimen shown in 7.1E; **F)** *Homophyllia australis*, same specimen shown in 7.1E; **G)** *Acanthastrea bowerbanki* IRD HS3066 from New Caledonia; **H)** *Acanthastrea hillae*, same specimen shown in 7.1H; **I)** *Acanthastrea hemprichii* UNIMIB BA115 from the Gulf of Aden; *Symphyllia wilson* from Australia. 162

Figure 7.3. Bayesian phylogeny reconstruction of the family Lobophylliidae for the analysis of the concatenated data set of COI, Histone H3, and ITS region. Numbers above branches indicate nodal support of shown topology by means of Bayesian posterior probabilities (>0.8), Maximum Likelihood Sh-like supports (>0.7), and Maximum Parsimony bootstrap supports (>50). Lower values of support not shown. Clades within Lobophylliidae are coloured and labelled A to I according to Arrigoni et al. (2014a). Specimens analyzed in this study are in bold. 169

Figure 7.4. Haplotype network of the genus *Micromussa* (clade A) obtained in Network 4.6.1.2 for the mitochondrial intergenic spacer region (IGR) between COI and 1-rRNA. The size of circles is proportional to the frequencies of specimens sharing the same haplotype. The black solid circles are indicative of mutations that differentiate each haplotype. 170

Figure 7.5. Top (A, C, E, G) and side (B, D, F, H) views of *Homophyllia australis* showing typical morphology: **A)** IRD HS3441, top view; **B)** side view of the same corallum as in A; **C)** IRD HS3470, top view; **D)** side view of the same corallum as in C; **E)** IRD HS3545, top view; **F)** side view of the same corallum as in E; **G)** IRD HS3424, top view; **H)** side view of the same corallum as in G. 172

Figure 7.6. Skelton macro-morphology of specimens of cf *Homophyllia australis* included in this study and showing a different morphology from the typical one: **A)** top and **B)** side view of IRD HS 3543; **C)** IRD HS 3359 polystomatous specimen, image shows detail of the linckage (dashed line); **D)** IRD HS 3483 polystomatous specimen; **E)** top and **F)** side view of IRD HS 3327; **G), H), I)** show top, side and lateral corallite view, respectively, of a specimen with two calices from Gambier. 173

Figure 7.7. Coralla and corallite of *Micromussa amakusensis* from the Gulf of Aden, Indian Ocean: **A)** corallum morphology of specimen MNHN-IK-2012-14232; **B)** corallite shape and organization in the same specimen as in A; **C)** corallite shape and organization in specimen UNIMIB MU183; **D)** specimen in the EPA Socotra collection; **E)** detail of the left hand side of the specimen in C showing smaller corallites; **F)** detail of the left hand side of the specimen in C showing larger corallites. 174

Figure 7.8. Scanning Electron Microscopy images of *Homophyllia australis* HS3311 with typical macro-morphology (A, F, K, P, U, Z), *Acanthastrea bowerbanki* 4629 (B, G, L, Q, V, AA), *Acanthastrea hillae* MH019 (C, H, M, R, W, AB), *Symphyllia wilsoni* WIL1 (D, I, N, S, X, AC), *Acanthastrea hemprichii* BA115 (E, J, O, T, Y, AD): **A-E)** top view of the examined fragments; **F-J)** side view of the examined fragments; **K-T)** view of septa size and ornamentation; **U-Y)** detail of septal teeth shape; **Z-AD)** granulation of the septal teeth. 176

Figure 7.9. Scanning Electron Microscopy images of *Micromussa amakusensis* (A, F, K, P, U, Z) from Japan, *Acanthastrea lordhowensis* 1642 (B, G, L, Q, V, AA), *Micromussa amakusensis* from the Gulf of Aden, Yemen (C, H, M, R, W, AB), *Phymastrea multipunctata* (D, I, N, S, X, AC), cf *Homophyllia australis* (E, J, O, T, Y, AD). **A-E)** top view of the examined fragments; **F-J)** top view of corallites; **K-O)** side view of adjoining corallite walls; **P-T)** detail of septal teeth shape; **U-Y)** granulation of the septal teeth; **Z-AD)** structure of the columella. 177

Figure 7.10. Morphology of *Symphyllia wilsoni*. **A)** meandering valleys and a hydnporphoid formation (white arrow) which can be found in this species; **B)** full sized corallite on the left hand side, side by side with a valley in which the centres have an unusual morphology and thicker septa (black arrows) seem to separate the columellae which are also almost split in two; **C)** a close up of the columellae shown in B; **D)** SEM of the columella sitting deep in the valleys; **E)** SEM top view of an hydnporphoid formation; **F)** SEM side view of the same hydnporphoid formation as in E; **G)** close up of F showing septal side granulation; **H)** in the foreground a columella and in the background behind it the thicker septa separating adjacent columellae indicated by the black arrows in B and C; **I)** a detail of the peculiar structure forming saddle-shaped structure on the two adjoining inner ends

of the thicker septa separating adjacent columellae; **J**) granulation of the saddle-shaped structure shown in I.

178

- LIST OF TABLES -

Table 1.1. Schematic timeline of the classification of the genera in the Lobophylliidae in the principal taxonomic studies from Vaughan and Wells (1943) until Budd et al. (2012). Only extant genera are included. = : synonymy.

32

Table 2.1. List of analyzed specimens. Y = Balhaf (Gulf of Aden, Yemen); BA = Bir Ali (Gulf of Aden, Yemen); AD= Aden (Gulf of Aden, Yemen); BU = Burum (Gulf of Aden, Yemen); MU and FP = Al Mukallah (Gulf of Aden, Yemen); SO = Socotra Island (Indian Ocean, Yemen); MA = Mayotte Island (Indian Ocean, France); KA = Kamaran Island (Red Sea, Yemen); SO = Socotra Island (Gulf of Aden Yemen); NC and HS = Côte Oubliée (New Caledonia).

41

Table 2.2. List of the taxa examined in this study. For each species the clade to which it is assigned and the traditional family are listed. If applicable, the divergence, or lack thereof, between Indian Ocean (IO) and Pacific Ocean (PO) material is indicated. Remarks on the main findings are listed. n.a. = not applicable; div. = divergence observed between IO and PO specimens; no div. = no divergence observed between IO and PO specimens. Species in bold were examined for the first time in this study. * indicates species for which IO populations are analysed for the first time in this study.

55

Table 3.1. List of the material examined in this study. For each specimen we list code, identification, family, sampling locality, COI and rDNA sequences used for the phylogenetic reconstructions. * indicates species analyzed for the first time from a molecular point of view. P.O. = Pacific Ocean; I.O. = Indian Ocean; IRD = Institut de Recherche pour le Développement, Nouméa, New Caledonia; UNIMIB = University of Milano – Bicocca, Milan, Italy; RMNH = Naturalis Biodiversity Center, former name of the present Rijksmuseum van Natuurlijke Historie, Leiden, the Netherlands. All the skeletons analyzed in this study are currently deposited at the University of Milano-Bicocca, Milan, Italy.

64

Table 3.2. Grouping at genus level of the 32 species analyzed based on molecular data in this study. Type species are in bold. * = species analyzed for the first time from the molecular point of view; ^ = molecularly based grouping candidate for new genus description; § = genus re-assignment pending a formal taxonomic revision.

71

Table 4.1. Annotation of the complete mitochondrial genome of *A. maxima*.

76

Table 5.1. List of the material examined in this study. For each specimen we list code, identification, sampling locality, collector, and COI, histone H3, and ITS

region sequences used for the phylogenetic reconstructions.

85

Table 5.2. Macromorphology and micromorphology of *Parascolymia vitiensis* and *P. rowleyensis* (previously *Australomussa*). Explanation of characters, their ID numbers (in brackets) and state names are from Budd et al. (2012).* = character examined on polycentric coralla; Csn= number of cycle of costosepta; Sn = number of cycle of septa. Names of characters which have different states in the two species in bold.

106

Table 6.1. Voucher number, identification, collection site, and EMBL accession numbers of the samples used for molecular and morphological analyses in this study. Source: ^a Arrigoni et al. (2014b); ^b Arrigoni et al. (2012); ^c Arrigoni et al. (2014a).

119

Table 6.2. Macromorphology and micromorphology of *Sclerophyllia margariticola*, *S. maxima* (this study) and *Cynarina lacrymalis* and *Acanthastrea echinata* (from Budd et al., 2012). Explanation of characters, their ID numbers (in brackets) and state names are from Budd et al. (2012).- = character examined on polycentric coralla; Csn= number of cycle of costosepta; Sn = number of cycle of septa.

143

Table 7.1. List of the material examined in this study. For each specimen we list code, identification, sampling locality, collector, and molecular markers used for the phylogenetic reconstructions. xxx: sequence newly obtained in this work.

157

- LIST OF APPENDICES -

Appendix 2.1. Map of the Indo-Pacific showing sampling localities for this study (numbered from 1 to 4) and sampling localities of the “Bigmessidae” samples included in published phylogenies (Fukami et al., 2008; Huang et al., 2009; Kitahara et al., 2010; Huang et al., 2011; Benzoni et al., 2011). 1 = Yemen, north-western Gulf of Aden coast, 2 = Socotra Island; 3 = Mayotte Island; 4 = New Caledonia. Geographical coordinates: Kamaran (Lat. 15°22.82' N, Long. 42°36.27' E), Aden (Lat. 12°46.60' N, Long. 44°56.28' E), Balhaf (Lat. 13°58.12' N, Long. 48°10.66' E), Bir Ali (Lat. 13°59.48' N, Long. 48°19.67' E), Burum (Lat. 14°18.76' N, Long. 48°59.84' E), Al Mukallah (Lat. 14°30.52' N, Long. 49°09.82' E), Socotra (Lat. 12°40.35' N, Long. 54°11.75' E), Mayotte Island (Lat. 12°38.48' S, Long. 45°02.74' E), Côte Oubliée (Lat. 21°55.78 S, Long. 166°41.11' E). 224

Appendix 2.2. *In-vivo*, corallum, and detail of corallites morphology of the species with Indian Ocean (IO) or Indo-Pacific (IP) analyzed in this study. A) *Leptastrea transversa* (IP); B) *L. bottae* (IP); C) *L. pruinosa* (IP); D) *Cyphastrea microphthalma* (IP); E) *C. serailia* (IP); F) *Plerogyra sinuosa* (IP); G) *Blastomussa wellsi* (IP); H) *B. merleti* (IP); I) *Parasimplastrea omanensis* (IO); J) *Echinopora gemmacea* (IP) (IP); K) *Favites peresi* (IO); L) *Favites halicora* (IP); M) *F. complanata* (IP); N) *F. abdita* (IP); O) *Hydnophora exesa* (IP); P) *Platygyra daedalea* (IP); Q) *Favia favius* (IP); R) *Favites pentagona* (IP); S) *Leptoria phrygia* (IP); T) *Micromussa amakusensis* (IP); U) *Cynarina lacrymalis* (IP); V) *Lobophyllia hemprichii* (IP); W) *Lobophyllia corymbosa* (IP); X) *Symphyllia radians* (IP); Y) *Acanthastrea maxima* (IO); Z) *A. echinata* (IP); AA) *Echinophyllia aspera* (IP). Please refer to Veron et al. (1977) and Veron (2000) for the diagnostic morphologic characters that correspond with each of these species. When all images refer to the same specimen its code is shown on the bottom left corner of the *in situ* image. In case images refer to different specimens this is indicated. Corallite detail on the right hand side always refer to the corallum shown in the centre image. For images of *Favia pallida* (IP), *F. rotumana* (IP), and *F. matthaii* (IP) refer to Fig. 2. For images of *Goniastrea retiformis* (IP) and *Plesiastrea versipora* (IP) refer to Benzoni et al. (2011). Sampling localities: Y = Balhaf (Gulf of Aden, Yemen); BA = Bir Ali (Gulf of Aden, Yemen); AD= Aden (Gulf of Aden, Yemen); BU = Burum (Gulf of Aden, Yemen); MU and FP = Al Mukallah (Gulf of Aden, Yemen); SO = Socotra Island (Indian Ocean, Yemen); MA = Mayotte Island (Indian Ocean, France); KA = Kamaran Island (Red Sea, Yemen); SO = Socotra Island (Gulf of Aden Yemen); NC and HS = Côte Oubliée (New Caledonia). 230

Appendix 2.3. Maximum Parsimony tree based on COI dataset. Numbers are bootstrap values. Clade numbers and sub-clade codes are the same ones reported respectively by Fukami et al. (2008) and Huang et al. (2011). Values <50% are not shown. IO samples are evidenced in blue and PO samples in black. 231

Appendix 2.4. Maximum Parsimony tree based on rDNA dataset. Numbers are bootstrap values. Clade numbers and sub-clade codes are the same ones reported respectively by Fukami et al. (2008) and Huang et al., (2011). Values <50% are not shown. IO samples are evidenced in blue and PO samples in black. 232

Appendix 3.1. *In situ* and corallum of species examined in this study: a) *Acanthastrea rotundoflora* from type locality (New Caledonia); b) *A. hemprichi*; c) *A. echinata*; d) *A. subechinata*; e) *Echinophyllia aspera* from the Indian Ocean; f) *E. orpheensis*; g) *E. echinoporoides*; h) *E. tarae*; i) *Cynarina lacrymalis*; j) *A. faviaformis*. Colour codes and capital letters in white circles refer to clades in Fig. 3.1. Specimen code on the images. 233

Appendix 3.2. *In situ* and corallum of species examined in this study: a) *Symphyllia valenciennesi*; b) *S. recta*; c) *S. agaricia*; d) *S. radians*; e) *Lobophyllia hemprichii*; f) *L. robusta*; g) *L. flabelliformis*; h) *L. cf diminuta*; i) *L. costata*; j) *S. erythraea*. Colour codes and capital letters in white circles refer to clades in Fig. 3.1. Specimen code on the image. 234

Appendix 3.3. ML tree based on COI dataset. Node values are ML SH-like support (> 70%). 235

Appendix 3.4. ML tree based on rDNA dataset. Node values are ML SH-like support (> 70%). 236

Appendix 5.1. Phylogenetic position of *Parascolymia vitiensis* and *P. rowleyensis* (previously *Australomussa*) within the family Lobophylliidae based on partial mitochondrial COI gene. Bayesian topology is shown. Numbers associated with branches indicate Maximum Likelihood bootstrap (>70%) support (left) and Bayesian posterior probabilities (>0.9) (right). Clades within Lobophylliidae are coloured and labelled A to I according to Arrigoni et al. (2014a). 237

Appendix 5.2. Phylogenetic position of *Parascolymia vitiensis* and *P. rowleyensis* (previously *Australomussa*) within the family Lobophylliidae based on nuclear histone H3. Bayesian topology is shown. Numbers associated with branches indicate Maximum Likelihood bootstrap (>70%) support (left) and Bayesian posterior probabilities (>0.9) (right). Clades within Lobophylliidae are coloured and labelled A to I according to Arrigoni et al. (2014a). 238

Appendix 5.3. Phylogenetic relationships between *Parascolymia vitiensis* and *P. rowleyensis* (previously *Australomussa*) within the family Lobophylliidae based on nuclear ITS region. Bayesian topology is shown. Numbers associated with branches indicate Maximum Likelihood bootstrap (>70%) support (left) and

Bayesian posterior probabilities (>0.9) (right). Clades within Lobophylliidae are coloured and labelled A to I according to Arrigoni et al. (2014a). 239

Appendix 5.4. *In situ* photos of the specimens of *Parascolymia vitiensis* analyzed in this study: A) 6816, B) 6830; C) IRD HS2955; D) IRD HS2964; E) IRD HS2985, F) IRD HS3255; G) UNIMIB PFB031; H) UNIMIB PFB032; I) UNIMIB PFB033; J) UNIMIB PFB052; K) UNIMIB PFB053; L) UNIMIB PFB055; M) UNIMIB PFB151; N) UNIMIB PFB152. 240

Appendix 6.1. List of sequences of COI, Histone H3, and rDNA used for the Ancestral character state reconstruction. 241

Appendix 6.2. Original illustration of *S. margariticola* by Klunzinger (1879). Arabic numerals at the outer end of the septa indicate the cycle number (from 1 to 5). 242

Appendix 7.1. ML tree based on mitochondrial COI dataset. Node values are ML SH-like support (> 0.7). 243

Appendix 7.2. ML tree based on nuclear Histone H3 dataset. Node values are ML SH-like support (> 0.7). 244

Appendix 7.3. ML tree based on ITS region dataset. Node values are ML SH-like support (> 0.7). 245

Appendix 7.4. Pairwise comparisons of genetic distance within and between clades of the family Lobophylliidae. Standard deviations listed on the upper right hand portions for each set of comparisons. 246

– CHAPTER 1 –

General Introduction

1.1 From traditional to reverse taxonomy

Stony corals (Cnidaria, Anthozoa, Scleractinia) are polypoidal marine invertebrates with relatively simple level of organization that are distributed throughout the world's oceans, from the tropics to polar regions and from the intertidal zone to the deepest depths (Cairns, 1999; Veron, 2000). This group is distinguished from the other related orders of the Hexacorallia, *i.e.* Corallimorpharia, Actiniaria, Antipatharia, Zoantharia, and Ceriantharia, by having the capacity to effectively secrete an aragonitic calcium carbonate skeleton and it is composed by more than 1,400 extant species (Wallace, 1999; Cairns, 1999, 2001; Veron, 2000; Cairns and Kitahara, 2012). Nearly 40% of these species are found deeper than 50 m and they do not live in association with phototrophic dinoflagellates of the genus *Symbiodinium* (Cairns, 1999, 2004, 2007, 2011; Cairns and Kitahara, 2012). The remaining species inhabit shallow waters, they are mostly colonial and zooxanthellate, and represent the major framework builders of tropical coral reefs (Hoeksema, 1989; Veron, 2000; Cairns, 1999; Wallace, 1999; Wallace et al., 2012).

Since the 19th century traditional classification of scleractinian corals has been conducted mainly on detailed examination of skeletal characters (Milne Edwards and Haime, 1857; Ogilvie, 1897; Vaughan and Wells, 1943; Wells, 1956). An exhaustive review of historical and modern accounts of coral evolutionary relationships and classification systems was published by Stolarski and Roniewicz (2001). After Linnean system of classification, several taxonomic publications raised during the 19th century describing and referring to the coral gross-morphology (Dana, 1846; Milne Edwards and Haime, 1857; Ogilvie, 1897). On the basis of their remarkably wide zoological and paleontological knowledge Milne Edwards and Haime (1857) presented the first thorough classification of scleractinian

corals. Their effort remains a most influential work, later revised in Vaughan and Wells's (1943) milestone work. During the 20th century, four main classification systems were proposed as a result of an increasing amount of data concerning extant and fossil corals and more in-depth analyses on macro- and micromorphological traits (Vaughan and Wells, 1943; Wells, 1956; Alloiteau, 1952; Chevalier and Beauvais, 1987). In particular, Vaughan and Wells (1943) and Wells (1956) provided the basic scheme of coral systematics for modern taxonomy based on conventional taxonomic keys of phenotypic traits of skeleton (Fig. 1.1). Summarizing the results of over one hundred years of study of recent and paleontological coral specimens, the authors subdivided the order Scleractinia into five suborders and 33 extant and fossil families (Fig. 1.2). Alloiteau (1952) and Chevalier and Beauvais (1987) relied upon these two aforementioned systems but focused their attention on innovative observations of microstructural characters, hypothesizing that gross-morphology could be highly confusing.

Finally, starting in the 1960s, an increasing number of field studies provided for the first time information about the living animal and *in-situ* morphology and plasticity, thus leading to the last phase of uniquely morphology-based coral taxonomy (Veron and Pichon, 1976, 1980, 1982; Veron et al., 1977; Veron and Wallace, 1984; Hoeksema, 1989; Wallace, 1999; Veron, 2000). These works demonstrated the extent of intraspecific variability and adopted the concept of “morphological discontinuity” to determine species boundaries (Wallace and Willis, 1994). However, morphological discontinuities between closely related species are frequently unclear and confused making the definition of species boundaries a hard task for coral specialists themselves (Veron and Pichon, 1976, 1980, 1982; Wallace, 1999). Environment-induced phenotypic plasticity, intraspecific variation caused by different genotypes, and evolutionary convergence of skeletal characters have been indicated as factors causing the overlap of intraspecific and interspecific variability (Hoeksema, 1993; Veron, 1995; Todd, 2008). Moreover, several studies showed that synchronized spawning among numerous species of hard corals, *i.e.* mass spawning *sensu* Willis et al.

(1985), occurs in the majority of reef regions (reviewed by Baird et al. (2009)). The simultaneously release of huge quantities of sperms and eggs in a limited period of time creates an incomparable opportunity for interspecific hybridization and introgression. Extensive introgressive hybridization has been demonstrated to occur in corals (reviewed by Willis et al. (2006)), especially within the genus *Acropora* (van Oppen et al., 2001, 2002a; Vollmer and Palumbi, 2002; Richards et al., 2008; Isomura et al., 2013). Based on these evidence, Veron (1995) proposed the hypothesis of “reticulate evolution” to mass-spawning corals, thrown into crisis the biological concept of species. In this scenario, coral species continuously fuse by hybridization, and separate via isolation and genetic drift and the entire process is under physical environmental control, *i.e.* changes in surface circulation patterns, and not under biological control (Veron, 1995)

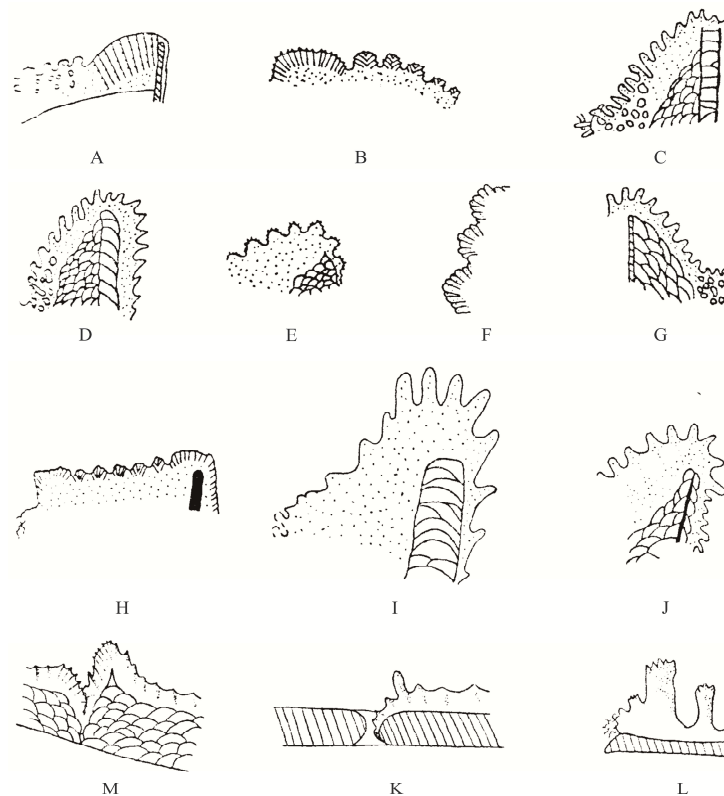


Figure 1.1. Illustration of septa of the genera traditionally ascribed to the Mussidae (A-J) and to the Pectiniidae (M-L) as reported in Vaughan and Wells (1943). Modified from Vaughan and Wells (1943). A, B) *Circophyllia truncate*, x3; C) *Mussismilia braziliensis*, x2; D) *Mussismilia harttii*, x2; E) *Syzygophyllia brevis*, x2; F) *Leptomussa variabilis*, x1^{1/2}; G) *Acanthastrea echinata*, x3; H) *Antillia gregorii*, x2; I) *Acanthophyllia dashayesiana*, x1; J) *Mussa angulosa*, x1^{1/2}; M) *Echinophyllia aspera*, x2.2; K) *Oxypora lacera*, x2.2; L) *Mycedium tubifex*, x2.2. Modified from Vaughan and Wells (1943).

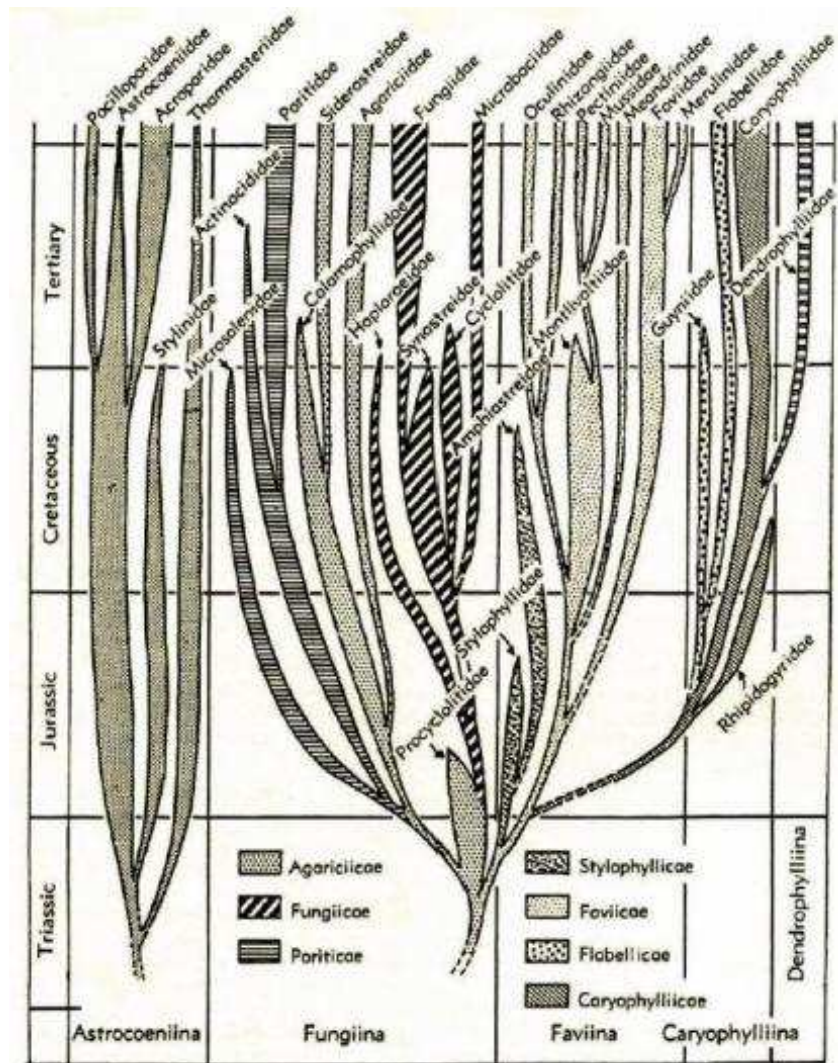


Figure 1.2. The classification system and evolutionary relationships among stony corals proposed by Wells (1956). Branches represent families, patterns represent superfamilies, and columns represent suborders. Modified from Wells (1956).

Since the late 1990s, molecular analyses have revolutionized the traditional systematics of corals at all levels showing that the conventional macromorphological classification in suborders, families, and genera is mostly unreliable (Romano and Palumbi, 1996; Romano and Cairns, 2000; Chen et al., 2002; Fukami et al., 2004a, 2008; Le Goff-Vitry et al., 2004; Kitahara et al. 2010; Huang et al. 2011) (Fig. 1.3). Mitochondrial and nuclear phylogeny reconstructions revealed that extant stony corals fall into three major groups, *i.e.* the Basal, Complex, and Robust clades, instead of seven traditional suborders, and pushed the evolutionary origin of the Scleractinia deep into the Paleozoic (Romani and Palumbi, 1996; Stolarski et al., 2011). Phylogenetics based on mitochondrial

nucleotides sequences strongly supported the monophyly of the Scleractinia (Brugler and France, 2007; Fukami et al., 2008; Kitahara et al., 2010; Stolarski et al., 2011; Kayal et al., 2013). Conversely, other molecular studies proposed that the Corallimorpharia arose by skeleton loss from a scleractinian ancestor at a time (during the mid-Cretaceous) of high oceanic CO₂ levels (Stanley and Fautin, 2001; Medina et al., 2006; Lin et al., 2014; Kitahara et al., 2014). Moreover, within the Scleractinia, the majority of traditional families have been found to be para- or polyphyletic (Fukami et al., 2004a, 2008; Kitahara et al., 2010; Huang et al., 2011) (Fig. 1.3).

This extensive and continuously growing amount of genetic data and the development in molecular tools made the evolutionary hypotheses based on genetics more robust and reliable. Well supported molecular phylogenies, together with the increasing number of unexpected genetic findings, encouraged the morphologists to search for new micromorphological and microstructural criteria in order to corroborate molecular phylogenies (Stolarski and Janiszewska, 2001; Cuif and Sorauf, 2001; Stolarski, 2003; Cuif et al., 2003; Benzoni et al., 2007; Brahmi et al., 2010; Budd and Stolarski, 2009, 2011; Janiszewska et al., 2011). On the one hand, some traditional microstructures, such as “trabeculae” and “centers of calcification” (Bourne, 1887; Vaughan and Wells, 1943), have been re-described and re-interpreted (Stolarski, 2003; Brahmi et al., 2010). On the other hand, fine-scale morphological analyses of taxa within molecularly-defined lineages allowed the identification of key and informative micromorphological and microstructural characters (Fig. 1.4) (Benzoni et al., 2007; Budd and Stolarski, 2009, 2011; Gittenberger et al., 2011; Benzoni et al., 2011; Janiszewska et al., 2011; Kitahara et al., 2012a, 2012b; Budd et al., 2012). This reverse taxonomy (Budd et al., 2010) led to several taxonomic revisions at family (Budd et al., 2012; Kitahara et al., 2012a, 2012b; Huang et al., 2014) and genus level (Wallace et al., 2007; Benzoni et al., 2010; Gittenberger et al., 2011; Schmidt-Roach et al., 2014), suggesting a great potential to better understand the evolution of scleractinian corals

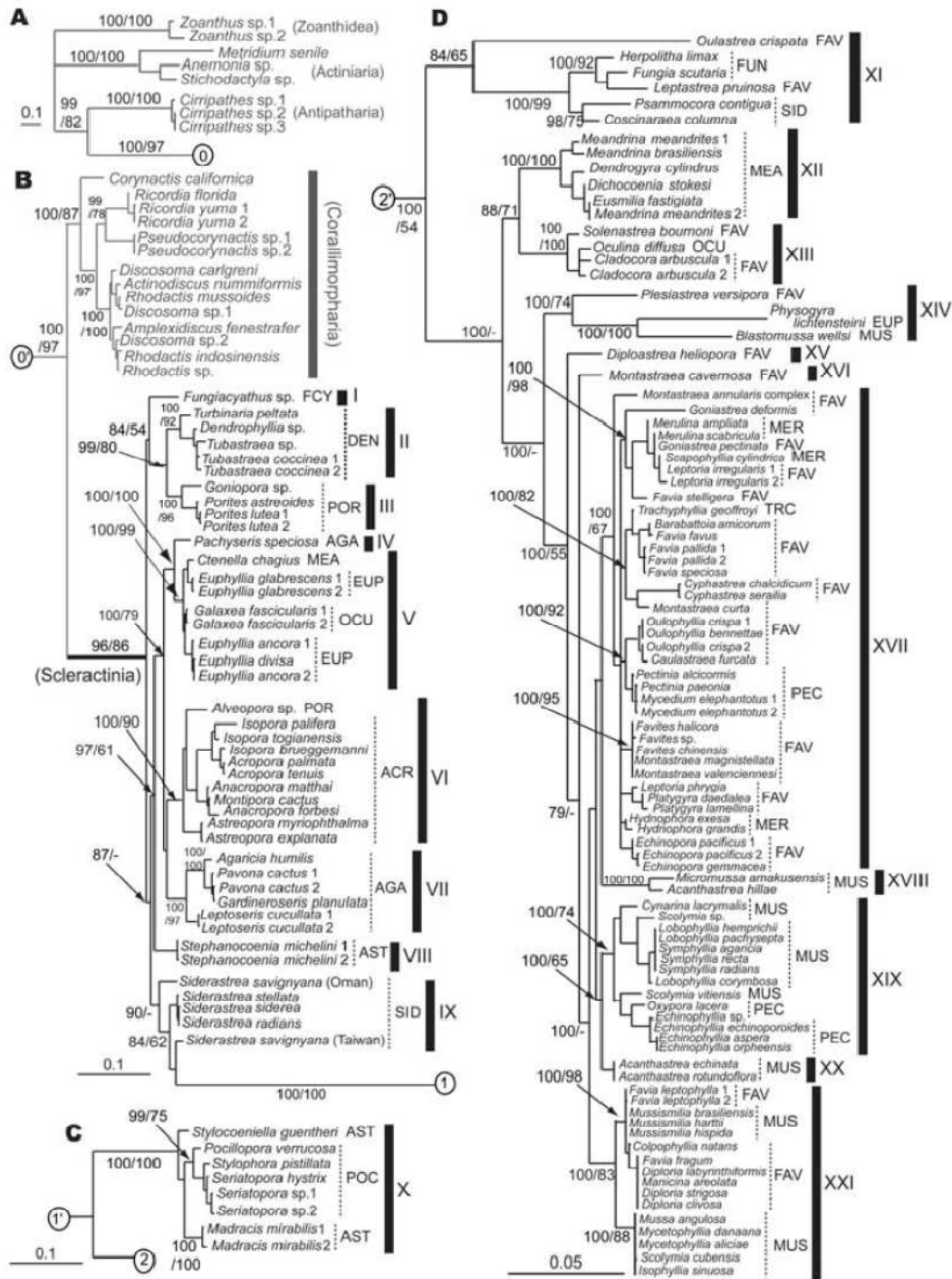


Figure 1.3. Phylogenetic relationships among scleractinian corals and outgroups. Topology was inferred by Bayesian analysis, based on combined mitochondrial COI and CYTB sequences. Numbers on main branches show percentages of Bayesian probability ($\geq 70\%$) and bootstrap values ($\geq 50\%$) in ML analysis. Dashes mean bootstrap values $< 50\%$ in ML. Numbers in circles show the connection of trees from A to D: A, outgroups; B, complex corals and corallimorpharians; C, the family Pocilloporidae; D, robust corals. Three-letter codes correspond with traditional families; numbers in Roman numerals indicate clades interpreted from the tree. Modified from Fukami et al. (2008).

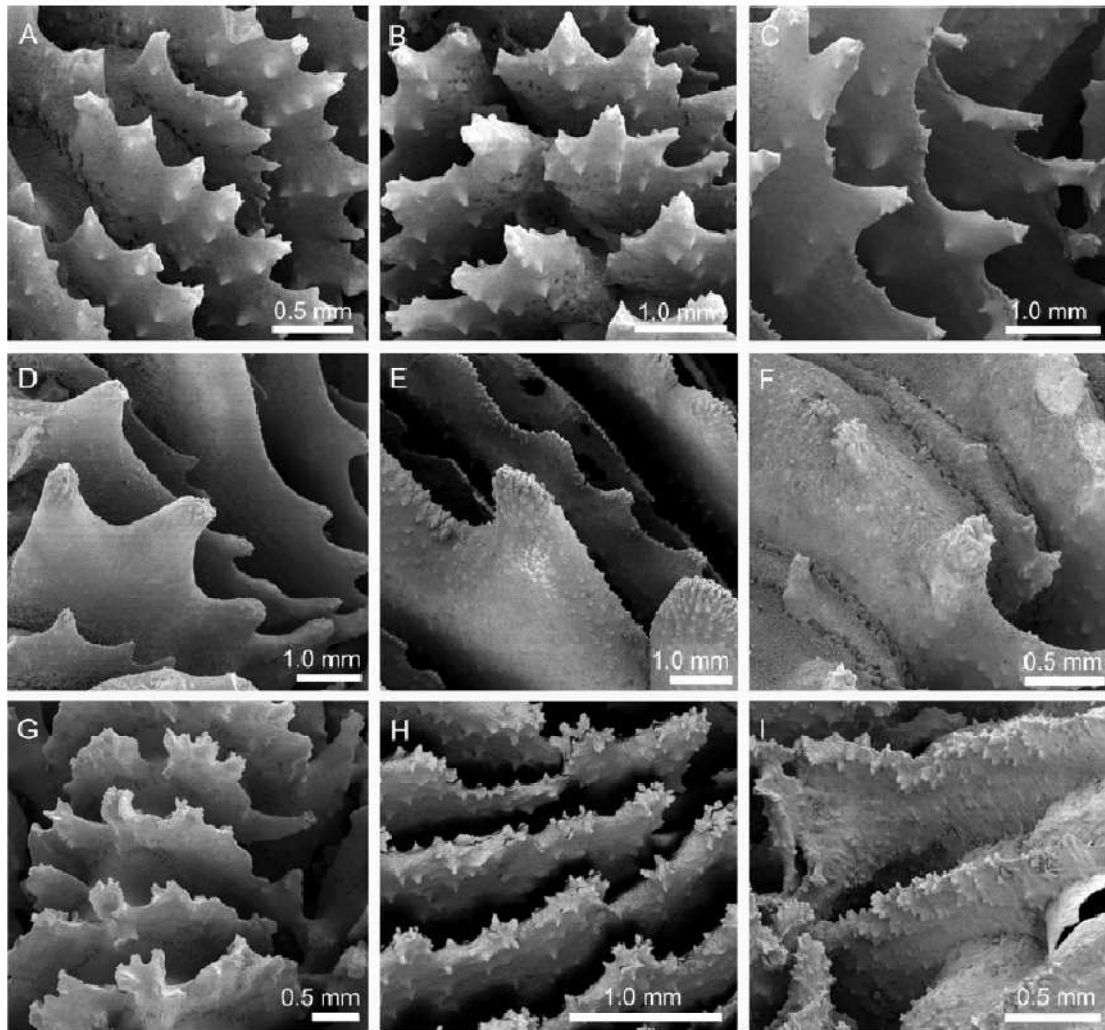


Figure 1.4. An example of micromorphology showing the study of the shape of septal teeth and the granulations on septal faces (Budd and Stolarski, 2009, 2011). Clade XXI *sensu* Fukami et al. (2008) (A-C) is distinguished by regular blocky teeth with pointed tips, and aligned granules. Clade XIX *sensu* Fuami et al. (2008) (D-F) is distinguished by irregular lobate or bulbous teeth with elliptical tooth bases, and rounded granules enveloped by extensive thickening deposits. Clade XVII *sensu* Fuami et al. (2008) (G-I) is distinguished by irregular multi-axial teeth with circular bases, and irregular scattered granules. A) XXI, *Pseudodiploria strigosa*; B) XXI, *Mussismilia braziliensis*; C) XXI, *Isophyllia sinuosa*; D) XIX, *Lobophyllia pachysepta*; E) XIX, *Parascolymia vitiensis*; F) XIX, *Echinophyllia echinoporoides*; G) XVII, *Merulina ampliata*; H) XVII, *Favites halicora*; I) XVII, *Hydnophora exesa*. Modified from Budd et al. (2012).

1.2 The family Lobophylliidae Dai and Horng, 2009

The family Lobophylliidae Dai and Horng, 2009 currently comprises 12 extant genera and 52 extant zooxathellate species and is widely distributed throughout the Indo-Pacific, from the Red Sea and east Africa, to French Polynesia (Veron, 2000; Dai and Horng, 2009; Budd et al., 2012; Benzoni, 2013). The Lobophylliidae are hermatypic, solitary and colonial forms, and are an ecologically dominant group in all coral reefs of the Indo-Pacific (Veron and Pichon, 1980; Scheer and Pillai, 1983; Sheppard and Sheppard, 1991; Veron, 1993, 2000). The family contains both widespread common and distinctive species as well as high latitude endemic species (Veron, 1985, 1986, 1992, 1993, 2000, 2002; Cairns, 1999). Table 1.1 summarizes the schematic outline of the taxonomic classification of the genera in the Lobophylliidae from Vaughan and Wells (1943) to Budd et al. (2012).

The family corresponds to molecular clades XVIII, XIX, and XX *sensu* Fukami et al. (2008) identified by Fukami et al. (2004a, 2008) (Fig. 1.3) using both mitochondrial and nuclear genes. It consists of the colonial genus *Moseleya* previously ascribed to the Faviidae (Veron, 2000) and other 12 Indo-Pacific genera that have conventionally been assigned to the families Mussidae Ortmann, 1890 or Pectiniidae Vaughan and Wells, 1943. Integrating molecular and morphological analyses, Budd et al. (2012) carried out a complete re-organization at family level and defined the Mussidae (clade XXI *sensu* Fukami et al. (2008)) as a group limited to Atlantic Ocean, the Merulinidae (clade XVII *sensu* Fukami et al. (2008)) as a predominantly Indo-Pacific taxon, and the Lobophylliidae (clades XVIII, XIX, and XX *sensu* Fukami et al. (2008)) as a family distributed throughout the Indo-Pacific. The Lobophylliidae are characterized by irregular lobate or bulbous teeth with elliptical tooth bases, rounded granules enveloped by extensive thickening deposits (Fig. 1.3), well-developed thickening deposits, parathecal corallite walls, and widely spaced clusters of calcification centres (Budd and Stolarski, 2009; Budd et al., 2012; Huang et al., 2014).

Despite the recent molecular and morphological insights (Fukami et al., 2004a, 2008; Budd and Stolarski, 2009), the family still remains poorly understood. Most of its taxa are unstudied and nothing is known about evolutionary relationships within the family as well as detailed micromorphological analyses still have to be conducted.

Table 1.1. Schematic timeline of the classification of the genera in the Lobophylliidae in the principal taxonomic studies from Vaughan and Wells (1943) until Budd et al. (2012). Only extant genera are included. = : synonymy.

Vaughan and Wells (1943)	Wells (1956)	Chevalier and Beauvais (1987)	Veron (2000)	Budd et al. (2012)
Mussidae	Mussidae	Mussidae	Mussidae	Lobophylliidae
<i>Acanthastrea</i>	<i>Acanthastrea</i>	<i>Acanthastrea</i>	<i>Acanthastrea</i>	(clades XVIII, XIX, XX)
<i>Acanthophyllia</i>	<i>Acanthophyllia</i>	<i>Acanthophyllia</i>	<i>Australomussa</i> ⁺	<i>Acanthastrea</i>
<i>Isophyllia</i>	<i>Homophyllia</i>	<i>Blastomussa</i> ⁺⁺	<i>Blastomussa</i> ⁺⁺	<i>Australomussa</i> ⁺
<i>Isophyllastrea</i>	<i>Isophyllia</i>	<i>Cynarina</i>	<i>Cynarina</i>	<i>Cynarina</i>
<i>Mycetophyllia</i>	<i>Isophyllastrea</i>	<i>Homophyllia</i>	(= <i>Acanthophyllia</i>)	(= <i>Indophyllia</i> ^{**} , <i>Acanthophyllia</i>)
<i>Mussa</i>	<i>Mycetophyllia</i>	<i>Isophyllia</i>	<i>Indophyllia</i> ^{**}	<i>Echinomorpha</i> ⁺
(= <i>Scolymia</i>)	<i>Mussa</i>	<i>Isophyllastrea</i>	<i>Isophyllia</i>	<i>Echinophyllia</i>
<i>Mussismilia</i>	(= <i>Scolymia</i>)	<i>Mycetophyllia</i>	<i>Micromussa</i> ⁺	<i>Homophyllia</i>
<i>Lobophyllia</i>	<i>Mussismilia</i>	<i>Mussa</i>	<i>Mycetophyllia</i>	<i>Micromussa</i> ⁺
(= <i>Cynarina</i> , <i>Homophyllia</i>)	<i>Lobophyllia</i>	<i>Mussismilia</i>	<i>Mussa</i>	<i>Moseleya</i>
<i>Palauphyllia</i>	(= <i>Cynarina</i> , <i>Palauphyllia</i>)	<i>Lobophyllia</i>	<i>Mussismilia</i>	<i>Lobophyllia</i>
<i>Symphyllia</i>	<i>Symphyllia</i>	(= <i>Palauphyllia</i>)	<i>Lobophyllia</i>	(= <i>Palauphyllia</i>)
		<i>Parascolymia</i> [*]	<i>Symphyllia</i>	<i>Oxypora</i>
		<i>Symphyllia</i>	<i>Scolymia</i>	<i>Parascolymia</i> [*]
		<i>Scolymia</i>	(= <i>Homophyllia</i> , <i>Parascolymia</i> [*])	<i>Symphyllia</i>
Pectiniidae	Pectiniidae			Mussidae
<i>Echinophyllia</i>	<i>Echinophyllia</i>	Pectiniidae		(clade XXI)
<i>Oxypora</i>	<i>Oxypora</i>	<i>Echinophyllia</i>	Pectiniidae	<i>Isophyllia</i>
<i>Myecedium</i>	<i>Myecedium</i>	<i>Oxypora</i>	<i>Echinomorpha</i> ⁺	(= <i>Isophyllastrea</i>)
<i>Pectinia</i>	<i>Pectinia</i>	<i>Myecedium</i>	<i>Echinophyllia</i>	<i>Mycetophyllia</i>
	<i>Physophyllia</i>	<i>Pectinia</i>	<i>Oxypora</i>	<i>Mussa</i>
Faviidae	Faviidae	<i>Physophyllia</i>	<i>Myecedium</i>	<i>Mussismilia</i>
<i>Moseleya</i>	<i>Moseleya</i>		<i>Pectinia</i>	<i>Scolymia</i>
.....	Trachyphylliidae	(= <i>Physophyllia</i>)	and other 5 genera
		<i>Moseleya</i>		
		Faviidae	
			<i>Moseleya</i>	
			
				Merulinidae
				(clade XVII)
				<i>Myecidium</i>
				<i>Pectinia</i>
				<i>Physophyllia</i>
			
				Incertae sedis
				(clade XIV)
				<i>Blastomussa</i> ⁺⁺

* *Parascolymia* was described by Wells (1964) to include *Parascolymia vitiensis* (Brüggemann, 1877), previously considered as *Scolymia vitiensis* by Vaughan and Wells (1943) and Wells (1956)

** *Indophyllia* was considered a fossil genus until the description of the living species *I. macassarensis* Best and Hoeksema, 1987

⁺ *Australomussa*, *Micromussa*, and *Echinomorpha* were firstly described by Veron (2000)

⁺⁺ *Blastomussa* was firstly described by Wells (1968)

1.3 Aims of the dissertation

The overall objective of this dissertation is to fill the existing gap in the knowledge of evolution and systematics of the Lobophylliidae using molecular and micromorphological data. As general outline, a basic and robust molecular background of the family (Chapters 2, 3, and 4) was provided and further integrated with newly obtained genetic data and gross- and fine-scale morphological observations in order to revise different taxa ascribed to the Lobophylliidae (Chapters 5, 6, and 7). In particular a molecular phylogeny reconstruction of the Robust clade was proposed and the evolutionary relationships between the Lobophylliidae and their closely related lineages investigated (Chapter 2). Then the levels of paraphyly of the traditional lobophylliid genera were summarized in a comprehensive multi-loci molecular phylogeny of the Lobophylliidae (Chapter 3). The complete mitochondrial genome of *Acanthastrea maxima* Sheppard and Salm, 1988 allowed to better understand the evolution of the family, suggesting also potential informative mitochondrial markers for future molecular studies of the other lobophylliid genera (Chapter 4). Finally, reverse taxonomy supported the revision of five conventional genera, *Australomussa* Veron, 1985 and *Parascolymia* Wells, 1964 (Chapter 5), *Sclerophyllia* Klunzinger, 1879 (Chapter 6), *Homophyllia* Brüggemann, 1877 and *Micromussa* Veron, 2000 (Chapter 7), and the description of two new species and a new genus (Chapter 7) through an innovative integrated morpho-molecular approach.

- CHAPTER 2 -

*Molecular phylogeny of the Robust Clade
(Faviidae, Mussidae, Merulinidae, and Pectiniidae):
an Indian Ocean perspective*

Roberto Arrigoni¹, Fabrizio Stefani², Michel Pichon³, Paolo Galli^{1,4}, Francesca Benzoni^{1,5}

¹ Department of Biotechnologies and Biosciences, University of Milan – Bicocca, Piazza della Scienza 2, 20126, Milan, Italy

² Water Research Institute-National Research Council (IRSA-CNR), Via del Mulino 19, 20861, Brugherio (MB), Italy

³ Museum of Tropical Queensland, Flinders street, Townsville 4810, Australia

⁴ MaRHE Center (Marine Research and High Education Center), Magoodhoo Island, Faafu Atoll, Maldives

⁵ Institut de Recherche pour le Développement, UMR227 CoReUs2, 101 Promenade Roger Laroque, 98848 Noumea, New Caledonia

Published in *Molecular Phylogenetics and Evolution*: 65, 183-193 (2012)

2.1 Abstract

Recent phylogenetic analyses have demonstrated the limits of traditional coral taxonomy based solely on skeletal morphology. In this phylogenetic context, Faviidae and Mussidae are ecologically dominant families comprising one third of scleractinian reef coral genera, but their phylogenies remain partially unresolved. Many of their taxa are scattered throughout most of the clades of the Robust group, and major systematic incongruences exist. Numerous genera and species remain unstudied, and the entire biogeographic area of the Indian Ocean remains largely unsampled. In this study, we analysed a portion of the mitochondrial cytochrome *c* oxidase subunit 1 gene and a portion of ribosomal DNA for 14 genera and 27 species of the Faviidae and Mussidae collected from the Indian Ocean and New Caledonia and this is the first analysis of five of these species. For some taxa, newly discovered evolutionary relationships were detected, such as the evolutionary distinctiveness of *Acanthastrea maxima*, the genetic overlap of *Parasimplastrea omanensis* and *Blastomussa merleti*, and the peculiar position of *Favites peresi* in clade XVII together with *Echinopora* and *Montastrea salebrosa*. Moreover, numerous cases of intraspecific divergences between Indian Ocean and Pacific Ocean populations were detected. The most striking cases involve the genera *Favites* and *Favia*, and in particular *Favites complanata*, *Favites halicora*, *Favia favius*, *F. pallida*, *F. matthai*, and *F. rotumana*, but divergence also is evident in *Blastomussa merleti*, *Cyphastrea serailia*, and *Echinopora gemmacea*. High morphological variability characterizes most of these taxa, thus traditional skeletal characteristics, such as corallite arrangement, seem to be evolutionary misleading and are plagued by convergence. Our results indicate that the systematics of Faviidae and Mussidae is far from being resolved and that the inclusion of conspecific populations of different geographical origin represents an unavoidable step when redescribing the taxonomy and systematics of scleractinian corals. More molecular phylogenies are needed to define the evolutionary lineages that could be corroborated by known and newly discovered micromorphological characters.

2.2 Introduction

Recent molecular discoveries have revolutionised the traditional classification of scleractinian corals (Cnidaria, Anthozoa, Scleractinia) that was based on the morphology of skeletal structures (Vaughan and Wells, 1943; Wells, 1956; Romano and Palumbi, 1996; Romano and Cairns, 2000; Fukami et al., 2004a, 2008; Budd et al., 2010; Kitahara et al., 2010). Indeed, most traditional macromorphological characters are affected by convergence, homoplasy, phenotypic plasticity, and intraspecific variability, which renders the definition of taxa boundaries and the reconstruction of evolutionary relationships very challenging (Lasker, 1981; Budd, 1990; Miller, 1992; Budd and Klaus, 2001; Todd et al., 2001, 2004; Klaus et al., 2007; Todd, 2008; Forsman et al., 2009).

Since Romano and Palumbi (1996, 1997) provided evidence based on the 16S gene that refuted the traditional subdivision of the Scleractinia into seven suborders (Veron, 1995), the adequacy of traditional morphotaxonomy and systematics has been questioned. Romano and Palumbi (1996,1997) showed the existence of two main molecularly defined clades of corals, the Complex and Robust, which later were confirmed using other markers (Romano and Cairns, 2000; Chen et al., 2002; Le Goff-Vitry et al., 2004). Moreover, Fukami et al. (2008) used two mitochondrial and two nuclear markers to show that at least 11 traditionally recognised scleractinian families are polyphyletic.

Two of the most challenging scleractinian coral families are the Faviidae Gregory, 1900 and the Mussidae Ortmann, 1890. They both are found in the Atlantic and the Pacific Oceans, and they include 37 of the 111 scleractinian reef coral genera (Veron, 2000). Despite their ecological importance and a considerable amount of taxonomic studies focused on them (e.g., Matthai, 1914; Vaughan and Wells, 1943; Wells, 1956; Chevalier, 1975; Wijsman-Best, 1976; Veron et al., 1977; Veron and Pichon, 1980; Zlatarski and Estalella, 1982; Veron, 2000; Budd and Stolarski, 2009; Budd and Stolarski, 2011), the systematics of these two families is in need of a major formal taxonomic overhaul. The genera traditionally

ascribed to the Faviidae and Mussidae are largely polyphyletic, with representatives scattered through 10 of the 12 clades of the Robust group (Fukami et al., 2008). Moreover, the Atlantic members of the two families are more closely related to each other than to their Pacific confamilials (Fukami et al., 2004a, 2008; Nunes et al., 2008; Kitahara et al., 2010).

The Atlantic clade XXI (sensu Fukami et al., 2008) contains *Favia fragum* Esper, 1795 and *Mussa angulosa* Pallas, 1766, which are the type species of the Faviidae and Mussidae, respectively. This phylogenetic affinity is also supported by several micromorphological and microstructural characters, such as the shapes and distribution of septal teeth and granules, the area between teeth, the development of thickening deposits, and the arrangement of the calcification centres and fibers, which are quite distinctive between Atlantic and Pacific Mussidae (Budd and Stolarski, 2009). Pursuing their search for new morphological diagnostic characters, Budd and Stolarski (2011) found that Atlantic and Pacific representatives of the Faviidae differ in teeth shape, teeth and septal granulation, and the structure of the inter-area between teeth, thus reflecting the same pattern found in the case of the Atlantic and Pacific Mussidae (Budd and Stolarski, 2009).

Among the Pacific mussids, the genera *Cynarina*, *Lobophyllia*, and *Symphyllia* are more closely related to the Pectiniidae Vaughan and Wells, 1943 genera *Echinophyllia* and *Oxypora* (clade XIX) than to the confamilial genera *Micromussa* and *Acanthastrea* (clades XVIII and XX, respectively), which present unclear or polyphyletic phylogenetic relationships (Fukami et al., 2004a, 2008). Within the genus *Scolymia*, the Atlantic species *S. cubensis* belongs to (Atlantic) clade XXI and the Pacific species *S. vitiensis* is included in clade XIX. Furthermore, the genus *Blastomussa* is highly divergent from the remainder of the Mussidae and is in clade XIV (Fukami et al., 2008; Kitahara et al., 2010). However, to date the phylogenetic relationships among Pacific mussids have not been investigated from a more detailed and exhaustive molecular point of view, and the phylogeny of several taxa needs to be addressed.

Among the faviids, the genera *Oulastrea*, *Leptastrea*, *Solenastrea*, *Cladocora*, and *Plesiastrea* are highly divergent and not closely related to their confamilials (Fukami et al., 2008; Kitahara et al., 2010). The majority of the Pacific Faviidae is nested within the families Trachyphylliidae Verrill, 1901 and Merulinidae Verrill, 1866 and with the Pectiniidae genera *Pectinia* and *Mycedium* in clade XVII. This group of taxa is informally called “Bigmessidae” (Huang et al., 2011) due to its untidiness and species richness (Fukami et al., 2004a, 2008; Knowlton et al., 2008; Budd, 2009; Huang et al., 2009; Kitahara et al., 2010; Huang et al., 2011). Huang et al. (2011) published a robust molecular phylogeny of clade XVII based on two mitochondrial markers and three nuclear markers, thereby producing the most complete and resolved molecular work on the “Bigmessidae” to date. Within clade XVII, Huang et al. (2011) detected eight well-supported genus-level subclades, which were substantiated by morphologic differences in the corallite wall structures and in the arrangement and distinctiveness of centers of rapid accretion (Budd and Stolarski, 2011). They also showed that the species *Moseleya latistellata* and *Montastraea multipunctata*, which chronologically were the last taxa investigated, do not cluster into clade XVII. This finding suggests that other as yet unstudied species or genera of Faviidae may be highly divergent and that more detailed studies including as many species as possible from different localities may unveil more unexpected relationships. Indeed, much remains unknown in terms of species boundaries and taxon validity in this group of reef corals.

To date, only a fraction of the 176 currently recognised species belonging to the Faviidae and Mussidae (Veron, 2000) have been investigated. Moreover, the main phylogenetic studies of the Faviidae and Mussidae (Fukami et al., 2004a, 2008; Nunes et al., 2008; Huang et al., 2009, 2011) have been conducted on material from the Atlantic and the Pacific Ocean (PO). Taxa and populations from the Indian Ocean (IO) remain largely unstudied (Fig. 2.1). A total of 124 species in the IO await molecular analyses and taxonomic re-evaluation. Among these, 10 are known only from the Red Sea and 13 from the IO, whereas 101 are also found in the PO. At the genus level, *Erythrastrea* and *Parasimplastrea*, which are ascribed

to the Faviidae and are known only from the IO, have never been studied. The only IO species analysed so far is *Plesiastrea devantieri* (Benzoni et al., 2011), and morphologic and molecular data suggest that the species actually does not belong to the genus *Plesiastrea*.

In this study, 90 specimens representing 14 genera and 27 species of Faviidae and Mussidae were collected from the IO and the PO. *Acanthastrea maxima*, *Favites peresi*, *Parasimplastrea omanensis*, *Plesiastrea bottae*, and *Blastomussa merleti* were included in a molecular phylogenetic study for the first time. While *L. bottae* and *B. merleti* are also found in the PO, the others are taxa typical or endemic to the Gulf of Aden and of the Arabian Sea. IO samples of the other 21 Indo-Pacific species had only been examined from the PO prior to this study. COI and rDNA were sequenced to infer phylogeny of the Robust clade. The phylogenetic relationships between newly studied taxa and the “Bigmessidae” already examined in the literature and between species inhabiting both the IO and PO are discussed in light of the coral polyps and skeleton morphology.

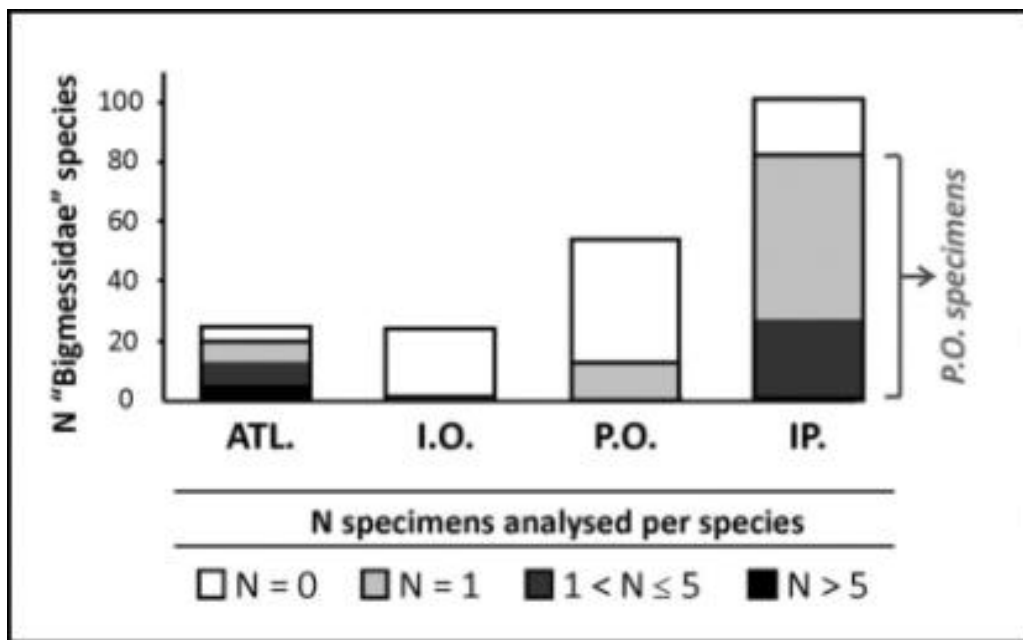


Figure 2.1. Number of “Bigmessidae” species currently known to have an Atlantic Ocean (ATL), Indian Ocean (IO), Pacific Ocean (PO), or Indo-Pacific (IP) distribution based on Veron’s (2000) distribution maps. For each column the white area represents the number species for which no published molecular phylogeny is available (October 2011), the light

grey area the species for which the published phylogeny is currently based on one specimen, the dark grey area the species for which the phylogeny is based on two to five specimens, and the black area the species for which more than five samples have been analyzed (data from Fukami et al., 2007, 2008; Nunes et al., 2008; Kitahara et al., 2010; Huang et al., 2011; Benzoni et al., 2011). Note that for all species with IP distribution only material from P.O. was studied in the examined molecular phylogenies (cf Fig. 2.2).

2.3 Material and methods

2.3.1 Sampling and specimen identification

96 specimens of scleractinian corals were collected from different sites in the southern Red Sea, the Gulf of Aden, Mayotte Island and New Caledonia (App. 2.1) (Table 2.1).

Corals were photographed in situ with an underwater Canon Powershot A720 digital camera in an Ikelite housing prior to collection (App. 2.2). For each sampled colony, 2 cm² of living tissue were fixed in 100% ethanol for molecular analyses, and a fragment of at least 10 cm² was bleached in sodium hypochlorite for 24 h, rinsed with freshwater, and air-dried for morphological analysis. In the laboratory, specimens were identified at the species level based on skeletal morphology using a Zeiss Stemi DV4 stereo-microscope following Wijsman-Best (1976), Wijsman-Best (1977), Veron et al. (1977), Veron and Pichon (1980), Sheppard and Sheppard (1991), and Veron (2000, 2002). Images of the skeletons were taken with a Canon G9 digital camera (App. 2.2).

Table 2.1. List of analyzed specimens. Y = Balhaf (Gulf of Aden, Yemen); BA = Bir Ali (Gulf of Aden, Yemen); AD= Aden (Gulf of Aden, Yemen); BU = Burum (Gulf of Aden, Yemen); MU and FP = Al Mukallah (Gulf of Aden, Yemen); SO = Socotra Island (Indian Ocean, Yemen); MA = Mayotte Island (Indian Ocean, France); KA = Kamaran Island (Red Sea, Yemen); SO = Socotra Island (Gulf of Aden Yemen); NC and HS = Côte Oubliée (New Caledonia).

Specimen code	Family	Species	COI	rDNA
Y715	Faviidae	<i>Cyphastrea microphthalma</i>	HE654555	HE648471
BA007	Faviidae	<i>Cyphastrea microphthalma</i>	HE654556	HE648472
BA035	Faviidae	<i>Cyphastrea microphthalma</i>	HE654557	HE648473
BA080	Faviidae	<i>Cyphastrea microphthalma</i>	HE654558	HE648474
Y713	Faviidae	<i>Cyphastrea serailia</i>	HE654559	HE648475
Y714	Faviidae	<i>Cyphastrea serailia</i>	HE654560	HE648476
Y727	Faviidae	<i>Echinopora gemmacea</i>	HE654561	HE648477
BA041	Faviidae	<i>Echinopora gemmacea</i>	HE654562	HE648478
AD029	Faviidae	<i>Favia fавus</i>	HE654563	HE648479
BA101	Faviidae	<i>Favia matthaii</i>	HE654564	HE648480
BU040	Faviidae	<i>Favia matthaii</i>	HE654565	HE648481
BA082	Faviidae	<i>Favia matthaii</i>	HE654566	HE648482
BA049	Faviidae	<i>Favia pallid</i>	HE654567	HE648483
BA050	Faviidae	<i>Favia pallid</i>	HE654568	HE648484
BA061	Faviidae	<i>Favia pallid</i>	HE654569	HE648485
BA067	Faviidae	<i>Favia pallid</i>	HE654570	HE648486
BA105	Faviidae	<i>Favia pallid</i>	HE654571	HE648487
BA119	Faviidae	<i>Favia pallid</i>	HE654572	HE648488
Y728	Faviidae	<i>Favia pallid</i>	HE654573	HE648489
BA065	Faviidae	<i>Favia rotumana</i>	HE654574	HE648490
BA083	Faviidae	<i>Favia rotumana</i>	HE654575	HE648491
BA141	Faviidae	<i>Favia rotumana</i>	HE654576	HE648492
BA048	Faviidae	<i>Favia rotumana</i>	HE654577	HE648493
BA069	Faviidae	<i>Favia rotumana</i>	HE654578	HE648494
BA086	Faviidae	<i>Favia rotumana</i>	HE654579	HE648495
BA112	Faviidae	<i>Favia rotumana</i>	HE654580	HE648496
MU195	Faviidae	<i>Favia cf rotumana</i>	HE654581	HE648497
BA143	Faviidae	<i>Favites abdita</i>	HE654582	HE648498
BA046	Faviidae	<i>Favites complanata</i>	HE654583	HE648499
BA125	Faviidae	<i>Favites complanata</i>	HE654584	HE648500
MU173	Faviidae	<i>Favites complanata</i>	HE654585	HE648501
MU194	Faviidae	<i>Favites complanata</i>	HE654586	HE648502
BA146	Faviidae	<i>Favites halicora</i>	HE654587	HE648503
BA047	Faviidae	<i>Favites halicora</i>	HE654588	HE648504
BA063	Faviidae	<i>Favites halicora</i>	HE654589	HE648505
BA084	Faviidae	<i>Favites halicora</i>	HE654590	HE648506
BA085	Faviidae	<i>Favites halicora</i>	HE654591	HE648507
BA144	Faviidae	<i>Favites halicora</i>	HE654592	HE648508
BA008	Faviidae	<i>Favites pentagona</i>	HE654593	HE648509
AD005	Faviidae	<i>Favites pentagona</i>	HE654594	HE648510
BA026	Faviidae	<i>Favites pentagona</i>	HE654595	HE648511
BA030	Faviidae	<i>Favites pentagona</i>	HE654596	HE648512
AD051	Faviidae	<i>Favites pentagona</i>	HE654597	HE648513
BA042	Faviidae	<i>Favites peresi</i>	HE654598	HE648514
BA054	Faviidae	<i>Favites peresi</i>	HE654599	HE648515

BA147	Faviidae	<i>Favites peresi</i>	HE654600	HE648516
Y751	Faviidae	<i>Leptastrea bottae</i>	HE654601	HE648517
BA044	Faviidae	<i>Leptastrea bottae</i>	HE654602	HE648518
BA079	Faviidae	<i>Leptastrea bottae</i>	HE654603	HE648519
BA111	Faviidae	<i>Leptastrea bottae</i>	HE654604	HE648520
BA068	Faviidae	<i>Leptastrea pruinosa</i>	HE654605	HE648521
BA081	Faviidae	<i>Leptastrea pruinosa</i>	HE654606	HE648522
BA103	Faviidae	<i>Leptastrea pruinosa</i>	HE654607	HE648523
BA127	Faviidae	<i>Leptastrea pruinosa</i>	HE654608	HE648524
BA131	Faviidae	<i>Leptastrea pruinosa</i>	HE654609	HE648525
Y716	Faviidae	<i>Leptastrea transversa</i>	HE654610	HE648526
BA004	Faviidae	<i>Leptoria phrygia</i>	HE654611	HE648527
MU094	Faviidae	<i>Parasimplastrea omanensis</i>	HE654612	HE648528
MU160	Faviidae	<i>Parasimplastrea omanensis</i>	HE654613	HE648529
MU205	Faviidae	<i>Parasimplastrea omanensis</i>	HE654614	HE648530
Y571	Faviidae	<i>Parasimplastrea omanensis</i>	HE654615	HE648531
BA005	Faviidae	<i>Platygyra daedalea</i>	HE654616	HE648532
BA045	Faviidae	<i>Platygyra daedalea</i>	HE654617	HE648533
BA059	Faviidae	<i>Platygyra daedalea</i>	HE654618	HE648534
BA075	Faviidae	<i>Platygyra daedalea</i>	HE654619	HE648535
BA051	Merulinidae	<i>Hydnophora exesa</i>	HE654620	HE648536
AD026	Merulinidae	<i>Hydnophora exesa</i>	HE654621	HE648537
AD056	Merulinidae	<i>Hydnophora exesa</i>	HE654622	HE648538
BA043	Mussidae	<i>Acanthastrea echinata</i>	HE654623	HE648539
BA115	Mussidae	<i>Acanthastrea echinata</i>	HE654624	HE648540
MA433	Mussidae	<i>Acanthastrea echinata</i>	HE654625	HE648541
BA136	Mussidae	<i>Acanthastrea maxima</i>	HE654626	HE648542
MU161	Mussidae	<i>Acanthastrea maxima</i>	HE654627	HE648543
MU163	Mussidae	<i>Acanthastrea maxima</i>	HE654628	HE648544
NC593	Mussidae	<i>Blastomussa merleti</i>	HE654629	HE648545
NC672	Mussidae	<i>Blastomussa merleti</i>	HE654630	HE648546
MU093	Mussidae	<i>Blastomussa merleti</i>	HE654631	HE648547
BA142	Mussidae	<i>Blastomussa merleti</i>	HE654632	HE648548
BU000	Mussidae	<i>Blastomussa merleti</i>	HE654633	HE648549
HS2630	Mussidae	<i>Blastomussa wellsi</i>	HE654634	HE648550
HS2681	Mussidae	<i>Blastomussa wellsi</i>	HE654635	HE648551
NC674	Mussidae	<i>Cynarina lacrymalis</i>	HE654636	HE648552
MA434	Mussidae	<i>Lobophyllia cf corymbosa</i>	HE654637	HE648553
AD003	Mussidae	<i>Lobophyllia corymbosa</i>	HE654638	HE648554
BA134	Mussidae	<i>Lobophyllia hemprichii</i>	HE654639	HE648555
MU202	Mussidae	<i>Lobophyllia hemprichii</i>	HE654640	HE648556
MU215	Mussidae	<i>Micromussa amakusensis</i>	HE654641	HE648557
FP	Mussidae	<i>Micromussa amakusensis</i>	HE654642	HE648558
BA117	Mussidae	<i>Micromussa amakusensis</i>	HE654643	HE648559
BA107	Mussidae	<i>Symphyllia radians</i>	HE654644	HE648560
BU033	Mussidae	<i>Symphyllia radians</i>	HE654645	HE648561
BU046	Mussidae	<i>Symphyllia radians</i>	HE654646	HE648562
MU204	Mussidae	<i>Symphyllia radians</i>	HE654647	HE648563
BA001	Pectiniidae	<i>Echinophyllia aspera</i>	HE654648	HE648564
KA079	Euphyllidae	<i>Plerogyra sinuosa</i>	HE654649	HE648565
SO038	Euphyllidae	<i>Plerogyra sinuosa</i>	HE654650	HE648566

2.3.2 DNA extraction, PCR amplification, and sequencing

Fixed coral tissue was scraped from the sample surface, and total DNA was extracted using DNAeasy® Tissue kit (Quiagen Inc., Valencia, CA, USA) according to the manufacturer's protocol.

Two different molecular markers were amplified: 1) a ~750 bp portion of mitochondrial COI and 2) a ~800 bp region of rDNA including the entire gene 5.8S and spacer regions ITS1 and ITS2 and a part of coding regions 18S and 28S. The utility of rDNA as a reliable marker for phylogenetic inferences was first questioned by Vollmer and Palumbi (2004) due to the presence in *Acropora* of elevated intraindividual and intraspecific variation and the retention of ancient lineages predating the origin of species (van Oppen et al., 2002a). Conversely the extremely high diversity of rDNA is typical of *Acropora* (Wei et al., 2006) that shows several atypical features different from other corals as the shortest ITS among metazoans (Odorico and Miller, 1997) and a unique secondary structure (Chen et al., 2004). Moreover the presence of rDNA pseudogenes, demonstrated for *Acropora* (Marquez et al., 2003), represents an exception in Scleractinia genera rather than a common rule (Chen et al., 2004; Wei et al., 2006). Consequently, the utility of rDNA marker in phylogenetic analysis of genera other than *Acropora* is currently accepted. The first locus was amplified using scleractinian-specific primers MCOIF and MCOIR and the protocols outlined in Fukami et al. (2004b). The coral-specific primer A18S (Takabayashi et al., 1998) and the universal primer ITS4 (White et al., 1990) were used to amplify the fragment of the rDNA following Benzoni et al. (2010). All sequences generated from this study were deposited with EMBL, and accession numbers are provided in Table 2.1.

2.3.3 Phylogenetic analyses

Electropherograms were checked and sequences were edited using CodonCodeAligner (version 3.7.0, Codon Code Corporation, Dedham, MA, USA). *Galaxea fascicularis* (Complex clade) was selected as the outgroup based on

previously published molecular data (Romani and Palumbi, 1996, 1997; Romano and Cairns, 2000; Chen et al., 2002; Le Goff-Vitry et al., 2004; Fukami et al., 2008), and other representatives of Faviidae and Mussidae were included (Fukami et al., 2008; Huang et al., 2009, 2011).

The two independent loci were concatenated in a partitioned dataset of 201 specimens in order to achieve a sub-genus level of phylogenetic resolution. The sequences were aligned using ClustalX (version 2.0, Thompson et al., 1997) with default parameters, and the alignments were refined manually using BioEdit (version 7.0.9.1, Hall, 1999). The BaseFreq option implemented in PAUP* (version 4.0.b.10, Swofford, 2003) was used to test homogeneity of base frequencies across taxa because compositional bias may provide a misleading signal in phylogenetic reconstruction involving many different taxa (Lyons-Weiler and Hoelzer, 1999). Indels, invariable and parsimony informative sites were detected using DnaSP (version 5.10.01, Librado and Rozas, 2009). Indels were treated as a fifth character in phylogenetic analyses.

A phylogenetic reconstruction by Bayesian inference (BI) was conducted using MrBayes (version 3.1.2, Huelsenbeck and Ronquist, 2001), by maximum likelihood (ML) using PhyML (version 3.0, Guindon and Gascuel, 2003), and by maximum parsimony (MP) using PAUP* (version 4.0.b.10, Swofford, 2003). Testing of the evolutionary model that best fit the data was conducted with MODELTEST (version 3.7, Posada and Crandall, 1998) using the Akaike information criterion based on the concatenated alignment. The general time reversible model (GTR) + invariable sites + gamma ($P_{inv} = 0.3811$, $\alpha = 0.6797$) was selected for both BI and ML analyses. BI was performed with four Markov chains run simultaneously for 5,000,000 generations, with trees sampled every 100 generations for a total of 50,000 saved trees and a burn-in to 20%; clade support was assessed based on posterior probability. A suitable burn-in and the convergence were established using Tracer (version 1.5, Drummond and Rambaut, 2007). For MP, a heuristic search was performed using starting trees obtained by random stepwise addition with 10 replicates and the tree bisection-reconnection (TBR)

branch-swapping-algorithm generating a strict consensus tree. Five hundred bootstrap replicates were used to verify the robustness of the internal branches of the tree. ML analysis used the default parameters of PhyML and the Shimodaira and Hasegawa (SH-like) test to check the nodes supports (Anisimova and Gascuel, 2006).

We also conducted a MP analysis for each separate locus. Parsimony searches were conducted in PAUP* using a heuristic search with 10 independent repetitions of random sequence addition and the TBR method of branch swapping. A strict consensus tree was calculated based on the set of the most parsimonious trees. Branch support was estimated using 500 bootstrap replicates.

2.4 Results

2.4.1 Sequence data characteristics

rDNA and COI sequences were obtained for each of the 96 coral specimens analysed in this study. rDNA chromatograms did not show high intra-individual polymorphisms, thereby avoiding the need to clone the amplified fragments. The sequences were aligned with 105 other specimens for which both COI and rDNA sequences were available in GenBank. In the case of *Goniastrea favulus* (HQ203358), *Goniastrea pectinata* (HQ203360), *Montastraea cf. annuligera* (HQ203369), *Platygyra acuta* (HQ203386), and *Platygyra contorta* (HQ203387), for which only rDNA sequences are published in GenBank, COI sequences of the most related congeneric species based on Huang et al. (2011) were used to infer phylogeny.

The aligned partial COI sequences consisted of 609 nucleotide sites, 197 (32%) of which were variable and 181 (30%) of which were parsimony informative. The aligned rDNA sequences comprised 991 positions, 664 (67%) of which were polymorphic, 589 (59%) of which were parsimony informative, and 555 of which were indels. The rDNA exhibited a high GC content (C = 29.7%, G = 26.5%, A = 22.4%, T = 21.4%), whereas the COI gene had a higher AT content than GC

percentage (A = 21.5%, T = 41.2%, C = 16.4%, G = 20.9%). Despite the differences in AT/GC contents between these two loci, the test of homogeneity of base composition did not detect significant differences across taxa. The p values were 1.00 for the two independent loci and for the combined data (for COI $\chi^2 = 51.57$ df = 597, for rDNA $\chi^2 = 307.96$ df = 597, all genetic data $\chi^2 = 243.98$ df = 597).

2.4.2 Phylogenetic analyses

COI and rDNA regions were combined to maximize the total numbers of characters for phylogenetic analyses. Generally, MP topology was less resolved than, but not contrasting with, the model-based methods (BI and ML). These latter phylogenetic reconstructions recovered trees with very similar topologies. Only the BI phylogram with branch support indicated by Bayesian posterior probability scores (Pp), Sh like-support (Ss), and MP bootstrapping support (Bs) is shown (Fig. 2.2). When using the terms clade and subclade hereafter, we refer to the main groups found and defined by Fukami et al. (2008) and Huang et al. (2011), respectively.

Clades XI, XIV, and XXI are resolved and very well supported (Pp = 99–100 and Ss = 89–98). *Oulastrea crispata* remains highly divergent from clade XI. The genus *Leptastrea* is divergent from clade XVII, and its monophyly is well supported (Pp = 100, Ss = 97, Bs = 100), as is also true in previously published phylogenies (Fukami et al., 2008; Kitahara et al., 2010). The IO faviid genus *Parasimplastrea* is closely related to species present in the mussid genus *Blastomussa*, which is monophyletic within clade XIV. Clades XV (*Diploastrea heliopora*) and XVI (*Montastraea cavernosa*), which are two highly divergent species found near the base of the Robust clade (Fukami et al., 2008; Kitahara et al., 2010), form a well-supported clade (Pp = 100, Ss = 98, Bs = 99) that is in agreement with the five-loci phylogeny proposed by Huang et al. (2011). Clade XVII is partially resolved: subclades XVII-C and XVII-I constitute a separate group, while the remaining subclades generate a monophyletic group.

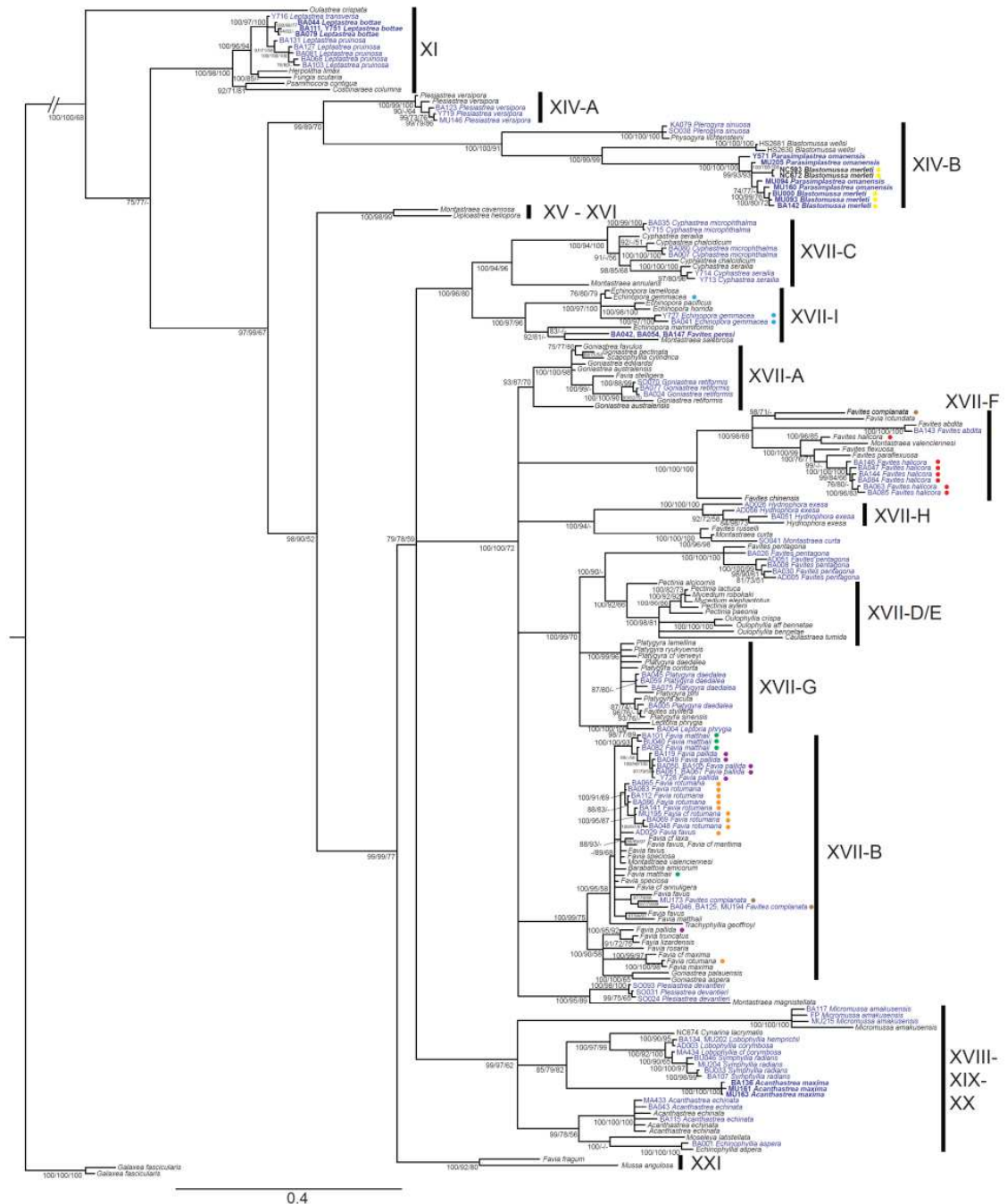


Figure 2.2. Bayesian tree of the combined rDNA and COI datasets. Posterior Bayesian probabilities (>70%), Sh-like support (>70%) and bootstrap values (>50%) are shown at nodes in the following order: BI, ML and MP. Dashes (-) indicate nodes that are statistically unsupported. Clade numbers and sub-clade codes are the same ones reported respectively by Fukami et al. (2008) and Huang et al. (2011). Species included for the first time in a molecular study are indicated in bold. IO samples are evidenced in blue and PO samples in black. Species with divergence between IO and PO populations are indicated with full circles: yellow circles = *Blastomussa merleti*; blue circles = *Echinopora gemmacea*; brown circles = *Favites complanata*; red circles = *Favites halicora*; green circles = *Favia matthaii*; purple circles = *Favia pallida*; orange circles = *Favia rotumana*.

These results are consistent with individually rDNA tree presented by Huang et al. (2011), but not with their combined five-gene phylogeny, which recovered clade XVII as a well-supported group conversely. Within subclade XVII-I, *Favites peresi* is closely related to *Echinopora mammiformis* and *Montastraea salebrosa*, which are the basal species of this subclade. Subclades XVII-A, XVII-B, XVII-C, XVII-D/E, XVII-H, and XVII-I are recovered and well supported. Subclades XVII-F and XVII-G are partially unresolved due to the divergence of their basal species, *Montastraea magnistellata* and *Leptoria phrygia*, respectively. The monophyly of clade XVIII-XIX-XX is supported in all of the analyses (Pp = 99, Ss = 97, Bs = 62); this is in contrast to the mitochondrial phylogeny proposed by Fukami et al. (2008) in which the Pacific mussids (with the exception of *Blastomussa*) and some of the pectiniids (*Echinophyllia* and *Oxypora*) are split into three clades. The IO species *Acanthastrea maxima* is included in this group but it is highly divergent within it.

Overall, most sequences from the IO populations of each species form monophyletic clades with moderate node supports. The only exceptions are the polyphyletic *Blastomussa merleti*, *Parasimplastrea omanensis*, *Cyphastrea microphthalma*, and *Platygyra daedalea*. Nevertheless, although the monophyly of IO clades is strongly supported at the species level in the combined tree, a paraphyletic or polyphyletic species status is detected when sequences from both the IO and the PO are analysed jointly. Indeed, 8 of 18 species represented by specimens from both the IO and the PO (*i.e.* *Cyphastrea serailia*, *Echinopora gemmacea*, *Favia favius*, *F. matthaii*, *F. pallida*, *F. rotumana*, *Favites halicora*, *F. complanata*) are not monophyletic on the base of concatenated COI and rDNA.

Individual MP analyses of COI and rDNA revealed general congruence in the phylogenetic signal. No substantial discordances or general patterns of conflict (Apps. 2.3-2.4).

2.5 Discussion

2.5.1 New contributions to the phylogeny of Faviidae and Mussidae

The genus *Leptastrea* is highly divergent from clade VXII (Fig. 2.2), and it is included in clade XI with the fungiids and most of the siderastreids (Romano and Palumbi, 1996, 1997; Romano and Cairns, 2000; Le Goff-Vitry et al., 2004; Fukami et al., 2008; Kitahara et al., 2010). In this case, both nuclear and mitochondrial phylogenies (Apps. 2.3-2.4) recover three species of *Leptastrea* in clade XI. Therefore, its classification within the family Faviidae is not supported by phylogeny, and further micromorphological and microstructural analyses must be conducted to discover new characters consistent with Fungiidae and inconsistent with Faviidae, if any. While the genus placement at the family level needs to be reexamined, *Leptastrea* as a genus is strongly supported monophyletic, and it is also distinct on the basis of morphological evidence. Even at the species level, *L. bottae* and *L. pruinosa* are also monophyletic, notwithstanding the high within-species morphological variability. Unfortunately, *L. transversa* is represented by only one specimen, and it is divergent from the remainder of the congeners examined.

The monotypic genus *Parasimplastrea* is known to occur only in the Gulf of Aden (Pichon et al., 2010), the Arabian Sea (Claereboudt, 2006), and from Mauritius (Moothien Pillai et al., 2002). *Parasimplastrea omanensis* from Oman was first described by Sheppard in 1985. Its generic name refers to the superficial morphological affinity with the genus *Simplastrea* Umbgrove, 1939 (Sheppard and Salm, 1988; Coles, 1996). The species was then renamed *Parasimplastrea sheppardi*, which was a questionable taxonomic decision, and moved from the Oculinidae to the Faviidae because of the occasional presence of thickened septa and rudimentary columellae (Veron, 2000). In fact, *P. omanensis* is highly divergent from clade XVII and other faviids, and it has no evolutionary relationships with the Oculinidae. Moreover, *P. omanensis* is closely related to the genus *Blastomussa* and especially to *B. merleti*, the type species of this genus.

These two species are genetically indistinguishable using rDNA and COI and, despite a cerioid vs. phaceloid arrangement, they are morphologically similar, though well distinct, both in terms of polyp and of corallite morphology (App. 2.2). If further analyses based on a larger geographical sample confirm this close relationship, the genus *Parasimplastrea* will have to be formally synonymised with the genus *Blastomussa*. *Blastomussa wellsi* is related but distinct from *B. merleti* and *P. omanensis*, thereby highlighting a strongly supported monophyly for this genus.

Acanthastrea maxima is a small sized and relatively uncommon coral species presently known only from the Gulf of Aden (DeVantier et al., 2004; Pichon et al., 2010), the Arabian Sea (Sheppard and Salm, 1988), and the Persian Gulf (Hodgson and Carpenter, 1995). *Acanthastrea maxima* shows the typical Pacific mussid skeletal morphology (sensu Budd and Stolarski, 2009) (App. 2.2) and, not surprisingly, it is in clade XVIII-XIX-XX together with the other PO Mussidae. Nevertheless, it has no close relationships with *A. echinata* and, more interestingly, it is highly distinct within the clade itself. Therefore, most of the approaches traditionally used to infer evolutionary distinctiveness may be powerful for this species (Cadotte and Davies, 2010), and coupling this with its restricted IO distribution suggests that it might be a case of priority for future coral species conservation strategies.

Favites peresi is a relatively common species recorded throughout the IO, from the Red Sea to Madagascar, but it is absent in the PO (Veron, 2000). Faure and Pichon (1978) and Scheer and Pillai (1983) described this species as *Favites* on the basis of, inter alia, septa of equal width throughout their length. However, Veron (2000) moved it to the genus *Goniastrea* on the basis of the crown of well-developed paliform lobes typically observed in this genus. Molecular results show that *F. peresi* is in subclade XVII-I, which includes all *Echinopora* species analysed so far from a molecular point of view and *Montastraea salebrosa*. Thus, *F. peresi* has no close phylogenetic relationship either with either genera *Favites* or *Goniastrea*. Therefore, its taxonomy needs to undergo a formal revision. However,

this revision might have to wait until all of the “Bigmessidae” are examined in one phylogeny, as more unexpected phylogenetic relationships could be unveiled as the taxa still to be examined are dealt with.

2.5.2. Within species divergences between Indian and Pacific Ocean populations

Some cases of evolutionary divergence between IO and PO populations were unveiled when we compared our IO sequences with other PO sequences (Fukami et al., 2008; Huang et al. 2009, 2011) of coral species with Indo-Pacific distribution (Table 2.2). The most striking case of divergence is that of *Favites complanata* (Fig. 2.2). The sample from Singapore is in subclade XVII-F, which includes most of the *Favites* species and the type species of the genus *Favites abdita*, whereas the IO specimens are nested within subclade XVII-B, which is a group consisting mainly of *Favia* spp.. This odd situation could be explained either by an incorrect identification of the examined material or by a morphological convergences.

Although misidentification may occur in *Favites* at the species level due to the lack of a formal revision and to the striking morphological similarity between certain taxa, misidentification is highly unlikely at the genus level. In fact, despite the well-known and documented morphologic plasticity in scleractinian corals (Todd, 2008), species typically characterized by a cerioid corallite arrangement, like *Favites* spp., do not develop the coenosteum found in plocoid taxa (e.g., *Favia* spp.). Conversely, it is not uncommon in some *Favia* species to observe a tendency towards a fusion of the corallite walls (Fig. 2.3).

This being said, the specimens identified in this study as *F. complanata* have fused corallite walls in the whole corallum (App. 2.2). We cannot exclude the possibility that the material we identified as *F. complanata* may belong to another species previously described under another name and later synonymised with *F. complanata* itself or with other species (e.g., *F. acuticollis* Ortmann, 1889 later synonymised with *F. chinensis* Verrill, 1866) or, even, of a new species morphologically similar to *F. complanata*. In the latter case the two morphs could

have undergone morphological convergence that led to this taxonomic confusion. Several examples of traditional morphological characters plagued by convergence have been found in the family Faviidae (Fukami et al., 2004a, 2008; Huang et al., 2009, 2011; Budd and Stolarski, 2011). Formal taxonomic revision of the genus, including study of the type material of the described species and collected specimens, is needed to determine the actual identity of this puzzling population of *F. complanata*.

Another phenomenon which might possibly explain this pattern is cryptic genetic divergence. However, it is unlikely because of the highly relevant and atypical amount of divergence between the two presumed cryptic lineages with respect to other cases of documented cryptic speciation (Souter, 2010 for *Pocillopora damicornis* within the IO; Stefani et al., 2011 for *Stylophora pistillata* between the IO and PO; Huang et al., 2011 for *Goniastrea australensis* between Australia and Singapore).

Numerous instances of more or less marked divergence between IO and PO specimens of the same species were detected for *Blastomussa merleti*, *Cyphastrea serailia*, *Echinopora gemmacea*, *Favites halicora*, *Favia favius*, *F. pallida*, *F. matthaii*, and *F. rotumana*. In the case of *B. merleti*, the molecular distinction between IO and PO specimens also is supported, to a certain extent, by morphology. The specimens sampled in the species type locality, New Caledonia, show typically phaceloid growth in which corallite walls are never joined and, overall, corallite diameter is smaller than that in the IO specimens. These, in turn, display a tendency towards a cerioid corallite arrangement in some, but not all, parts of the corallum and a larger corallite diameter. The variability in coral species morphology across large distribution ranges was discussed by Veron (1995), who introduced the concept of “geographic subspecies” of scleractinian corals. In our case, however, the co-occurrence of genetic and at least partial morphologic divergence would suggest that the species so far identified as *B. merleti* in the IO could actually be a new species rather than a geographic sub-species of this taxon. It could be argued that given the strong genetic affinities between the IO *B. merleti*

and *Parasimplastrea omanensis* and the fact that the latter is typically cerioid, the examined specimens assigned to the former could in fact be specimens of *P. omanensis* with aberrant corallite organization. However, the morphology of the living polyps remains markedly distinct between the two species, even in case of specimens with partial fusion of the corallite walls (App. 2.2), and *P. omanensis* has consistently fewer septa (App. 2.2).

For each of the four *Favia* species analysed in this study, the IO and PO samples did not cluster together. The IO samples of *F. rotumana* and *F. pallida* are recovered together in distinct clade but are evolutionary distinct from their PO conspecific samples (Fig. 2.2). A remarkable intraspecific morphological variation characterized the IO specimens of both species sampled for this study, especially in terms of the fusion of the corallite walls (Fig. 2.3B). In fact, while *Favia* is typically cerioid and *Favites* plocoid, several specimens presented *Favia*-like and *Favites*-like morphology within the same colony (Fig. 2.3A-B). This finding provides more evidence that this character is not a phylogenetically informative one at either the genus or the species level. Finally, a remarkable case of interspecific morphologic plasticity among the *Favia* species involves the IO samples of *F. pallida* and *F. matthaii*, which are two very closely related species as shown in the phylogeny and confirmed by their morphology (Fig. 2.3C-F). The IO specimens of these two species were recovered in two distinct and monophyletic clades, each distantly related from their conspecific PO population. However, they share many morphological features. While some specimens had intermediate morphology (Fig. 2.3D), others had part of the colony showing a typical *F. pallida* appearance and the other part typically looking like *F. matthaii* (Fig. 2.3F). This lack of well-defined morphological boundaries could be originated by interspecific hybridization (Willis et al., 2006), whose influence is increased by evidences of simultaneous mass spawning of many species of corals worldwide (Harrison et al., 1984; Baird et al., 2009). In particular five species of *Favia*, including *F. pallida* and *F. matthaii*, show a substantial overlap in spawning time and reproduction and a similar development of gametes in Thailand (Kongjandtre et al., 2010). These

observations suggest that beyond the now-proven polyphyletic status of most traditional families and genera and with more taxa awaiting study and more unexpected findings likely to emerge as more samples from multiple localities are studied together, species level issues are crucial to the study of the evolution and phylogeny of the scleractinian corals.

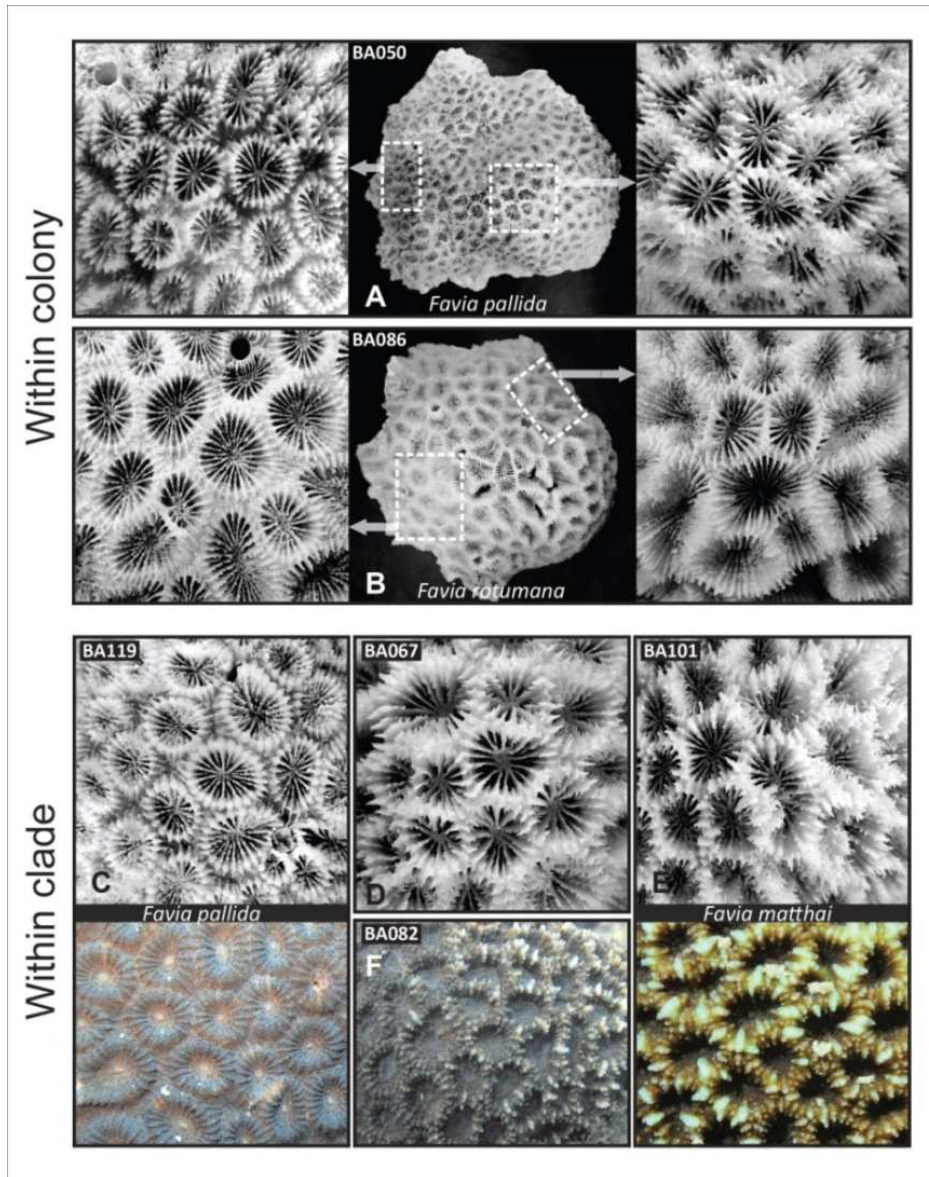


Figure 2.3. Within colony plasticity of the skeleton morphology in the genus *Favia*. A) colony of *Favia pallida* (BA050) and B) of *F. rotumana* (BA086) showing a typically plocoid (left) as well as sub-ceriod or ceriod (right) corallite arrangement within the same specimen, respectively. Within clade plasticity of *F. pallida* and *F. matthaii*, and intermediate morphs C) skeleton (above) and *in vivo* morphology (below) of a *F. pallida* colony (BA119), and D) skeleton morphology of a colony (BA067) of the same species and in the same clade (Fig. 2.2) but with more exert septa; E) skeleton (above) and *in vivo* morphology (below) of a *F. matthaii* colony (BA101) showing the typically exert septa in

this species; F) *in vivo* morphology of specimen BA082 displaying a *F. pallida* morphology of the left and a *F. matthaii* morphology on the right hand side of the image. This specimen was identified as *F. matthaii*, however, note its intermediate position in the phylogeny in Fig. 2.2.

Table 2.2. List of the taxa examined in this study. For each species the clade to which it is assigned and the traditional family are listed. If applicable, the divergence, or lack thereof, between Indian Ocean (IO) and Pacific Ocean (PO) material is indicated. Remarks on the main findings are listed. n.a. = not applicable; div. = divergence observed between IO and PO specimens; no div. = no divergence observed between IO and PO specimens. Species in bold were examined for the first time in this study. * indicates species for which IO populations are analysed for the first time in this study.

Clade	Taxon	Family	IO vs PO	Remarks
XI	<i>Leptastrea bottae</i> *	Faviidae	n.a.	monophyletic with the other species in the genus
XI	<i>Leptastrea pruinosa</i> *	Faviidae	n.a.	very high plasticity
XI	<i>Leptastrea transversa</i> *	Faviidae	n.a.	one specimen
XIV-A	<i>Plesiastrea versipora</i>	Faviidae	no div.	-
XIV-B	<i>Blastomussa merleti</i> *	Mussidae	div.	monophyletic with <i>B. Wellsi</i> and <i>B. omanensis</i>
XIV-B	<i>Blastomussa wellsii</i>	Mussidae	n.a.	monophyletic with but deeply divergent from <i>B. Merleti</i> and <i>B. omanensis</i>
XIV-B	<i>Parasimplastrea omanensis</i> *	Faviidae	n.a.	monophyletic and to be placed in synonymy with the genus <i>Blastomussa</i>
XVII-A	<i>Goniastrea retiformis</i>	Faviidae	no div.	-
XVII-B	<i>Favia favius</i> *	Faviidae	div.	one specimen
XVII-B	<i>Favia matthaii</i> *	Faviidae	div.	close to <i>F. pallida</i>
XVII-B	<i>Favia pallida</i> *	Faviidae	div.	close to <i>F. matthaii</i>
XVII-B	<i>Favia rotumana</i> *	Faviidae	div.	very high plasticity
XVII-B	<i>Favites complanata</i> *	Faviidae	div.	low plasticity
XVII-C	<i>Cyphastrea microphthalma</i> *	Faviidae	n.a.	no genetic boundaries for a well-defined morpho-species
XVII-C	<i>Cyphastrea serailia</i> *	Faviidae	div.	no genetic boundaries for a well-defined morpho-species
XVII-D/E	<i>Favites pentagona</i> *	Faviidae	no div.	-
XVII-F	<i>Favites abdita</i> *	Faviidae	no div.	one specimen
XVII-F	<i>Favites halicora</i> *	Faviidae	div.	-
XVII-G	<i>Leptoria phrygia</i>	Faviidae	no div.	one specimen
XVII-G	<i>Platygyra daedalea</i> *	Faviidae	no div.	no genetic boundaries for a well-defined morpho-species
XVII-H	<i>Hydnophora exesa</i> *	Merulinidae	no div.	-

XVII-I	<i>Echinopora gemmacea*</i>	Faviidae	div.	-
XVII-I	<i>Favites peresi*</i>	Faviidae	n.a.	neither close to <i>Goniastrea</i> nor to <i>Favites</i>
XVII	<i>Montastraea curta</i>	Faviidae	no div.	genetic affinity with <i>Montastraea curta</i> - one specimen
XVII	<i>Plesiastrea devantieri</i>	Faviidae	n.a.	affinity with <i>Montastraea magnistellata</i> not resolvable for the final taxonomic revision of this species
XVIII-XIX-XX	<i>Echinophyllia aspera*</i>	Pectiniidae	no div.	one specimen
XVIII-XIX-XX	<i>Acanthastrea echinata*</i>	Mussidae	no div.	-
XVIII-XIX-XX	<i>Acanthastrea maxima*</i>	Mussidae	n.a.	confirmed in the former Mussidae but evolutionarily distinct
XVIII-XIX-XX	<i>Cynarina lacrymalis</i>	Mussidae	n.a.	one specimen
XVIII-XIX-XX	<i>Lobophyllia corymbosa*</i>	Mussidae	n.a.	one specimen
XVIII-XIX-XX	<i>Lobophyllia hemprichii*</i>	Mussidae	n.a.	one specimen
XVIII-XIX-XX	<i>Micromussa amakusensis*</i>	Mussidae	no div.	-
XVIII-XIX-XX	<i>Symphyllia radians*</i>	Mussidae	n.a.	-

2.5.3 Molecular and phylogenetic implications

However, in the Anthozoa, COI is characterized by a lower rate of genetic variation, resulting in a phylogenetic resolution merely at higher systematic levels due to an insufficient intrageneric divergence (Shearer et al., 2002; Hellberg, 2006; Shearer and Coffroth, 2008; Huang et al., 2008). This molecular locus may constitute the basic backbone of a phylogeny when combined with hypervariable markers in order to build a more comprehensive phylogenetic tree of scleractinian corals. In this study, rDNA provided robust details about scleractinian coral evolution at different levels, from populations to genera (Chen et al., 2004; Forsman et al., 2006; Wei et al., 2006), and the information carried by COI compensated for the homoplasy traditionally associated with rDNA at the inner nodes.

The two-loci phylogeny proposed in this paper is consistent with those published by Fukami et al. (2008) based on mitochondrial COI and cytB and by Huang et al. (2011) using five markers (COI, rDNA, IGR, histone H3, and 28S). Regarding the “Bigmessidae”, the present phylogeny highlights how unstudied taxa might have unexpected relationships at different taxonomic levels and suggests that general conclusions are far from being definitive in modern coral taxonomy whenever the entire set of interrelated species of interest are not considered together in a comprehensive analysis. In the present study, some taxa ascribed to the Faviidae based on traditional skeletal characters and thus were expected to be in the “Bigmessidae” were found to be highly divergent and did not cluster in clade XVII. *Parasimplastrea omanensis* in this study and *Moseleya latistellata* and *Montastraea multipunctata* (Huang et al., 2011) are recent examples of these taxonomic misunderstandings. Moreover, other faviid groups within clade XVII were found to be not closely related to congeneric species or conspecific populations as expected based on traditional taxonomy. *Favites peresi* and IO specimens of *Favites complanata* illustrated this type of phylogenetic feature in relation to the other *Favites* species and the PO *F. complanata* population, respectively. Besides these unexpected evolutionary relationships, the “Bigmessidae” can be considered to be a well-defined group composed of eight subclades. Subclades are strongly supported by both molecular (Huang et al., 2011 and the present study) and micromorphological analyses (Budd and Stolarski, 2011). The inclusion into the analysis of species from the IO, a geographic area hitherto largely understudied, for which PO sequences are available does not involve any substantial change in the structure of the subclades.

The sister group of clade XVII is a monophyletic cluster that encompasses three different clades (XVIII, XIX, and XX) and this is the first time that this cohesive group is supported by a phylogenetic work. Trying to assign taxonomic units to these clades implies that they could be unified into a single lineage based on the combined COI and rDNA phylogeny, and this is also partially confirmed by the morphological analysis published by Budd and Stolarski (2009). Indeed,

Acanthastrea echinata (previously in clade XX) shares with other Indo-Pacific mussids (previously in clade XIX) most of the micromorphological and microstructural characters reported by Budd and Stolarski (2009), and the main difference between the two is the structure of the columella of *A. echinata*. Unfortunately, the authors did not evaluate *Micromussa* (clade XVIII), which exhibits a high molecular divergence within clade XVIII-XIX-XX.

Clade XIV, introduced by Fukami et al. (2008) on the basis of a small number of samples and species, was established in reason of the close phylogenetic relationships between *Plesiastrea versipora*, *Physogyra lichtensteini*, and *Blastomussa wellsi* regardless of the strong morphologic divergences between these taxa. Subsequently, Kitahara et al. (2010) added *Plerogyra* sp. and two non-reef-dwelling species, *Cyathelia axillaris* and *Trochocyathus efateensis*, to the clade. The present work shows for the first time that *Plerogyra sinuosa*, *Blastomussa merleti*, and *Parasimplastrea omanensis* are also nested within clade XIV. Thus, clade XIV is even more heterogeneous from the molecular, morphologic, taxonomic, and ecologic point of view. On the one hand, it is increasingly accepted (Kitahara et al. 2010; Benzoni et al., 2011) that clades including taxa with extremely different ecological traits and different taxonomic placement exist and that perhaps more will be discovered. However, on the other hand, an update of the status of this group is clearly needed, and a preliminary identification of two main subclades might help in reconstructing their evolutionary and taxonomic relationships. We suggest that subclade XIV-A, composed of *P. versipora*, *C. axillaris*, and *T. efateensis*, which are species with pali in front of each septal cycle before the last, a papillose columella, and well-developed costae (Kitahara et al., 2010; Benzoni et al., 2011), be formally separated from subclade XIV-B, which contains *B. wellsi*, *B. merleti*, and *P. omanensis* on the one hand and *Plerogyra lichtensteini*, *Physogyra sinuosa*, and *Pysogyra* sp. on the other hand, all of which are characterized by large and fleshy polyps.

Our results indicate that the taxonomy of the Faviidae and Mussidae is still unresolved, especially for those taxa not yet analysed phylogenetically, and confirm

that molecular approach is necessary for detecting the evolutionary lineages obscured by traditional taxonomy. However, it is also evident that the pending formal taxonomic decisions are necessary because clades and subclades cannot be used interchangeably with taxa. Their use in the specialized literature, together with the establishment of formally non-existent names such as the “Bigmessidae”, can only generate more confusion for the non-specialist, who is unavoidably left behind with outdated taxonomic references.

– CHAPTER 3 –

*Lobophylliidae (Cnidaria, Scleractinia) reshuffled: pervasive
non-monophyly at genus level*

Roberto Arrigoni¹, Tullia Isotta Terraneo¹, Paolo Galli^{1,2}, Francesca Benzoni^{1,3}

¹ Department of Biotechnologies and Biosciences, University of Milan – Bicocca, Piazza della Scienza 2, 20126, Milan, Italy

² MaRHE Center (Marine Research and High Education Center), Magoodhoo Island, Faafu Atoll, Maldives

³ Institut de Recherche pour le Développement, UMR227 CoReUs2, 101 Promenade Roger Laroque, 98848 Noumea, New Caledonia

Published in *Molecular Phylogenetics and Evolution*: 73, 60-64 (2014)

3.1 Abstract

The Indo-Pacific scleractinian coral family Lobophylliidae was recently described on the basis of molecular data and micromorphological and microstructural characters. We present the most comprehensive molecular phylogeny reconstruction of the family to date based on COI and rDNA including 9 genera and 32 species, 14 of which were investigated for the first time. The monophyly of the family is now strongly supported, with the inclusion of the genera *Acanthastrea* and *Micromussa*, whereas previously it was based on uncertain molecular relationships. Nevertheless, these and the other lobophylliid genera *Echinophyllia*, *Micromussa*, *Oxypora*, and *Symphyllia*, are not themselves monophyletic and need to be investigated from a morphological point of view. *Acanthastrea faviaformis* is nested within the family Merulinidae. This study highlights the need for further analyses at species level and of formal taxonomic actions.

3.2 Introduction

Molecular analyses have revolutionized our understanding of evolutionary relationships within the Scleractinia and shown that the order is subdivided into three clades (Robust, Complex, and Basal) instead of seven traditional suborders (Romano and Palumbi, 1996; Stolarski et al., 2011). Genetics have challenged the validity of most families and genera as traditionally described based on skeleton macromorphology (Fukami et al., 2004a, 2008; Benzoni et al., 2007, 2011, 2012a; Gittenberger et al., 2011; Huang et al., 2011; Arrigoni et al., 2012). In turn, unexpected molecular findings have prompted coral morphologists to search for new micromorphological and microstructural characters to corroborate molecular phylogenies (Benzoni et al., 2007; Budd and Stolarski, 2009, 2011; Kitahara et al., 2012a, 2012b). The combination of molecular and morphological research has led to taxonomic revisions of scleractinian corals at different levels and to the formal description of new taxa like, for example, three new families in the Robust clade:

the Lobophylliidae Dai and Horng, 2009, the Deltocyathiidae Kitahara et al, 2012, and the Coscinaraeidae Benzoni et al, 2012 (Budd et al., 2012; Kitahara et al., 2012a; Benzoni et al., 2012a).

The Indo-Pacific family Lobophylliidae currently comprises 12 extant genera (Budd et al., 2012) and 51 extant zooxanthellate species (Veron, 2000). All extant species are colonial with the exception of the solitary genera *Cynarina* Brüggemann, 1877 and *Homophyllia* Brüggemann, 1877 (Veron, 2000). The family is characterized by irregular lobate or bulbous teeth with elliptical tooth bases, rounded granules enveloped by extensive thickening deposits with vertical palisade-like structures between teeth, and differences in size/shape of teeth amongst septal cycles (Budd and Stolarski, 2009, Budd et al., 2012). Dai and Horng (2009) and Budd et al. (2012) grouped clades XVIII, XIX, and XX *sensu* Fukami et al. (2008) in a single lineage, thus defining the Lobophylliidae. Budd et al. (2012) anticipated, however, that further molecular analyses on *Acanthastrea* Milne Edwards & Haime, 1848 and *Micromussa* Veron, 2000, would be needed to assess their relationships within the family. Fukami et al. (2008) analyzed 17 Lobophylliidae species based on samples from the Pacific Ocean. Arrigoni et al. (2012) investigated 9 species adding Indian Ocean material (Obura, 2012) and confirmed for the first time the presence of a monophyletic cluster encompassing clades XVIII, XIX, and XX. To date, 30 species of Lobophylliidae, and the genera *Australomussa* Veron, 1985, and *Echinomorpha* Veron, 2000, have not been studied from a molecular point of view.

We present the most comprehensive molecular phylogeny of the Lobophylliidae so far, based on two loci, COI and nuclear rDNA, and widespread sampling in the Indo-Pacific, analyzing 9 genera and 32 species, including 14 that were not molecularly investigated before. The use of COI and rDNA allowed inference of the phylogeny at higher and lower systematic levels respectively, due to their different evolution rate (Hellberg, 2006; Wei et al., 2006; Gittemberg et al., 2011; Benzoni et al., 2012a).

3.3 Material and methods

Seventy coral colonies were sampled from different localities in the Indian and Pacific Ocean (Table 3.1). Each colony was photographed underwater and a fragment about 10 cm² area was collected, of which 2 cm² were preserved in absolute or 95% ethanol, or CHAOS solution (Sargent et al., 1986) (Apps. 3.1, 3.2). Samples were identified following Chevalier (1975), Veron and Pichon (1980), and Veron (2000), and illustrations of holotypes in their original descriptions.

Total DNA was extracted using DNAeasy® Tissue kit (Qiagen Inc., Valencia, CA, USA) for samples conserved in ethanol, and a phenol-chloroform based method for samples in CHAOS (Fukami et al., 2004b). The mitochondrial cytochrome *c* oxidase subunit I gene (COI, partially) and a selection of nuclear rDNA (the entire ITS1, 5.8S, ITS2 and a fragment of 18S and 28S) were investigated. COI and rDNA were amplified using respectively MCOIF - MCOIR primers (Fukami et al., 2004a) and ITS4 (Takabayashi et al., 1998) - A18S (White et al., 1990) primers and the protocol by Benzoni et al. (2011). All newly obtained sequences were deposited with EMBL (Table 3.1). The obtained rDNA electropherograms did not show any signal of intra-individual polymorphisms avoiding the need to clone rDNA (Wei et al., 2006).

A partition-homogeneity test was run in PAUP 4.0b10 (Swofford, 2003) to examine whether the sequences from the two loci should be combined in a single analysis. No conflicting phylogenetic signals between the datasets ($P = 0.95$) were detected and the two independent markers were concatenated in a partitioned dataset of 104 sequences. Sequences were aligned with ClustalW algorithm in BioEdit Sequence Alignment Editor 7.0.9.1 (Hall, 1999) and then manually checked. ITS1 and ITS2 regions were easy to align, with the exception of *A. maxima* Sheppard and Salm, 1988 due its high divergence within the family and the presence of repeated fragments, requiring more careful alignment. Maximum Parsimony (MP), Bayesian Inference (BI), and Maximum Likelihood (ML) were used to infer phylogeny of

the Lobophylliidae. MP analysis was conducted with PAUP 4.0b10 using heuristic searches and 500 bootstrap replicates. The GTR + I + G model was selected as an appropriate model of nucleotide substitution with MrModeltest2.3 (Nylander, 2004). BI analysis was run with MrBayes 3.1.2 (Ronquist and Huelsenbeck, 2003) using 9 million generations, saving a tree every 100 generations and discarding the first 22,500 trees as burn-in. ML analysis was performed with PhyML 3.0 (Guindon and Gascuel, 2003) using Shimodaira and Hasegawa test (SH-like) to check the support of each internal branch.

Table 3.1. List of the material examined in this study. For each specimen we list code, identification, family, sampling locality, COI and rDNA sequences used for the phylogenetic reconstructions. * indicates species analyzed for the first time from a molecular point of view. IRD = Institut de Recherche pour le Développement, Nouméa, New Caledonia; UNI = University of Milano – Bicocca, Milan, Italy; RMNH = Naturalis Biodiversity Center, former name of the present Rijksmuseum van Natuurlijke Historie, Leiden, the Netherlands. All the skeletons analyzed in this study are currently deposited at the University of Milano-Bicocca, Milan, Italy.

Code	Species	Locality	COI	rDNA
HS3285	<i>Acanthastrea bowerbanki</i> *	New Caledonia	HF954208	HF954295
HS3298	<i>Acanthastrea bowerbanki</i> *	New Caledonia	HF954209	HF954296
UNI DJ288	<i>Acanthastrea echinata</i>	Djibouti	HF954214	HF954301
HS3195	<i>Acanthastrea echinata</i>	New Caledonia	HF954213	HF954300
UNI MY211	<i>Acanthastrea echinata</i>	Mayotte	HF954215	HF954302
UNI BA115	<i>Acanthastrea echinata</i>	Gulf of Aden	HE654624	HE648540
HS3197	<i>Acanthastrea echinata</i>	New Caledonia	HF954217	HF954304
-	<i>Acanthastrea echinata</i>	Japan	AB117249	AB441401
HS3233	<i>Acanthastrea faviaformis</i> *	New Caledonia	HF954212	HF954299
HS3065	<i>Acanthastrea hemprichii</i> *	New Caledonia	HF954221	HF954309
HS3141	<i>Acanthastrea hemprichii</i> *	New Caledonia	HF954222	HF954310
HS3227	<i>Acanthastrea hemprichii</i> *	New Caledonia	HF954220	HF954308
HS3169	<i>Acanthastrea hillae</i>	New Caledonia	HF954206	HF954293
HS3225	<i>Acanthastrea hillae</i>	New Caledonia	HF954207	HF954294
HS3127	<i>Acanthastrea ishigakiensis</i> *	New Caledonia	HF954205	HF954292
UNI MU203	<i>Acanthastrea maxima</i>	Gulf of Aden	HF954210	HF954297
UNI S0132	<i>Acanthastrea maxima</i>	Socotra	HF954211	HF954298
UNI BA136	<i>Acanthastrea maxima</i>	Gulf of Aden	HE654626	HE648542
UNI MU161	<i>Acanthastrea maxima</i>	Gulf of Aden	HE654627	HE648543
UNI MU163	<i>Acanthastrea maxima</i>	Gulf of Aden	HE654628	HE648544
HS3166	<i>Acanthastrea rotundoflora</i>	New Caledonia	HF954216	HF954303
UNI PFB259	<i>Acanthastrea rotundoflora</i>	Papua New Guinea	HF954218	HF954305
UNI PFB260	<i>Acanthastrea rotundoflora</i>	Papua New Guinea	HF954238	HF954306
HS3228	<i>Acanthastrea subechinata</i> *	New Caledonia	HF954219	HF954307
HS1604	<i>Cynarina lacrymalis</i>	New Caledonia	HE654636	HE648552
UNI MY011	<i>Cynarina lacrymalis</i>	Mayotte	HF954201	HF954288
UNI DJ262	<i>Echinophyllia aspera</i>	Djibouti	HF954242	HF954329
HS2990	<i>Echinophyllia aspera</i>	New Caledonia	HF954245	HF954332

HS3224	<i>Echinophyllia aspera</i>	New Caledonia	HF954244	HF954331
UNI MU211	<i>Echinophyllia aspera</i>	Gulf of Aden	HF954243	HF954330
UNI BA001	<i>Echinophyllia aspera</i>	Gulf of Aden	HE654648	HE648564
-	<i>Echinophyllia aspera</i>	Palau	AB117252	AB441400
HS3171	<i>Echinophyllia echinata*</i>	New Caledonia	HF954232	HF954320
HS3179	<i>Echinophyllia echinata*</i>	New Caledonia	HF954233	HF954321
HS3278	<i>Echinophyllia echinata*</i>	New Caledonia	HF954234	HF954322
UNI M901	<i>Echinophyllia echinoporoides</i>	Maldives	HF954239	HF954326
UNI MY350	<i>Echinophyllia echinoporoides</i>	Mayotte	HF954237	HF954325
UNI PFB189	<i>Echinophyllia echinoporoides</i>	Papua New Guinea	HF954235	HF954323
UNI PFB379	<i>Echinophyllia echinoporoides</i>	Papua New Guinea	HF954236	HF954324
HS3248	<i>Echinophyllia orpheensis</i>	New Caledonia	HF954240	HF954327
UNI PFB200	<i>Echinophyllia orpheensis</i>	Papua New Guinea	HF954241	HF954328
UNI GA071	<i>Echinophyllia tarae*</i>	Gambier	HF954229	HF954317
UNI GA084	<i>Echinophyllia tarae*</i>	Gambier	HF954230	HF954318
UNI GA099	<i>Echinophyllia tarae*</i>	Gambier	HF954231	HF954319
UNI DJ120	<i>Lobophyllia corymbosa</i>	Djibouti	HF954255	HF954342
UNI MY010	<i>Lobophyllia corymbosa</i>	Mayotte	HF954254	HF954341
UNI AD003	<i>Lobophyllia corymbosa</i>	Gulf of Aden	HE654638	HE648554
UNI MA434	<i>Lobophyllia corymbosa</i>	Mayotte	HE654637	HE648553
UNI GA024	<i>Lobophyllia costata*</i>	Gambier	HF954246	HF954333
UNI GA058	<i>Lobophyllia costata*</i>	Gambier	HF954247	HF954334
UNI MY199	<i>Lobophyllia cf diminuta*</i>	Mayotte	HF954252	HF954339
UNI MY325	<i>Lobophyllia cf diminuta*</i>	Mayotte	HF954253	HF954340
UNI PFB103	<i>Lobophyllia flabelliformis*</i>	Papua New Guinea	HF954248	HF954335
UNI PFB297	<i>Lobophyllia flabelliformis*</i>	Papua New Guinea	HF954249	HF954336
UNI KA139	<i>Lobophyllia hemprichii</i>	Red Sea	HF954256	HF954343
UNI BA134	<i>Lobophyllia hemprichii</i>	Gulf of Aden	HE654639	HE648555
UNI MU202	<i>Lobophyllia hemprichii</i>	Gulf of Aden	HE654640	HE648556
UNI PFB183	<i>Lobophyllia robusta*</i>	Papua New Guinea	HF954250	HF954337
UNI PFB296	<i>Lobophyllia robusta*</i>	Papua New Guinea	HF954251	HF954338
UNI SO071	<i>Micromussa amakusensis</i>	Socotra	HF954198	HF954285
UNI BA117	<i>Micromussa amakusensis</i>	Gulf of Aden	HE654643	HE648559
UNI FP	<i>Micromussa amakusensis</i>	Gulf of Aden	HE654642	HE648558
UNI MU215	<i>Micromussa amakusensis</i>	Gulf of Aden	HE654641	HE648557
-	<i>Micromussa amakusensis</i>	Japan	AB441200	AB441403
G61909	<i>Moseleya latistellata</i>	Australia	HQ203293	HQ203376
HS3103	<i>Oxypora glabra*</i>	New Caledonia	HF954224	HF954312
HS3270	<i>Oxypora glabra*</i>	New Caledonia	HF954223	HF954311
HS3274	<i>Oxypora glabra*</i>	New Caledonia	HF954225	HF954313
UNI KA131	<i>Oxypora lacera</i>	Red Sea	HF954226	HF954314
HS3172	<i>Oxypora lacera</i>	New Caledonia	HF954227	HF954315
HS3203	<i>Oxypora lacera</i>	New Caledonia	HF954228	HF954316
HS3255	<i>Parascalymia vitiensis</i>	New Caledonia	HF954202	HF954289
UNI PFB031	<i>Parascalymia vitiensis</i>	Papua New Guinea	HF954203	HF954290
RMNH Coel 40070	<i>Phymastrea multipunctata</i>	Sabah, Malaysia	HF954199	HF954286
RMNH Coel 40099	<i>Phymastrea multipunctata</i>	Sabah, Malaysia	HF954200	HF954287
P131	<i>Phymastrea multipunctata</i>	Philippines	HQ203289	HQ203372
UNI PFB104	<i>Symphyllia agaricia</i>	Papua New Guinea	HF954263	HF954350
UNI PFB213	<i>Symphyllia agaricia</i>	Papua New Guinea	HF954264	HF954351
UNI DJ277	<i>Symphyllia erythraea*</i>	Djibouti	HF954257	HF954344
UNI MY045	<i>Symphyllia erythraea*</i>	Mayotte	HF954258	HF954345

UNI SO011	<i>Symphyllia erythraea</i> *	Socotra	HF954259	HF954346
UNI MY230	<i>Symphyllia radians</i>	Mayotte	HF954265	HF954352
UNI SO087	<i>Symphyllia radians</i>	Socotra	HF954266	HF954353
UNI BA107	<i>Symphyllia radians</i>	Gulf of Aden	HE654644	HE648560
UNI BU046	<i>Symphyllia radians</i>	Gulf of Aden	HE654646	HE648562
HS3118	<i>Symphyllia recta</i>	New Caledonia	HF954267	HF954354
HS3131	<i>Symphyllia recta</i>	New Caledonia	HF954268	HF954355
HS3157	<i>Symphyllia valenciennesii</i> *	New Caledonia	HF954261	HF954348
UNI PFB277	<i>Symphyllia valenciennesii</i> *	Papua New Guinea	HF954262	HF954349
HS3135	<i>Symphyllia cf valenciennesii</i> *	New Caledonia	HF954260	HF954347
S048	<i>Diploastrea heliopora</i>	Singapore	EU371660	HQ203315
G61880	<i>Dipsastraea favus</i>	Australia	HQ203255	HQ203322
G61883	<i>Dipsastraea matthaii</i>	Australia	HQ203259	HQ203331
S068	<i>Dipsastraea rotumana</i>	Singapore	FJ345427	HQ203339
S109	<i>Echinopora lamellose</i>	Singapore	FJ345419	HQ203318
S002	<i>Favites abdita</i>	Singapore	HQ203267	HQ203345
S083	<i>Goniastrea retiformis</i>	Singapore	EU371700	HQ203361
P127	<i>Hydnophora exesa</i>	Philippines	HQ203276	HQ203362
S081	<i>Leptoria phrygia</i>	Singapore	EU371705	HQ203365
P114	<i>Merulina scabricula</i>	Philippines	HQ203281	HQ203366
S055	<i>Oulophyllia crispa</i>	Singapore	EU371721	HQ203381
P115	<i>Pectinia lactuca</i>	Philippines	HQ203300	HQ203384
G61887	<i>Platygyra lamellina</i>	Australia	HQ203302	HQ203389

3.4 Results and Discussion

Our sequences were analyzed together with 20 other lobophylliids from GenBank for a total alignment of 1572 bp. Topologies resulting from BI, ML, and MP analyses were largely congruent with a consistent composition of major clades and discrepancies at nodes, which are poorly supported in all three phylogenies, especially in the MP tree (Fig. 3.1). ML individual trees of COI and rDNA were largely congruent with no conflicting patterns among clades and taxa (Apps. 3.3, 3.4).

The monophyly of the family Lobophylliidae is well-supported in all analyses. *Acanthastrea* and *Micromussa*, whose evolutionary relationships were uncertain (Fukami et al., 2008), are nested within the family (Fig. 3.1). This result corroborates previous molecular findings by Arrigoni et al. (2012) and supports morphological analyses by Budd et al. (2012).

Our combined phylogeny reconstruction includes the type species of the investigated genera and pinpoints generic boundaries in need of further study. Nine main monophyletic genus-level lineages are supported (Fig. 3.2) and they are

mostly in disagreement with the previous systematic positions of most Lobophylliidae (Veron, 2000; Budd et al., 2012). All polytypic genera, *i.e.* *Acanthastrea*, *Echinophyllia* Klunzinger, 1879, *Lobophyllia* de Blainville, 1830, *Oxypora* Saville Kent, 1871, and *Symphyllia* Milne Edwards & Haime, 1848, are not monophyletic (Table 3.2). In turn, the close relationship between the only studied species of *Micromussa* and the lobophylliid-like *Phymastrea multipunctata* (Hodgson, 1985) in sub-clade A (Fig. 3.1) suggests that a formal taxonomic action is timely for the latter (Table 3.2).

The most notable and complex case is that of the highly polyphyletic genus *Acanthastrea*, whose representatives are scattered throughout sub-clades B, C, E, and I (Fig. 3.1). The sister group relationship between *A. bowerbanki* Milne Edwards and Haime, 1851 and *A. hillae* Wells, 1955 in sub-clade B is genetically well supported and corroborated by morphologic similarities of their coralla and corallites (Veron and Pichon, 1980). However, these species are more closely related to sub-clade A than to sub-clade E, including the type species, *A. echinata* (Dana, 1846). The genetic boundaries between the latter and *A. hemprichii* (Ehrenberg, 1834), *A. rotundoflora* Chevalier, 1975, and *A. subechinata* Veron, 2000 remain undefined and are in need of additional molecular analyses. Moreover, the Indian Ocean *Acanthastrea maxima* is confirmed as an evolutionarily distinct species that is self-standing in sub-clade C (Arrigoni et al., 2012). This species and *A. bowerbanki* and *A. hillae* will have to be subsumed within two new genera corresponding to sub-clades C and B, respectively (Table 3.2). Finally, *A. ishigakiensis* Veron, 1990 is nested in sub-clade I and closely related to *Symphyllia recta* (Dana, 1846), which is the type species of its genus, thus prompting this species re-assignment. Morphologic similarity between this *Acanthastrea* species and *Symphyllia erythraea* (Klunzinger, 1879), have been highlighted before (Veron, 2000) although the latter is a genetically distinctive species (Fig. 3.1). A different case again is that of *A. faviaformis* Veron, 2000 which clusters in the Merulinidae Verrill, 1865, and appears to be a sister taxon of *Dipsastraea* de Blainville, 1830, and therefore needs formal reclassification.

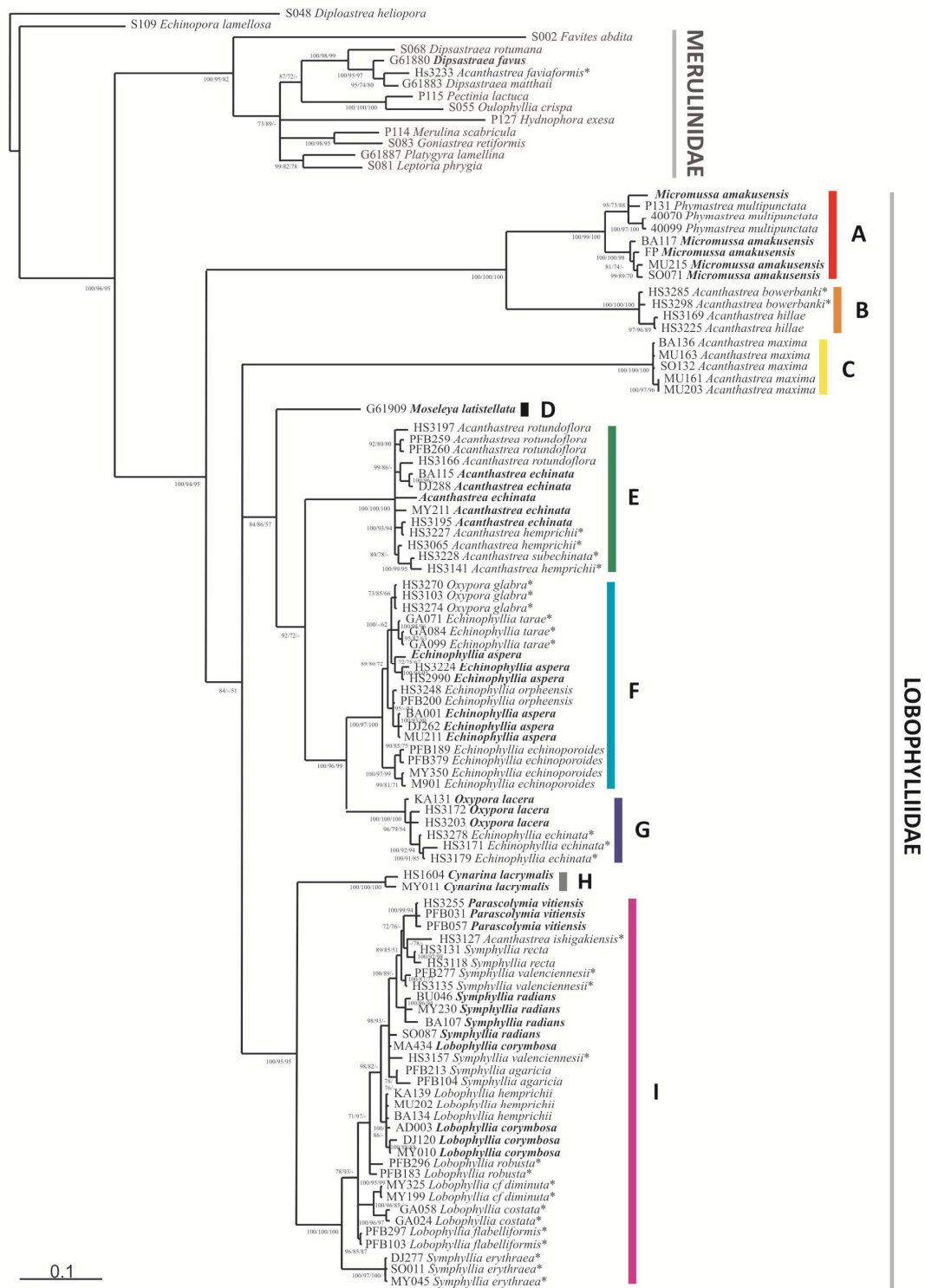


Figure 3.1. Phylogeny of the Lobophylliidae inferred from Bayesian Inference analyses of COI and rDNA. Node values are Posterior Bayesian probabilities (> 70%), ML SH-like support (> 70%) and MP (> 50%) bootstrap values. Dashes (-) indicate nodes that are statistically unsupported. Uppercase letters and colour codes delineate lineages referred to in Fig. 3.2 and Table 3.2. Type species in bold. * species analyzed for the first time from a molecular point of view.

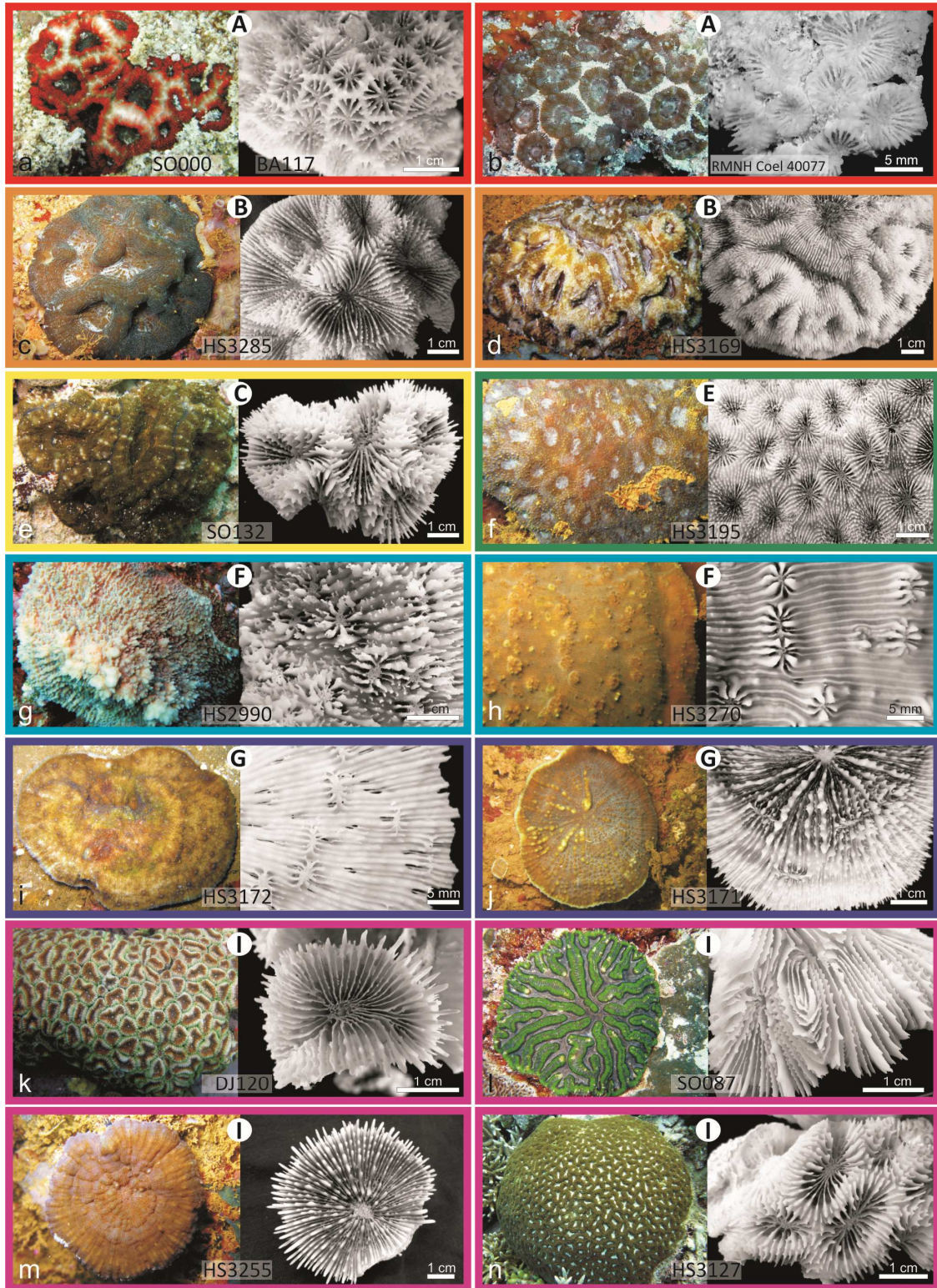


Figure 3.2. *In situ* and corallum photos of species with unexpected phylogenetic relationships: a) *Micromussa amakusensis*; b) *Phymastrea multipunctata*; c) *A. bowerbanki*; d) *A. hillae*; e) *A. maxima*; f) *A. echinata*; g) *Echinophyllia aspera*; h) *Oxypora glabra*; i) *O. lacera*; j) *E. echinata*; k) *Lobophyllia corymbosa*; l) *Symphyllia radians*; m) *Parascalymia vitiensis*; n) *A. ishigakiensis*. Colour codes and uppercase letters in white circles indicate clades in Fig. 3.1. Specimen code on the corallum image.

Echinophyllia and *Oxypora* nest into each other and their genetic boundaries remain unclear, as are those based on morphology (Veron and Pichon, 1980; Budd and Stolarski, 2009; Veron, 2000). *Oxypora glabra* Nemenzo, 1959 is part of the *Echinophyllia* clade (sub-clade F) while *E. echinata* (Saville-Kent, 1871) is closest to the type species *O. lacera* (Verrill, 1864) in sub-clade G, a situation at least partially foreseen by Chevalier (1975) who had already placed *O. glabra* in *Echinophyllia*.

The phaceloid *Lobophyllia* and the meandroid *Symphyllia* belong to a single lineage (sub-clade I) and their traditional separation based on corallum organization seems evolutionarily meaningless as already shown in other cases (Arrigoni et al., 2012). These genera are known to share several micromorphological and microstructural characters (Budd and Stolarski, 2009) and the genus *Lobophyllia* should be expanded to include the genus *Symphyllia* (Table 3.2). Moreover, the inclusion of the monotypic genus *Parascolymia* in sub-clade I was not previously envisaged (Budd et al., 2012) and needs to be synonymised with *Lobophyllia*. In fact, colonial coralla of *Parascolymia* (Veron and Pichon, 1980: Fig. 417) do bear similarities with some *Symphyllia* species and, most of all, with *Australomussa*.

Unexpected genetic affinities of coral taxa have already been shown in several instances (Fukami et al., 2004a, 2008; Benzoni et al., 2007, 2011, 2012b; Huang et al., 2011; Kitahara et al., 2012a, 2012b; Arrigoni et al., 2012) and are not surprising *per se*. However, our phylogeny model suggests that more unexpected results could emerge from the genetic characterization of the 17 still unstudied known Lobophylliidae species, and of the monotypic genera *Australomussa* and *Echinomorpha* (Veron, 2000; Budd et al., 2012). Overall, the results presented in this study will represent a solid basis for a formal revision at genus level of the Lobophylliidae (Table 3.2).

Table 3.2. Grouping at genus level of the 32 species analyzed based on molecular data in this study. Type species are in bold. * = species analyzed for the first time from the molecular point of view; ^ = molecularly based grouping candidate for new genus description; § = genus re-assignment pending a formal taxonomic revision.

Clade	Genus	Traditional species
A	<i>Micromussa</i>	<i>Micromussa amakusensis</i> , <i>Phymastrea multipunctata</i> §
B	<i>Incertae sedis 1</i> [^]	<i>Acanthastrea bowerbanki</i> *§, <i>Acanthastrea hillae</i> §
C	<i>Incertae sedis 2</i> [^]	<i>Acanthastrea maxima</i> §
D	<i>Moseleya</i>	<i>Moseleya latistellata</i>
E	<i>Acanthastrea</i>	<i>Acanthastrea echinata</i> , <i>Acanthastrea hemprichii</i> *, <i>Acanthastrea rotundoflora</i> , <i>Acanthastrea subechinata</i> *
F	<i>Echinophyllia</i>	<i>Echinophyllia aspera</i> , <i>Echinophyllia echinoporoides</i> , <i>Echinophyllia orpheensis</i> , <i>Echinophyllia tarae</i> *, <i>Oxypora glabra</i> *§
G	<i>Oxypora</i>	<i>Oxypora lacera</i> , <i>Echinophyllia echinata</i> *§
H	<i>Cynarina</i>	<i>Cynarina lacrymalis</i>
I	<i>Lobophyllia</i>	<i>Lobophyllia corymbosa</i> , <i>Lobophyllia costata</i> *, <i>Lobophyllia diminuta</i> *, <i>Lobophyllia flabelliformis</i> *, <i>Lobophyllia hemprichii</i> , <i>Lobophyllia robusta</i> *, <i>Symphyllia radians</i> §, <i>Symphyllia agaricia</i> §, <i>Symphyllia erythraea</i> *§, <i>Symphyllia recta</i> §, <i>Symphyllia valenciennesii</i> *§, <i>Acanthastrea ishigakiensis</i> *§, <i>Parascolymia vitiensis</i> §
	<i>Dipsastraea</i> (family Merulinidae)	<i>Acanthastrea faviaformis</i> *§

- CHAPTER 4 -

*The complete mitochondrial genome of *Acanthastrea maxima*
(Cnidaria, Scleractinia, Lobophylliidae)*

Roberto Arrigoni¹, Benoît Vacherie², Francesca Benzoni¹, Valerie Barbe²

¹ Department of Biotechnologies and Biosciences, University of Milan – Bicocca, Piazza della Scienza 2, 20126, Milan, Italy

² CEA/DSV/IG/Genoscope, Rue Gaston Crémieux, 91000, Évry, Cedex, France

In press in *Mitochondrial DNA*: DOI, 10.3109/19401736.2014.926489

4.1 Abstract

The complete nucleotide sequence of the mitochondrial genome of the scleractinian coral *Acanthastrea maxima* has been obtained, representing the first sequenced mitogenome of a member of the Lobophylliidae. The mitochondrial genome is 18,278 bp in length, the longest sequence among the robust corals sequenced mitogenome to date. The overall GC composition (33.7%) and the gene arrangement are similar to those of the other scleractinian corals, including 13 protein-coding genes, 2 rRNA genes (rnl and rns) and 2 tRNA genes (tRNA^{Met} and tRNA-Trp). All genes except tRNA-Trp, atp8, cox1, tRNA-Met and rnl are engulfed by a large group I intron in the nad5 gene. A second group I intron of 1077 bp in length is inserted in the cox1 gene and it encodes a putative homing endonuclease. There are four regions of gene overlaps totalling 22 bp and nine intergenic spacer regions for a total of 2220 bp, of which the cox3-cox2 region may correspond to the putative control region.

4.2 Introduction

Acanthastrea maxima Sheppard and Salm (1988) (Cnidaria, Anthozoa, Scleractinia) is an uncommon coral species known only from the Gulf of Aden, Arabian Sea, Gulf of Oman, and Persian Gulf (Veron, 2000) (Figs. 4.1-4.2). Phylogenetic studies based on molecular tools have revealed that the species belongs to the robust group and it is highly divergent within the family Lobophylliidae (Arrigoni et al., 2012, 2014a). Moreover, it has been listed as a Near Threatened species in IUCN Red List (Turak et al., 2008) because of extensive reduction of its natural coral reef habitat and its susceptibility to a number of threats, such as bleaching.

In this work, we present the complete mitochondrial genome sequence for *A. maxima* (EMBL No. FO904931), which makes it the first sequenced mitogenome for a representative of the Lobophylliidae.

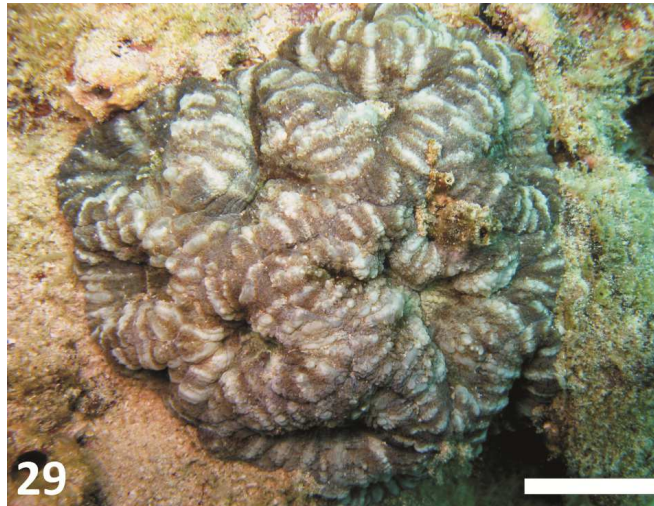


Figure 4.1. In-vivo picture of the analyzed specimen of *A. maxima* (SO131).



Figure 4.2. Distribution map of *A. maxima*. Modified from Veron (2000).

4.3 Material and methods

The entire mitogenome was obtained using Illumina technology. Two overlapping paired-end libraries (478 bp (A) and 574 bp (B) insert size) were constructed and sequenced on MiSeq instrument (2X250 nt(A) and 2X300 nt (B)) (Illumina, San Diego, CA). To identify mitochondrial reads, the reads were compared with the NCBI Metazoan mitochondrial database (<http://www.ncbi.nlm.nih.gov/genomes/MITOCHONDRIA/Metazoa/>) using a home-made program based on BWA (<http://bio-bwa.sourceforge.net/>). A total of

11,394 reads were merged (representing a minimum of 100-fold coverage) and assembled using Roche's Newbler v2.9 assembler (Roche, Mannheim, Germany). The assembly accuracy and final consensus construction was performed using Consed (www.phrap.org).

4.4 Results and Discussion

The complete mitochondrial genome was 18,278 bp long, the longest length among the robust corals sequenced mitogenome to date (Lin et al., 2011). The G+C content was 33.7% and the genome had the common gene organization of scleractinian coral mitochondrial genome (Fukami and Knowlton, 2005; Medina et al., 2006; Wang et al., 2013). The mitogenome contains 13 protein-coding genes (*nad1-6*, *nad4L*, *cob*, *atp6*, *atp8*, *cox1-3*), 2 ribosomal RNA genes (*rnl* and *rns*), and 2 transfer RNA genes (*trnM* and *trnW*) (Table 4.1).

Nearly all of the 13 protein-coding genes used methionine (ATG) as the translation initiation codon whereas *nad2* used isoleucine (ATA) and *cox3* started with valine (GTG).

As in other cnidarians, all the protein-coding genes had complete stop codon (TAA and TAG). The *nad5* gene was interrupted by a large group I intron which contains ten protein-coding genes and *rns*. A second group I intron of 1077 bp in length was inserted in the *cox1* gene and it was similar to those of other lobophylliids and robust corals (Fukami et al., 2007). The insertion site of this intron was identical to that of robust corals (Fukami et al., 2007) and its open reading frame of 310 amino acids contains the LAGLI-DADG motif encoding a putative homing endonuclease.

There are four cases of gene overlap totalling 22 bp, while the nine intergenic regions make up a total of 2220 nucleotides. 83.7% of these non-coding nucleotides are found in two regions, the *cox3-cox2* region (1278 bp) and the *cox1-trnM* one (580 bp). The former region possesses typical characteristics of a putative

control region, such as long length, presence of tandem repeats and the potential to form secondary structures (van Oppen et al., 2002b).

Table 4.1. Annotation of the complete mitochondrial genome of *A. maxima*.

Gene/region	Strand*	Location	Length (bp)	AT (%)	Start codon	Stop codon	IGR length (bp)†
<i>trnM</i>	H	1-72	72	56.9			0
<i>Rnl</i>	H	73-2077	2005	68.9			0
<i>nad5</i> (5')	H	2078-2788	711	66.4	ATG		0
Group I Intron (<i>nad5</i> (5'))	H	2789-2899	111	68.5			0
<i>nad1</i>	H	2900-3847	948	65.0	ATG	TAG	2
<i>Cob</i>	H	3850-4989	1140	67.5	ATG	TAA	25
<i>nad2</i>	H	5015-6301	1287	68.9	ATA	TAA	1
<i>nad6</i>	H	6303-6863	561	69.0	ATG	TAA	-1
<i>atp6</i>	H	6863-7540	678	67.7	ATG	TAA	-1
<i>nad4</i>	H	7540-8979	1440	66.1	ATG	TAG	138
<i>Rns</i>	H	9118-10,019	902	65.2			191
<i>cox3</i>	H	10,211-10,990	780	62.4	GTG	TAA	1278
<i>cox2</i>	H	12,269-12,976	708	64.9	ATG	TAA	-19
<i>nad4L</i>	H	12,958-13,257	300	71.1	ATG	TAA	2
<i>nad3</i>	H	13,260-13,601	342	68.1	ATG	TAA	0
Group I Intron (<i>nad5</i> (3'))	H	13,602-13,658	57	73.7			0
<i>nad5</i> (3')	H	13,659-14,762	1104	69.3		TAG	0
<i>trnW</i>	H	14,763-14,830	68	60.3			3
<i>atp8</i>	H	14,834-15,031	198	79.8	ATG	TAA	-1
<i>cox1</i> (5')	H	15,031-15,759	729	64.2	ATG		0
Group I Intron (<i>cox1</i>)	H	15,760-16,836	1077	64.3			0
<i>cox1</i> (3')	H	16,837-17,697	861	65.5		TAA	580

Notes: *H indicates heavy strand; † Numbers correspond to the nucleotides separating different genes/regions. Negative numbers indicate overlapping nucleotides between adjacent genes/regions.

– CHAPTER 5 –

Taxonomy and phylogenetics relationships of the coral genera

Australomussa and Parascolymia

(Scleractinia, Lobophylliidae)

Roberto Arrigoni¹, Zoe T. Richards², Chaolun Allen Chen^{3,4}, Andrew H. Baird⁵,
Francesca Benzoni^{1,6}

¹ Department of Biotechnologies and Biosciences, University of Milan – Bicocca, Piazza della Scienza 2, 20126, Milan, Italy

² Aquatic Zoology, Western Australian Museum, 49 Kew Street, Welshpool, WA 6106, Australia

³ Biodiversity Research Centre, Academia Sinica, Nangang, Taipei 115, Taiwan

⁴ Institute of Oceanography, National Taiwan University, Taipei 106, Taiwan

⁵ ARC Centre of Excellence for Coral Reef Studies, James Cook University, Townsville, QLD 4811, Australia

⁶ Institut de Recherche pour le Développement, UMR227 CoReUs2, 101 Promenade Roger Laroque, 98848 Noumea, New Caledonia

Published in *Contributions to Zoology*: 83, 195-215 (2014)

5.1 Abstract

Novel micromorphological characters in combination with molecular studies have led to an extensive revision of the taxonomy and systematics of scleractinian corals. In the present work, we investigate the macro- and micromorphology and the phylogenetic position of the genera *Australomussa* and *Parascolymia*, two monotypic genera ascribed to the family Lobophylliidae. The molecular phylogeny of both genera was addressed using three markers, the partial mitochondrial COI gene and the nuclear histone H3 and the ribosomal ITS region. Based on molecular data, *Australomussa* and *Parascolymia* belong to the Lobophylliidae and they cluster together with the genera *Lobophyllia* and *Symphyllia* within the same clade. While *A. rowleyensis* and *P. vitiensis* are closely related based on the three gene regions examined, their macro and micromorphology suggest that these species are distinct, differing in several characters, such as continuity and thickness of the costosepta, the number of septa, septal tooth height, spacing, and shape, and the distribution and shape of granules. Thus, we revise the taxonomic status of the genus *Australomussa* as a junior synonym of *Parascolymia*.

5.2 Introduction

Over the last two decades, our understanding of the evolution and the systematics of hard corals (Cnidaria, Anthozoa, Scleractinia) has rapidly advanced due to the progressive increase of molecular studies (Romano and Palumbi, 1996; Chen et al., 2002; Fukami et al., 2004a, 2008; Kitahara et al., 2010; Stolarski et al., 2011). The new molecular phylogenies are, however, often very different from phylogenies based on macro-morphology (Fukami et al., 2004a, 2008; Budd and Stolarski, 2009, 2011; Huang et al., 2011). Several recent papers integrating molecular and morphological approaches have led to formal taxonomic revisions of scleractinian corals at different taxonomic ranks (e.g. Wallace et al., 2007; Gittenberger et al., 2011; Kitahara et al., 2012a, 2012b, 2013; Benzoni et al., 2012a, 2012b, 2014; Kitano et al., 2014; Huang et al., 2014a, b). This integrated

approach has proved effective at resolving long-standing issues, for example a comprehensive revision of the taxonomy and systematics of 23 nominal species of *Psammocora* Dana, 1846 (Stefani et al., 2008; Benzoni, 2006; Benzoni et al., 2010, 2012b) and 21 nominal species of *Pocillopora* Lamarck, 1816 (Flot et al., 2008; Pinzon et al., 2013; Schmidt-Roach et al., 2013a, 2013b, 2014).

The stony coral family Lobophylliidae Dai and Horng, 2009 has recently been studied by several authors using an integrated morpho-molecular approach, and is undergoing several taxonomic changes, although this process is far from complete. For example, Indo-Pacific taxa traditionally ascribed to the Mussidae Ortmann, 1890 have been moved to the Lobophylliidae as a result of the molecular work by Fukami et al. (2004a, 2008), and the finding of a deep divergence between Indo-Pacific and Atlantic species based on morphological characters (Budd and Stolarski, 2009; Budd et al., 2012). The family Lobophylliidae is now comprised of the genera *Lobophyllia* de Blainville, 1830, *Acanthastrea* Milne Edwards and Haime, 1848, *Cynarina* Brüggemann, 1877, *Echinophyllia* Klunzinger, 1879, *Homophyllia* Brüggemann, 1877, *Micromussa* Veron, 2000, *Moseleya* Quelch, 1884, *Oxypora* Saville Kent, 1871, *Parascolymia* Wells, 1964 and *Symphyllia* Milne Edwards and Haime, 1848 (Budd et al., 2012). Also included in the family are two genera that have not been examined at a molecular level, namely *Echinomorpha* Veron, 2000 and *Australomussa* Veron, 1985, hence their phylogenetic placement is unresolved.

The macromorphology (budding, colony form, size and shape of corallites, numbers of septal cycles), the micromorphology (shapes and distributions of septal teeth and granules), and the microstructure (arrangement of calcification centres and thickening deposits within costosepta) of the lobophylliid genera *Acanthastrea*, *Cynarina*, *Echinophyllia*, *Homophyllia*, *Lobophyllia*, *Micromussa*, *Oxypora*, *Parascolymia*, and *Symphyllia* were examined by Budd and Stolarski (2009) and Budd et al. (2012). They concluded that the shape and distribution of septal teeth and granules, the area between teeth, and the development of thickening deposits are informative characters for distinguishing the Lobophylliidae from

representatives of the other coral families. Arrigoni et al. (2014a) presented a comprehensive molecular phylogeny that shows that the Lobophylliidae is a monophyletic family comprising nine main molecular clades (clades A–I), and that several genera are not monophyletic. The authors also showed that the monospecific genus *Parascolymia* belongs to clade I (*sensu* Arrigoni et al., 2014a) together with all the species of *Lobophyllia* and *Symphyllia* for which molecular data is available, including the two type species *Lobophyllia corymbosa* (Forskål, 1775) and *Symphyllia radians* Milne Edwards and Haime, 1849. The authors did not, however, undertake any formal taxonomic revision of the status of the genus *Parascolymia*.

Australomussa rowleyensis Veron, 1985 was described from Western Australia and ascribed to the Mussidae. It is a colonial and zooxanthellate scleractinian coral, characterized by flattened, helmet- or dome-shaped coralla, valleys approximately 20mm wide, with very thick walls and a well-developed columella (Veron, 1985). In the original description of *A. rowleyensis*, Veron (1985) stated that this genus showed ‘little resemblances to any other genus’ with the exception of *Parascolymia* and *Symphyllia*, and ‘its closest affinities are probably with the former’. The author referred only to the macromorphology of the coralla for the comparison of *Australomussa* with *Parascolymia* and *Symphyllia* and did not consider any micromorphological characters. Budd and Stolarski (2009) and Budd et al. (2012) showed that the majority of macromorphological characters traditionally used in the taxonomy and systematics of Lobophylliidae and Mussidae exhibit homoplasy. In contrast, novel micromorphological characters separate these two families and are useful for the description and formalization of species. Nevertheless, while the micromorphology of *P. vitiensis* (Brüggemann, 1877) was described by Budd and Stolarski (2009) and Budd et al. (2012), *A. rowleyensis* was not analysed in these studies.

The known distribution of *A. rowleyensis* includes the Western Pacific region known as the Coral Triangle (for definition see Hoeksema, 2007; Veron et al., 2009) and partially overlaps with the distribution of *P. vitiensis* which is absent

from Western Australia but extends to the west in the Indian Ocean and to the east in the central Pacific (Veron, 2000). *Australomussa rowleyensis* and *P. vitiensis* have very different histories of nomenclature. Perhaps due to its recent description and rarity (Veron, 1985), *A. rowleyensis* has always been described as *A. rowleyensis* despite its morphological similarity to *Parascolymia* and *Symphyllia* (Veron, 1985, 2000). Conversely, *P. vitiensis* has a long history of nomenclatural confusion. It was originally ascribed to *Litophyllia* Milne Edwards and Haime, 1857 (Gardiner, 1899; Crossland, 1952) and later described as *Protolobophyllia japonica* Yabe and Sugiyama, 1935. In agreement with Matthai (1928), Wells (1937) and Vaughan and Wells (1943) considered *Scolymia* Haime, 1852 and *Protolobophyllia* Yabe and Sugiyama, 1935 as junior synonyms of *Lobophyllia*, presuming that the solitary forms were juvenile monostomatous stages of this colonial genus. Based on differences in macromorphology, Wells (1964) separated the Atlantic species *Scolymia lacera* (Pallas, 1766) from the Indo-Pacific species *Scolymia vitiensis* and established the genus *Parascolymia* for the latter one because he verified that the holotype of *Protolobophyllia japonica* was a specimen of *Cynarina lacrymalis* (Milne Edwards and Haime, 1848). Subsequently, Veron and Pichon (1980) synonymised *Parascolymia* with *Scolymia* based on the fact that these two genera are almost entirely monocentric, questioning also the validity of the geographical separation. Finally, Budd et al. (2012) restored the distinction between *Parascolymia* (Indo-Pacific) and *Scolymia* (Atlantic) based on molecular and micromorphological analyses (Fukami et al., 2004a, 2008; Budd and Stolarski, 2009).

Although *P. vitiensis* is generally monocentric, it can also form polystomatous coralla (Chevalier, 1975; Veron and Pichon, 1980: figs. 416–417) (Figs. 5.1B–D, 5.2F–I). The macro-morphologic observation of a large series of mono- to polystomatous specimens of *P. vitiensis* from Papua New Guinea and New Caledonia and the similarity of the larger specimens with *A. rowleyensis* prompted the detailed study of the morphological affinities and molecular relationship between these two species and the two monospecific genera they are currently

ascribed to.

Here we selected three DNA regions, the barcoding region of cytochrome oxidase subunit I gene, the nuclear ribosomal ITS region, and the nuclear histone H3 for molecular analysis of these species. The former two molecular loci have been extensively used in phylogenetic studies of scleractinian corals (Fukami et al., 2008; Gittenberger et al., 2011; Huang et al., 2011; Benzoni et al., 2011, 2014) and, moreover, the most comprehensive phylogeny reconstruction of the Lobophylliidae to date is based on these two markers (Arrigoni et al., 2014a). The latter locus was revealed to be informative for a broad-based phylogeny of the Merulinidae Verrill, 1865 (Huang et al., 2011, 2014b), a family closely related to the Lobophylliidae (Fukami et al., 2008; Arrigoni et al., 2012). Several phylogenetic studies of scleractinian corals achieved a well-resolved phylogeny using a concatenated species-tree, combining mitochondrial and nuclear molecular markers (Huang et al., 2009, 2011; Souter, 2010; Gittenberger et al., 2011; Benzoni et al., 2012a, 2012b; Richards et al., 2013; Arrigoni et al., 2014a). This kind of approach is a powerful way to obtain a robust phylogeny, resolving all key nodes and yielding good resolution at species level.

In the present paper, the phylogenetic relationships of *A. rowleyensis* with the rest of the Lobophylliidae are explored for the first time on the basis of three molecular loci, the barcoding region of cytochrome oxidase subunit I gene, the nuclear histone H3, and the nuclear ribosomal ITS region. In addition, we examined the macromorphology and micromorphology of *A. rowleyensis* and compared it to *P. vitiensis*.

5.3 Materials and methods

5.3.1 Sampling

Specimens of *Parascolymia vitiensis* for this study were sampled in New Caledonia, Papua New Guinea, and Eastern Australia, while samples of *Australomussa rowleyensis* were collected in the Kimberley, North-West Australia (Table 5.1). Coral specimens were photographed and collected while SCUBA diving from 2 to 35 meters depth. Digital images of living corals in the field were taken with a Canon Powershot G9 in an Ikelite underwater housing system in New Caledonia and Papua New Guinea (Figs. 5.1 and App. 5.4), and with an Olympus XZ1 in a PT-050 underwater housing in Australia (Fig. 5.1 and App. 5.4). Coral specimens were collected, tagged, and preserved in 95% ethanol for further molecular analysis. After the sampling of fixed tissues for DNA extraction, each corallum was immersed in sodium hypochlorite for 48 hours to remove all soft parts, rinsed in freshwater and dried for microscope observation. Specimens were identified at the species level based on skeletal morphology using a Leica M80 microscope following the descriptions and illustrations by Chevalier (1975), Veron and Pichon (1980), and Veron (1985).

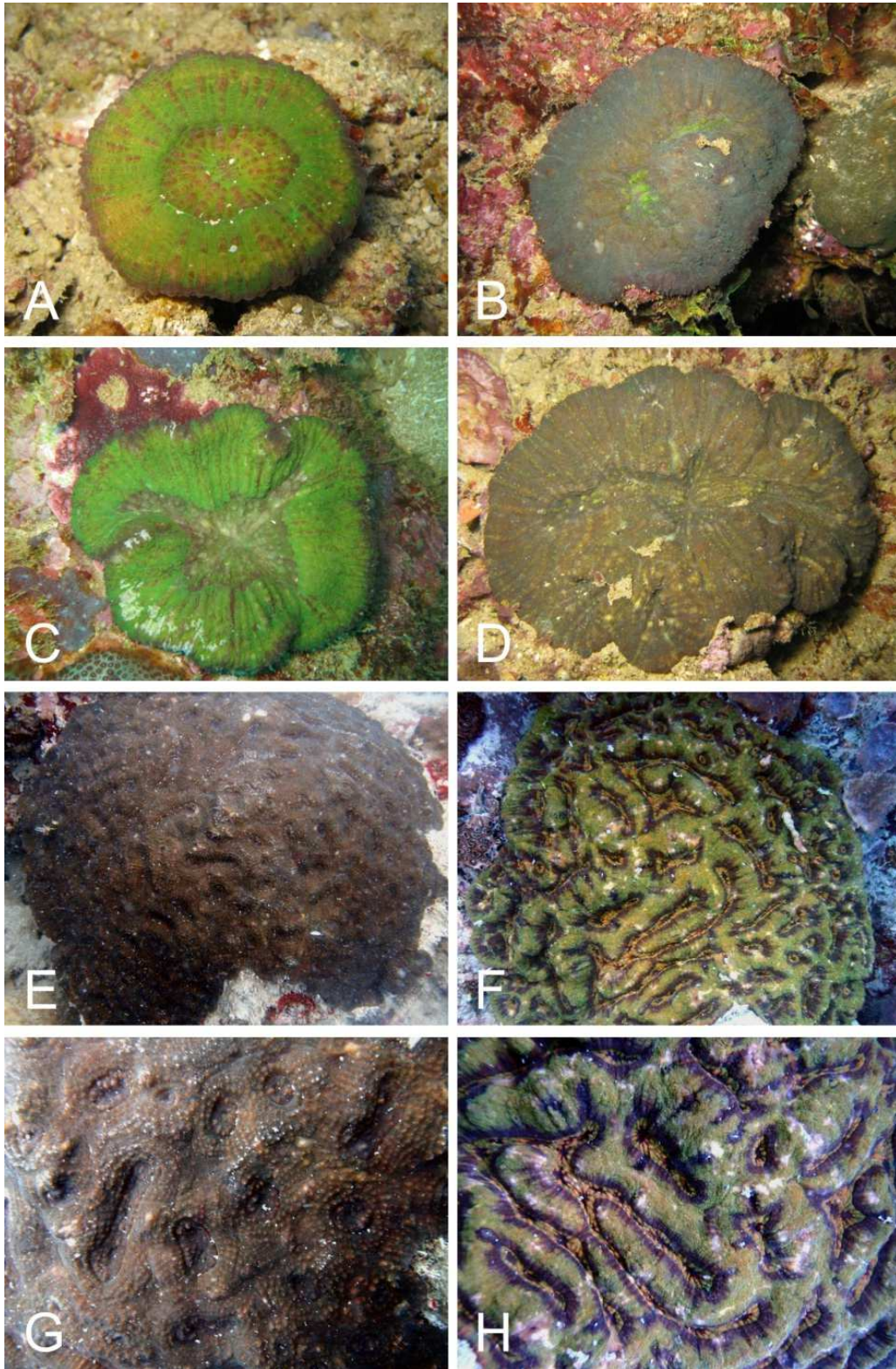


Figure 5.1. *Parascolymia vitiensis* (A-D) and *P. rowleyensis* (previously *Australomussa*) (E-G) *in situ*: A) IRD HS2984 (monostomatous); B) UNIMIB PFB056 (bistomatous); C) IRD HS3139 (polystomatous, same as in Figure 5.2H); D) UNIMIB PFB057 (polystomatous, same as in Figure 5.2I); E) WAM Z65786; F) WAM Z65785; G) close up of the same colony as in E; H) close up of the same colony as in F.

Table 5.1. List of the material examined in this study. For each specimen we list code, identification, sampling locality, collector, and COI, histone H3, and ITS region sequences used for the phylogenetic reconstructions.

Code	Species	Locality	Collector	COI	H3	ITS
WAM Z65785	<i>Australomuss a rowleyensis</i>	Australia	Richards	LK022344	LK022380	LK022359
WAM Z65786	<i>Australomuss a rowleyensis</i>	Australia	Richards	LK022345	LK022381	LK022360
WAM Z65787	<i>Australomuss a rowleyensis</i>	Australia	Richards	LK022346	LK022382	LK022361
WAM Z65788	<i>Australomuss a rowleyensis</i>	Australia	Richards	LK022347	LK022383	LK022362
WAM Z65789	<i>Australomuss a rowleyensis</i>	Australia	Richards	LK022348	LK022384	LK022363
6816	<i>Parascolymia vitiensis</i>	Australia	Baird		LK022385	LK022364
6830	<i>Parascolymia vitiensis</i>	Australia	Baird	LK022349	LK022386	LK022365
IRD HS2955	<i>Parascolymia vitiensis</i>	New Caledonia	Benzoni	LK022350	LK022387	LK022366
IRD HS2964	<i>Parascolymia vitiensis</i>	New Caledonia	Benzoni	LK022351		LK022367
IRD HS2984	<i>Parascolymia vitiensis</i>	New Caledonia	Benzoni	LK022352	LK022388	LK022368
IRD HS2985	<i>Parascolymia vitiensis</i>	New Caledonia	Benzoni	LK022353	LK022389	LK022369
IRD HS3139	<i>Parascolymia vitiensis</i>	New Caledonia	Benzoni	LK022354	LK022390	LK022370
IRD HS3255	<i>Parascolymia vitiensis</i>	New Caledonia	Benzoni	HF954202	LK022391	HF954289
UNI PFB031	<i>Parascolymia vitiensis</i>	Papua New Guinea	Benzoni	HF954203	LK022392	HF954290
UNI PFB032	<i>Parascolymia vitiensis</i>	Papua New Guinea	Benzoni		LK022393	LK022371
UNI PFB033	<i>Parascolymia vitiensis</i>	Papua New Guinea	Benzoni			LK022372
UNI PFB052	<i>Parascolymia vitiensis</i>	Papua New Guinea	Benzoni	LK022355	LK022394	LK022373
UNI PFB053	<i>Parascolymia vitiensis</i>	Papua New Guinea	Benzoni			LK022374
UNI PFB054	<i>Parascolymia vitiensis</i>	Papua New Guinea	Benzoni	LK022356	LK022395	LK022375
UNI PFB055	<i>Parascolymia vitiensis</i>	Papua New Guinea	Benzoni		LK022396	LK022376
UNI PFB056	<i>Parascolymia vitiensis</i>	Papua New Guinea	Benzoni	LK022357		LK022377
UNI PFB057	<i>Parascolymia vitiensis</i>	Papua New Guinea	Benzoni	HF954204	LK022397	HF954291
UNI PFB151	<i>Parascolymia vitiensis</i>	Papua New Guinea	Benzoni	LK022358	LK022398	LK022378
UNI PFB152	<i>Parascolymia vitiensis</i>	Papua New Guinea	Benzoni		LK022399	LK022379
UNI	<i>Micromussa</i>	Gulf of	Benzoni		LK022400	

BA117	<i>amakusensis</i>	Aden		
UNI	<i>Micromussa</i>	Gulf of	Benzoni	LK022401
MU215	<i>amakusensis</i>	Aden		
RMNH	<i>Phymastrea</i>	Sabah,	Hoeksema	LK022402
coel	<i>multipunctata</i>	Malaysia		
40070				
IRD	<i>Acanthastrea</i>	New	Benzoni	LK022403
HS3169	<i>hillae</i>	Caledonia		
IRD	<i>Acanthastrea</i>	New	Benzoni	LK022404
HS3225	<i>hillae</i>	Caledonia		
IRD	<i>Acanthastrea</i>	New	Benzoni	LK022405
HS3298	<i>bowerbanki</i>	Caledonia		
UNI	<i>Acanthastrea</i>	Gulf of	Benzoni	LK022406
BA136	<i>maxima</i>	Aden		
UNI	<i>Acanthastrea</i>	Gulf of	Benzoni	LK022407
MU161	<i>maxima</i>	Aden		
UNI	<i>Acanthastrea</i>	Djibouti	Benzoni	LK022408
DJ288	<i>echinata</i>			
IRD	<i>Acanthastrea</i>	New	Benzoni	LK022409
HS3228	<i>subechinata</i>	Caledonia		
UNI	<i>Acanthastrea</i>	Papua New	Benzoni	LK022410
PFB259	<i>rotundoflora</i>	Guinea		
IRD	<i>Acanthastrea</i>	New	Benzoni	LK022411
HS3065	<i>hemprichii</i>	Caledonia		
UNI	<i>Echinophyllia</i>	Gulf of	Benzoni	LK022412
BA001	<i>aspera</i>	Aden		
UNI	<i>Echinophyllia</i>	Papua New	Benzoni	LK022413
PFB189	<i>echinoporoides</i>	Guinea		
IRD	<i>Echinophyllia</i>	New	Benzoni	LK022414
HS3248	<i>orpheensis</i>	Caledonia		
IRD	<i>Echinophyllia</i>	New	Benzoni	LK022415
HS3171	<i>echinata</i>	Caledonia		
IRD	<i>Oxypora</i>	New	Benzoni	LK022416
HS3172	<i>lacera</i>	Caledonia		
IRD	<i>Oxypora</i>	New	Benzoni	LK022417
HS3203	<i>lacera</i>	Caledonia		
UNI	<i>Cynarina</i>	Mayotte	Benzoni	LK022418
MY011	<i>lacrymalis</i>			
IRD	<i>Cynarina</i>	New	Benzoni	LK022419
HS1604	<i>lacrymalis</i>	Caledonia		
UNI	<i>Lobophyllia</i>	Gulf of	Benzoni	LK022420
AD003	<i>corymbosa</i>	Aden		
UNI	<i>Lobophyllia</i>	Gambier	Benzoni	LK022421
GA024	<i>costata</i>			
UNI	<i>Lobophyllia</i>	Gulf of	Benzoni	LK022422
BA134	<i>hemprichii</i>	Aden		
UNI	<i>Lobophyllia</i>	Papua New	Benzoni	LK022423
PFB183	<i>robusta</i>	Guinea		
UNI	<i>Symphyllia</i>	Papua New	Benzoni	LK022424
PFB104	<i>agaricia</i>	Guinea		
UNI	<i>Symphyllia</i>	Gulf of	Benzoni	LK022425
BA107	<i>radians</i>	Aden		
IRD	<i>Symphyllia</i>	New	Benzoni	LK022426

HS3118	<i>recta</i>	Caledonia		
IRD	<i>Symphyllia</i>	New	Benzoni	LK022427
HS3135	<i>valenciennesii</i>	Caledonia		

5.3.2 Morphological analyses

Images of coral skeletons were taken with a Canon G5 digital camera and through a Leica M80 microscope equipped with a Leica IC80HD camera. For high resolution and deep field close ups of three-dimensional details of corallites and septa, a series of images of the same subject at different focus intervals were taken (approximately 10) and the images were fused using the Helicon Focus 5.3 software (Kozub et al., 2000–2012). To compare macromorphology and micromorphology of *P. vitiensis* and *A. rowleyensis* we used a subset of 21 characters from Budd et al. (2012) (Table 5.2). We adopted their character name, ID number (in brackets) and state names and, when relevant quantitative differences between the two species were observed within a character state, this information was added after it. Given the large size of the skeletal structures in *P. vitiensis* and *A. rowleyensis*, the majority of macromorphological and micromorphological characters considered in this study, with the notable exception of characters 43 (granule shape and distribution) and 44 (interarea) from Budd et al. (2012), were examined using light microscopy. Scanning Electron Microscopy (SEM) was used to analyze the shape and distribution of granules on septal faces and the interarea of teeth on representative specimens of *P. vitiensis* (UNIMIB PFB151) and one of *A. rowleyensis* (WAM Z65789). Specimens were mounted using silver glue, sputter-coated with conductive gold film and examined using a Vega Tescan Scanning Electron Microscopy at the SEM Laboratory, University of Milano–Bicocca. For glossary of skeletal terms we refer to Budd et al. (2012).

Abbreviations:

CC1: IRD CoralCal1 Expedition, Côte Oubliée, New Caledonia, 2007

CC4: IRD CoralCal4 Expedition, New Caledonia, IRD, 2012

CCAP: IRD CoralCap Expedition, New Caledonia, 2007

Cs: cycle of costosepta

IRD: Institut de Recherche pour le Développement, Nouméa, New Caledonia

NIUGINI: Niugini Biodiversity Expedition, Papua New Guinea, 2012

RMNH: Naturalis Biodiversity Center (former Rijksmuseum van Natuurlijke Historie), Leiden, the Netherlands

S: cycle of septa

UNIMIB: Università di Milano-Bicocca, Milan, Italy

WAM: Western Australian Museum, Perth, Australia

In the list of examined material for IRD specimens the station number (ST) is provided, when available, after the sampling locality. Station numbers can be searched in the IRD online database LagPlon (http://lagplon.ird.nc/consultv2_5/rechSimple.faces) where additional details on the reef habitat, GPS coordinates, and a map of each station can be found.

5.3.3 Molecular analyses

Whole genomic DNA was extracted from tissue samples using the DNeasy Blood and Tissue kit (Qiagen Inc., Valencia, CA, USA) according to the manufacturer's protocols. DNA concentration of extracts was quantified using a Nanodrop 1000 spectrophotometer (Thermo Scientific, Wilmington, DE, USA). A total of three molecular markers were amplified and sequenced for the majority of the specimens (Table 5.1): (1) a ~750 bp fragment of the cytochrome oxidase subunit I gene (COI) from mitochondrial DNA, (2) a ~350 bp portion of the nuclear histone H3, and (3) a ~800 pb portion of the ITS region, including the 3' end of 18S, the entire ITS1, 5.8S, and ITS2, and the 5' end of the 28S, as nuclear loci. COI was amplified using MCOIF - MCOIR primers (Fukami et al., 2004b) and the protocol by Benzoni et al. (2011), the histone H3 using H3F – H3R primers (Colgan et al., 1998), and the ITS region using ITS4 (Takabayashi et al., 1998) - A18S (White et al., 1990) primers and the protocol by Benzoni et al. (2011), or alternately using 1S and 2SS primers (Wei et al., 2003) and the protocol by Kitano *et al.* (2014). Sequencing was carried out by Genomics and Bioscience and

Technology Co., Ltd, Xizhi City, Taipei County, Taiwan. Sequences obtained in this study have been deposited in EMBL, and accession numbers are listed in Table 5.1.

Sequences were viewed, edited and assembled using CodonCode Aligner 4.2.5 (CodonCode Corporation, Dedham, MA, USA) and manually checked using BioEdit 7.2.5 (Hall, 1999). Alignments of the four separated datasets (three single gene trees and one concatenated) were carried out using the E-INS-i option in MAFFT 7.110 (Kato et al., 2002; Kato and Standley, 2013) under default parameters. *Plesiastrea versipora* (Lamarck, 1816) and several species from the family Merulinidae were selected as outgroups due their divergence from the family Lobophylliidae (Fukami et al., 2008; Kitahara et al., 2010; Benzoni et al., 2011). Indels, invariable, and parsimony informative sites were detected with DnaSP 5.10.01 (Librado and Rozas, 2009) and Indels were treated as a fifth character in phylogenetic analyses. Genetic distances and their standard deviation were calculated as *p*-distance with 500 bootstrap replicates using MEGA 5.2 (Tamura et al., 2011). To reconstruct the single gene trees Bayesian Inference (BI) and Maximum Likelihood (ML) analyses were used as implemented in MrBayes 3.1.2 (Ronquist and Huelsenbeck, 2003) and PhyML 3.0 (Guindon and Gascuel, 2003), respectively. The best-fit substitution model for each locus was determined using the Akaike Information Criterion (AIC) as implemented in MrModeltest 2.3 (Nylander, 2004) in conjunction with PAUP4.0b10 (Swofford, 2003). As most suitable models AIC selected the General Time-Reversible (GTR) model with a proportion of sites being invariable (+I) and the remainder following a gamma distribution (+I) for COI and rDNA, and the Kimura (K80) model with a proportion of invariable sites (+I) for histone H3.

The Maximum Likelihood (ML) tree was calculated with PhyML and a total of 500 bootstrap replicates were performed to assess the robustness of each clade. Four independent Markov Chain Monte Carlo (MCMC) runs were conducted for 1.4×10^7 generations for COI dataset (1.7×10^7 generations for histone H3 and 4×10^7 generations for ITS region) with trees sampled every 100 generation for each

analysis. The 25% first trees were discarded as burn-in, and posterior probabilities were estimated from the remaining trees in each run (10,500 remaining trees for COI, 12,750 for histone H3, and 30,000 for ITS region). To determine if the runs had achieved stationarity, we visualized log-likelihood scores and model parameter values across each run using Tracer 1.5 (Rambaut and Drummond, 2007). Finally, the three single gene datasets were concatenated in a single partitioned alignment and the phylogeny was reconstructed using Bayesian Inference and Maximum Likelihood analyses. Four independent Markov Chain Monte Carlo (MCMC) runs were conducted for 2.2×10^7 generations with trees sampled every 100 generation and the 25% first trees were discarded as burn-in. The ML tree was built in PhyML and a total of 500 bootstrap replicates were performed to assess the robustness of each clade. Branches with >70% bootstrap support values and >0.90 posterior probabilities are considered significantly supported.

5.4 Results

5.4.1 Macromorphology

In *P. vitiensis* coralla can be solitary (Figs. 5.1A, 5.2A–E) or colonial (Figs. 5.1B–D, 5.2F–I) and formed by intracalicular and extracalicular budding (*i. e.* Fig. 5.2I). In colonial coralla, as a result of circumoral budding, corallites are highly polymorphic (Figs. 5.2G–I) and corallite integration is uni- or multiserial. Corallum shape is generally flattened or concave (Figs. 5.1–5.2). Calice or valley width is larger than 2.5cm (Fig. 5.2) and variable. In some specimens the central part of the calice can have a shallow depression (Figs. 5.2D–F, H). Continuity of costosepta is mostly confluent in di-tricentric coralla (Figs. 5.2F–G), but becomes mostly not confluent in polycentric coralla (Fig. 5.2I; Veron and Pichon, 1980: Fig. 417). There are six cycles of septa in the calices, rarely seven (Fig. 5.2E; Chevalier, 1975), those of the sixth are free. Septa spacing is large, with 4-5 septa per 5mm (Figs. 5.4A–B). Relative costosepta thickness between Cs1 and Cs2 *versus* Cs3 is unequal (Figs. 5.5C–D). In polycentric coralla linkage between centres of adjacent

corallites within series is lamellar (Figs. 5.4B–C). Columella trabecular and spongy (indicated by arrows in Figs. 5.4B–C) and its size relative to calice width is less than 1/5 (Fig. 5.2). The endotheca is vesicular (Fig. 5.6A).

In *A. rowleyensis* coralla are flattened or massive and ‘helmet- or dome-shaped’ (Figs. 5.1E–H). Coralla are colonial as a result of primary circumoral budding and both intra and extracalicular budding occur (Fig. 5.3D–E). Corallites display polymorphism in smaller colonies where the central corallite is still larger as in the paratype WAM 173-84 (Veron, 1985: Fig. 25) and corallite integration is uni- or multiserial. Calice or valley width is large according to the character state in Budd *et al.* (2012) but smaller than 2.5 cm (Figs. 5.4D–F). Calices at the periphery of the coralla can be inclined and the part of their calice which is not adjacent to other calices can be wide (Figs. 5.3A–B, 5.6D). Continuity of costosepta is mostly confluent (Figs. 5.3A–E, 5.4E–F). There are four cycles of septa (Fig. 5.3D), those of the fourth are free. Septa spacing is large, with five septa per 5 mm (Figs. 5.4D–E). Relative costosepta thickness between Cs1 and Cs2 *versus* Cs3 is slightly unequal (Figs. 5.5A–B). Linkage between centres of adjacent corallites within a series is lamellar (Figs. 5.4D–F). Columella are trabecular and spongy (indicated by arrows in Figs. 5.4E–F) and the size relative to calice width less than or equal to 1/4 of calice width (Figs. 5.3D–E, 5.4D–F). The endotheca is vesicular (Figs. 5.6B–C).

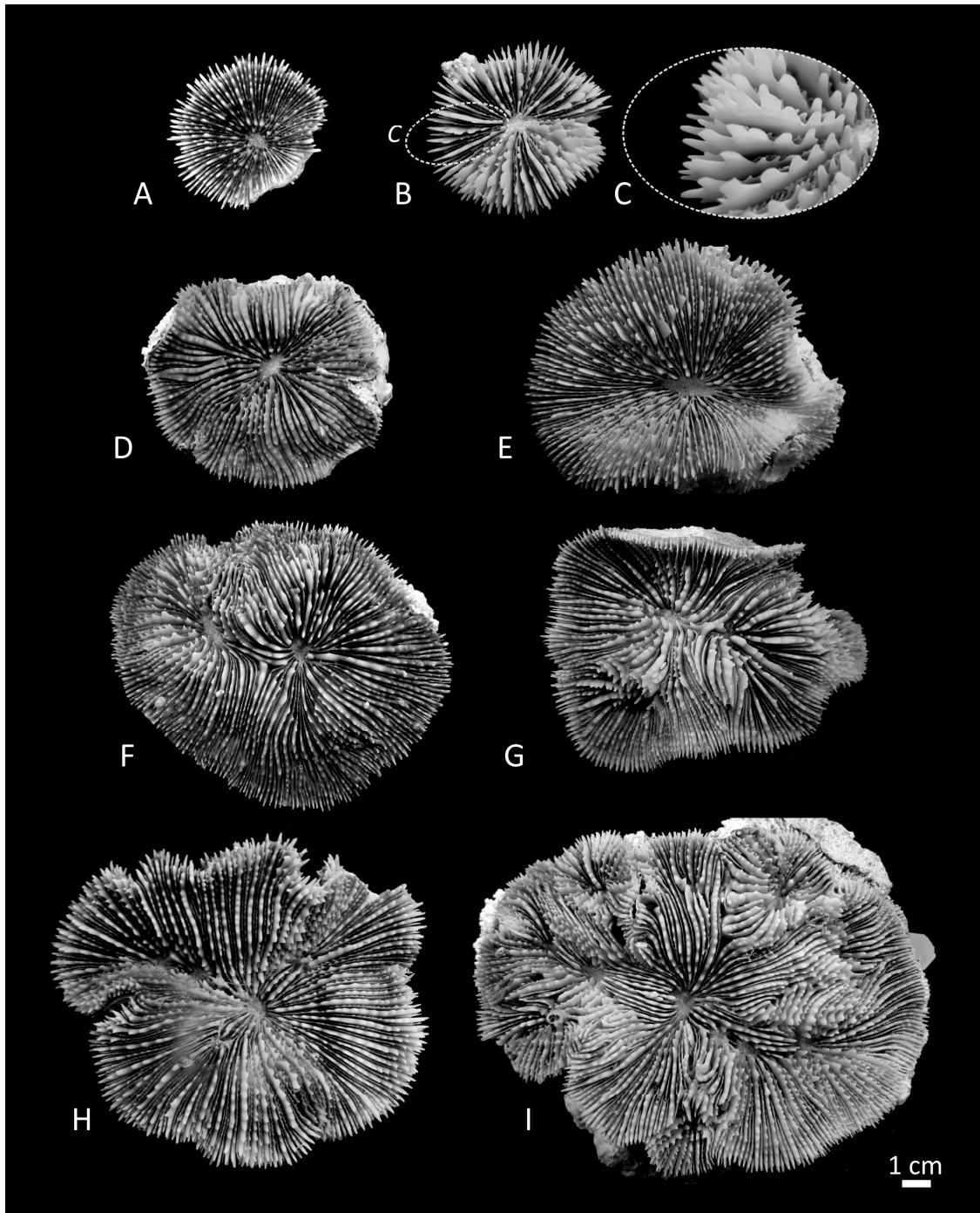


Figure 5.2. Corallum morphology in *Parascolymia vitiensis*: A) IRD HS3255; B) IRD HS2955; C) detail of the same specimen in B showing variability in shape and size of septal teeth; D) UNIMIB PFB031; E) IRD HS2985; F) UNIMIB PFB056; G) UNIMIB PFB055; H) IRD HS3139; I) UNIMIB PFB057. All specimens are in the phylogenetic trees in Figures 5.9, Apps. 5.1-5.3.

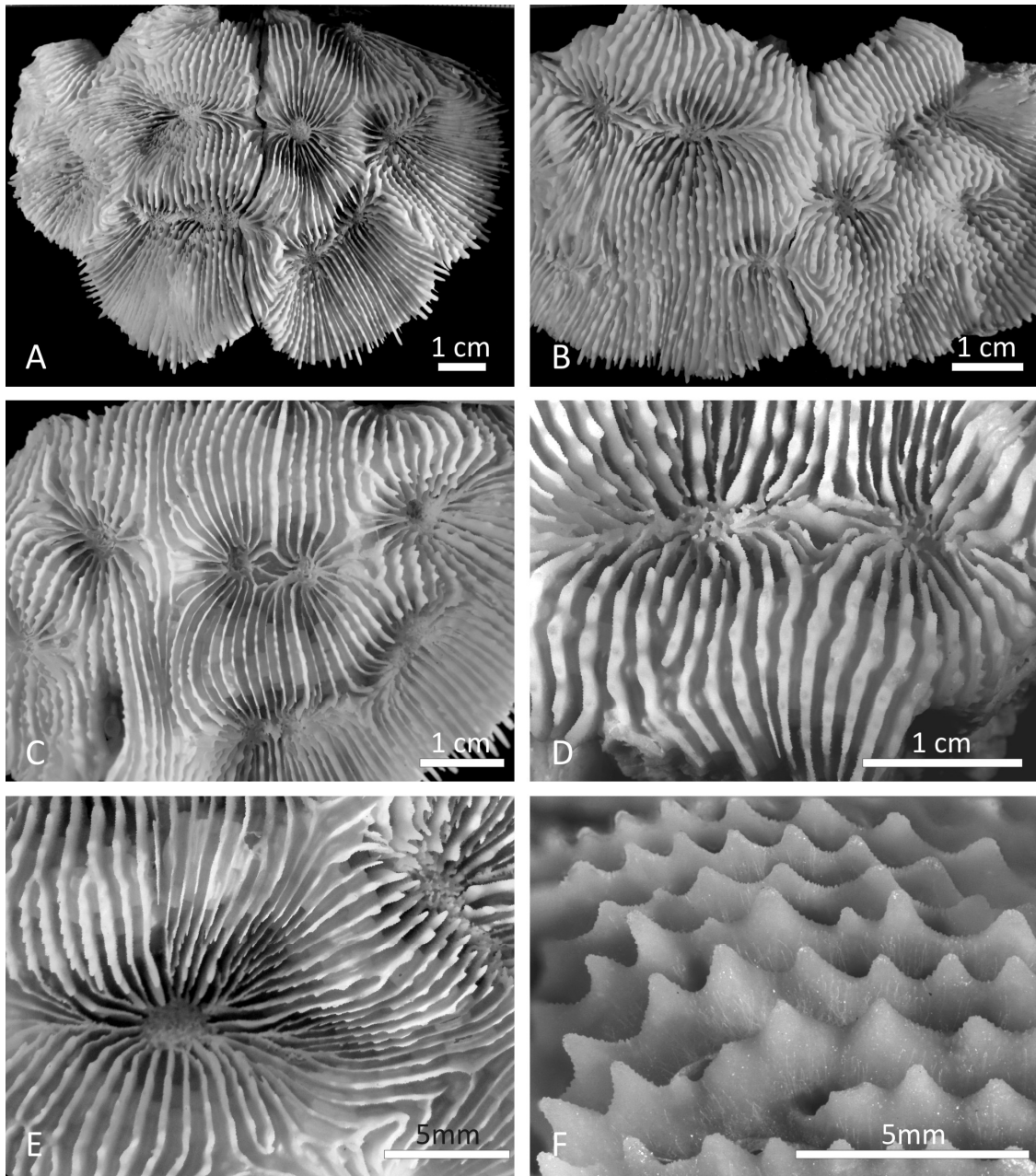


Figure 5.3. Corallum morphology in *Parascolyxia rowleyensis* (previously *Australomussa*): A) WAM Z65785; B) WAM Z65788; C) WAM Z65786; D) lamellar linkage between centres of adjacent corallites in same specimen as in B ; E) corallite polymorphism in the same specimen as in A; F) size and shape of costosepta in specimen WAM Z65787. All specimens are in the phylogenetic trees in Figures 5.9, Apps. 5.1-5.3.

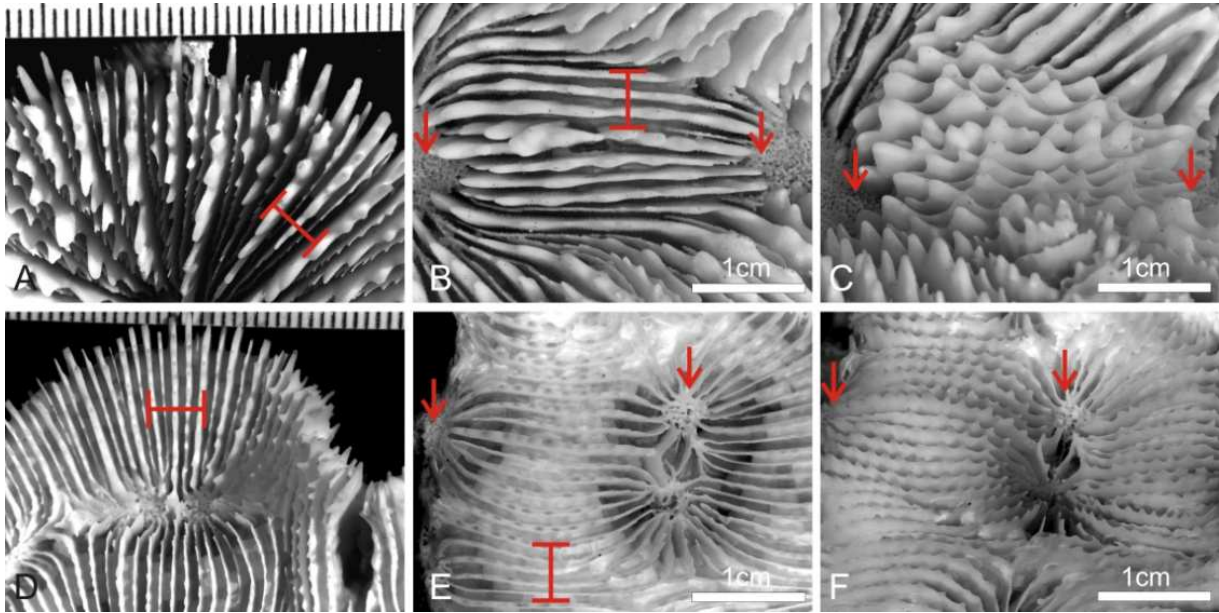


Figure 5.4. Comparison of the macromorphology of *Parascolymia vitiensis* (A-C) and *P. rowleyensis* (D-E): A) septa in the monocentric specimen IRD HS2964; B) top view of the costosepta in the polycentric specimen UNIMIB PFB057; C) side view of the same portion of the specimen in B; D) peripheral calices in specimen WAM Z65786; E) top view of the costosepta in the same specimen as D; F) side view of the same portion of the specimen in E. Red arrows indicate the position of the columella in adjacent corallites, red brackets placed perpendicularly to the costosepta show the number of costosepta intercepted by a 1 cm transect.

5.4.2 Micromorphology

In *P. vitiensis* tooth base at mid-septum is elliptical in shape and parallel to the direction of the septum (Figs. 5.5C-D). Tooth tips are irregular and overall mainly lobate (Figs. 5.5D, 5.7A-B, D). Teeth on S1 are 1mm or higher (Figs. 5.4C, 5.7) and their spacing is very wide, with adjacent teeth more than 2 mm apart. Tooth shape and size is very variable within and between septa (Fig. 5.7) as also noted by previous authors (Chevalier, 1975; Veron and Pichon, 1980) with some teeth becoming round in section towards the tip and having an overall pointed, or spiniform Chevalier (1975), shape (Fig. 5.7C). Granulation on the side of septa is weak and granules are enveloped by thickening deposits (Figs. 5.7A-B). The inter-area structure is generally smooth (Fig. 5.5D) or with palisade. Tooth shape between Cs3 and Cs1 is unequal (Figs. 5.5C-D).

In *A. rowleyensis* tooth base at mid-septum is elliptical in shape and parallel to

the direction of the septum (Figs. 5.5A–B). Tooth tips are irregular and lobate (Figs. 5.5B, 5.8). Teeth on S1 range between 0.8 – 0.9 mm (Figs. 5.4F, 5.8) and their spacing is wide, with adjacent teeth between 1 and 2 mm apart. Granulation on the side of septa is strong and granules are scattered (Figs. 5.5B, 5.8A). The inter-area structure has a palisade structure (Figs. 5.8A). Tooth shape between Cs3 and Cs1 is equal (Fig. 5.5B). In general, in this species tooth shape is not very variable within and between septa (Figs. 5.5A-B) especially when compared to the variability described in *P. vitiensis*.

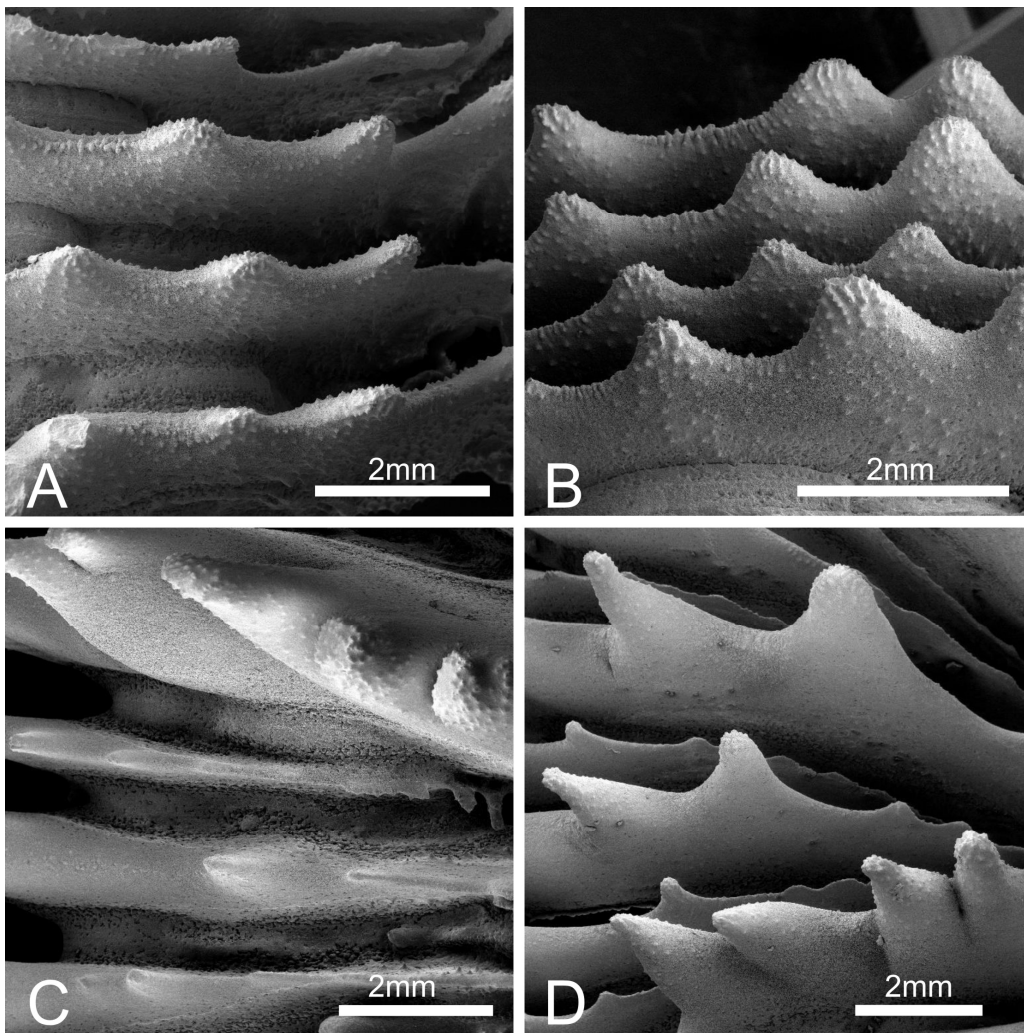


Figure 5.5. SEM images of radial elements of *Parascolymia rowleyensis* (previously *Australomussa*) (WAM Z65789: A-B) and *P. vitiensis* (UNIMIB PFB151: C-D): A) top view of septa reaching the wall; B) side view of septa of different cycles showing some variability in septal teeth size between cycles but overall homogeneous shape; C) top view of septa reaching the wall; D) side view of septa of different cycles showing high variability in septal teeth size and shape between cycles.

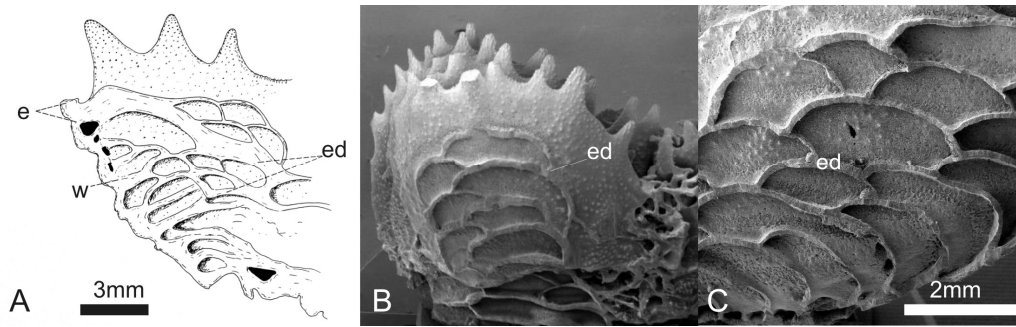


Figure 5.6. Vesicular endotheca: A) longitudinal section of the periphery of a calice of *Parascalymia vitiensis* (modified from Chevalier, 1975: Fig. 190); B) SEM image of a longitudinal section along the septa of *P. rowleyensis* (WAM Z65789); C) detail of vesicular endothecal dissepiments in the same specimen as in B. e = epitheca; w = wall; ed = endothecal dissepiments.

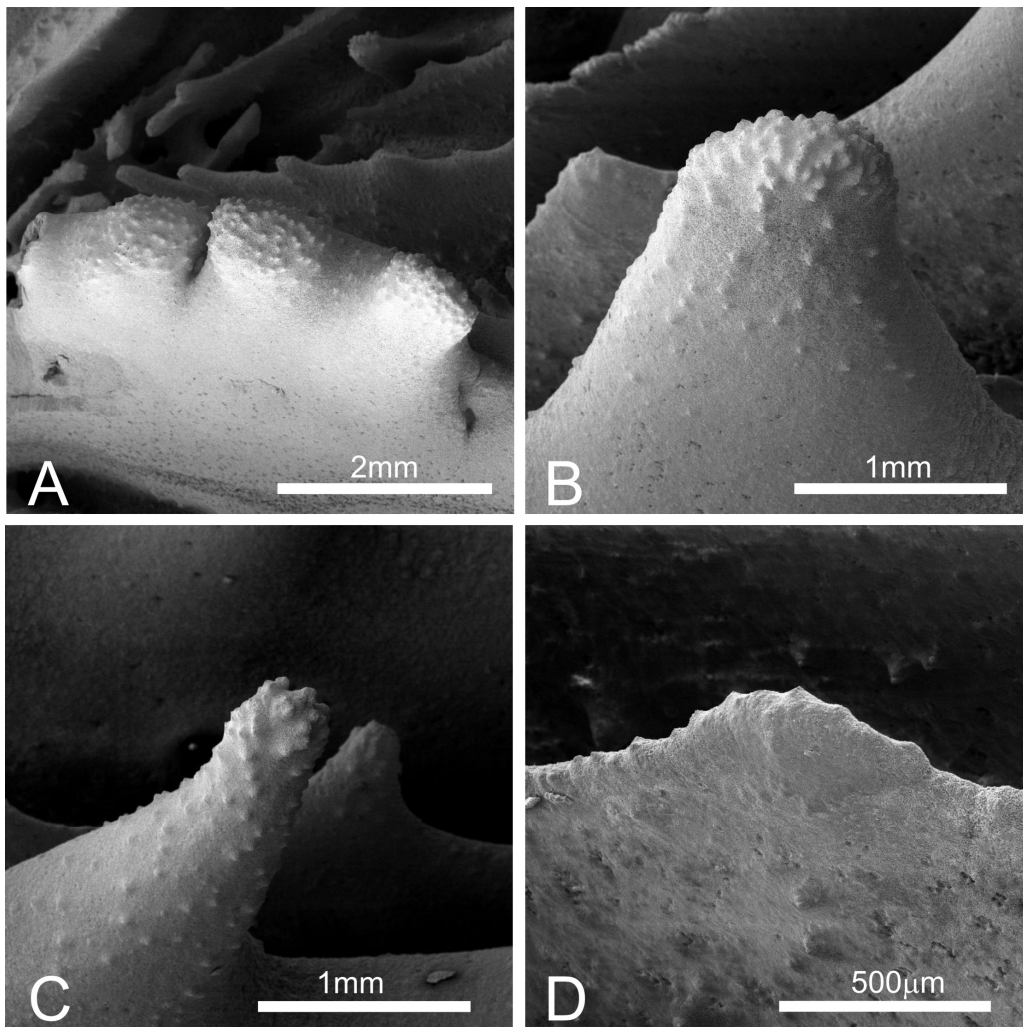


Figure 5.7. SEM of *Parascalymia vitiensis* (UNIMIB PFB151): A) top view of a S1 showing its thickness and clumped teeth; B) side view of an S2 septum tooth; C) side view of an S2 septum tooth, note the difference in shape of the tooth tip compared to B; D) side view of an S5 septum tooth.

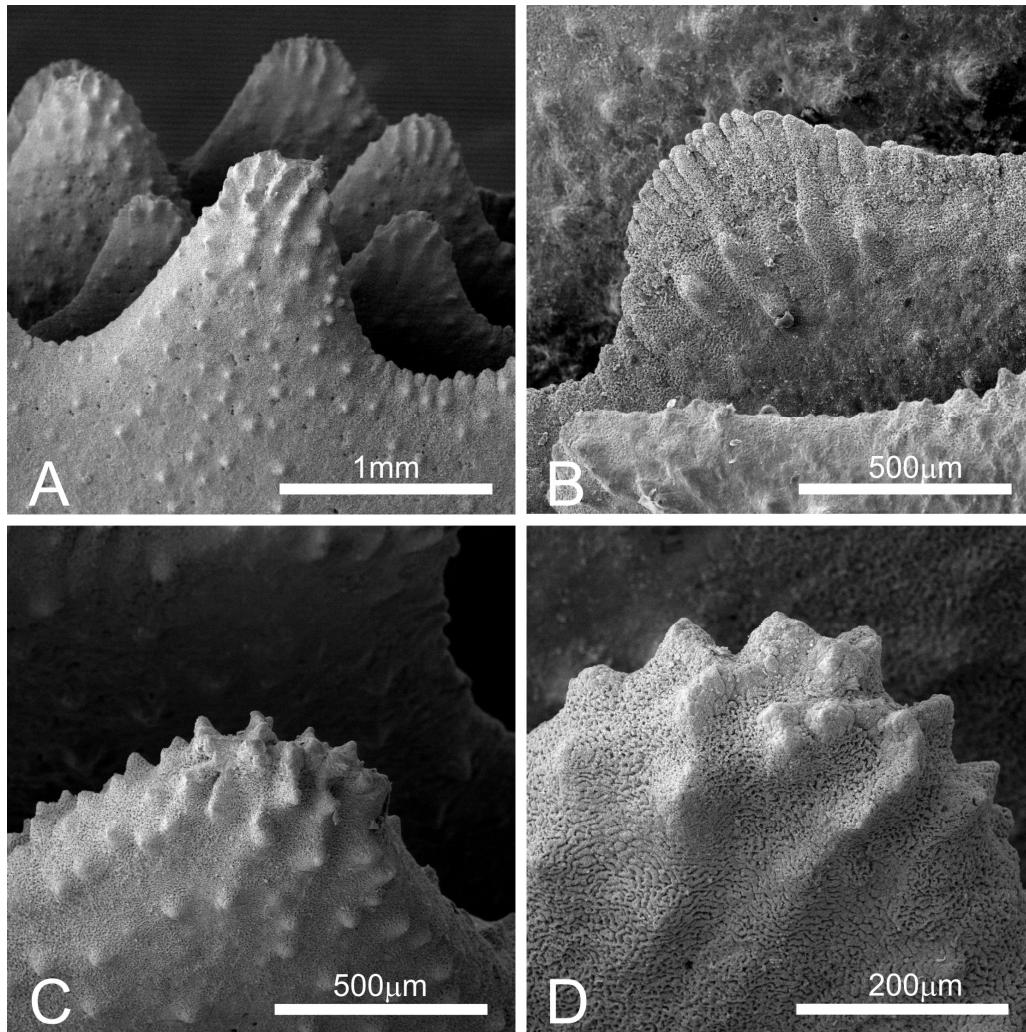


Figure 5.8. SEM of *Parascolymia rowleyensis* (previously *Australomussa*) (WAM Z65789): A) side view of septa of different cycles showing homogeneous shape of septum teeth between cycles; B) side view of an S4 septum tooth; C) side view of an S2 septum tooth showing granulation; D) side view of the tip of an S1 septum tooth.

5.4.3 Molecular analyses

The final alignment of COI data consisted of 580 bp, of which 48 were parsimony informative sites, with a total of 84 mutations. The aligned histone H3 matrix was 318 bp long with 86 parsimony informative sites and 122 mutations. The total alignment of ITS region was composed by 951 bp, 160 parsimony informative sites and 294 mutations. No intra-individual polymorphisms or double peaks were observed in the chromatograms of the two nuclear loci, thereby avoiding the need to clone the amplified fragments. The phylogeny reconstruction of the combined molecular data is in Fig. 5.9, while the three single gene trees are

in the Supplementary Information (Apps. 5.1-5.3). Phylogenetic analyses under BI and ML criteria yielded congruent results, with no contrasting signals. Bayesian topologies with significant branch support indicated by ML bootstrapping support (MLs) and Bayesian posterior probability scores (BIs) are reported in Figs 5.9 and Apps. 5.1-5.3.

The phylogram based on the concatenated (COI, histone H3, and ITS) molecular dataset shows high ML and BI supports at all key nodes (Fig. 5.9). Clade I *sensu* Arrigoni et al. (2014a) contains all species of *Lobophyllia* and *Symphyllia* analyzed so far and all our sequences of *A. rowleyensis* and *P. vitiensis*. The latter two species group together in a strongly supported lineage (MLs = 100 and BIs = 0.9) and their genetic boundaries remain unclear being indistinguishable from each other with these molecular markers. The average genetic distance of *A. rowleyensis* from *P. vitiensis* is $1.1 \pm 0.2\%$, while genetic variability within *A. rowleyensis* is $1.1 \pm 0.3\%$ and within *P. vitiensis* is $0.7 \pm 0.2\%$. The majority of the other species in this clade, *L. costata* (Dana, 1846), *L. robusta* Yabe, Sugiyama and Eguchi, 1936, *S. agaricia* Milne Edwards and Haime, 1849, *S. radians*, *S. recta* (Dana, 1846), and *S. valenciennesii* Milne Edwards and Haime, 1849 are recovered as monophyletic lineages. The only exceptions are represented by *L. corymbosa* and *L. hemprichii* (Ehrenberg, 1834) that are not monophyletic and nested in two distinct lineages.

The Bayesian COI topology (App. 5.1) indicates that all newly obtained sequences of *A. rowleyensis* and *P. vitiensis* are nested together with the genera *Lobophyllia* and *Symphyllia* within clade I (MLs = 94% and BIs = 0.93). While the two species are not monophyletic and they occur together in two main groups within clade I, the mitochondrial phylogenetic reconstruction is similar to that of the nuclear histone H3 (App. 5.2). Again, all newly obtained sequences of *A. rowleyensis* and *P. vitiensis* form clade I *sensu* Arrigoni et al. (2014a) (MLs = 95% and BIs = -) together with several species of *Lobophyllia* and *Symphyllia*. Clade I is composed of 10 species represented by a total of 28 sequences, of which 26 share the same haplotype and they are thus identical, while the remaining two sequences

differ from the others by only one bp substitution. Moreover, all of the Merulinidae subclades defined by Budd and Stolarski (2011) and Huang et al. (2011) are recovered with the exception of D/E. Interestingly, also in the family Lobophylliidae, all of the molecular clades defined by Arrigoni et al. (2014a) based on COI and rDNA molecular markers, except F, are supported in our BI and ML analyses. The Bayesian topology obtained from the ITS region alignment is similar to both COI and histone H3ones, but has a higher resolution at species level with significant supports for the majority of key nodes (App. 5.3). Again, all our sequences of *A. rowleyensis* and *P. vitiensis* are found together in a strongly supported group (MLs = 90 and BIs = 1) within clade I (App. 5.3). A similar situation is apparent for *L. hemprichii* and *S. agaricia* which occur in a strongly supported monophyletic group. The other *Lobophyllia* and *Symphyllia* species within clade I, *i.e.* *L. costata*, *L. diminuta* Veron, 1985, *L. flabelliformis* Veron, 2000, *L. robusta*, *S. erythraea* (Klunzinger, 1879), *S. radians*, *S. recta*, and *S. valenciennesii*, are recovered as monophyletic lineages, while the only specimen of *Acanthastrea ishigakiensis* Veron, 1990 is closely related to *S. recta*.

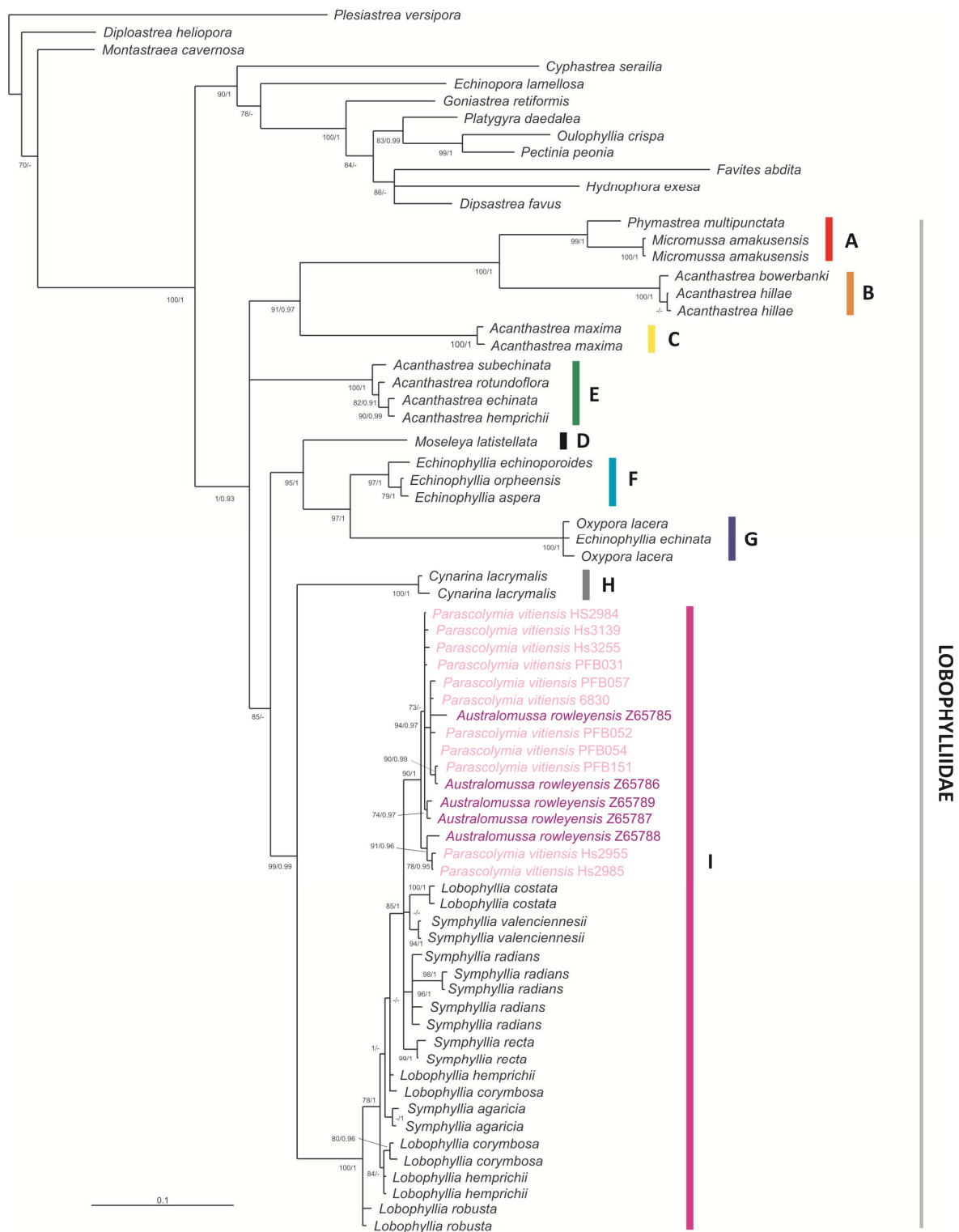


Figure 5.9. Phylogenetic position of *Parascolymia vitiensis* and *P. rowleyensis* (previously *Australomussa*) and their relationships within the family Lobophylliidae based on concatenated matrix (COI, histone H3, and ITS region). Bayesian topology is shown. Numbers associated with branches indicate Maximum Likelihood bootstrap (>70%) support (left) and Bayesian posterior probabilities (>0.9) (right). Clades within Lobophylliidae are coloured and labelled A to I according to Arrigoni et al. (2014a).

5.5 Taxonomic account

5.5.1 Examined material

Parascolymia vitiensis (Brüggemann, 1877)

Australia – (AIMS monograph coral collection, Coll. M. Pichon and J.E.N. Veron): MTQ G43171 Esk Island, Palm Islands, QLD (18°46'S; 146°31'E), 1-22m; MTQ G43207 Hook Island, Whitsunday Islands, QLD (20°04'S; 148°57'E), 2-8m; (Coll. A. Baird): 6830 Great Barrier Reef, Orpheus Island, Little Pioneer Bay (18°36'S, 146°29' E), 23/05/2013; 6816 Great Barrier Reef, Orpheus Island, Little Pioneer Bay (18°36'S, 146°29' E), 23/05/2013; **Papua New Guinea** – (NIUGINI, Coll. F. Benzoni): UNIMIB PFB031, site PCT50, 10/11/2012; UNIMIB PFB032, PCT50, 10/11/2012; UNIMIB PFB052, PCT44 Kranget Island (-5,18927; 145,8273), 11/11/2012; UNIMIB PFB053, PCT44 Kranget Island (-5,18927; 145,8273), 11/11/2012; UNIMIB PFB054, PCT44 Kranget Island (-5,18927; 145,8273), 11/11/2012; UNIMIB PFB055, PCT44 Kranget Island (-5,18927; 145,8273), 11/11/2012; UNIMIB PFB056 PCT44 Kranget Island (-5,18927; 145,8273), 11/11/2012; UNIMIB PFB057, PCT44 Kranget Island (-5,18927; 145,8273), 11/11/2012; UNIMIB PFB151, PCT29, Paeowa Island (-5,1745; 145,8334), 13/11/2012; PFB152, PCT29 Paeowa Island (-5,1745; 145,8334), 13/11/2012; **New Caledonia** – (CC1, Coll. F. Benzoni and G. Lasne): IRD HS1440, ST1069, 19/03/2007; IRD HS1443, ST1069, 19/03/2007; IRD HS1452, ST1069, 19/03/2007; IRD HS1456, ST1069, 19/03/2007 - (CCAP, Coll. F. Benzoni and G. Lasne): IRD HS1722, ST1117, 30/10/2007; IRD HS1740, ST1119, 31/10/2007; IRD HS1796, ST1121, 01/11/2007; IRD HS1812, ST1123, 02/11/2007- (CC4, Coll. F. Benzoni): IRD HS2955, ST1452, 06/04/2012; IRD HS2964, ST1453, 06/04/2012; IRD HS2984, ST1455, 07/04/2012; IRD HS2985, ST1455, 07/04/2012; IRD HS3139, ST 1469, 16/04/2012; IRD HS3255, ST 1479, 22/04/2012.

Australomussa rowleyensis Veron, 1985

Australia – (Woodside Collection (Kimberley) Expeditions 2009-2012, Coll. Z. Richards): WAM Z65785, Stn. 114/K12, Patricia Is. (14.25.298°S; 125.30.443°E) 12m, 22/10/2012 (K10); WAM Z65789, Stn. 6, Adele Is. (15.26.676°S; 123.10.249°E) 12m, 15/10/2009 (K60); WAM Z65788, Stn. 9/K12, Adele Is. (15.30.248°S; 123.05.766°E) 12m, 16/10/2009 (K93); WAM Z65787, Stn. 75/K12, Beagle Reef (15.35.217S; 123.53.654°E) 12m, 20/10/2011 (K94); WAM Z65786, Stn. 78/K12, Mavis Reef (15.50.519°S; 123.60.824°E) 12m, 21/10/2012 (K141); **Solomon Islands** – (Coll. E. Turak) MTQ G57901 Santa Isabel Island, Palunhukura (07°50.8'S; 158°43.3'E), 2-26m, 16/05/2004; **Indonesia** – (Coll. B.W. Hoeksema) RMNH Coel. 23309, W Sumatra, off Padang, Gusung Sipakal reef, 02/05/1995; RMNH Coel. 24941, SW Sulawesi, Spermonde Archipelago, Kudingareng Keke reef, 22/05/1996; RMNH Coel. 24178, SW Sulawesi, Spermonde Archipelago, Bone Lola reef, 11m, 05/03/1996.

5.5.2 Taxonomy

Based on the aforementioned molecular data and morphologic observations discussed above, *Australomussa* is considered a junior synonym of *Parascolymia* and *A. rowleyensis* is hereafter formally moved to this genus.

Order Scleractinia Bourne, 1900

Family Lobophylliidae Dai and Horng, 2009

Genus *Parascolymia* Wells, 1964

TYPE SPECIES: *Scolymia vitiensis* Brüggemann, 1877, p. 304

REVISED DIAGNOSIS: Corallum attached, monocentric or polycentric by intracalicular and extracalicular budding. Corallite can display polymorphism. Corallite integration uni or multiserial. Calice or valley width is large (see Budd et al. 2012). Continuity of costosepta mostly confluent in polycentric coralla. Septa of the last cycle free. Septa spacing large. Relative costosepta thickness between Cs1

and Cs2 *versus* Cs3 unequal or slightly unequal. In polycentric coralla linkage between centres of adjacent corallites within series is lamellar. Columella trabecular and spongy. Endotheca vesicular. Septal tooth base at mid-septum is elliptical in shape and parallel to the direction of the septum. Tooth tips irregular and lobate. Teeth on S1 high and their spacing is wide. The inter-area structure is generally smooth or with palisade. Tooth shape between Cs3 and Cs1 equal or unequal.

SPECIES INCLUDED:

Parascolymia vitiensis (Brüggemann, 1877)

Scolymia vitiensis Brüggemann, 1877, p. 304; Veron 2000, p. 68, figs 1–7; Hoeksema and Van Ofwegen, 2004; Dai and Horng, 2009, p. 71, figs 1–2; Turak and DeVantier, 2011, p. 174.

Scolymia cf vitiensis Veron and Pichon, 1980, pp. 244–250, figs 410, 411, 413–417.

Parascolymia vitiensis (Brüggemann, 1877) Budd and Stolarski, 2009, figs 2, 4, 6–7, 9, 11; Budd *et al.*, 2012, fig 4; Arrigoni *et al.*, 2014a, fig 2.

TYPE MATERIAL: The holotype (1862.2.4.49) is deposited at NHMUK.

TYPE LOCALITY: Fiji.

Parascolymia rowleyensis (Veron, 1985)

Australomussa rowleyensis Veron, 1985, p.171, figs 23–25; Veron, 2000, p. 80, figs 1–5; Hoeksema and Van Ofwegen, 2004; Dai and Horng, 2009, p. 69, figs 1-2; Turak and DeVantier, 2011, p. 175.

TYPE MATERIAL: The holotype (907) is deposited at WAM. Two paratypes (172-84 from Mermaid Reef, Rowley Shoals, Western Australia, 183-84 from Phuket Peninsula, western Thailand) are deposited at WAM.

TYPE LOCALITY: Legendre Island, Dampier Archipelago, Western Australia.

5.6 Discussion

In this study we explore the gross- and fine-scale morphology and the phylogeny of the two traditionally described monotypic genera *Australomussa* and *Parascolymia*. We provide a detailed description of diagnostic micromorphological characters of *A. rowleyensis* and *P. vitiensis* and we define the phylogenetic position of both these two species within the family Lobophylliidae using three molecular markers. As a result we propose a taxonomic revision for the genus *Australomussa* and we formally consider *Australomussa* as a junior synonym of *Parascolymia*.

5.6.1 Morphology of *P. rowleyensis* and *P. vitiensis* and consequences for taxonomy

The lack of genetic resolution between *P. vitiensis* and *P. rowleyensis* in all our molecular analyses might suggest that these two species are in fact synonyms. The skeleton morphology, however, indicates that although the two species share some macro- and micromorphologic character, they are morphologically distinct and they have a different state for 10 of the 21 characters used by Budd et al. (2012) (in bold in Table 5.2).

Veron (1985) stated that *Australomussa* ‘differs from *Symphyllia* in having an initial central corallite which buds daughter corallites extracalicularly, in lacking meandering valleys (which some *Symphyllia* ecomorphs also lack) and in having widely separated series of centres without a true common wall between them’. However, he provided no detailed information on the morphologic characters that differentiate *Australomussa* from *Parascolymia* (= *Scolymia*). Our observations of the macro- and micromorphology of *P. rowleyensis* and *P. vitiensis* confirm that these species share a number of characters, namely intracalicular and extracalicular budding, corallite polymorphism associated with circumoral budding, uni or multiserial corallite integration, free septa, wide septa spacing with less than six septa per 5mm, discontinuous linkage between corallite centres (lamellar linkage), a trabecular spongy columella, a vesicular endotheca, septum tooth elliptical at the

base, and irregular lobate tooth tips (Table 5.2). Nevertheless *P. vitiensis* has wider calices or series, a larger variability of continuity of costosepta over the wall, more cycles of septa, different relative costosepta thickness, a smaller columella size relative to calice width, higher and more widely spaced septum teeth, weakly developed septa granulation, a smoother inter-area structure, and unequal tooth shape between costosepta of different cycles (Table 5.2 in bold). We propose therefore that these morphological differences are sufficient to distinguish two species despite the fact that the unresolved genetic boundaries based on multiple markers strongly argue against retaining the species as distinct. Thus we formally consider *Australomussa* as a junior synonym of *Parascolymia* and retain *P. vitiensis* and *P. rowleyensis* as separate sister species.

In *P. vitiensis* the teeth in different septal cycles differ significantly in shape as already discussed by Veron and Pichon (1980) and Budd and Stolarski (2009). In *P. rowleyensis* the teeth in different septal cycles do not differ significantly in shape as described by Veron (1985) in the species original description. The type specimen of *P. rowleyensis* displays an obvious variability of thickening of costosepta between specimens as remarked by Veron (1985). However, the variability of shape and size of septal dentation is far more reduced in this species than in *P. vitiensis*. One of the specimens of *P. rowleyensis* in the series we examined, Z65786, has relatively thin septa and costosepta and is similar in this respect to the paratype WAM 173-84 (Veron, 1985: Fig. 25). The remainder have a similar thickness of costosepta to the holotype WAM 171-84 (Veron, 1985: Fig. 23). However, none of the specimens we examined in this study has radial elements as thick as paratype WAM 172-84 (Veron, 1985: Fig. 24). The thickness of radial elements of this paratype comes close to that of the radial elements of higher cycles of some *P. vitiensis*. Nevertheless, the number of septal cycles, and the relative thickness of septa from different cycles, as well as the size of the dentation of the septa fall within the range of *P. rowleyensis* rather than in that of *P. vitiensis*.

Table 5.2. Macromorphology and micromorphology of *Parascolymia vitiensis* and *P. rowleyensis* (previously *Australomussa*). Explanation of characters, their ID numbers (in brackets) and state names are from Budd et al. (2012). * = character examined on polycentric coralla; Csn= number of cycle of costosepta; Sn = number of cycle of septa. Names of characters which have different states in the two species in bold.

Character	<i>P. vitiensis</i>	<i>P. rowleyensis</i> (previously <i>Australomussa</i>)		
Macromorphology	Intracalicular budding (1)	Present *	Present	
	Extracalicular budding (2)	Present *	Present	
	Circumoral budding and associated corallite polymorphism (3)	Present *	Present	
	Corallite integration (4)	Uni or multiserial *	Uni or multiserial	
	Calice or valley width (7)	Large, >2.5cm	Large, <2.5cm	
	Continuity of costosepta (9)	Mostly not confluent *	Mostly confluent	
	Number of septa (10)	4 cycles	6-7 cycles	
	Free septa (11)	Present	Present	
	Septa spacing (per 5mm) (12)	Wide, <6	Wide, <6	
	Relative costosepta thickness (Cs1andCs2 -vs- Cs3) (13)	Unequal	Slightly unequal	
	Corallite centres linkage (14)	Discontinuous by lamellar linkage	Discontinuous by lamellar linkage	
	Columella structure (15)	Trabecular spongy	Trabecular spongy	
	Columella size relative to calice width (16)	Small, <1/4	Small to medium, ≤1/4	
	Endotheca (19)	Abundant/vesicular	Abundant/vesicular	
	Micromorphology	Tooth base (mid-septum) (35)	Elliptical parallel	Elliptical parallel
		Tooth tips (38)	Irregular lobate	Irregular lobate
Tooth height (S1) (39)		High, and ≥ 1mm	High, but <1mm	
Tooth spacing (S1) (40)		Very wide, >2mm	Wide, 1-2mm	
Granules shape and distribution (43)		Weak enveloped by thickening depositis	Strong scattered	
Interarea structure (44)		Smooth and palisade	Palisade	
Cs3/Cs1 tooth shape (45)		Unequal	Equal	

In some genera of lobophylliids (*e.g. Lobophyllia, Symphyllia, Parascolymia*), the teeth in different septal cycles differ significantly in shape while in other genera (*e.g. Acanthastrea* and *Homophyllia*) such differentiation is not observed (Budd and Stolarski, 2009). Our results confirm that the size and shape of septal teeth of *P. vitiensis* is highly variable within and between septa of the same specimen (Chevalier, 1975; Veron and Pichon, 1980; Budd and Stolarski, 2009) (Figs. 5.4A–C, 5.5C–D, 5.7). The remarkable variation of these characters in *P. vitiensis*, and their within and between septa variability was also described by other authors (Veron and Pichon, 1980) and led Chevalier (1975) to describe the variety

dentorotundata (namely, with rounded teeth) for some specimens from New Caledonia (*i.e.* Figs. 5.2B–C). However, in *P. rowleyensis* the variability in size and shape of septal teeth is much less developed, with septal and costoseptal teeth being of more uniform size and shape than in *P. vitiensis* (for *P. rowleyensis* see Figs. 5.4D–F, 5.5A–B, 5.8).

5.6.2 Molecular phylogeny of *P. rowleyensis* and *P. vitiensis*

Our multi-locus molecular analyses showed that *P. rowleyensis* belongs to the family Lobophylliidae (Fig. 5.9), as proposed by Dai and Horng (2009) and Budd et al. (2012) based on the macromorphology of the colony and on traditional taxonomy (Veron, 1985, 1992, 2000). Moreover, the species, traditionally ascribed to the monotypic genus *Australomussa*, does not occur in a distinct molecular clade, rather it is nested within the well-supported clade I *sensu* Arrigoni *at al.* (2014a), which comprises the genera *Lobophyllia*, *Symphyllia*, and *Parascolymia* (Fig. 5.9).

Parascolymia rowleyensis and *P. vitiensis* could not be separated in any single gene tree or the concatenated phylogeny (Fig. 5.9, Apps. 5.1–5.3) and the intraspecific and interspecific divergences within and between the two species completely overlap. The lack of genetic variation suggests that these two nominal species could be just one species or that lineage sorting is incomplete because the two species have a recent common ancestor. The former explanation is unlikely because *P. rowleyensis* and *P. vitiensis* differ in several micromorphological characters (Table 5.2) and, therefore, it is more likely these two species have not completely diverged although divergence time estimates are not available. An alternative hypothesis is hybridization between the two species, as reported for other genera (Diekmann et al., 2001; van Oppen et al., 2002a; Vollmer and Palumbi, 2004; Richards et al., 2008). However, the lack of intra-individual polymorphism in nuclear sequences of both species and the absence of intermediate morphologies challenges this hypothesis.

5.6.3 Utility of the examined molecular markers

The three single gene trees gave congruent phylogeny reconstructions (Apps. 5.1-5.3), however higher resolution at the species level was achieved by the ITS region (App. 5.3). The best overall BI and ML support was obtained for the concatenated dataset (Fig. 5.9).

The scleractinian COI gene is usually characterized by low evolution rate and consequently by an overlap of intraspecific and interspecific divergences that do not allow this marker to be used as a barcoding gene in the order Scleractinia (Hellberg, 2006; Shearer and Croffroth, 2008; Huang et al., 2008). The main exception to this general scenario in scleractinian corals is *Stylophora pistillata* Esper, 1797, for which Keshavmurthy et al. (2013) detected four deeply divergent lineages corresponding to four particular geographic regions. COI can also be informative when combined or compared in multi-marker analyses (Fukami et al., 2008; Forsman et al., 2009; Huang et al., 2011; Benzoni et al., 2011, 2012a; Gittenberger et al., 2011) (Fig. 5.4, App. 5.1). This mitochondrial region does however resolve the majority of the inner nodes, *i.e.* older relationships, within the family Lobophylliidae (this study and Arrigoni et al., 2012, 2014a), Fungiidae Dana, 1846 (Gittenberger et al., 2011), and Poritidae Gray, 1842 (Kitano et al., 2014). In our phylogenetic reconstruction based on this mtDNA region, *P. vitiensis* and *P. rowleyensis* are nested within clade I (*sensu* Arrigoni et al., 2014a) but they appear to be polyphyletic (App. 5.1). The intra-specific variability of *P. vitiensis* ($0.9 \pm 0.2\%$) and *P. rowleyensis* ($0.9 \pm 0.2\%$) overlaps the inter-specific distance between the two species ($0.9 \pm 0.2\%$) and the last value is comparable to the mean closest congeneric inter-specific distances among Anthozoa ($0.71 \pm 0.15\%$) found by Huang et al. (2008).

The nuclear histone H3 gene has been extensively used in phylogenetic studies of arthropods (Colgan et al., 1998; Maxmen et al., 2003), annelids (Novo et al., 2011), and mollusks (Colgan et al., 2000; Pola and Gosliner, 2010) because it is easily amplifiable, highly conserved at the amino acid level, (transiently) highly

expressed, and the presence of multiple histone repeats is an uncommon feature (Colgan et al., 1998, 2000; Maxson et al., 1983). It has recently been used in a coral phylogenetic analysis by Huang et al. (2011, 2014b) where it supported all higher-level lineages within the Merulinidae except clade D/E. Our phylogeny reconstruction based on histone H3 resolved all molecular clades within the Lobophylliidae with high node-support values (App. 5.2). These results suggest that histone H3 could be used to evaluate the broad-base phylogeny of other families, in both the Robust and Complex groups, and the phylogenetic relationships among their genera.

The ITS region has been extensively used to resolve species boundaries in scleractinian corals (Diekmann et al., 2001; Forsmann et al., 2009; Benzoni et al., 2010, 2012b, 2012b, 2014; Flot et al., 2011; Gittenberger et al., 2011; Stefani et al., 2011; Schmidt-Roachet et al., 2013a; Arrigoni et al., 2012, 2014a; Keshavmurthy et al., 2013; Kitano et al., 2013, 2014). Despite the phylogenetic utility of this marker being questioned because of its unique pattern of secondary structure in the genus *Acropora* Oken, 1815 (van Oppen et al., 2002a; Vollmer and Palumbi, 2004; Chen et al., 2004; Wei et al., 2006), it is currently accepted and considered as the most suitable molecular locus to resolve phylogenetic relationships among closely related species. Here, the ITS region resolved the majority of lobophylliid species (App. 5.3), except for species in clade E (Arrigoni et al., 2014a). Within clade I (sensu Arrigoni et al., 2014a) the majority of species included were monophyletic, with the notable exception of *P. rowleyensis* and *P. vitiensis*. Therefore, these results confirmed the usefulness of this marker in phylogenetic studies and we strongly encourage its application for the delimitation of species boundaries in scleractinian corals until new highly variable markers are discovered.

In conclusion, this study demonstrated that comprehensive studies conducted both at molecular and micromorphological levels are and will be essential to evaluate the evolutionary relationships of scleractinian corals and their taxonomy. We strongly believe that different disciplines, such as morphology, molecular systematics, ecology, and reproduction, should be used for taxonomical studies to

reach a more complete and comprehensive approach towards the understanding of coral species diversity and biogeography.

– CHAPTER 6 –

*Forgotten in the taxonomic literature: resurrection
of the scleractinian coral genus *Sclerophyllia*
(*Scleractinia*, *Lobophylliidae*) from the Arabian Peninsula
and its phylogenetics relationships*

Roberto Arrigoni¹, Michael Lee Berumen², Tullia Isotta Terraneo^{1,2}, Annalisa Caragnano¹, Jessica Bouwmeester², Francesca Benzoni¹

¹ Department of Biotechnologies and Biosciences, University of Milan – Bicocca, Piazza della Scienza 2, 20126, Milan, Italy

² Red Sea Research Center, King Abdullah University of Science and Technology, 23955 Thuwal, Kingdom of Saudi Arabia

³ Institut de Recherche pour le Développement, UMR227 CoReUs2, 101 Promenade Roger Laroque, 98848 Noumea, New Caledonia

In press in *Systematics and Biodiversity*:

DOI, [10.1080/14772000.2014.978915](https://doi.org/10.1080/14772000.2014.978915)

6.1 Abstract

The monospecific scleractinian coral genus *Sclerophyllia* Klunzinger, 1879 was originally described from Al-Qusayr (Egypt) in the Red Sea based on a series of solitary specimens. Thenceforth, it has been considered a junior synonym of *Symphyllia* and *Cynarina* based on corallum macromorphology. In this study, several specimens of *Sclerophyllia margariticola* were collected on the coasts of Saudi Arabia in the northern and central Red Sea. Four molecular markers were sequenced, COI and the intergenic spacer between COI and 1-rRNA from mitochondrial DNA and Histone H3 and ribosomal ITS2 from nuclear DNA. Phylogenetic trees and haplotype network analyses show that *S. margariticola* belongs to the family Lobophylliidae and that it is closely related to *Acanthastrea maxima*, an uncommon species from waters around the Arabian peninsula (the Gulf of Aden, Arabian Sea, Gulf of Oman, and Persian Gulf). *Sclerophyllia margariticola* and *A. maxima* share several macro- and micromorphological characters, such as the presence of free septa, high elliptical septal teeth perpendicular to the septal margin, irregular lobate tips, very wide tooth spacing, a very strong granulation with granules scattered all along the septal sides, and a palisade interarea structure, and their micromorphology differs substantially from that of *Acanthastrea echinata*, the type species of *Acanthastrea*. Therefore, we formally resurrect *Sclerophyllia*, provide a revised diagnosis for the genus, and move *A. maxima* into *Sclerophyllia*.

6.2 Introduction

The scleractinian coral family Lobophylliidae Dai and Horng, 2009 has been defined in detail by Budd et al. (2012) based on the combination of phylogenetic analyses of mitochondrial and nuclear data (Fukami et al., 2004a, 2008) and micromorphological and microstructural observations (Budd and Stolarski, 2009; Budd et al., 2012). To date, the family includes 11 extant genera and 52 species distributed in the Red Sea, Indian Ocean, and Pacific Ocean (Veron, 2000; Budd et

al., 2012; Benzoni, 2013; Arrigoni et al., 2014b). Evolutionary relationships within this group were poorly understood until a comprehensive molecular phylogeny reconstruction of the Lobophylliidae showed that the family is monophyletic, whereas the majority of genera as previously described, e.g. *Acanthastrea* Milne Edwards and Haime, 1848, *Echinophyllia* Klunzinger, 1879, *Lobophyllia* de Blainville, 1830, *Micromussa* Veron, 2000, *Oxypora* Saville Kent, 1871, and *Symphyllia* Milne Edwards and Haime, 1848 are not (Arrigoni et al., 2014a). In the same study the need of formal taxonomic actions in this family was highlighted pending detailed micromorphological and microstructural analyses performed on a larger dataset of species, as already done for the families Acroporidae Verrill, 1902 (Wallace et al., 2007), Fungiidae Dana, 1846 (Gittenberger et al., 2011), Merulinidae Verrill, 1865 (Huang et al., 2011, 2014a, 2014b), Mussidae Ortmann, 1890 (Budd et al., 2012), Poritidae Gray, 1842 (Kitano et al., 2014), Coscinaraeidae Benzoni et al. 2012a, and Psammocoridae Chevalier and Beauvais, 1987 (Benzoni et al., 2007, 2010, 2012a). A first step in this direction for the family Lobophylliidae led to the revision of the genus *Australomussa* Veron, 1985, now a junior synonym of *Parascolymia* Wells, 1964 based on an integrated morpho-molecular approach (Arrigoni et al., 2014b).

One of the unresolved and complex issues concerning the taxonomy and systematics of the Lobophylliidae is the validity of the genera representing solitary corals *Acanthophyllia* Wells, 1937, *Cynarina* Brüggemann, 1877, *Homophyllia* Brüggemann, 1877, *Indophyllia* Gerth, 1921, *Rhodocyathus* Bourne, 1905, *Parascolymia* Wells, 1964, *Protolobophyllia* Yabe and Sugiyama, 1935, and *Sclerophyllia* Klunzinger, 1879 (Matthai, 1928; Wells, 1964; Veron and Pichon, 1980). Several monostomatous species have been described and ascribed to distinct solitary genera based on the macromorphology of the corallum (Best and Hoeksema, 1987; Brüggemann, 1877; Wells, 1937, 1964). All these genera were subsequently considered junior synonyms of the genera *Lobophyllia* or *Symphyllia* with colonial coralla on the assumption that they represented early monocentric stages of the latter (Matthai, 1928; Wells, 1937; Vaughan and Wells, 1943). Other

authors synonymized some genera of these monostomatous corals with each other, for example *Sclerophyllia* as a junior synonym of *Cynarina* (Wells, 1964), and recognized only a few valid genera (Wells, 1964; Chevalier, 1975; Veron and Pichon, 1980). Nowadays, *Cynarina* and *Homophyllia* are the only two monostomatous taxa assigned to the family (Budd et al., 2012) while the valid genus *Parascalymia* has been shown to consist of monocentric and polystomatous corals (Chevalier, 1975; Veron and Pichon, 1980; Arrigoni et al., 2014b).

The monospecific genus *Sclerophyllia* was described by Klunzinger (1879) based on a series of monocentric specimens collected in the northern Red Sea, in Al-Qusayr (Egypt). *S. margariticola* is solitary and the corallite outline is circular or elliptical (Klunzinger, 1879). According to its original description, corallites are up to 3-4 cm in diameter, two times larger than the height, and contain numerous (60-96) septa arranged in five orders of which the first two or three are thicker than the others (Klunzinger, 1879). In this species, the columella is well developed and elliptical in outline, and composed of a mass of anastomosing trabeculae (Klunzinger, 1879). Notably, all of the samples recorded by Klunzinger (1879) were attached to big pearl oyster shells even though the author did not mention a specific number of specimens and only showed two syntypes (Klunzinger, 1879, p. 5, pl. 1, fig. 12). *S. margariticola* Klunzinger, 1879 was also reported from Djibouti by Gravier (1907, 1911) and by Vaughan (1907), who based this new geographic record on three specimens collected by Gravier. Subsequently, the species was mentioned as *Symphyllia margariticola* (Montanaro-Gallitelli, 1943) but this was a misidentification according to Wells (1964). Moreover, *Sclerophyllia* was considered a junior synonym of *Symphyllia* (Matthai, 1928; Wells, 1937; Vaughan and Wells, 1943) and of *Cynarina* Milne Edwards and Haime, 1849 (Wells, 1964; Veron and Pichon, 1980). The latter synonymy has never been contradicted by later authors (Veron, 2000; Budd et al., 2012) and, hence, the genus has not been considered valid since the work of Gravier (1911).

In 2013, surveys conducted along the coasts of Saudi Arabia as part of the project “Biodiversity in the Saudi Arabian Red Sea” organized by the King

Abdullah University of Science and Technology (KAUST) allowed the collection of several specimens matching the original description and illustration of *S. margariticola* in the northern and central Red Sea from 20 to 60 m depth. The availability of this material thus prompted the re-examination of the taxonomic status of this long-forgotten species from a morpho-molecular point of view. Therefore, in this study we test the validity of the genus *Sclerophyllia* and its phylogenetic relationships within the family Lobophylliidae (Arrigoni et al., 2014a) by sequencing four molecular markers, the mitochondrial regions cytochrome c oxidase subunit I (COI) and the non-coding intergenic spacer region (IGR) between COI and large ribosomal RNA subunit (l-rRNA) and the nuclear loci Histone H3 and the internal transcribed spacer 2 (ITS2). Moreover, we explore the gross- and fine-scale morphology of *S. margariticola* and compare it with that of other lobophylliid species that are genetically closely related to it.

6.3 Material and methods

6.3.1 Sampling

Fifteen specimens of *Sclerophyllia margariticola*, five colonies of *Acanthastrea echinata* (Dana, 1846), and a specimen of *Cynarina lacrymalis* were collected from 5 to 60 m depth along the Saudi Arabia coast of the Red Sea at various localities from the Gulf of Aqaba to Thuwal in March and September 2013 within the KAUST project “Biodiversity in the Saudi Arabian Red Sea” (Figs. 6.1, 6.2–6.9). Seven colonies of *A. maxima* were collected along the coasts of Yemen at Balhaf, Al Mukallah, and at Socotra Island in the Gulf of Aden during several missions between 2007 and 2010 within the frame of the Total EandP - Creoccean - University of Milano-Bicocca “Yemen Scleractinia Biodiversity Project” (Figs. 6.1, 6.10–6.17).

Corals were photographed *in situ* with an underwater Canon G9 digital camera in an Ikelite housing prior to collection (Figs. 6.2–6.9, 6.10–6.17). Coral samples were collected, tagged, and preserved in 95% ethanol for molecular analyses (Table

6.1). After DNA extraction, each corallum was bleached in sodium hypochlorite, rinsed with freshwater, and air-dried for identification and morphological analyses. Corals were identified examining the type material and following Klunzinger (1879), Pichon et al. (2010), Sheppard and Salm (1988), and Sheppard and Sheppard (1991).

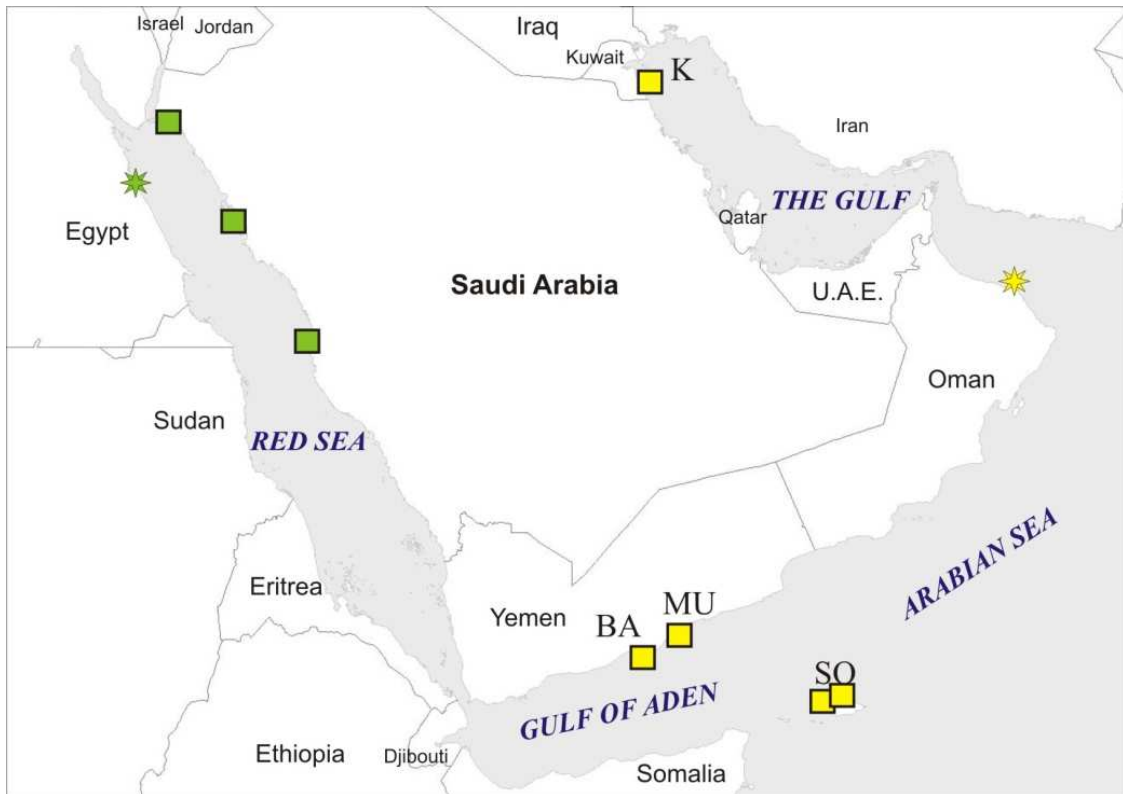
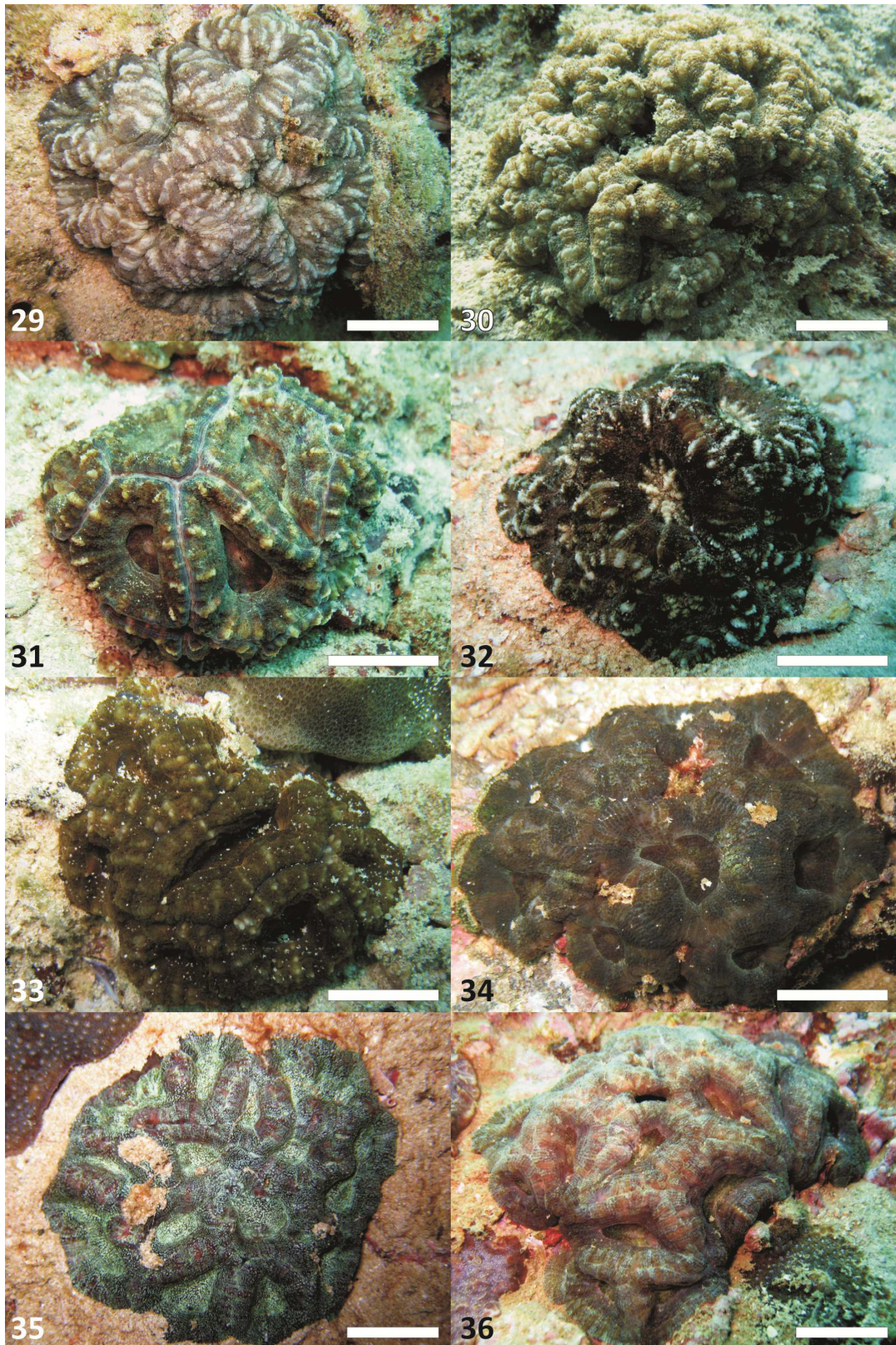


Figure 6.1. Map of the type and sampling localities of *S. margariticola* (green) and *S. maxima* (previously *Acanthastrea*) (yellow) for this study. Squares indicate sampling localities, stars indicate type localities. BA = Bir Ali, Yemen; MU = Al Mukallah, Yemen; SO = Socotra Island; K = Kuwait.



Figures 6.2-6.9. *Sclerophyllia margariticola* in situ: **6.2**, encrusting round-shaped corallum, KAUST SA880; **6.3**, round-shaped corallum, KAUST SA932; **6.4**, oval-shaped corallum, KAUST SA1016; **6.5**, triangular-shaped corallum, KAUST SA934; **6.6**, cyathiform oval-shaped corallum with obvious paliform lobes, KAUST SA976; **6.7**, cyathiform oval-shaped corallum, KAUST SA977; **6.8**, round-shaped corallum, KAUST SA1297; **6.9**, round-shaped corallum with obvious paliform lobes, KAUST SA1298. Scale bars represent 1 cm.



Figures 6.10-6.17. *Sclerophyllia maxima* (previously *Acanthastrea*) *in situ*: **6.10**, UNIMIB SO131; **6.11**, colony at Al Mukallah, Yemen; **6.12**, UNIMIB BA136; **6.13**, UNIMIB MU163, Yemen; **6.14**, UNIMIB SO132; **6.15**, colony at Al Mukallah, Yemen; **6.16**, colony at Burum, Yemen; **6.17**, colony at Al Mukallah, Yemen. Scale bars represent 1 cm.

Table 6.1. Voucher number, identification, collection site, and EMBL accession numbers of the samples used for molecular and morphological analyses in this study. Source: ^a Arrigoni et al. (2014b); ^b Arrigoni et al. (2012); ^c Arrigoni et al. (2014a).

Code	Identification	Locality	H3	COI	ITS2	IGR
BA136	<i>Sclerophyllia maxima</i>	Gulf of Aden, Yemen	LK022406 ^a	HE654626 ^b	HE648542 ^b	LM993358
MU161	<i>Sclerophyllia maxima</i>	Gulf of Aden, Yemen	LK022407 ^a	HE654627 ^b	HE648543 ^b	LM993359
MU163	<i>Sclerophyllia maxima</i>	Gulf of Aden, Yemen	LM993306	HE654628 ^b	HE648544 ^b	LM993360
MU203	<i>Sclerophyllia maxima</i>	Gulf of Aden, Yemen	LM993307	HF954210 ^c	HF954297 ^c	LM993361
SO131	<i>Sclerophyllia maxima</i>	Socotra, Yemen	LM993308	LM993329	LM993346	LM993362
SO132	<i>Sclerophyllia maxima</i>	Socotra, Yemen	LM993309	HF954211	HF954298	LM993363
SA880	<i>Sclerophyllia margariticola</i>	Red Sea	LM993310	LM993330	LM993347	LM993364
SA881	<i>Sclerophyllia margariticola</i>	Red Sea	LM993311		LM993348	LM993365
SA932	<i>Sclerophyllia margariticola</i>	Red Sea	LM993312	LM993331	LM993349	LM993366
SA933	<i>Sclerophyllia margariticola</i>	Red Sea	LM993313	LM993332	LM993350	LM993367
SA934	<i>Sclerophyllia margariticola</i>	Red Sea	LM993314	LM993333	LM993351	LM993368
SA935	<i>Sclerophyllia margariticola</i>	Red Sea	LM993315	LM993334	LM993352	LM993369
SA975	<i>Sclerophyllia margariticola</i>	Red Sea	LM993316	LM993335	LM993353	LM993370
SA976	<i>Sclerophyllia margariticola</i>	Red Sea	LM993317	LM993336	LM993354	LM993371
SA977	<i>Sclerophyllia margariticola</i>	Red Sea	LM993318	LM993337		LM993372
SA1014	<i>Sclerophyllia margariticola</i>	Red Sea	LM993319		LM993355	LM993373
SA1015	<i>Sclerophyllia margariticola</i>	Red Sea	LM993320	LM993338	LM993356	LM993374
SA1016	<i>Sclerophyllia margariticola</i>	Red Sea	LM993321		LM993357	LM993375
SA1017	<i>Sclerophyllia margariticola</i>	Red Sea	LM993322	LM993339		LM993376
SA019	<i>Acanthastrea echinata</i>	Red Sea	LM993323	LM993340		
SA375	<i>Acanthastrea echinata</i>	Red Sea	LM993324	LM993341		
SA1009	<i>Acanthastrea echinata</i>	Red Sea	LM993325	LM993342		
SA1041	<i>Acanthastrea echinata</i>	Red Sea	LM993326	LM993343		
SA1145	<i>Acanthastrea echinata</i>	Red Sea	LM993327	LM993344		
SA473	<i>Cynarina lacrymalis</i>	Red Sea	LM993328	LM993345		

6.3.2 DNA extraction, amplification, and sequence analyses

Genomic DNA was extracted from tissue samples using the standard procedure implemented in the DNeasy Tissue Kit (Qiagen, Valencia, California). The barcoding portion of COI was amplified using MCOIF – MCOIR primers (Fukami et al., 2004a) and the protocol by Benzoni et al. (2011). The IGR between COI and 1-rRNA was amplified using MNC1F – MNC1R primers (Fukami et al., 2004b; Huang et al., 2009) and a thermal cycler profile of 94° for 2 min, 35 cycles of 94° for 45 sec, 53° for 1 min, 72° for 1 min, with a final phase of 72° for 5 min. Histone H3 was amplified using H3F – H3R primers (Colgan et al., 1998) and ITS2 was amplified using ITS4 (Takabayashi et al., 1998) – A18S (White et al., 1990) primers and the protocol proposed by Benzoni et al. (2011). All PCR products were purified with Illustra ExoStar (GE Healthcare, Buckinghamshire, United Kingdom) and directly sequenced in forward and reverse directions using an ABI 3130xl Genetic Analyzer (Applied Biosystems, Carlsbad, California). Chromatograms of products obtained using primers ITS4 – A18S did not show any intra-individual polymorphisms or double peaks, thereby allowing direct sequencing of ITS2. Sequences obtained in this study were deposited in EMBL, and accession numbers are listed in Table 6.1.

Histone H3 and COI allow inference at a higher systematic level due to their low evolution rates in scleractinian corals (Colgan et al., 1998; Hellberg, 2006; Huang et al., 2008) and they have been demonstrated to be powerful in the definition of genus boundaries, especially within merulinids and lobophylliids (Fukami et al., 2008; Huang et al., 2011, 2014b; Arrigoni et al., 2012, 2014a, 2014b). Furthermore we define the genetic boundaries between species throughout haplotype network analyses of ITS2 and IGR, as already reported for other taxa (Benzoni et al., 2007; Stefani et al., 2007; Flot et al., 2008, 2011; Schmidt-Roach et al., 2013a). Recently, the complete mitochondrial genome of *Acanthastrea maxima* was published (Arrigoni et al., 2014c) which showed that the IGR between COI and 1-rRNA (580 bp), represents the second largest intergenic region of the entire

mitogenome, and thus promises to be a suitable variable marker for this species.

Sequences were viewed, edited, and assembled using CodonCode Aligner 4.2.5 (CodonCode Corporation, Dedham, MA, USA) and manually checked using BioEdit 7.2.5 (Hall, 1999). Alignments of the four separate datasets were carried out using the E-INS-i option in MAFFT 7.110 (Kato et al., 2002; Kato and Standley, 2013) under default parameters. Genetic distances and their standard deviation were calculated as *p*-distance with 1000 bootstrap replicates using MEGA 5.2 (Tamura et al., 2011). Prior to the phylogenetic analysis, the Akaike Information Criterion in MrModeltest 2.3 (Posada and Crandal, 1998) was used to determine the appropriate substitution model of sequence evolution that best fitted the data. The preferred model of nucleotide substitution was Hasegawa-Kishino-Yano (HKY) with gamma-distributed rate heterogeneity ($\Gamma = 0.175$) for COI and Kimura (K80) with gamma-distributed rate heterogeneity ($\Gamma = 0.171$) for Histone H3. We conducted phylogenetic analyses using Bayesian inference (BI) and maximum-likelihood (ML) methods for the separate COI and Histone H3 datasets. We performed BI analyses using MrBayes 3.1.2 (Ronquist and Huelsenbeck, 2003). Four independent Markov Chain Monte Carlo (MCMC) were run for 2.5×10^7 generations and trees were sampled every 100th generation for the COI partition, while we used 3×10^7 generations with trees sampled every 100th generation for Histone H3. Based on the parameter estimations and convergence examined by Tracer (Rambaut and Drummond, 2007), the first 25% of trees were discarded as burn-in. We performed ML analyses in PhyML 3.0 (Guindon and Gascuel, 2003) and node support for the two separated gene trees was examined using 1000 bootstrap replicates. The trees include the posterior probabilities (PP) from BI and bootstrap support values (B) from the ML analysis in this order (Figs. 18, 19). Posterior probability values were considered statistically significant when $PP \geq 0.95$ and bootstrap support values when $B \geq 70$.

We constructed a median-joining network (Bandelt et al., 1999) for separate IGR and ITS2 datasets using Network 4.6.1.2 (<http://www.fluxus-technology.com>) in order to define species boundaries between *S. margariticola* and *A. maxima*

(Figs. 6.20–6.21). The median-joining method uses a maximum parsimony approach to search for all the shortest phylogenetic trees of given dataset (Bandelt et al., 1999).

6.3.3 Morphological analyses

Scleractinian coral samples were analyzed both at macro- and micromorphological levels using light microscopy and SEM, respectively. Images of coral skeletons were taken with a Canon G5 digital camera as well as through a Leica M80 microscope equipped with a Leica IC80HD camera. For scanning electron microscope (SEM) imaging, fragments of specimens were grinded, mounted on stubs using silver glue, sputter-coated with conductive gold film and examined using a Vega Tescan Scanning Electron Microscope at the University of Milano-Bicocca. Specimens were sputter-coated with Au-Pd and imaged using a Quanta 200 FEG SEM at the King Abdullah University of Science and Technology. For a glossary of skeletal terms we follow Budd et al. (2012).

6.3.4 Ancestral character state reconstruction

In order to reconstruct ancestral state evolution of the character “development of multiple mouths” within the family Lobophylliidae, we performed an ancestral character state reconstruction mapping this character onto a reduced taxa ML tree using Maximum Parsimony method with Mesquite 2.75 (Maddison and Maddison, 2011). The reduced taxa ML tree contained only one representative for each lobophylliid species for which sequences of COI, Histone H3 and rDNA are available (App. 6.1). The concatenated alignment consisted of 1845 bp for 30 taxa and ML analysis was performed with PhyML 3.0 (Guindon and Gascuel, 2003), as described in the previous section. *Plesiastrea versipora* (Lamarck, 1816), *Diploastrea heliopora* (Lamarck, 1816), and *Montastraea cavernosa* (Linnaeus, 1767) were selected as outgroups (Fukami et al., 2008; Budd et al., 2012). The following three character states were assigned: 0 as polystomatous (= colonial) for all species with the exception of *Sclerophyllia margariticola*, *Cynarina lacrymalis*

and *Parascolymia vitiensis*, 1 as monostomatous (= solitary) for *S. margariticola* and *C. lacrymalis*, and 2 as polystomatous or monostomatous for *P. vitiensis* (Brüggemann, 1877) (Fig. 6.22).

6.3.5 Museum collections and other examined specimens

Type material and specimens examined for this study are deposited in different institutions listed hereafter.

Abbreviations:

KAUST: King Abdullah of Science and Technology, Thuwal, Kingdom of Saudi Arabia

MNHN: Muséum National d'Histoire Naturelle, Paris, France

NHM: Natural History Museum, London, UK

UNIMIB: University of Milano-Bicocca, Milan, Italy

ZMB: Museum für Naturkunde, Berlin, Germany

The holotype of *Acanthastrea maxima* (1986.11.17.2) is deposited at NHM. Although various specimens of *Sclerophyllia margariticola* were mentioned by Klunzinger (1879) and illustrations of two syntypes were published (App. 6.2), only specimen ZMB Cni 2181 is available and hereby designated lectotype. The original descriptions and illustrations of both species were used as reference.

6.4 Results

6.4.1 Phylogenetic and haplotype network analyses

The four molecular markers were analyzed separately. The final alignment of Histone H3 consisted of 318 bp with a total of 90 polymorphic sites of which 77 were parsimony-informative, while the partial COI gene matrix was composed of 609 bp and 70 sites were variable (40 parsimony-informative). The ITS2 dataset contained 247 total characters of which 27 were polymorphic and 19 were parsimony-informative, whilst the total alignment of IGR consisted of 744 sites (9

variable and parsimony-informative characters).

Plesiastrea versipora was selected as outgroup in both Histone H3 and COI phylogenetic trees because of its divergence from the families Lobophylliidae, Merulinidae Verrill, 1865, Diploastreidae Chevalier and Beauvais, 1987, and Montastraeidae Yabe and Sugiyama, 1941 (Fukami et al., 2008; Huang et al., 2011; Benzoni et al., 2011; Budd et al., 2012).

The results of BI and ML analyses for both separate Histone H3 and COI datasets are similar, despite the presence of some differences between the two main topologies (Figs. 6.18, 6.19). For example, the phylogenetic reconstruction based on Histone H3 recovered a sister relationship between clade E and G that it is not present in the COI analysis. Moreover the inter-relationships between clades H, D, and (E, F, G, and I) are better resolved in the mitochondrial tree than in the nuclear one.

In detail, phylogeny reconstruction based on Histone H3 (Fig. 6.18) recovers the family Lobophylliidae as monophyletic group (PP = 0.97 and B = 95) while the monophyly of the Merulinidae is supported though not as strongly (PP = - and B = 73). The Diploastreidae form the sister-group to the Merulinidae and the Lobophylliidae, while the Montastraeidae are at the base of the tree. Within the lobophylliid clade, the majority of the nine main genus-level lineages proposed by Arrigoni et al. (2014a), based on a concatenated COI and rDNA analyses, are resolved with low or moderate branch supports using Histone H3 locus. *Sclerophyllia margariticola* and *Acanthastrea maxima* cluster together in the strongly supported clade C (PP = 1 and B = 100) and, notably, all of the newly obtained Histone H3 sequences of these two species share the same exclusive haplotype. Furthermore *S. margariticola* and *A. maxima* are not related to clade E, which comprises the majority of *Acanthastrea* species and the genus type species *Acanthastrea echinata*, and clade H, composed by the solitary species *Cynarina lacrymalis*.

The evolutionary relationships among lobophylliids investigated with the partial COI gene (Fig. 6.19) are congruent with Histone H3 phylogenetic reconstruction.

Within this family, the mitochondrial tree confirms all of the nine major lineages, although support for Clade E is lacking. Again, *S. margariticola* and *A. maxima* form a strongly supported clade C (PP = 1 and B = 87). Moreover, concordantly to Histone H3 analysis, *S. margariticola* and *A. maxima* are highly divergent regarding both *A. echinata* and the other species of *Acanthastrea* found in clade E, and *C. lacrymalis* in clade H.

Haplotype network analyses of *S. margariticola* and *A. maxima* based on the molecular loci ITS2 and IGR are reported in Figs. 6.20–6.21. In both networks, no haplotypes are shared between the two species even if *S. margariticola* and *A. maxima* are weakly distinguished in both analyses. A total of four haplotypes are identified for IGR: two related haplotypes differing by two base changes for the six samples of *A. maxima* and two other haplotypes specific of the thirteen specimens of *S. margariticola* that differ by three mutations, while *A. maxima* and *S. margariticola* haplotypes are separated by four to nine base pairs substitutions (Fig. 6.20). Two major clusters corresponding to the two species *A. maxima* and *S. margariticola* can be revealed in the ITS2 haplotype network (Fig. 6.21) as already weakly shown in the IGR haplotype one.

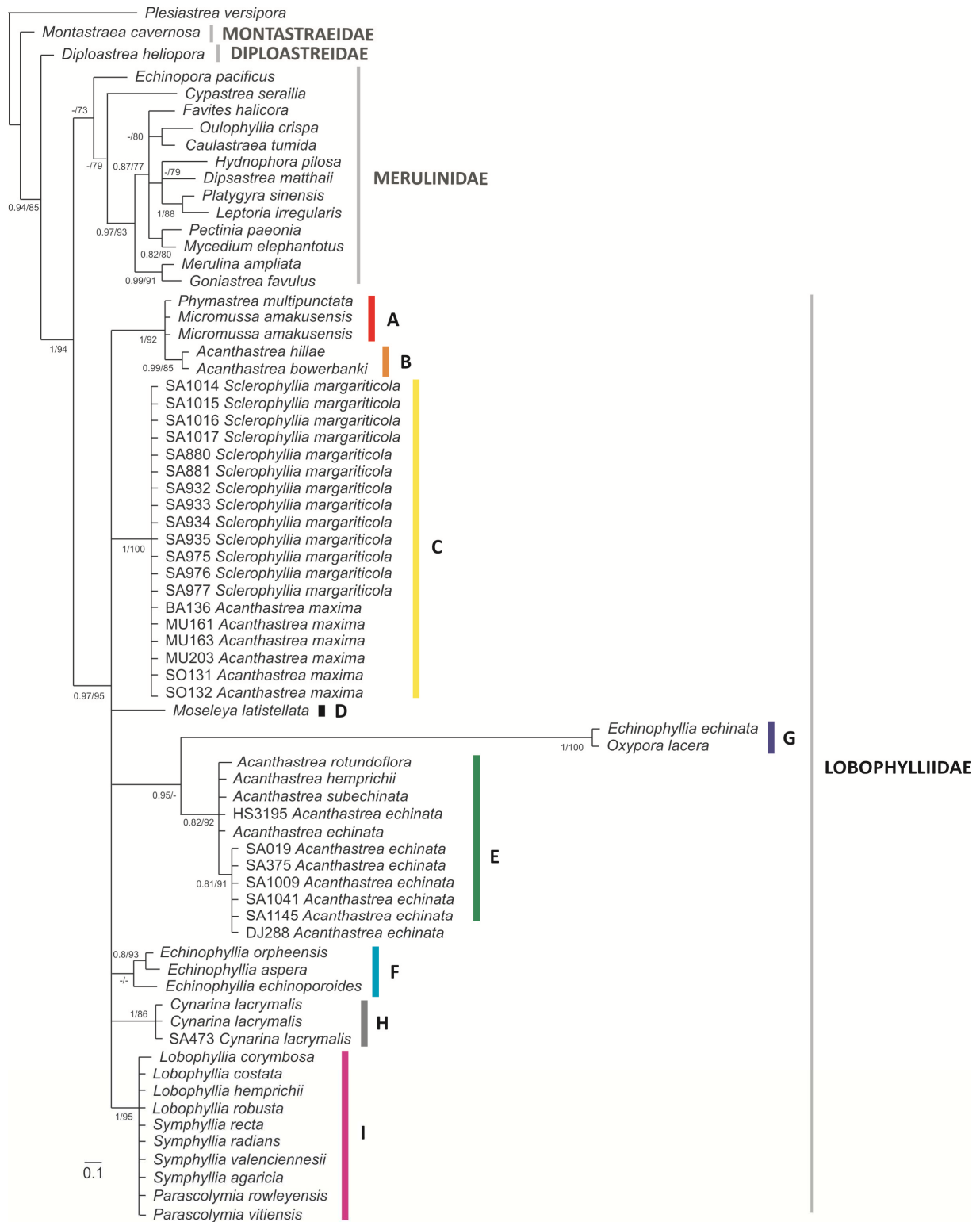


Figure 6.18. Phylogeny reconstruction of *Sclerophyllia margariticola* and *Sclerophyllia maxima* (previously *Acanthastrea*) within the family Lobophylliidae, based on Bayesian Inference (BI) analysis of the nuclear gene Histone H3. Bayesian posterior probability (left) higher than 0.95 and ML bootstrap values (right) higher than 70 are displayed on the nodes. Clades within Lobophylliidae are coloured and labelled A to I according to Arrigoni et al. (2014a).

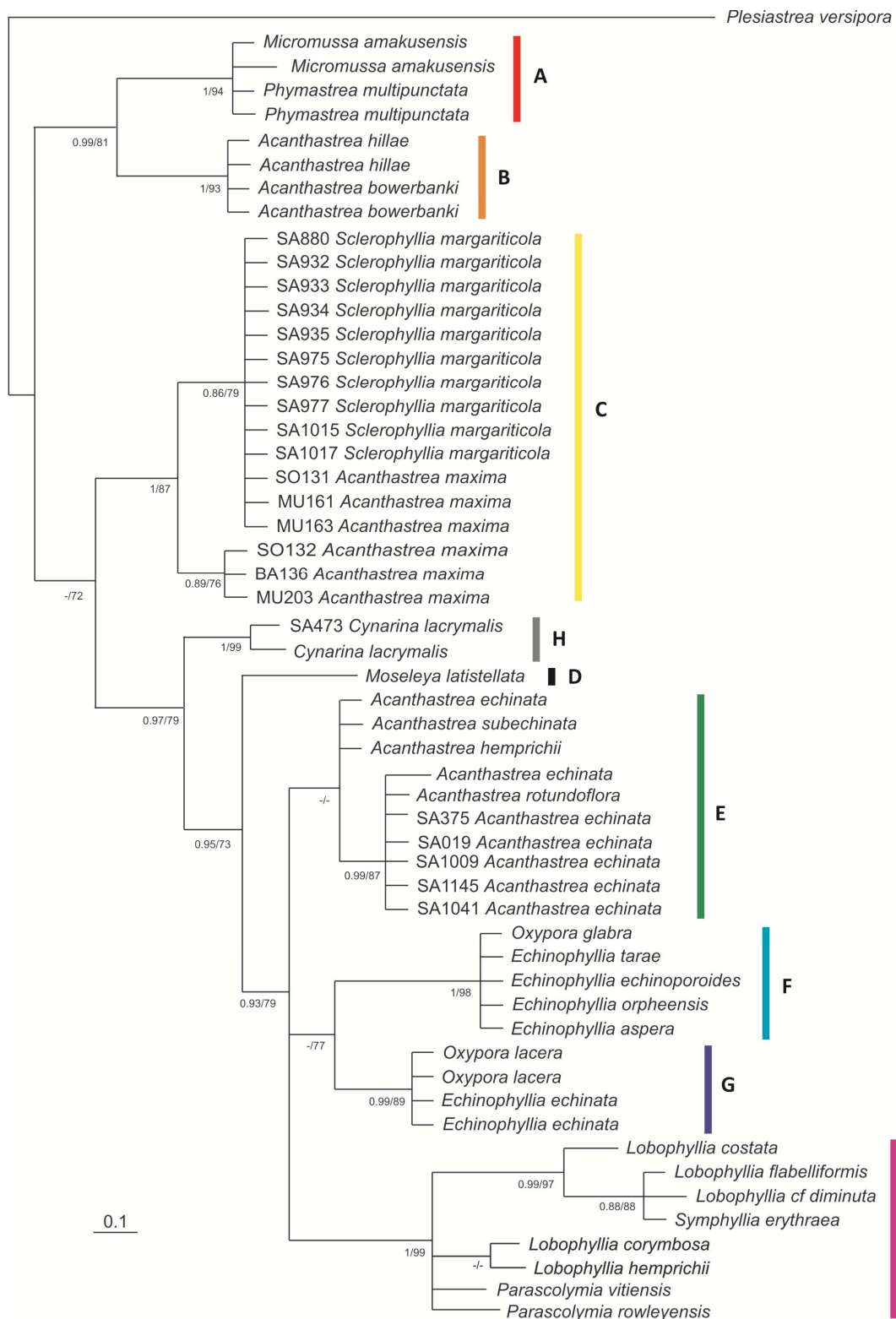
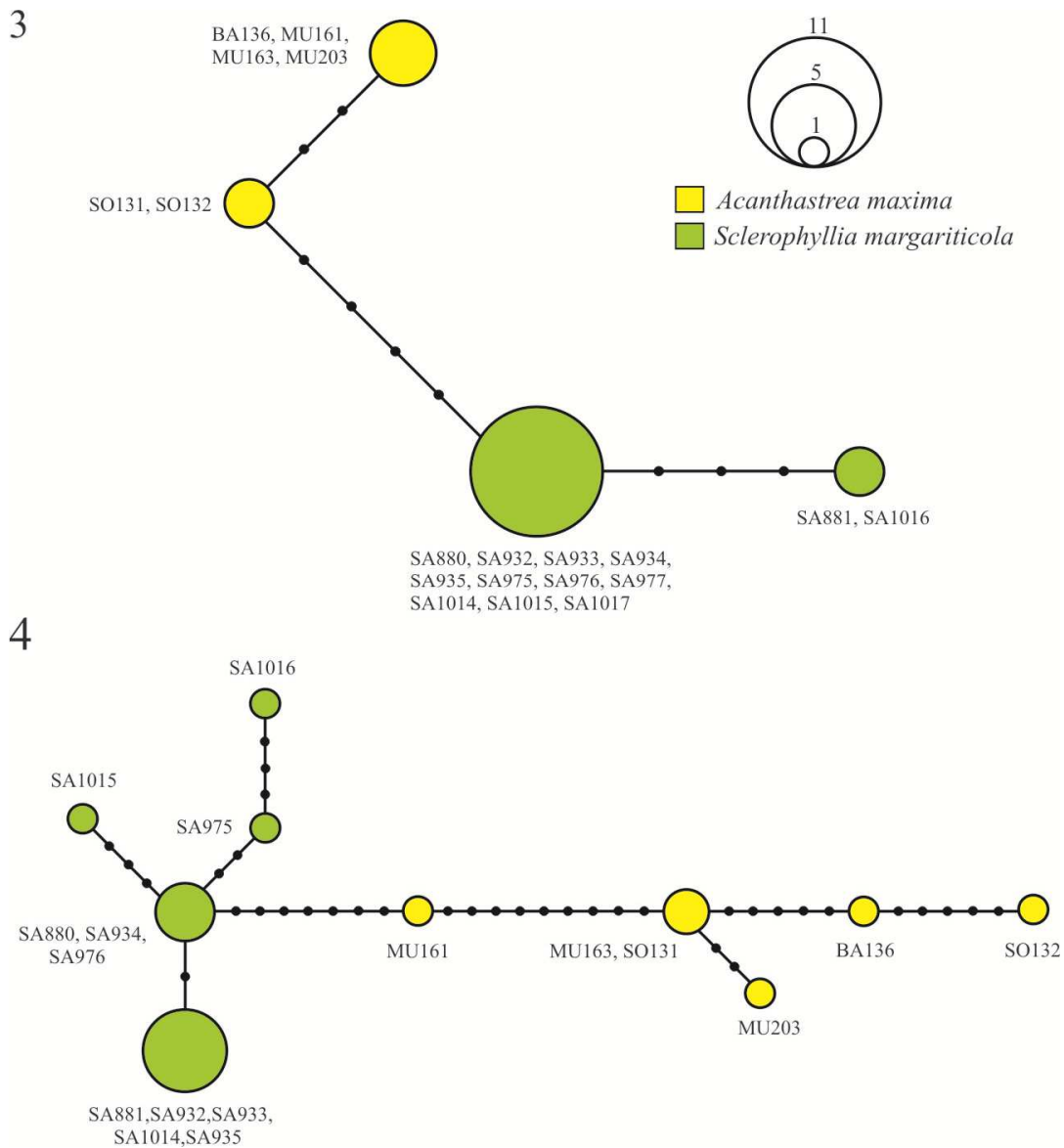


Figure 6.19. Phylogeny reconstruction of *Sclerophyllia margariticola* and *Sclerophyllia maxima* (previously *Acanthastrea*) within the family Lobophylliidae, based on Bayesian Inference (BI) analysis of the partial mitochondrial gene COI. Bayesian posterior probability (left) higher than 0.95 and ML bootstrap values (right) higher than 70 are displayed on the nodes. Clades within Lobophylliidae are coloured and labelled A to I according to Arrigoni et al. (2014a).

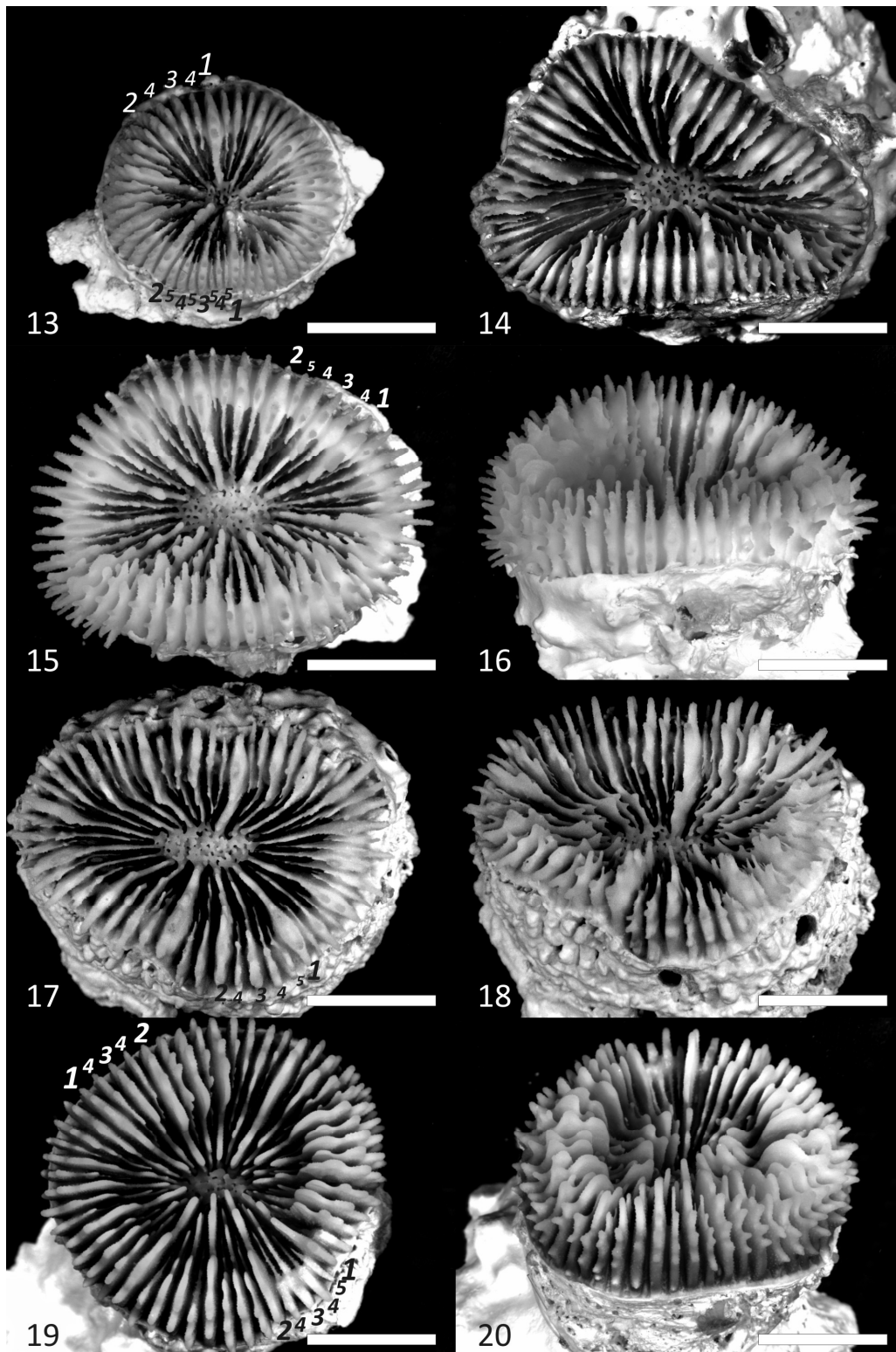


Figures 6.20-6.21. Most-parsimonious median-joining networks of *Sclerophyllia margariticola* (in green) and *Sclerophyllia maxima* (previously *Acanthastrea*) (in yellow): **6.20**, network inferred from the mitochondrial intergenic spacer region (IGR) between COI and 1-rRNA; **6.21**, network inferred from the nuclear internal transcribed spacer 2 (ITS2) region. The size of circles is proportional to the frequencies of specimens sharing the same haplotype. The black solid circles are indicative of mutations that differentiate each haplotype.

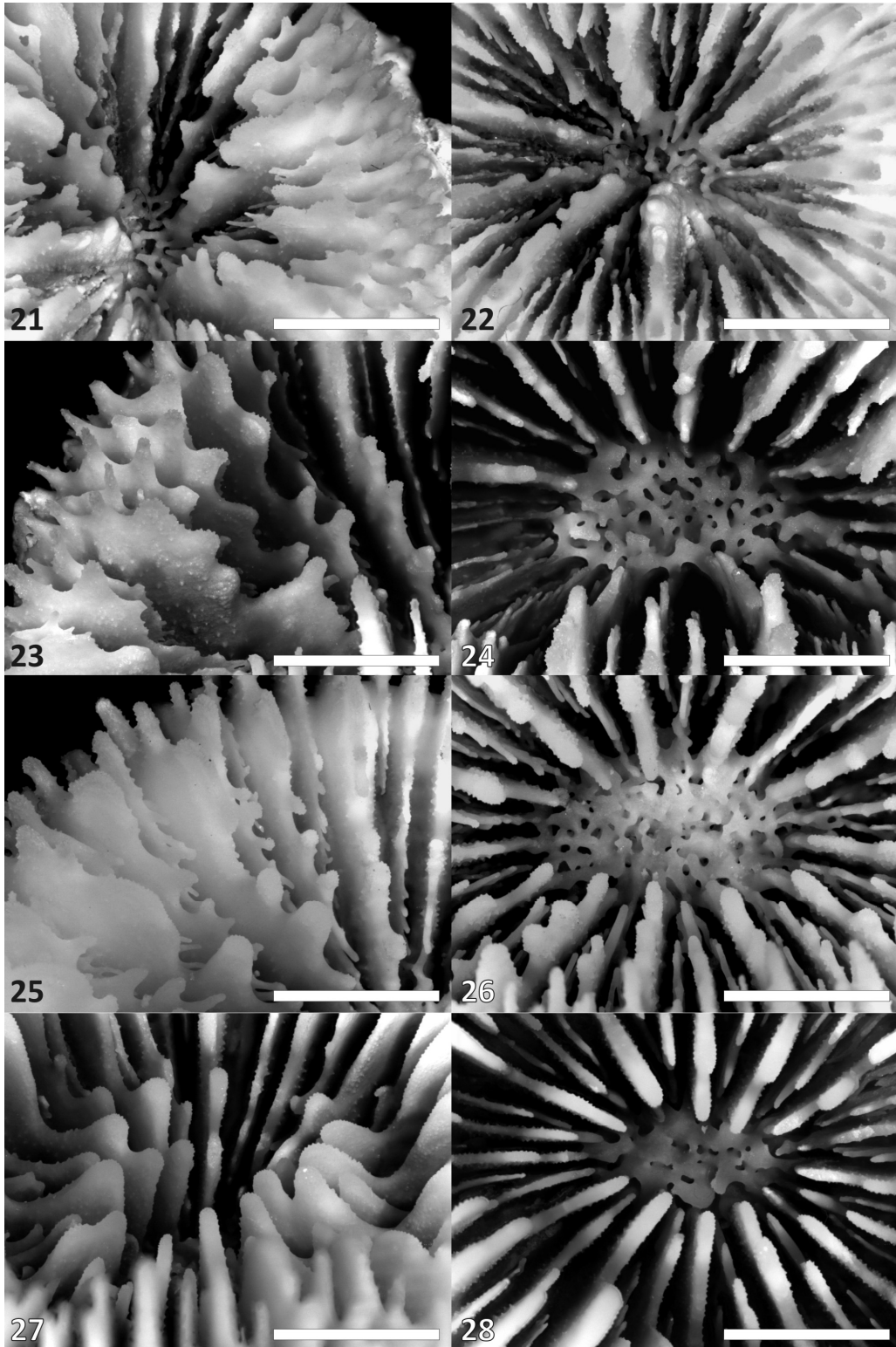
6.4.2 Morphological analyses

6.4.2.1 Macromorphology

In *Sclerophyllia margariticola* coralla are solitary and the corallum is cyathiform (Figs. 6.2–6.9, 6.23–6.30, App. 6.2). Calice width is large (> 15 mm) as a character state in Budd et al. (2012). Smaller coralla are circular in shape (Figs. 6.2–6.3, 6.8–6.23, 6.29–6.30) but the calice outline can become irregular and almost triangular (Figs. 6.4–6.5, 6.24, 6.27) or oval (Figs. 6.6–6.7, 6.25) in the largest specimen we observed, which is 35 mm in diameter (Fig. 6.7). There are four complete cycles of septa in the calices, and a fifth incomplete cycle (Figs. 6.23, 6.25, 6.27, 6.29). In the largest of the two specimens figured by Klunzinger (1879) a sixth cycle is found (App. 6.2). Septa of the major cycles are thicker. Septa of the last cycle are free (Figs. 6.23, 6.25, 6.27, 6.29), those of the cycle before the last can be free or slightly bend towards those of the lower cycle (Figs. 6.32, 6.38) and fuse at their base and with the columella (Figs. 6.34, 6.36, App. 6.2). Septa spacing is large, with 4–5 septa per 5 mm (Figs. 6.32, 6.34, 6.36, 6.38). Costae are well developed and extend 5–6 mm below the corallite wall (Figs. 6.26, 6.28, 6.30). Costae of the major cycles are thicker, hence relative costosepta thickness between Cs1 and Cs2 *versus* Cs3 is slightly unequal (Figs. 6.26, 6.28, 6.30). Columella is trabecular and spongy (Figs. 6.32, 6.34, 6.36, 6.38, App. 6.2) and its size relative to calice width is variable and less than 1/4 of calice width (Figs. 6.23–6.25, 6.27, 6.29, App. 6.2). Epitheca is well developed (Figs. 6.26, 6.28, 6.30). Internal lobes are weakly or well developed (Figs. 6.7, 6.30, 6.31, 6.37).

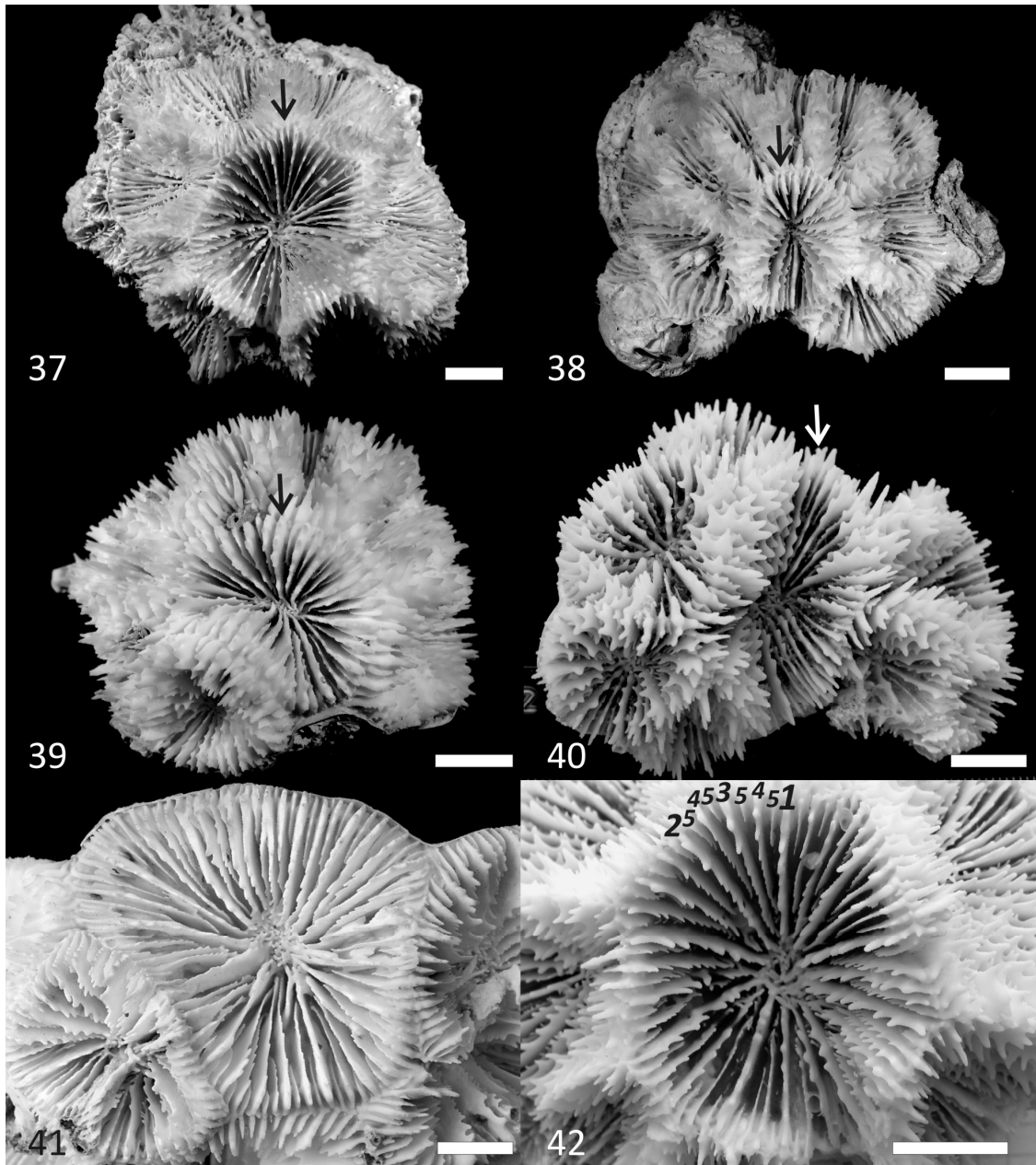


Figures 6.23–6.30. Coralla of *Sclerophyllia margariticola*: **6.23**, KAUST SA1017; **6.24**, KAUST SA934; **6.25**, top view of KAUST SA1014; **6.26**, side view of KAUST SA1014; **6.27**, top view of KAUST SA976; **6.28**, side view of KAUST SA976; **6.29**, top view of KAUST SA933; **6.30**, side view of KAUST SA933. Arabic numerals at the outer end of the septa in 6.23, 6.25, 6.27, and 6.29 indicate the cycle number (from 1 to 5). Scale bars represent 1 cm.



Figures 6.31–6.38. Radial elements (6.31, 6.33, 6.35, 6.37) and columella (6.32, 6.34, 6.36, 6.38) of *Sclerophyllia margariticola*: **6.31**, KAUST SA1017; **6.32**, KAUST SA1017; **6.33**, KAUST SA1014; **6.34**, KAUST SA1014; **6.35**, KAUST SA976; **6.36**, KAUST SA976; **6.37**, well formed crown of paliform lobes in KAUST SA933; **6.38**, relatively small columella in the same specimen as in 6.37. Scale bars represent 5 mm.

In *Acanthastrea maxima* coralla are flattened or massive (Figs. 6.10–6.17, 6.39–6.44). Coralla are colonial as a result of primary circumoral budding, and both intra and extracalicular budding occur (Figs. 6.39–6.43). Corallite display polymorphism and a central larger corallite can be observed (arrows in Figs. 6.39–6.42), calical series are not formed. Corallite integration is mostly discrete. Coenosteum is absent and walls of adjacent corallites are fused (Figs. 6.39, 6.40, 6.42), although in some coralla it is limited and the two adjacent walls can be distinguished (Figs. 6.41, 6.43) forming the “double wall” *sensu* Budd et al. (2012). Overall, calice width is large according to the character state in Budd et al. (2012) although some medium sized calices can surround the central corallite (Figs. 6.39–6.44). Calices found at the periphery of the coralla can be inclined and the part of their calice that is not adjacent to other calices can be wider (Fig. 6.39). Continuity of costosepta is mostly not confluent (Figs. 6.43–6.44). There are five complete cycles of septa in the calices (Fig. 6.44), septa of the major cycles are thicker (Figs. 6.39–6.44). Septa of the last cycle are free (Figs. 6.43–6.44), those of the cycle before the last can be free or slightly bent towards those of the lower cycle and fuse at their base and with the columella (Figs. 6.43–6.44). Septa spacing is large, with 4–5 septa per 5 mm (Figs. 6.43–6.44). Relative costosepta thickness between Cs1 and Cs2 *versus* Cs3 is slightly unequal (Fig. 6.44). Linkage between centres of adjacent corallites is absent. Columella trabecular and spongy and its size relative to calice width is less than 1/4 of calice width (Figs. 6.43–6.44, 6.48). Epitheca well developed (Fig. 6.41). Internal lobes not developed.

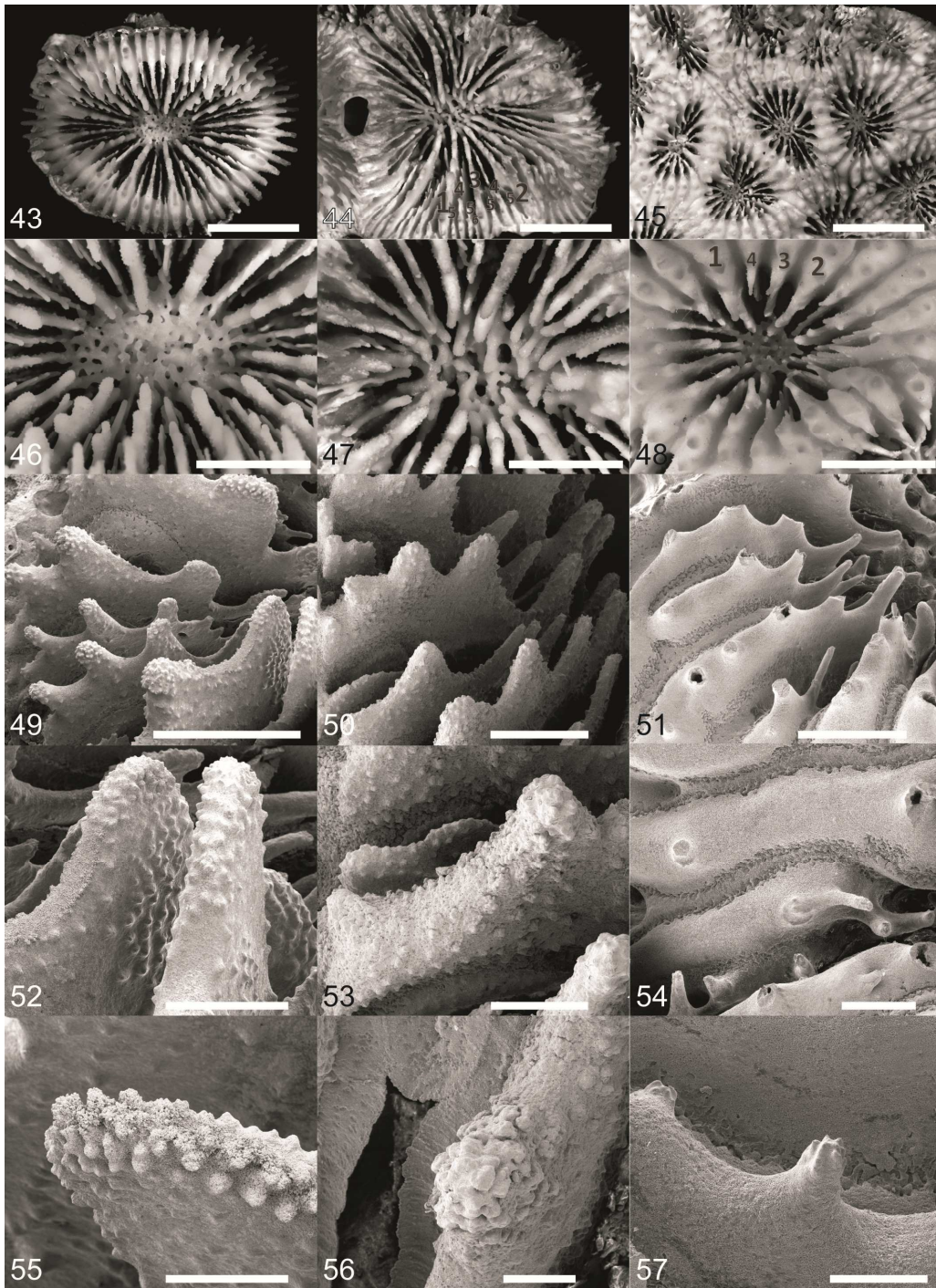


Figures 6.39-6.44. *Sclerophyllia maxima* (previously *Acanthastrea*): **6.39**, UNIMIB MU163, same specimen as in Fig. 11; **6.40**, UNIMIB BA136, same specimen as in Fig. 6.12; **6.41**, view of specimen UNIMIB K001 showing a top view of the central corallite (arrow); **6.42**, view of same specimen as in 6.41 showing a lateral view of the central corallite (arrow); **6.43**, largest calice in the holotype BMNH 1986.11.17.2; **6.44**, largest calice in UNIMIB MU163. Black arrows indicate the central and larger corallite. Arabic numerals at the outer end of the septa in 6.44 indicate the cycle number (from 1 to 5). Scale bars represent 1 cm.

6.4.2.2 Micromorphology

In *Sclerophyllia margariticola* tooth base at mid-septum is elliptical in shape and parallel to the length of the septum (Figs. 6.48, 6.51). Tooth tips are irregular and lobate (Figs. 6.51, 6.54). Teeth on S1 are high and their spacing is very wide, with adjacent teeth more than 2 mm apart (Figs. 6.48, 6.51). Tooth shape is regular, but size is larger on major septa (Figs. 6.45, 6.51). Granulation on the side of septa is strong and granules scattered (Figs. 6.51, 6.54, 6.57). The inter-area structure is generally smooth or with palisade. In septa of the major cycles its upper margin is almost flattened rather than rounded in section (Fig. 6.54). Tooth shape between Cs3 and Cs1 is unequal (Fig. 6.51).

In *Acanthastrea maxima* tooth base at mid-septum is elliptical in shape and parallel to the length of the septum (Figs. 6.49, 6.52). Tooth tips are irregular and lobate (Figs. 6.49, 6.52). Teeth on S1 are high and their spacing is very wide, with adjacent teeth more than 2 mm apart (Fig. 6.52). Tooth shape is regular, but size is larger on major septa (Figs. 6.52, 6.55). Granulation on the side of septa is strong and granules scattered (Figs. 6.52, 6.55). The inter-area structure is with palisade. In septa of the major cycles its upper margin is almost flattened rather than rounded in section (Fig. 6.55). Tooth shape between Cs3 and Cs1 is unequal (Fig. 6.52).



Figures 6.45-6.59. Macro and micro-morphology of *S. margariticola* (6.45, 6.48, 6.51, 54, 6.57), *S. maxima* (previously *Acanthastrea*) (6.46, 6.49, 6.52, 6.55, 6.58), and *Acanthastrea echinata* (6.47, 6.50, 6.53, 6.56, 6.59): **6.45**, KAUST SA1017; **6.46**, UNIMIB MU161; **6.47**, IRD HS3126; **6.48**, columella of the same corallite as in 6.45; **6.49**, columella of the same corallite as in 6.46; **6.50**, corallite of the same specimen as in 6.47; **6.51**, SEM image of the septa of KAUST SA1175 showing granulated septal sides; **6.52**, SEM image of the septa of UNIMIB MU161 showing granulated septal sides; **6.53**, SEM image of the septa of IRD HS3126 showing smooth septal sides; **6.54**, SEM image of two septa of the same specimen as in 6.51 showing margin and side ornamentation; **6.55**, SEM image of a septum of the same specimen as in 6.52 showing margin and side ornamentation; **6.56**, SEM image

of septa of the same specimen as in 6.53 showing septal margin ornamentation; **6.57**, top view of a septal teeth in the same specimen as in 6.51 and 6.54; **6.58**, top view of a septal teeth in the same specimen as in 6.52 and 6.55; **6.59**, septal teeth in the same specimen as in 6.53 and 6.56. Arabic numerals on the septa in 6.46 and 6.50 indicate the cycle number (from 1 to 6). Scale bars represent: Figs. 6.45-6.47, 1 cm; Figs. 6.48-6.50, 5 mm; Figs. 6.51-6.53, 2 mm; Figs. 6.54-6.56, 1 mm; Figs. 6.57-6.59, 500 μm .

6.4.3 Ancestral character state reconstruction

MP ancestral state reconstruction indicates that the polystomatous character state is likely ancestral within the family Lobophylliidae (Fig. 6.22). Moreover the acquisition of a single mouth seems to have occurred independently at least twice in this family within the lineage leading to *Cynarina lacrymalis* and *Sclerophyllia margariticola* (Fig. 6.22).

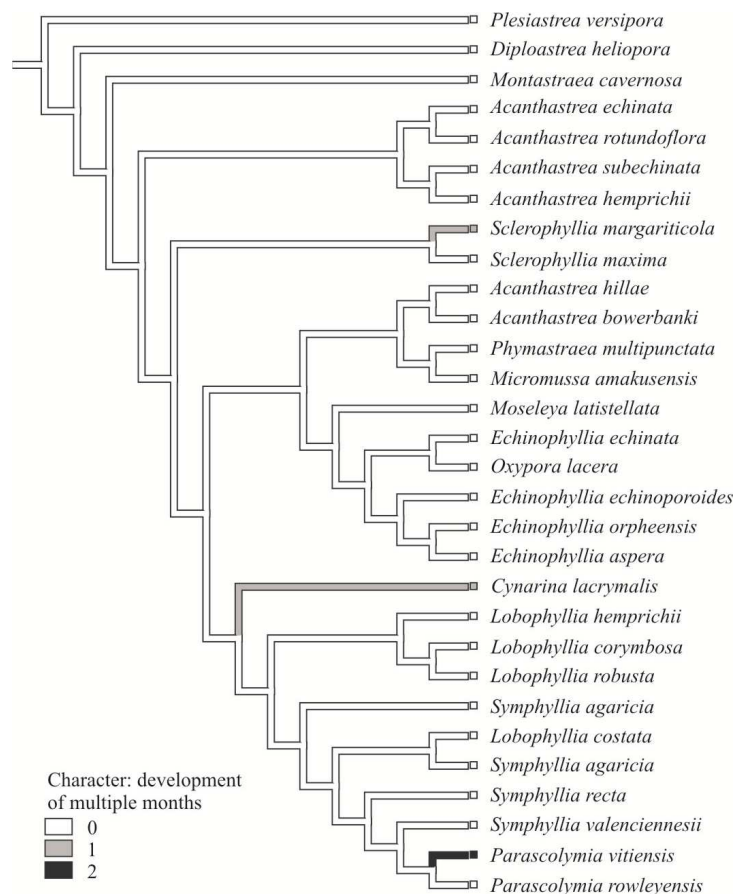


Figure 6.22. Ancestral state reconstruction of the character “development of multiple mouths” within the family Lobophylliidae obtained using Maximum Parsimony with Mesquite 2.75. Character states as follows: 0, white, polystomatous; 1, grey, monostomatous; 2, black, polystomatous or monostomatous.

6.5 Taxonomic account

6.5.1 Examined material

Sclerophyllia margariticola Klunzinger, 1879

Red Sea – ZMB Cni 2181, syntype, Al-Qusayr, Egypt, coll. C.B. Klunzinger; MNHN IK-2012-14250, 1837, coll. T. Lefebvre; **Saudi Arabia, Red Sea** – (Aqaba Biodiversity expedition): KAUST SA880, Jazirat Burcan site 7 (27°54'N; 35°03'E), 28/09/2013, coll. F. Benzoni; KAUST SA881, Jazirat Burcan site 07 (27°54'N; 35°03'E), 28/09/2013, coll. F. Benzoni; KAUST SA932, Magna Coast Guard st. 8 (28°24'N; 34°44'E), 29/09/2013, coll. F. Benzoni; KAUST SA933, Magna Coast Guard st. 8 (28°24'N; 34°44'E), 29/09/2013, coll. J.P.A. Hobbs; KAUST SA934, Magna Coast Guard st. 8 (28°24'N; 34°44'E), 29/09/2013, coll. F. Benzoni; KAUST SA935, Magna Coast Guard st. 8 (28°24'N; 34°44'E), 29/09/2013, coll. F. Benzoni; KAUST SA975, Magna Coast Guard st. 9 (28°24'N; 34°44'E), 30/09/2013, coll. F. Benzoni; KAUST SA976, Magna Coast Guard st. 9 (28°24'N; 34°44'E), 30/09/2013, coll. J.P.A. Hobbs; KAUST SA977, Magna Coast Guard st. 9 (28°24'N; 34°44'E), 30/09/2013, coll. F. Benzoni; KAUST SA1014, Magna Coast Guard st. 10 (28°24'N; 34°44'E), 29/09/2013, coll. F. Benzoni; KAUST SA1015, Magna Coast Guard st. 10 (28°24'N; 34°44'E), 29/09/2013, coll. F. Benzoni; KAUST SA1016, Magna Coast Guard st. 10 (28°24'N; 34°44'E), 29/09/2013, coll. F. Benzoni; KAUST SA1017, Magna Coast Guard st. 10 (28°24'N; 34°44'E), 29/09/2013, coll. F. Benzoni; KAUST SA1175, Thuwal Shark Reef st. 13 (22°18'N; 39°07'E), 04/10/2013, coll. F. Benzoni; KAUST SA1297, Thuwal Shark Reef (22°18'N; 39°07'E), 08/10/2013, coll. F. Benzoni; KAUST SA1298, Thuwal Shark Reef (22°18'N; 39°07'E), 08/10/2013, coll. F. Benzoni.

Acanthastrea maxima Sheppard and Salm, 1988

Gulf of Aden, Yemen – (coll. F. Benzoni, M. Pichon): UNIMIB MU161, Al Mukallah st. MU7 (14°31'N; 49°10'E), 20/03/2007; UNIMIB MU163, Al Mukallah st. MU7 (14°31'N; 49°10'E), 20/03/2007; UNIMIB MU203, Al

Mukallah st. MU9 (14°31'N; 49°10'E), 21/03/2007; UNIMIB BU019, Burum st. 2, 22/03/2007; UNIMIB BA136, Bir Ali st. BA15, 23/11/2008; **Socotra** – (coll. F. Benzoni, A. Caragnano): UNIMIB SO131, Ras Adho st. 14 (12°38'N; 54°16'E), 18/03/2010; UNIMIB SO132, Ras Adho st. 14 (12°38'N; 54°16'E), 18/03/2010.

6.5.2 Taxonomy

We re-establish the genus name *Sclerophyllia* on the basis of the molecular and morphologic results and we place *Acanthastrea maxima* in it.

Order Scleractinia Bourne, 1900

Family Lobophylliidae Dai and Horng, 2009

Genus *Sclerophyllia* Klunzinger, 1879

TYPE SPECIES: *Sclerophyllia margariticola* Klunzinger, 1879 (by monotypy)

REVISED DIAGNOSIS: Corallum attached, solitary or colonial as a result of primary circumoral budding, and secondary intra and extracalicular budding. In colonial coralla corallites display polymorphism. Coenosteum absent or limited to a “double wall”. Calice width is large (see Budd et al., 2012). Septa of the last cycle are free, those of the cycle before the last can be free or slightly bend towards those of the lower cycle and fuse at their base and with the columella. Septa spacing is large. Relative costosepta thickness between Cs1 and Cs2 versus Cs3 is slightly unequal. Columella is trabecular and spongy. Septal tooth base at mid-septum is elliptical in shape and parallel to the direction of the septum. Tooth tips are irregular and lobate. Teeth on S1 high and their spacing is very wide. Granulation on the side of septa is strong and granules scattered. The inter-area structure is with palisade. In septa of the major cycles inter-area structure upper margin is almost flattened rather than rounded in section. Tooth shape between Cs3 and Cs1 is unequal.

DISTRIBUTION: Red Sea, Gulf of Aden, Arabian Sea, Gulf of Oman, and the Gulf.

SPECIES INCLUDED:

Sclerophyllia margariticola Klunzinger, 1879

(Figs. 6.2–6.9, 6.23–6.38, 6.45, 6.48, 6.51, 6.54, 6.57, App. 6.2)

Sclerophyllia margariticola Klunzinger, 1879, vol. 3, p. 4, pl. 1, Fig. 12; not Gravier, 1911, vol. 2, p. 42, pl. II, Fig. 45;

TYPE MATERIAL: lectotype ZMB Cni 2181 (designated herein), deposited at the MFN.

TYPE LOCALITY: Al-Qusayr, Egypt, Red Sea.

DISTRIBUTION: Egypt, Saudi Arabia.

REMARKS: Specimen MNHN IK-2012-14250 was collected 60 years before Klunzinger's description of this species. According to the museum tags, the specimen was collected in 1837 by the French explorer C.T. Lefebvre (1811-1870) in the Red Sea and later identified by DJ Laborel as *Parascolymia*. The last author re-discovered this specimen in the MNHN collections in early 2014. Lefebvre led several expeditions in Abissinia (Eritrea and Ethiopia) (Lefebvre et al., 1845) and this specimen could represent the first record of the species in the south west coasts of the Red Sea, a notable example of the importance of historical collections as sources of unknown biodiversity (Benzoni et al., 2012a; Rocha et al., 2014) as well as baselines to determine biotic changes of coral reefs (Hoeksema et al., 2011).

Sclerophyllia maxima (Sheppard and Salm, 1988) comb. nov.

(Figs. 6.10–6.17, 6.39–6.44, 6.46, 6.49, 6.52, 6.55, 6.58)

Acanthastrea maxima Sheppard and Salm, 1988, vol. 22, pp. 276-279, Figs. 4-5; Veron, 2000, vol. 3, p. 27, Figs. 4-5; Coles, 1996, p. 54, pl. 47; Claereboudt, 2006, pp. 216-217, Figs. 1-4; Carpenter et al. 1997, 61; Pichon et al. 2010, pp. 188-189, Figs. 1-4; Arrigoni et al. 2012, Fig. S2Y; Arrigoni et al. 2014a, Fig. 2E.

TYPE MATERIAL: The holotype (1986.11.17.2) is deposited at the BMNH.

DISTRIBUTION: Yemen (Gulf of Aden), Socotra Island, Oman, Kuwait.

6.6 Discussion

An approach that combines mitochondrial and nuclear sequence data with detailed micromorphological investigation has already proved useful in the family Lobophylliidae in the formal revision of the genera *Australomussa* and *Parascolymia* (Arrigoni et al., 2014b). In the present work, it allowed the phylogenetic investigation of clade C *sensu* Arrigoni et al. (2014a) and led to resurrection of the genus *Sclerophyllia*, a long-forgotten genus incorrectly synonymized with the genera *Symphyllia* and *Cynarina* over the last century (Vaughan and Wells, 1943; Wells, 1964; Veron and Pichon, 1980), and led to the placement of *Acanthastrea maxima* in *Sclerophyllia*, henceforth referred to as *Sclerophyllia maxima*.

6.6.1 Morphology of *Sclerophyllia* vs *Acanthastrea* and *Cynarina*

Mitochondrial and nuclear phylogenetic reconstructions suggest that *Sclerophyllia margariticola* and *S. maxima* grouped together in clade C *sensu* Arrigoni et al. (2014a) within the family Lobophylliidae (Figs. 6.18, 6.19). Neither is molecularly closely related to *C. lacrymalis*, the species previously considered a senior synonym of *S. margariticola* (Veron and Pichon, 1980; Wells, 1964), nor to *A. echinata*, the type species of *Acanthastrea* in which *S. maxima* was originally described (Sheppard and Salm, 1988; Veron, 2000). Moreover, *S. margariticola* and *S. maxima* display discrete ITS2 and IGR haplotypes even if the molecular distinction between them is poorly inferred based on the haplotype network analyses (Figs. 6.20–6.21). Hence, molecular results demonstrate the taxonomic validity of *S. margariticola*, despite the taxonomic confusion and the erroneous synonymizations of this species (Matthai, 1928; Vaughan and Wells, 1943; Wells, 1964; Veron and Pichon, 1980).

The genetic data in this study is strengthened by macro- and micromorphologic results. The two species in the genus *Sclerophyllia* are distinguished by different macromorphologic characters, the most notable being the corallum condition –

solitary in *S. margariticola* and colonial in *S. maxima* (Table 6.2).

Moreover, in *S. margariticola* internal lobes are weakly or well developed (Figs. 6.28, 6.30) while they are not observed in *S. maxima* (Figs. 6.39, 6.44), and the trabecular processes forming the columella are more numerous, more tightly fused, and smaller in the former species (Fig. 6.48) than in the latter (Fig. 6.49). However, the two species share the large size of the corallite, the high number of septa cycles, the presence of free septa, the wide septal spacing, the slightly unequal relative costosepta thickness, and a trabecular spongy columella $<1/4$ of calice width (Table 6.2). In terms of micromorphology, *S. margariticola* and *S. maxima* are very similar for all the characters we examined (Table 6.2, Figs. 6.51–6.52) and are characterized by high elliptical septal teeth parallel to the septum direction, irregular lobate tips, very wide tooth spacing, a very strong granulation with granules scattered all along the septal sides, and a palisade interarea structure (Table 6.2, Figs. 6.51–6.52). Moreover, the interarea of major septa of both species has a characteristic flattened shape (Figs. 6.53–6.55). A comparison of the macro- and micromorphological features of *S. maxima* and *A. echinata* reveals that these two species, previously considered congeners, are different for 8 of the 14 macromorphological characters, and for 4 of the 7 micromorphological characters listed in Table 6.2. While *A. echinata* can form colonies with more numerous medium-sized corallites, it is usually devoid of polymorphism, and has mostly confluent costosepta with equal relative thickness, lamellar linkage of the centres, and a trabecular compact columella (Table 6.2; Budd and Stolarski, 2009), *S. maxima* forms colonies with less numerous large-sized corallites with obvious polymorphism, and has mostly not confluent costosepta with slightly unequal relative thickness, trabecular linkage of the centres, and a trabecular spongy columella. Visually, the most striking micromorphological character that distinguishes the two *Sclerophyllia* species from the type species of the genus *Acanthastrea* is the strong scattered granulation of the septal sides in *S. margariticola* and *S. maxima* (Figs. 6.54–6.55) and the weakly developed granules enveloped by thickening deposits in *A. echinata* (Fig. 6.56). The sides of the large

septal lobes in the two *Sclerophyllia* species are coarsely beaded (Figs. 6.57–6.58) while those in *A. echinata* are mostly smooth (Fig. 6.59). Furthermore, while the interarea in the major septa is rounded in section in *A. echinata* (Fig. 6.56), in *S. margariticola* and *S. maxima* it is typically flattened (Figs 6.54–6.55). In conclusion, in this study the morphological results were in agreement with the molecular results in defining *S. margariticola* and *S. maxima* as species belonging to the same genus, and in differentiating *S. maxima* from *A. echinata*.

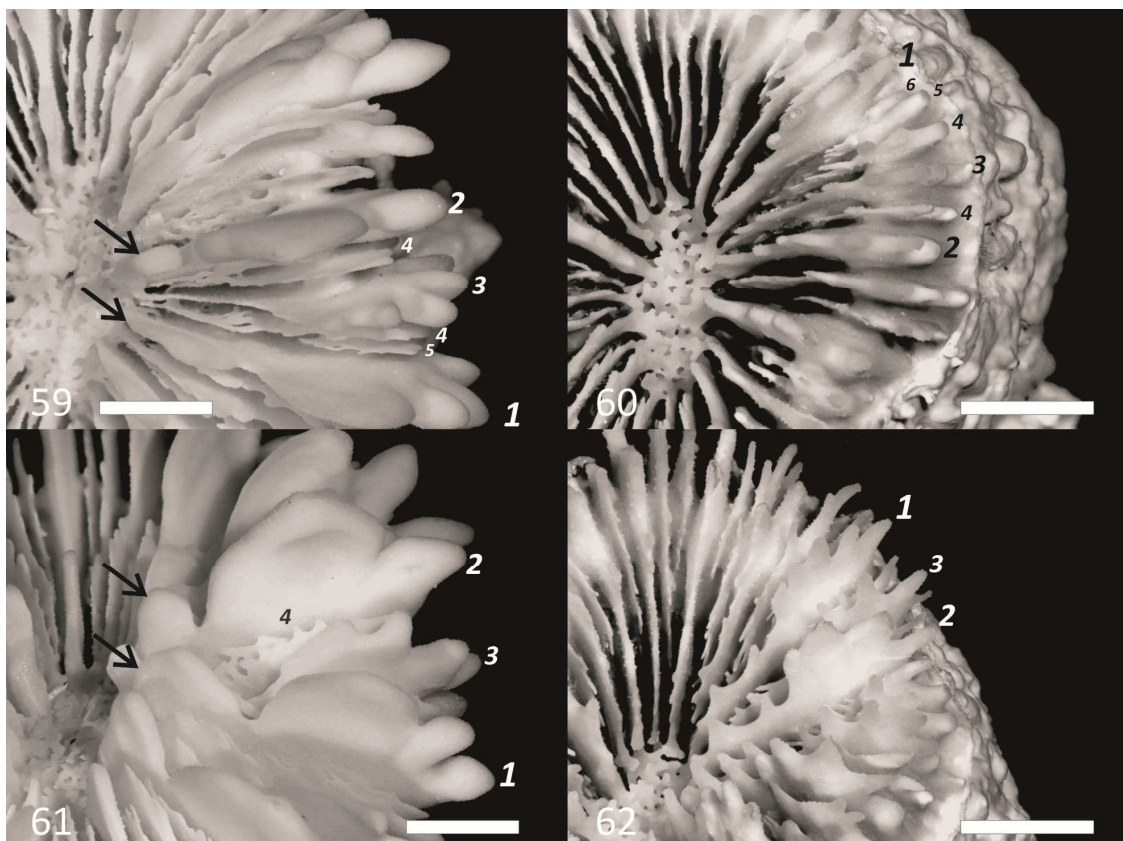
The past synonymy of *Sclerophyllia margariticola* with *Cynarina lacrymalis* can be explained by several shared morphologic characters (Table 6.2), first of all the solitary condition of the corallum. However, a direct comparison of specimens of the two species shows that *C. lacrymalis* has more spaced septa, with those of the first three cycles much thicker than in any of the studied specimens of *S. margariticola* (Figs. 6.60–6.61, respectively).

While in *C. lacrymalis* the relative costosepta thickness of Cs1 and Cs2 -vs- Cs3 is unequal, and that of Cs3 and Cs4 is very unequal, in *S. margariticola* the relative costosepta thickness is slightly unequal in all cases. Moreover, septal teeth in *C. lacrymalis* (Fig. 6.60) are wider and higher than in *S. margariticola* (Fig. 6.63) and the internal lobes in the former species are more obvious and well-developed (arrows in Figs. 6.60, 6.62) than in the latter. Finally, in *C. lacrymalis* there are 4 complete septa cycles and a fifth incomplete cycle, while in *S. margariticola* there are 5 complete septa cycles and a sixth incomplete cycle (Table 6.2).

Table 6.2. Macromorphology and micromorphology of *Sclerophyllia margariticola*, *S. maxima* (this study) and *Cynarina lacrymalis* and *Acanthastrea echinata* (from Budd *et al.*, 2012). Explanation of characters, their ID numbers (in brackets) and state names are from Budd *et al.* (2012).- = character examined on polycentric coralla; Csn= number of cycle of costosepta; Sn = number of cycle of septa.

	Character	<i>C. lacrymalis</i>	<i>S. margariticola</i>	<i>S. maxima</i>	<i>A. Echinata</i>	
Macromorphology	Intracalicular budding (1)	-	-	Present	Present	
	Extracalicular budding (2)	-	-	Present	Present	
	Circumoral budding and associated corallite polymorphism (3)	-	-	Present	Absent	
	Corallite integration (4)	-	-	Discrete	Discrete	
	Calice or valley width (7)	Large	Large	Large	Medium	
	Continuity of costosepta (9)	-	-	Mostly not confluent	Mostly confluent	
	Number of septa (10)	5 cycles	6 cycles	5 cycles	3 cycles	
	Free septa (11)	Present	Present	Present	Present	
	Septa spacing (per 5mm) (12)	Wide	Wide	Wide	Wide	
	Relative costosepta thickness (Cs1 and Cs2 -vs- Cs3) (13)	Unequal	Slightly unequal	Slightly unequal	Equal	
	Corallite centres linkage (14)	Lamellar	-	Trabecular	Lamellar	
	Columella structure (15)	Trabecular spongy	Trabecular spongy	Trabecular spongy	Trabecular compact	
	Columella size relative to calice width (16)	< ¼	< ¼	< ¼	1/2	
	Internal lobes (21)	Septal	Well developed	Absent	Absent	
	Micromorphology	Tooth base (mid-septum) (35)	Elliptical parallel	Elliptical parallel	Elliptical parallel	Elliptical parallel
		Tooth tips (38)	Irregular lobate	Irregular lobate	Irregular lobate	Irregular lobate
		Tooth height (S1) (39)	High	High	High	Medium
		Tooth spacing	Very wide	Very wide	Very wide	Very wide

(S1) (40)				
Granules shape and distribution (43)	Well-formed, scattered	Strong, scattered	Strong, scattered	Weak, enveloped by thickening deposits
Interarea structure (44)	Palisade	Palisade	Palisade	Weakly palisade/smooth
Cs3/Cs1 tooth shape (45)	Unequal	Unequal	Unequal	Equal



Figures 6.60-6.63. Morphology and dimensions of septa and septal teeth in *Cynarina lacrymalis* (6.60, 6.62) and *Sclerophyllia margariticola* (6.61, 6.63): **6.60**, top view of the septa; **6.61**, top view of the septa of (KAUST SA934); **6.62**, side view of the septa shown in 6.60; **6.63**, side view of the septa shown in 6.61. Arabic numerals at the end of the septa indicate the cycle number (from 1 to 6). Black arrows point at the large septal internal lobes in the major septa of *C. lacrymalis*. Scale bars represent 5 mm.

6.6.2 Biogeographical patterns revealed by genetic evidence

Based on the distribution ranges of its two species, the genus *Sclerophyllia* can be actually considered an endemic of the seas around the Arabian Peninsula, occurring in the Red Sea, Gulf of Aden, Arabian Sea, Gulf of Oman, and Persian Gulf (Klunzinger, 1879; Sheppard and Salm, 1988; Sheppard and Sheppard, 1991; Hodgson and Carpenter, 1995; Coles, 1996; Carpenter et al., 1997; DeVantier et al., 2004; Claereboudt, 2006; Pichon et al., 2010) (Fig. 6.1). Interestingly, both species exhibit allopatric ranges based on the fact that *S. margariticola* is only known from the Red Sea while *S. maxima* is an uncommon species found in the Gulf of Aden, Arabian Sea, Gulf of Oman, and Persian Gulf (Klunzinger, 1879; Carpenter et al., 1997; Claereboudt, 2006; Pichon et al., 2010) (Fig. 6.1). Although the divergence time between these two sister species cannot be estimated, it is likely that the geological history of the Arabian region has played a key role in the definition of geographic distribution of *S. margariticola* and *S. maxima* (Le Pichon and Gaulier, 1988; Omar and Steckler, 1995). In fact, the Red Sea remained repeatedly isolated from the Gulf of Aden over the last 5 Ma due to the near-closure of the narrow and shallow strait of the Bab al Mandab (Siddal et al., 2003). Despite the fact that the Red Sea fauna is understudied in comparison to those of other tropical reef regions (Berumen et al., 2013), some authors have demonstrated the importance of Red Sea geological events for the distribution and genetic structuring of fishes and corals (e.g., DiBattista et al., 2013; Keshavmurthy et al., 2013).

The increasing number of genetic and phylogenetic data for scleractinian corals has revealed several peculiar biogeographical patterns at different taxonomic levels previously obscured by a traditional taxonomy based solely on the macromorphology of the corallum (e.g., Fukami et al., 2004a; Keshavmurthy et al., 2013; Pinzon et al., 2013). For example, Fukami et al. (2004a, 2008) showed a deep divergence between the Indo-Pacific and the Atlantic representatives of the traditional families Mussidae and Faviidae Gregory, 1900 suggesting an evolutionary convergence of macromorphological characters. Moreover, several

cases of intraspecific divergences between Pacific and Indian Ocean populations have been discovered within the families Merulinidae (Arrigoni et al., 2012; Huang et al., 2011, 2014b), Lobophylliidae (Arrigoni et al., 2014a), and Poritidae (Kitano et al., 2014), supporting the existence of an Indian Ocean center of origin (Obura, 2012). The widespread pocilloporid genera *Pocillopora* Lamarck, 1816, and *Stylophora* Schweigger, 1820, have been extensively studied resulting in unforeseen geographic patterns that are mostly in disagreement with traditional taxonomy (Stefani et al., 2011; Flot et al., 2011; Keshavmurthy et al., 2013; Klueter and Andreakis, 2013; Pinzon et al., 2013; Schmidt-Roach et al., 2013a;). Indeed, genetics revealed the existence of several widespread species and few endemisms in *Pocillopora* (Pinzon et al., 2013; Schmidt-Roach et al., 2013a) explained by fine-scale morphology analyses (Schmidt-Roach et al., 2013b, 2014), while *S. pistillata* Esper, 1797, has been demonstrated to be currently subdivided in four deeply divergent lineages corresponding to four specific regions (Flot et al., 2011; Stefani et al., 2011; Keshavmurthy et al., 2013). Similar unforeseen distributional patterns have been reported for fish (Cowman and Bellwood, 2013) and octocorals (Reijnen et al., 2014). For example, species within the gorgonian family Melithaeidae Gray, 1870, did not cluster according to their traditional taxonomy but instead they grouped into different molecular clades that corresponded to specific regions, such as the Red Sea, East and South Africa, and the North and West Indian Ocean (Reijnen et al., 2014).

6.6.3 The relevance of being solitary

Monostomatism has often challenged the traditional taxonomy and systematics of several scleractinian coral groups (Vaughan and Wells, 1943; Wells, 1964; Hoeksema, 1989, 1991; Cairns, 2001, 2004). The taxonomic relevance of the solitary condition in corals has been revised in light of molecular phylogeny reconstructions published in recent years. Barbeitos et al. (2010) provided robust phylogenetic evidence that polystomatism has been repeatedly acquired and/or lost throughout the history of the order Scleractinia. These findings have been

subsequently corroborated by detailed phylogenetic analyses revealing that evolution from a solitary to a colonial condition, and the reverse, in the Fungiidae and Dendrophylliidae Gray, 1847, has occurred frequently in these two families characterized by congeneric monostomatous and polystomatous species (Gittenberger et al., 2011; Arrigoni et al., 2014d). For example, the highly speciose genus *Balanophyllia* Wood, 1844, is exclusively composed of solitary species but a phylogenetic reconstruction of dendrophylliids demonstrated the extensive polyphyly of this genus (Arrigoni et al., 2014d). Also, the genus *Cycloseris* Milne Edwards and Haime, 1849, originally consisted of monostomatous and free-living species (Hoeksema, 1989) but new molecular and micromorphological data showed that the polystomatous and attached species *C. explanulata* (van der Horst, 1922), *C. mokai* (Hoeksema, 1989), and *C. wellsi* (Veron and Pichon, 1980) belong to this genus (Benzoni et al., 2012b; Gittenberger et al., 2011; Hoeksema, 2014). Again, the monostomatous *Verrillofungia* Wells, 1966, is now considered a junior synonym of the polystomatous genus *Lithophyllon* Rehberg, 1892, based on a combined morpho-molecular approach (Gittenberger et al., 2011). Similarly, *Sclerophyllia* was originally described and maintained as a monotypic and solitary taxon (Klunzinger, 1879; Gravier, 1907; Wells, 1964; Veron and Pichon, 1980) until the present work, in which we reveal that the colonial species *S. maxima* belongs to the same lineage. The ancestral character state reconstruction reported in Fig. 6.22 suggests that the colonial condition was lost at least twice within the lobophylliids in the lineages leading to the species *S. margariticola* and *C. lacrymalis*. Once other solitary lobophylliid species, such as *Homophyllia australis* (Milne Edwards and Haime, 1849) and *Cynarina macassarensis* (Best and Hoeksema, 1987), are examined in a phylogenetic context, the actual evolutionary meaning of the solitary vs colonial condition will be better understood.

6.7 Conclusions

The present work points out the foremost importance of taxonomic literature and museum collections as information sources of known but forgotten taxa (Hoeksema et al., 2011; Rocha et al., 2014), as previously reported in the case of the genus *Craterastrea* Head, 1983 (Benzoni et al., 2012a). Indeed the examination of the original description of *S. margariticola* and its type material together with the study of new material from the coasts of Saudi Arabia in the northern and central Red Sea allowed us to resurrect the long-ignored genus *Sclerophyllia*. Furthermore, a detailed morpho-molecular approach of their taxonomy disclosed the unforeseen sister relationship between *S. margariticola* and *S. maxima*, which previously had been overlooked by the traditional systematics (Vaughan and Wells, 1943; Veron and Pichon, 1980; Wells, 1964). This phylogenetic and evolutionary distinct lineage shows also a peculiar geographic distribution, *i.e.* seas around the Arabian Peninsula, suggesting the importance of this area as marine biodiversity hotspot (Sheppard, 1985; Sheppard and Sheppard, 1991; Roberts et al., 2002; Berumen et al., 2013; Bowen et al., 2013).

– CHAPTER 7 –

*Integrating genetics and morphology:
revision of the reef coral genera *Micromussa* and *Homophyllia*
(*Scleractinia*, *Lobophylliidae*)
with description of two new species*

Roberto Arrigoni¹, Andrew H Baird², Chaolun Allen Chen^{3,4}, Hironobu Fukami⁵, Danwei Huang^{6,7,8}, Damian Thomson⁹, Mia Hoogenboom¹⁰, Bert W Hoeksema¹¹, Yuna Zayasu¹², Ann F Budd⁶, Tullia Isotta Terraneo^{1,13}, Yuko F Kitano⁵, Francesca Benzoni^{1,14}

¹ Department of Biotechnologies and Biosciences, University of Milan – Bicocca, Piazza della Scienza 2, 20126, Milan, Italy

² ARC Centre of Excellence for Coral Reef Studies, James Cook University, Townsville, QLD 4811, Australia

³ Biodiversity Research Centre, Academia Sinica, Nangang, Taipei 115, Taiwan

⁴ Institute of Oceanography, National Taiwan University, Taipei 106, Taiwan

⁵ Faculty of Agriculture, University of Miyazaki, 1-1 Gakuenkibanadai-Nishi, Miyazaki, 889-2192, Japan

⁶ Department of Earth and Environmental Sciences, University of Iowa, Iowa City, IA, 52242, USA

⁷ Scripps Institution of Oceanography, University of California, San Diego, La Jolla, CA 92093, USA

⁸ Department of Biological Sciences, National University of Singapore, Singapore 117543, Singapore

⁹ CSIRO Marine and Atmospheric Research, Wembley, WA 6014, Australia

¹⁰ School of Marine and Tropical Biology, James Cook University, Townsville, QLD 4811, Australia

¹¹ Department of Marine Zoology, Naturalis Biodiversity Center, P.O. Box 9517, 2300, RA Leiden, the Netherlands

¹² Seto Marine Biological Laboratory, Field Science and Education Center, Kyoto University, 459, Shirahama, Nishimuro-gun, Wakayama 649-2211, Japan

¹³ Red Sea Research Center, King Abdullah University of Science and Technology, 23955 Thuwal, Kingdom of Saudi Arabia

¹⁴ Institut de Recherche pour le Développement, UMR227 CoReUs2, 101 Promenade Roger Laroque, 98848 Noumea, New Caledonia

In preparation for *Organisms, Diversity & Evolution*

7.1 Abstract

The reef coral family Lobophylliidae is undergoing a widespread taxonomic revision thanks to the reciprocal illumination provided by both molecular and morphological tools. In this study, we investigate the evolutionary relationships and the macro- and micromorphology of six nominal coral species belonging to two of the nine molecular clades of the Lobophylliidae, *i.e.* clades A and B. Sequence data from mitochondrial DNA, COI and the intergenic spacer between COI and 1-rRNA, and nuclear DNA, Histone H3 and ITS region, are used to generate robust molecular phylogenies and median-joining haplotype network. Molecular analyses are strongly in agreement with detailed observations of gross- and fine-scale morphology of skeletons, leading to the formal revision of the genera *Homophyllia* and *Micromussa* and the description of two novel zooxanthellate shallow-water species, *Micromussa pacifica* sp. nov. and *Micromussa indiana* sp. nov. In particular, *Acanthastrea bowerbanki* and *A. hillae* are transferred to *Homophyllia* as well as *A. lordhowensis* and *Phymastrea multipunctata* to *Micromussa*, and a revised diagnosis for both two genera is provided. *Micromussa pacifica* sp. nov. is described from the Gambier Islands, New Caledonia, and Australia and, despite a superficial resemblance with *Homophyllia australis*, it has distinctive macro and micromorphological features at the septal level. *Micromussa indiana* sp. nov., previously considered an Indian Ocean population of *M. amakusensis*, is here described from the Gulf of Aden as a distinct species being genetically separated from *M. amakusensis* from which it can be distinguished on the basis of the smaller corallites size and by a smaller number of septa. Furthermore, molecular trees show that *Symphyllia wilsoni* is closely related but molecularly separated from clades A and B, and, based also on a unique combination of corallite and sub-corallite characters, the species is moved into a new genus, *Hydnophyllia* gen. nov. These findings highlight the need for integrating genetic and morphological datasets for taxonomic revision of scleractinian corals and description of new taxa.

7.2 Introduction

In the last decade, the increasing use of molecular tools and novel morphological analyses have shed new light on the evolution and systematics of scleractinian corals (Stolarski, 2003; Fukami et al., 2004a, 2008; Wallace et al., 2007; Budd and Stolarski, 2009, 2011; Gittenberger et al., 2011; Stolarski et al., 2011; Huang et al., 2011; Kitano et al., 2014). The reciprocal illumination between genetics and morphology has proven to be a successful and meaningful approach in order to formulate reliable hypothesis on reef coral evolutionary history and revolutionized the classical taxonomy at all systematic ranks (Stolarski and Janiszewska, 2001; Budd et al., 2010, 2012; Benzoni et al., 2012a; Kitahara et al., 2012b; Huang et al., 2014a).

The family Lobophylliidae Dai and Horng, 2009 is an ecologically dominant group in all tropical reefs of the Indo-Pacific (Veron and Pichon, 1980; Scheer and Pillai, 1983; Veron, 1993, 2000). It currently comprises 12 extant genera and 52 zooxathellate species and is widely distributed throughout the Indo-Pacific, from the Red Sea and east Africa to French Polynesia (Veron, 2000; Dai and Horng, 2009; Budd et al., 2012; Benzoni, 2013). To date, based on mitochondrial and nuclear phylogenies this taxon is a monophyletic lineage consisting of nine main genus-level molecular clades, denoted as clades A to I *sensu* Arrigoni et al. (2014a), that are mostly in disagreement with the previous systematic position of most lobophylliid representatives (Arrigoni et al., 2012, 2014a). Indeed, all polytypic genera analyzed so far, *i.e.* *Acanthastrea* Milne Edwards and Haime, 1848, *Echinophyllia* Klunzinger, 1879, *Lobophyllia* de Blainville, 1830, *Micromussa* Veron, 2000, *Oxypora* Saville Kent, 1871, and *Symphyllia* Milne Edwards and Haime, 1848, are not monophyletic (Arrigoni et al., 2014a). Furthermore, the two monospecific genera *Echinomorpha* Veron, 2000 and *Homophyllia* Brüggemann, 1877 have not been investigated at a molecular level, and their phylogentic position and taxonomy are still uncertain (Budd et al., 2012). Subsequently, these molecular findings have been integrated with novel skeletal macro- and micromorphological

criteria resulting in a better understanding of coral diversity and taxonomy (Budd and Stolarski, 2009; Budd et al., 2012; Arrigoni et al., 2014b, 2015). In particular, new micromorphological characters, such as the height, spacing, and shape of septal tooth, the distribution and shape of granules on septal face, and the structure of the interarea of teeth (Budd and Stolarski, 2009, 2011), resulted informative and diagnostic in the Lobophylliidae (Budd and Stolarski, 2009; Budd et al., 2012; Arrigoni et al., 2014b, 2015) as already demonstrated in other coral families (Benzoni et al., 2007, 2012a; Gittenberger et al., 2011; Budd and Stolarski, 2011; Janiszewska et al., 2011, 2013, 2015; Budd et al., 2012; Schmidt-Roach et al., 2014; Huang et al., 2014a, 2014b). In this taxonomic framework, the Lobophylliidae is undergoing a revision started with the phylogenetic classification of the genera *Australomussa* Veron, 1985, *Parascolymia* Wells, 1964, and *Sclerophyllia* Klunzinger, 1879 as a result of an integrated morpho-molecular approach (Arrigoni et al., 2014b, 2015).

The monotypic genus *Homophyllia* has a complicated nomenclatural history (Vaughan and Wells, 1943; Wells, 1964; Veron and Pichon, 1980; Veron, 2000; Budd et al., 2012). Previously considered a junior synonymy of *Lobophyllia* (Matthai, 1928; Vaughan and Wells, 1943) and *Scolymia* (Veron and Pichon, 1980; Veron, 2000), it was re-introduced by Budd et al. (2012) following novel morphological evidence proposed by Budd and Stolarski (2009). The authors showed that the micromorphology (granules and area between teeth) and the microstructure (arrangement of calcification centres) of the monostomatous species *Homophyllia australis* (Milne Edwards and Haime, 1849) (Figs. 7.1F, 7.2F) are unrelated and clearly distinguished from those of the solitary species *Scolymia lacera* (Pallas, 1766) and *Parascolymia vitiensis* (Brüggemann, 1877) (Budd and Stolarski, 2009; Budd et al., 2012; Arrigoni et al., 2014b). Nevertheless, despite the increasing amount of genetic data concerning the Lobophylliidae (Arrigoni et al., 2014a, 2014b, 2014c, 2015), no molecular information is available for *H. australis*. In this study we studied a large collection of specimens encompassing the whole range of morphologic variability shown in Veron and Pichon (1980), thus including

specimens with typical morphology (Figs. 7.1F, 7.2F; Figs. 408, 410 and 420 Veron and Pichon, 1980) and other specimens with thinner and less numerous septa (Figs. 7.1E, 7.2E; Figs. 412 and 424 Veron and Pichon, 1980).

Within the Lobophylliidae, the sister clades A and B *sensu* Arrigoni et al. (2014a) showed unexpected genetic affinities when compared with traditional taxonomy and the species included in these two clades are in need of formal taxonomic actions (Arrigoni et al., 2014a). Clade A *sensu* Arrigoni et al. (2014a) is composed by *Phymastrea multipunctata* (Hodgson, 1985) (Figs. 7.1D, 7.2D) and *Micromussa amakusensis* (Veron, 1990) (Figs. 7.1A, 7.2A) to date (Arrigoni et al., 2014a). The former species is currently formally assigned to the Merulinidae Verrill, 1865 but its phylogenetic placement within the Lobophylliidae revealed a taxonomic issue and a need for revision (Huang et al., 2011; Arrigoni et al., 2014a). Nevertheless, no detailed morphological studies have been conducted to elucidate the taxonomic status of this species. The poorly studied type species *M. amakusensis* has been recorded throughout the Indo-Pacific, from the Gulf of Aden to Central Indo-Pacific and West Pacific (Veron, 1990, 1992, 1993, 2000; Wallace et al., 2009; Pichon et al., 2010), regardless of remarkable morphological differences, such as number of septa and septal orders, between Indian Ocean (Figs. 7.1C, 7.2C) and Pacific Ocean (Figs. 7.1A, 7.2A) populations (Wallace et al., 2009; Pichon et al., 2010). In his description of *M. amakusensis*, Veron (1990) also highlighted that, on the basis of macromorphology and *in-situ* appearance, the closest species is *A. lordhowensis* Veron and Pichon, 2002 (Figs. 7.1B, 7.2B) which has larger and less regular corallites and more septa. Nevertheless, Veron (2000) erected the genus *Micromussa* to include species previously ascribed to *Acanthastrea* with corallites less than 5 mm diameter, thus excluding *A. lordhowensis*. The author also described *Micromussa diminuta* Veron, 2000 from Sri Lanka, but this species has never been examined further and no genetic or microstructural data is available.

Clade B *sensu* Arrigoni et al. (2014a) currently contains *Acanthastrea bowerbanki* Milne Edwards and Haime, 1857 (Figs. 7.1G, 7.2G) and *Acanthastrea*

hillae Wells, 1955 (Figs. 7.1H, 7.2H). At a molecular level, *A. bowerbanki* and *A. hillae* are clearly not related to the genus type species *Acanthastrea echinata* (Dana, 1846), recovered in clade E *sensu* Arrigoni et al. (2014a and figures therein), and the establishment of a new genus to accommodate these species is thus pending. The sister-relationship between the two species is corroborated also by remarkable morphologic similarities of their coralla and corallites (Veron and Pichon, 1980; Veron, 1992, 2000; Wallace et al., 2009). Their coralla are similar in growth form and mode of budding, while their corallites are the largest in *Acanthastrea* (Veron and Pichon, 1980; Veron, 2000). Furthermore, *A. bowerbanki* and *A. hillae* show a partially overlapping geographic distribution, living mainly in the Central Pacific (Veron and Pichon, 1980; Veron, 1993, 2000; Wallace et al., 2009). They are generally rare and uncommon throughout the tropics but more abundant in high latitude non-reef localities (Veron, 1993). *Acanthastrea hillae* has been also reported from the Western Indian Ocean but these records are doubtful (Veron, 2000).

The present study aims to provide a reliable molecular phylogeny reconstruction of six nominal species included in clades A and B *sensu* Arrigoni et al. (2014a), using sequences of the mitochondrial DNA regions cytochrome c oxidase subunit I (COI) and the non-coding intergenic spacer region between COI and large ribosomal RNA subunit, and the nuclear markers ribosomal internal transcribed spacers 1 and 2 and Histone H3 gene. Furthermore we investigate gross- and fine-scale morphology of skeletons of each examined coral species and, with the exception of *Phymastrea multipunctata*, all species were collected from their type locality.

7.3 Material and methods

7.3.1 Coral sampling and identification

A total of 87 coral specimens were collected while SCUBA diving between 1 and 35 m depth from different localities in the Indian and Pacific Ocean (Figs. 7.1, 7.2, Table 7.1). Samples of *A. bowerbanki*, *A. hillae*, *A. lordhowensis*, *H. australis*, and *Symphyllia wilsoni* Veron, 1985 were sampled from their type locality, Australia, as well as *M. amakusensis* from Japan. Each coral sample was underwater photographed and then collected, tagged, and approximately 1 cm² of the entire specimen was broken off and put in CHAOS solution to dissolve the tissue or fixed in 95% ethanol for further molecular analyses. The remaining corallum was immersed in sodium hypochlorite for 48 hours to remove all soft parts, rinsed in freshwater and air-dried for identification and microscope observations (Figs. 7.1, 7.2). Specimens were identified at species level based on their morphological structures following Milne Edwards and Haime (1848), Wells (1964), Veron and Pichon (1980, 1982), Hodgson (1985), Veron (1985, 1990, 2000), Wallace et al. (2009), Pichon et al. (2010), and using illustrations of holotypes in their original descriptions. Voucher samples were deposited at the University of Milano-Bicocca (Milano, Italy), the University of Miyazaki (Miyazaki, Japan), Institut de Recherche pour le Développement (Noumea, New Caledonia), Naturalis Biodiversity Center (Leiden, the Netherlands), and Museum of Tropical Queensland (Townsville, Australia).

Table 7.1. List of the material examined in this study. For each specimen we list code, identification, sampling locality, collector, and molecular markers used for the phylogenetic reconstructions. xxx: sequence newly obtained in this work.

Code	Species	Locality	Collector	CO I	Histon e H3	ITS region	IG R
4629	<i>Acanthastrea bowerbanki</i>	Australia	Baird AH	xxx	xxx	xxx	
MH019	<i>Acanthastrea bowerbanki</i>	Australia	Hoogenboom M	xxx	xxx	xxx	
HS3285	<i>Acanthastrea bowerbanki</i>	New Caledonia	Benzoni F	xxx	xxx	xxx	
HS3286	<i>Acanthastrea bowerbanki</i>	New Caledonia	Benzoni F	xxx	xxx	xxx	
HS3287	<i>Acanthastrea bowerbanki</i>	New Caledonia	Benzoni F	xxx	xxx	xxx	
HS3288	<i>Acanthastrea bowerbanki</i>	New Caledonia	Benzoni F	xxx	xxx	xxx	
HS3298	<i>Acanthastrea bowerbanki</i>	New Caledonia	Benzoni F	xxx	xxx	xxx	
HS3446	<i>Acanthastrea bowerbanki</i>	New Caledonia	Benzoni F	xxx	xxx	xxx	
HS3489	<i>Acanthastrea bowerbanki</i>	New Caledonia	Benzoni F	xxx	xxx	xxx	
MH043	<i>Acanthastrea hillae</i>	Australia	Hoogenboom M	xxx	xxx	xxx	
MH046	<i>Acanthastrea hillae</i>	Australia	Hoogenboom M	xxx	xxx	xxx	
HS3066	<i>Acanthastrea hillae</i>	New Caledonia	Benzoni F	xxx	xxx	xxx	
HS3163	<i>Acanthastrea hillae</i>	New Caledonia	Benzoni F	xxx	xxx	xxx	
HS3169	<i>Acanthastrea hillae</i>	New Caledonia	Benzoni F	xxx	xxx	xxx	
HS3225	<i>Acanthastrea hillae</i>	New Caledonia	Benzoni F	xxx	xxx	xxx	
HS3438	<i>Acanthastrea hillae</i>	New Caledonia	Benzoni F	xxx	xxx	xxx	
HS3501	<i>Acanthastrea hillae</i>	New Caledonia	Benzoni F	xxx	xxx	xxx	
HS3531	<i>Acanthastrea hillae</i>	New Caledonia	Benzoni F	xxx	xxx	xxx	
1597	<i>Acanthastrea lordhowensis</i>	Australia	Baird AH	xxx	xxx	xxx	xxx
1598	<i>Acanthastrea lordhowensis</i>	Australia	Baird AH	xxx	xxx	xxx	xxx
1642	<i>Acanthastrea lordhowensis</i>	Australia	Baird AH	xxx	xxx	xxx	xxx
5019	<i>Acanthastrea</i>	Australia	Baird AH	xxx	xxx	xxx	xxx

5023	<i>lordhowensi</i> <i>Acanthastrea</i>	Australia	Baird AH	xxx	xxx	xxx	xxx
5038	<i>lordhowensi</i> <i>Acanthastrea</i>	Australia	Baird AH	xxx	xxx	xxx	xxx
5050	<i>lordhowensi</i> <i>Acanthastrea</i>	Australia	Baird AH	xxx	xxx	xxx	xxx
5063	<i>lordhowensi</i> <i>Acanthastrea</i>	Australia	Baird AH	xxx	xxx	xxx	xxx
5079	<i>lordhowensi</i> <i>Acanthastrea</i>	Australia	Baird AH	xxx	xxx	xxx	xxx
5085	<i>lordhowensi</i> <i>Acanthastrea</i>	Australia	Baird AH	xxx	xxx	xxx	xxx
5087	<i>lordhowensi</i> <i>Acanthastrea</i>	Australia	Baird AH	xxx	xxx	xxx	xxx
5098	<i>lordhowensi</i> <i>Acanthastrea</i>	Australia	Baird AH	xxx	xxx	xxx	xxx
5099G	<i>lordhowensi</i> <i>Acanthastrea</i>	Australia	Baird AH	xxx	xxx	xxx	xxx
5099R	<i>lordhowensi</i> <i>Acanthastrea</i>	Australia	Baird AH	xxx	xxx	xxx	xxx
MH042	<i>lordhowensi</i> <i>Acanthastrea</i>	Australia	Hoogenboom M	xxx	xxx	xxx	xxx
4631	<i>Homophyllia</i> <i>australis</i>	Australia	Baird AH	xxx	xxx	xxx	
HS3311	<i>Homophyllia</i> <i>australis</i>	New Caledonia	Benzoni F	xxx	xxx	xxx	
HS3441	<i>Homophyllia</i> <i>australis</i>	New Caledonia	Benzoni F	xxx	xxx	xxx	
HS3447	<i>Homophyllia</i> <i>australis</i>	New Caledonia	Benzoni F	xxx	xxx	xxx	
HS3470	<i>Homophyllia</i> <i>australis</i>	New Caledonia	Benzoni F	xxx	xxx	xxx	
HS3524	<i>Homophyllia</i> <i>australis</i>	New Caledonia	Benzoni F	xxx	xxx	xxx	
HS3525	<i>Homophyllia</i> <i>australis</i>	New Caledonia	Benzoni F	xxx	xxx	xxx	
HS3526	<i>Homophyllia</i> <i>australis</i>	New Caledonia	Benzoni F	xxx	xxx	xxx	
HS3544	<i>Homophyllia</i> <i>australis</i>	New Caledonia	Benzoni F	xxx	xxx	xxx	
HS3545	<i>Homophyllia</i> <i>australis</i>	New Caledonia	Benzoni F	xxx	xxx	xxx	
HS3469	<i>Homophyllia</i> <i>australis</i>	New Caledonia	Benzoni F	xxx	xxx	xxx	
GA130	<i>cf Homophyllia</i> <i>australis</i>	Gambier Islands	Benzoni F	xxx	xxx	xxx	
GA150	<i>cf Homophyllia</i> <i>australis</i>	Gambier Islands	Benzoni F	xxx	xxx	xxx	

GA186	<i>cf Homophyllia australis</i>	Gambier Islands	Benzoni F	xxx	xxx	xxx	
HS3202	<i>cf Homophyllia australis</i>	New Caledonia	Benzoni F	xxx	xxx	xxx	xxx
HS3359	<i>cf Homophyllia australis</i>	New Caledonia	Benzoni F	xxx	xxx	xxx	xxx
HS3471	<i>cf Homophyllia australis</i>	New Caledonia	Benzoni F	xxx	xxx	xxx	xxx
HS3527	<i>cf Homophyllia australis</i>	New Caledonia	Benzoni F	xxx	xxx	xxx	xxx
HS3528	<i>cf Homophyllia australis</i>	New Caledonia	Benzoni F	xxx	xxx	xxx	xxx
HS3543	<i>cf Homophyllia australis</i>	New Caledonia	Benzoni F	xxx	xxx	xxx	xxx
HS3327	<i>cf Homophyllia australis</i>	New Caledonia	Benzoni F	xxx	xxx	xxx	xxx
HS3483	<i>cf Homophyllia australis</i>	New Caledonia	Benzoni F	xxx	xxx	xxx	xxx
AM65	<i>Micromussa amakusensis</i>	Japan	Fukami H	xxx	xxx	xxx	xxx
346	<i>Micromussa amakusensis</i>	Japan	Fukami H	xxx	xxx	xxx	xxx
359	<i>Micromussa amakusensis</i>	Japan	Fukami H	xxx	xxx	xxx	xxx
364	<i>Micromussa amakusensis</i>	Japan	Fukami H	xxx	xxx	xxx	xxx
368	<i>Micromussa amakusensis</i>	Japan	Fukami H	xxx	xxx	xxx	xxx
AD069	<i>Micromussa cf amakusensis</i>	Gulf of Aden	Benzoni F	xxx	xxx	xxx	xxx
BA117	<i>Micromussa cf amakusensis</i>	Gulf of Aden	Benzoni F	xxx	xxx	xxx	xxx
BU001	<i>Micromussa cf amakusensis</i>	Gulf of Aden	Benzoni F	xxx	xxx	xxx	xxx
FP	<i>Micromussa cf amakusensis</i>	Gulf of Aden	Benzoni F	xxx	xxx	xxx	xxx
MU185	<i>Micromussa cf amakusensis</i>	Gulf of Aden	Benzoni F	xxx	xxx	xxx	xxx
MU215	<i>Micromussa cf amakusensis</i>	Gulf of Aden	Benzoni F	xxx	xxx	xxx	xxx
SO071	<i>Micromussa cf amakusensis</i>	Gulf of Aden	Benzoni F	xxx	xxx	xxx	xxx
40070	<i>Phymastrea multipunctata</i>	Malaysia	Hoeksema BW	xxx	xxx	xxx	xxx
40077	<i>Phymastrea multipunctata</i>	Malaysia	Hoeksema BW	xxx	xxx	xxx	xxx
40099	<i>Phymastrea multipunctata</i>	Malaysia	Hoeksema BW	xxx	xxx	xxx	xxx
WIL1	<i>Symphyllia</i>	Australia	Thomson D	xxx	xxx	xxx	xxx

WIL2	<i>wilsoni</i> <i>Symphyllia</i>	Australia	Thomson D	xxx	xxx	xxx	xxx
WIL3	<i>wilsoni</i> <i>Symphyllia</i>	Australia	Thomson D	xxx	xxx	xxx	xxx
WIL4	<i>wilsoni</i> <i>Symphyllia</i>	Australia	Thomson D	xxx	xxx	xxx	xxx
WIL5	<i>wilsoni</i> <i>Symphyllia</i>	Australia	Thomson D	xxx	xxx	xxx	xxx
BA115	<i>Acanthastrea</i> <i>hemprichii</i>	Gulf of Aden	Benzoni F	xxx	xxx	xxx	
DJ274	<i>Acanthastrea</i> <i>hemprichii</i>	Djibouti	Benzoni F	xxx	xxx	xxx	
AD073	<i>Acanthastrea</i> <i>echinata</i>	Gulf of Aden	Benzoni F	xxx	xxx	xxx	
BU036	<i>Acanthastrea</i> <i>echinata</i>	Gulf of Aden	Benzoni F	xxx	xxx	xxx	
MH005	<i>Acanthastrea</i> <i>echinata</i>	Australia	Hoogenboom M	xxx	xxx	xxx	
MH006	<i>Acanthastrea</i> <i>echinata</i>	Australia	Hoogenboom M	xxx	xxx	xxx	
MH024	<i>Acanthastrea</i> <i>echinata</i>	Australia	Hoogenboom M	xxx	xxx	xxx	
MH040	<i>Acanthastrea</i> <i>echinata</i>	Australia	Hoogenboom M	xxx	xxx	xxx	
MH041	<i>Acanthastrea</i> <i>echinata</i>	Australia	Hoogenboom M	xxx	xxx	xxx	
HS3126	<i>Acanthastrea</i> <i>echinata</i>	New Caledonia	Benzoni F	xxx	xxx	xxx	
HS3150	<i>Acanthastrea</i> <i>echinata</i>	New Caledonia	Benzoni F	xxx	xxx	xxx	
HS3195	<i>Acanthastrea</i> <i>echinata</i>	New Caledonia	Benzoni F	xxx	xxx	xxx	

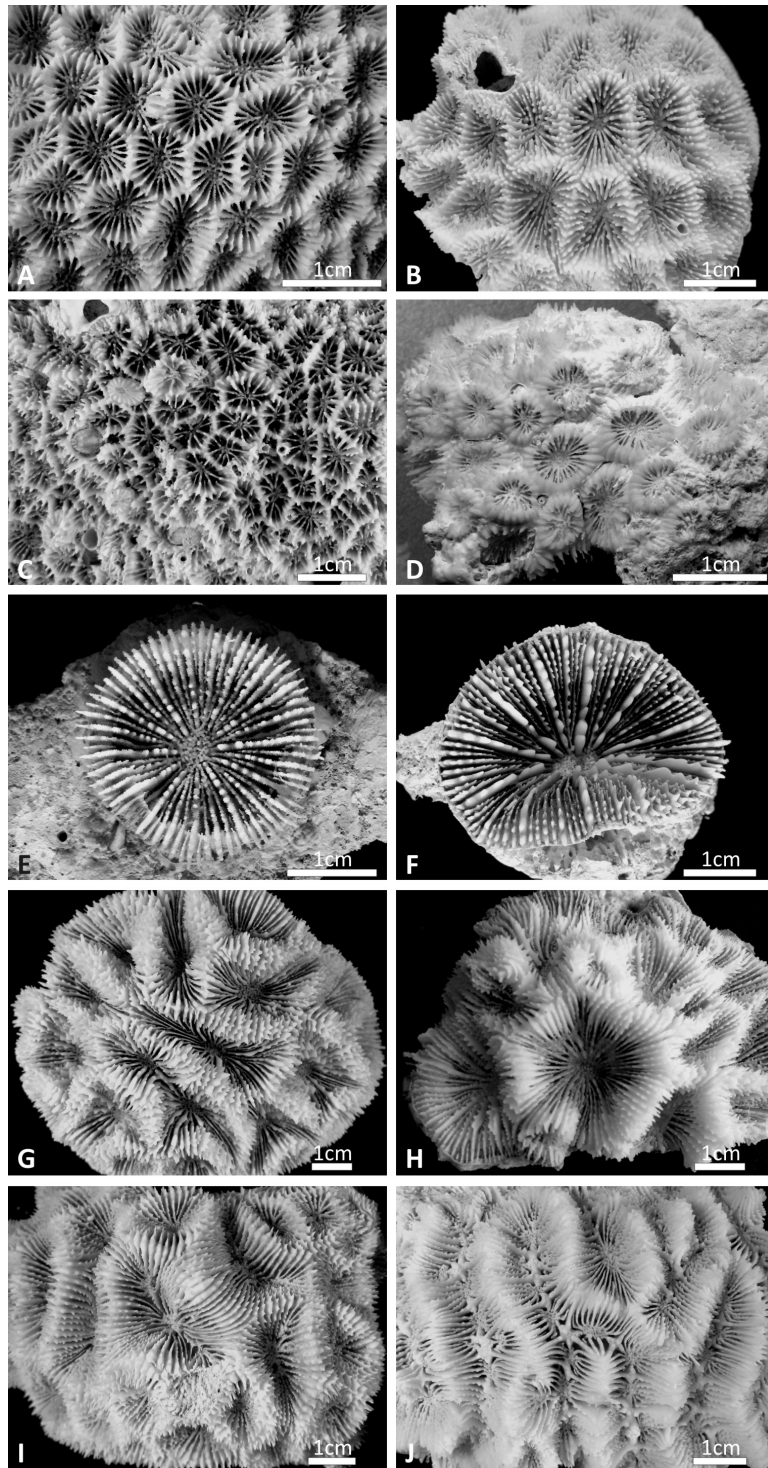


Figure 7.1. Skeleton macro-morphology of the Lobophylliidae included in this study: **A)** holotype of *Micromussa amakusensis* MTQ G32485 from Japan; **B)** *Acanthastrea lordhowensis* 1642 from Australia; **C)** *Micromussa amakusensis* MNHN-IK-2012-14232 from the Gulf of Aden; **D)** *Phymastrea multipunctata* RMNH Coel 40090 from Malaysia; **E)** cf *Homophyllia australis* IRD HS3543 from New Caledonia; **F)** *Homophyllia australis* IRD HS3424 from New Caledonia; **G)** *Acanthastrea bowerbanki* MH043 from Australia; **H)** *Acanthastrea hillae* IRD HS3287 from New Caledonia; **I)** *Acanthastrea hemprichii* UNIMIB BA115; **J)** *Symphyllia wilsoni* from Australia.



Figure 7.2. In situ morphology of the Lobophylliidae included in this study: **A)** *Micromussa amakusensis* from Japan; **B)** *Acanthastrea lordhowensis* from Lord Howe, Australia; **C)** *Micromussa amakusensis* from the gulf of Aden, same specimen shown in 7.1C; **D)** *Phymastrea multipunctata* RMNH Coel 40090 from Malaysia; **E)** cf *Homophyllia australis*, same specimen shown in 7.1E; **F)** *Homophyllia australis*, same specimen shown in 7.1E; **G)** *Acanthastrea bowerbanki* IRD HS3066 from New Caledonia; **H)** *Acanthastrea hillae*, same specimen shown in 7.1H; **I)** *Acanthastrea hemprichii* UNIMIB BA115 from the Gulf of Aden; *Symphyllia wilson* from Australia.

7.3.2 DNA preparation, amplification and sequence analyses

Total genomic DNA was extracted using the DNeasy Blood and Tissue kit (Qiagen Inc., Valencia, CA, USA) for coral tissue preserved in ethanol, and using a phenol-chloroform-based method with a phenol extraction buffer (100 mM Tris-Cl pH 8, 10 mM EDTA, 0.1% SDS) (Fukami et al., 2004; Huang et al., 2011). For all coral specimens we amplified and directly sequenced one mitochondrial marker, the barcoding region of cytochrome c oxidase subunit I (COI), and two nuclear markers, the Histone H3 gene and the ribosomal ITS region including the 3' end of 18S, the entire ITS1, 5.8S, and ITS2, and the 5' end of the 28S (ITS region). COI gene, Histone H3, and ITS region were amplified using the primer pairs MCOIF and MCOIR and the protocol proposed by Benzoni et al. (2011), H3F and H3R (Colgan et al., 1998), ITS4 (White et al., 1990) and A18S (Takabayashi et al., 1998) and the protocol published by Benzoni et al. (2011) respectively. Furthermore, for species included in clade A *sensu* Arrigoni et al. (2014a) the mitochondrial non-coding intergenic spacer region (IGR) between COI and large ribosomal RNA subunit was amplified using MNC1F and MNC1R primers (Fukami et al., 2004b; Huang et al., 2009) and the protocol described by Arrigoni et al. (2014c). Both strands of PCR fragments were purified and directly sequenced by Genomics Ltd. (Taipei, Taiwan) or alternately by Macrogen Inc. (Seoul, South Korea) with the same primers as used in the PCR. Chromatograms were manually corrected for misreads, if necessary, and forward and reverse strands were merged into one sequence file using CodonCode Aligner 3.6.1 (CodonCode Corporation, Dedham, MA, USA). In particular, chromatograms of products obtained with ITS4 and A18S primers did not show any intra-individual polymorphisms or double peaks, thereby allowing direct sequencing of ITS region. All newly obtained sequences were deposited in EMBL, and accession numbers are listed in Table 7.1.

Sequence alignments were generated using the E-INS-i option in MAFFT 7.110 (Kato et al., 2002; Kato and Standley, 2013) under default parameters. For phylogenetic analyses, sequences of COI, Histone H3, and ITS region were

concatenated into one partitioned data set. Three methods, Maximum Parsimony (MP), Maximum Likelihood (ML), and Bayesian Inference (BI), were employed to reconstruct the phylogenetic relationships within the Lobophylliidae. For MP analysis, tree searches were generated in PAUP* 4.0b10 (Swofford, 2003) using heuristic searches with 10000 random additions. Branch support was estimated with the bootstrap confidence levels using 1000 replicates. Prior to the model-based phylogenetic analyses, the best-fit model of nucleotide substitution was identified for each gene partition separately by means of the Akaike Information Criterion calculated with MrModeltest 2.3 (Nylander, 2004). The following substitution models were suggested: the GTR + I + G for ITS region, the HKY + G + I for COI, and the K80 + I for Histone H3. ML topologies were calculated with PhyML (Guindon and Gascuel, 2003) and relative support for individual clades was estimated using the Shimodaira and Hasegawa (SH-like) test. BI analysis was performed employing MrBayes 3.1.2 (Huelsenbeck and Ronquist, 2001). Two simultaneous runs of four Markov Monte Carlo chains were conducted for 3×10^7 generations, sampling every 100 generations to ensure independence of the successive samples. Results were analyzed for stationarity and convergence using Tracer 1.6 (Rambaut and Drummond, 2007), with a burn-in of 25% of sampled generations. Additionally, ML phylogenetic reconstructions for each separate COI, Histone H3, and ITS region were obtained using PhyML (Guindon and Gascuel, 2003) under the substitution models proposed by MrModeltest 2.3 (Nylander, 2004). The SH-like test replicates was performed to assess the branch support of ML trees.

Within clade A *sensu* Arrigoni et al. (2014a), Network 4.6.1.2 (<http://www.fluxus-technology.com>) was used to construct a median-joining haplotype network (Bandelt et al., 1999) for the IGR dataset. This method is especially applicable to non-recombinant DNA sequences, like mitochondrial DNA, and combines all minimum spanning trees to a single network. Alignment was converted to the Roehl format using DnaSP (Librado and Rozas, 2009), invariable sites were removed and sites with gaps were not considered.

7.3.3 Morphological analyses

Scleractinian coral skeletons of the sequenced lobophylliids were analyzed both at macro- and micromorphological levels using light microscopy and Scanning Electron Microscopy (SEM), respectively. Images of coral skeletons were taken with a Canon G5 digital camera as well as through a Leica M80 microscope equipped with a Leica IC80HD camera. For scanning electron microscope (SEM) imaging, skeleton fragments were grinded, mounted on stubs using silver glue, sputter-coated with conductive gold film, and examined using a Vega Tescan Scanning Electron Microscope at the University of Milano-Bicocca. For a glossary of skeletal terms we followed Budd et al. (2012). We adopted their character names, ID numbers (in brackets), and state names.

Abbreviations:

IRD: Institut de Recherche pour le Développement, Nouméa, New Caledonia

MNHN: Muséum National d'Histoire Naturelle, Paris, France

MTQ: Museum of Tropical Queensland, Australia

NHMK: Natural History Museum, London, UK (formerly British Museum of Natural History, BMNH)

QM: Queensland Museum, Brisbane, Australia

UNIMIB: Università di Milano-Bicocca, Milan, Italy

UP: Marine Science Institute, University of the Philippines, Manila, the Philippines

WAM: Western Australian Museum, Perth, Australia

7.4 Results

7.4.1 Phylogenetic and haplotype network analyses

New sequence data of COI, Histone H3, and ITS region generated in this study from 87 coral samples representing 11 species was combined with published sequences of the families Lobophylliidae, Merulinidae, Diploastreidae Chevalier

and Beauvais, 1987, and Montastraeidae Yabe and Sugiyama, 1941, resulting in an alignment composed by 50 nominal species. *Plesiastrea versipora* was selected as outgroup because of its divergence from the Lobophylliidae, Merulinidae, Diploastreidae, and Montastraeidae (Fukami et al., 2008; Huang et al., 2011; Budd et al., 2012). The final concatenated data set of aligned sequences of the three molecular fragments had a total length of 1939 bp (COI: 580 bp, Histone H3: 318 bp, ITS region: 1041 bp). The ITS region was the most variable, with 191 variable sites (148 positions parsimony-informative PI), the COI gene fragment showed 87 bp variable sites (57 positions PI), and the Histone H3 sequences featured 90 bp variable sites (84 positions PI).

The three single gene trees do not show any supported topological conflicts, although the resolution differs notably among the three topologies (Apps. 7.1, 7.2, 7.3). Moreover, each of the analyzed specimens belongs to the same molecular clade in all of the three phylogenetic reconstructions. The tree based on ITS region shows more resolution than the COI and Histone H3 analyses, contributing to a greater extent to the combined tree topology. The phylogenetic reconstruction obtained from the concatenated gene analyses is shown in Fig. 7.3. Bayesian, Maximum likelihood, and Maximum parsimony topologies are highly concordant and node support values are high across the ingroup and outgroup. In particular, the Maximum parsimony tree is less resolved than Bayesian and Maximum likelihood ones even if it does not conflict with the other two topologies. The phylogram based on the concatenated (COI, histone H3, and ITS region) molecular dataset is broadly consistent with published phylogenies (Huang et al., 2011; Arrigoni et al., 2014a, 2014b, 2015), confirming the Lobophylliidae and Merulinidae as monophyletic groups (Fig. 7.3). All of the nine main genus-level lineages proposed by Arrigoni et al. (2014a) for the Lobophylliidae are highly supported by all methods of phylogeny reconstruction. Surprisingly within this family a novel clade is detected and it is constituted by only one species, *S. wilsoni*. Its monophyly is strongly supported (Bayesian posterior probability score $P_p = 1$, ML SH-like support $S_s = 1$, MP bootstrapping support $B_s = 99$) and the lineage is deeply

divergent from clade I which contains the genera *Lobophyllia*, *Parascolymia*, and all of the other *Symphyllia* species analyzed so far. *Symphyllia wilsoni* falls at the base of the sister clades A and B that are both very well resolved and supported (Pp = 1, Ss = 1, Bs = 99 for both clades). Clade A contains three nominal species: the genus type species *M. amakusensis*, *P. multipunctata*, and *A. lordhowensis*. The monophyly of the latter two species is highly supported while *M. amakusensis* is split in two main lineages. In particular, the colonies of *M. amakusensis* from the type locality Japan are grouped together, with the exception of the uncertain position of a sample AM65, and they are sister to *P. multipunctata*, while specimens of *M. amakusensis* from Yemen form a monophyletic lineage with strong supports (Pp = 1, Ss = 1, Bs = 95) that is sister to the group *M. amakusensis* from Japan – *P. multipunctata*. Moreover, within clade A we find a basal well-supported group (Pp = 1, Ss = 1, Bs = 99) composed by all of the specimens identified as cf *Homophyllia australis* characterized by thinner and less numerous septa (Figs. 7.1E, 7.2E). This lineage is clearly not related to the samples of *H. australis* showing the typical morphology of the species (Figs. 7.1F, 7.2F) that form a well-supported group (Pp = 0.9, Ss = 0.89, Bs = 83) within the clade B and that are, therefore, also separated from *Parascolymia vitiensis* in clade I. *Homophyllia australis* is sister to the well-supported lineage (Pp = 0.95, Ss = 0.94, Bs = 90) composed by *A. bowerbanki* and *A. hillae*. The latter two species cannot be distinguished using these three molecular markers. In particular, the average genetic distance between these two species is $2.3 \pm 0.3\%$, and fully overlaps with the interspecific distances within *A. bowerbanki* and *A. hillae* that are $2.1 \pm 0.3\%$ and $2.4 \pm 0.4\%$, respectively. Finally, all of the analyzed colonies of *A. echinata* and *A. hemprichii* Ehrenberg, 1834 fall within clade E, together with the published sequences of *A. rotundoflora* and *A. subechinata*, although their genetic boundaries remain unclear.

Haplotype network analysis of clade A inferred from the mtDNA IGR locus is shown in Fig. 7.4. The results obtained with this mitochondrial region are highly concordant with the phylogeny reconstruction of clade A based on COI, Histone H3, and ITS region. A total of nine haplotypes are detected and five main clusters

corresponding to the five lineages found using the other markers are revealed. These clusters are separated by a minimum of seven mutations (between *M. amakusensis* from Japan and *M. lordhowensis*) and no haplotypes are shared between two or more clusters. In particular, we found two closely related haplotypes specific of *M. amakusensis* from Japan differing by three base changes, two closely related haplotypes for *P. multipunctata* separated by one mutations, two closely related haplotypes specific of *A. lordhowensis* showing one mutation event, a single haplotype for all eight specimens of cf *H. australis*, and two closely related haplotypes for *M. amakusensis* from Yemen differing by one base changes. Notably, *M. amakusensis* from Japan and *M. amakusensis* from Yemen are again unrelated and separated by 35-39 mutations.

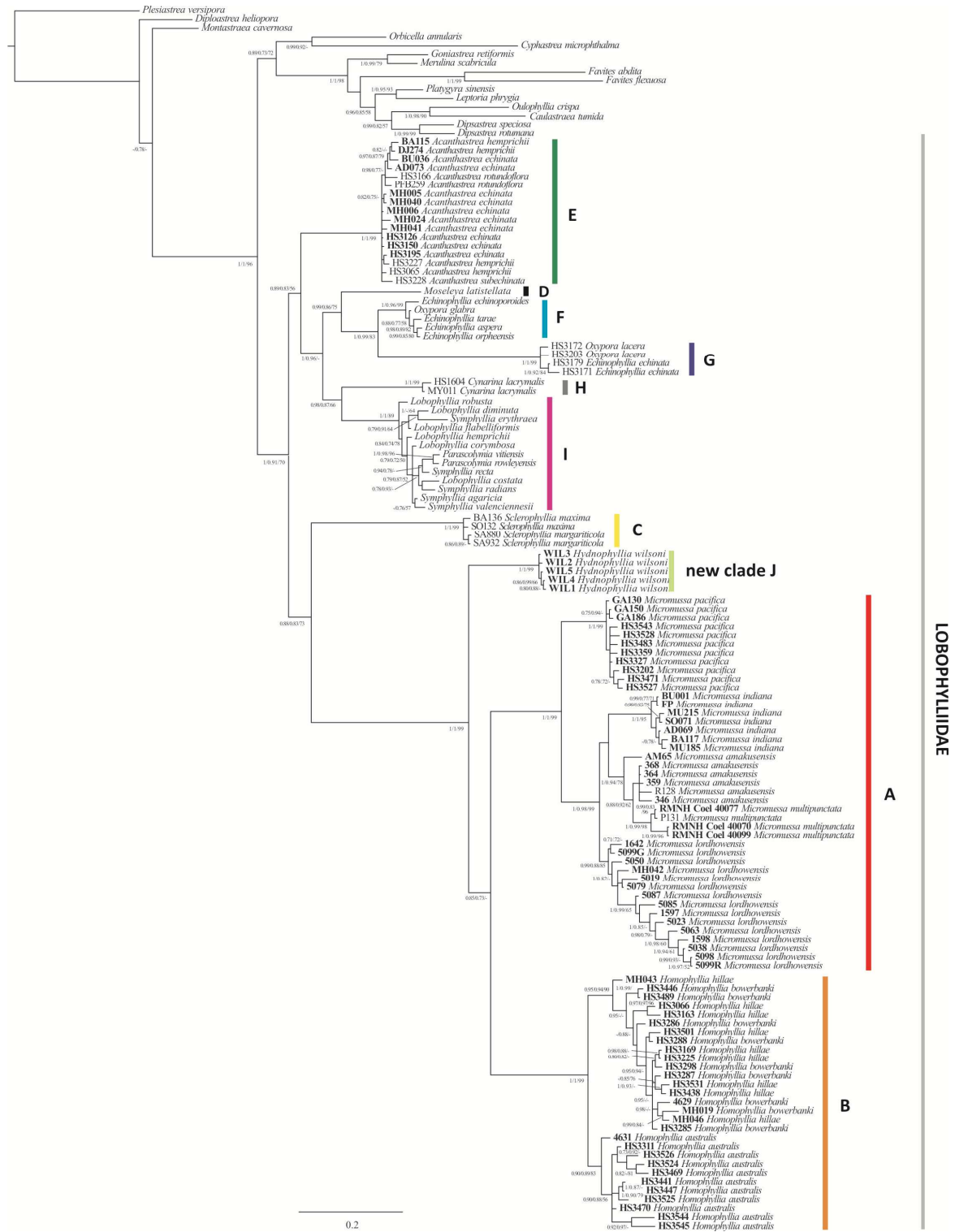


Figure 7.3. Bayesian phylogeny reconstruction of the family Lobophylliidae for the analysis of the concatenated data set of COI, Histone H3, and ITS region. Numbers above branches indicate nodal support of shown topology by means of Bayesian posterior probabilities (>0.8), Maximum Likelihood Sh-like supports (>0.7), and Maximum Parsimony bootstrap supports (>50). Lower values of support not shown. Clades within Lobophylliidae are coloured and labelled A to I according to Arrigoni et al. (2014a). Specimens analyzed in this study are in bold.

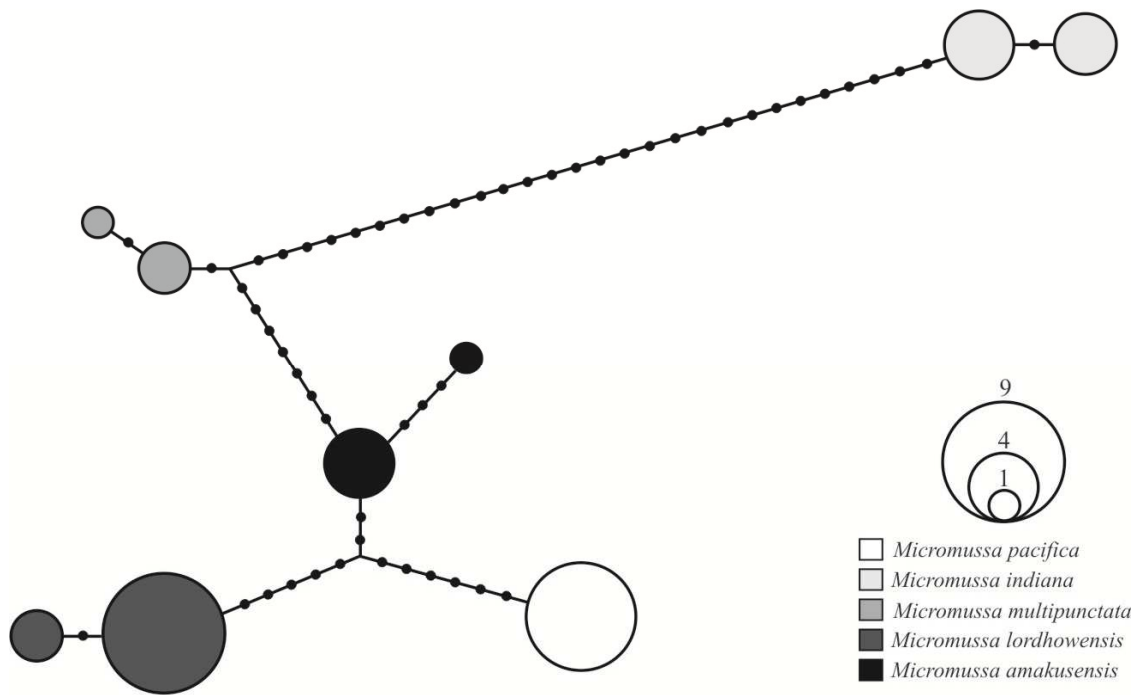


Figure 7.4. Haplotype network of the genus *Micromussa* (clade A) obtained in Network 4.6.1.2 for the mitochondrial intergenic spacer region (IGR) between COI and 1-rRNA. The size of circles is proportional to the frequencies of specimens sharing the same haplotype. The black solid circles are indicative of mutations that differentiate each haplotype.

7.4.2 Morphological analyses

7.4.2.1 Macromorphology

The examined lobophyllid species present a wide array of corallum macromorphology and corallite size and organization (Fig. 7.1). *Micromussa amakusensis*, *A. lordhowensis*, *P. multipunctata*, *A. bowerbanki*, *A. hillae*, and *S. wilsoni* are colonial species forming encrusting to massive coralla. Corallite organization is plocoid in *P. multipunctata*, cerioid in *M. amakusensis* and *A. lordhowensis*, cerioid to sub-meandroid in *A. bowerbanki* and *A. hillae*, and cerioid and meandroid in *S. wilsoni*. *Homophyllia australis* is a solitary species forming large and predominantly monocentric coralla. This species, however, shows a considerable range of corallum size and in some specimens a tendency to polystomatism is observed (Veron and Pichon, 1980). Two different morphs could be distinguished in the examined material, some with typical morphology (Figs. 7.1F, 7.5) having numerous septa with those of the first two cycles thicker and with

more pronounced teeth (black arrows in Figs. 7.5B, D, F, H), and others with thinner and less numerous septa (Figs. 7.1E, 7.6) and a more pronounced tendency to polystomatism (Figs. 7.6C-I). In these, both intracalicular (dashed arrows in Figs. 7.6C, E-F) and extracalicular (Figs. 7.6G-I) modes of budding were observed. Among the examined specimens, material previously identified as *M. amakusensis* from the Indian Ocean (Yemen) shows smaller corallite and columella size and a more polygonal outline (Fig 7.1C) than the material from Japan, the type locality (Fig. 7.1A). Moreover, the Yemen specimens have no more than 2-3 cycles of widely spaced septa while the Japan material has 4 cycles of septa (Fig. 7.1A). The macromorphological examination of *S. wilsoni* showed that this species has some peculiar features (Fig. 7.1J) which distinguish it from the other species in the same genus, and from any other lobophylliid examined. In this species, both monocentric corallites and series of corallites are observed. In the latter, the columellae in the valleys are not rounded or flattened in outline but have a roughly bilateral symmetry, the axis of this symmetry being a skeletal structure running in the centre of the valleys along their length and joining corallite centres. Finally, the walls of adjoining corallites series can be discontinuous and form hydnochoroid structures (Figs. 7.10A, E, F, G), similar to those observed in the merulinid genus *Hydnophora* and in some *Pavona* species (Veron and Pichon, 1980).

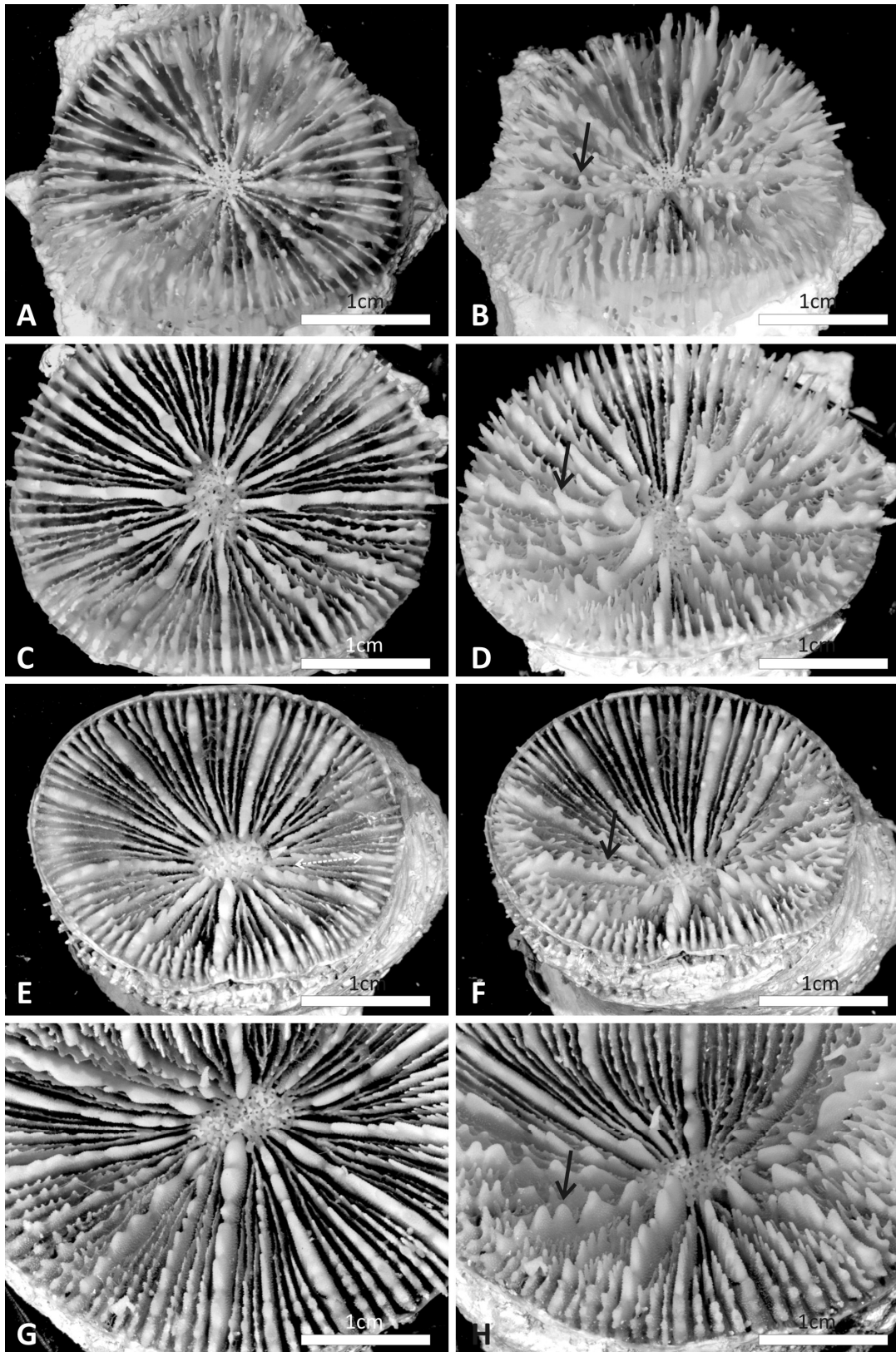


Figure 7.5. Top (A, C, E, G) and side (B, D, F, H) views of *Homophyllia australis* showing typical morphology: **A)** IRD HS3441, top view; **B)** side view of the same corallum as in A; **C)** IRD HS3470, top view; **D)** side view of the same corallum as in C; **E)** IRD HS3545, top view; **F)** side view of the same corallum as in E; **G)** IRD HS3424, top view; **H)** side view of the same corallum as in G.

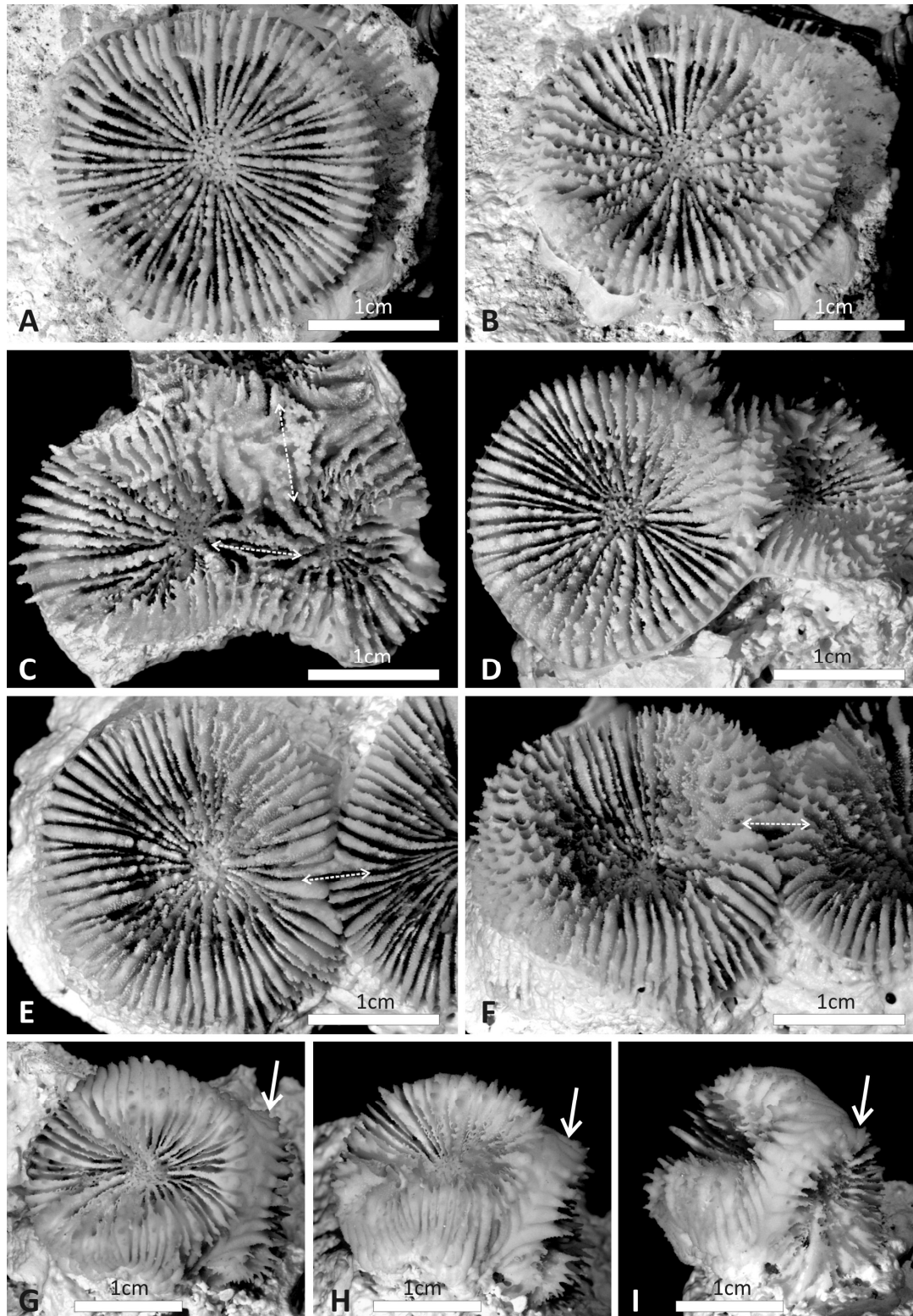


Figure 7.6. Skelton macro-morphology of specimens of *cf Homophyllia australis* included in this study and showing a different morphology from the typical one : **A)** top and **B)** side view of IRD HS 3543; **C)** IRD HS 3359 polystomatous specimen, image shows detail of the linkage (dashed line); **D)** IRD HS 3483 polystomatous specimen; **E)** top and **F)** side view of IRD HS 3327; **G), H), I)** show top, side and lateral corallite view, respectively, of a specimen with two calices from Gambier.

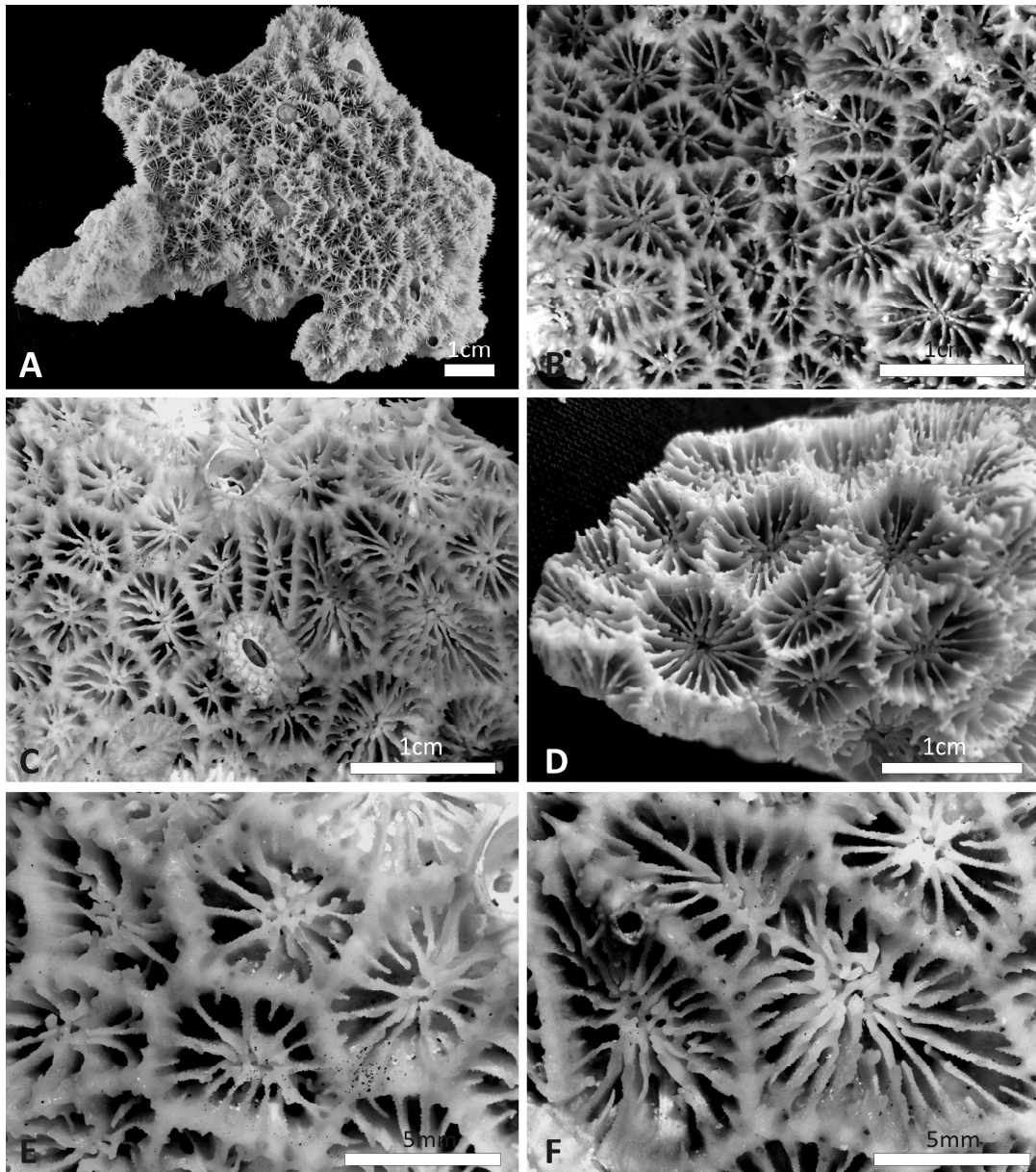


Figure 7.7. Coralla and corallite of *Micromussa amakusensis* from the Gulf of Aden, Indian Ocean: **A)** corallum morphology of specimen MNHN-IK-2012-14232; **B)** corallite shape and organization in the same specimen as in A; **C)** corallite shape and organization in specimen UNIMIB MU183; **D)** specimen in the EPA Socotra collection; **E)** detail of the left hand side of the specimen in C showing smaller corallites; **F)** detail of the left hand side of the specimen in C showing larger corallites.

7.4.2.2 Micromorphology

Despite the above mentioned macromorphological variability of skeletal structures including corallite organization, calice size, and number of cycles of septa, all the examined taxa share similar micro-morphology and, in particular, a similar strong typically lobophylliid dentation (Figs. 7.8, 7.9) with septal teeth being variable in size but similarly having an elliptical base at mid-septum and being parallel to the direction of the septum. Although tooth size varies being larger in septa of higher orders and smaller in septa of lower orders, their shape is consistently uniform within the same species (Figs. 7.8K-T, 7.9K-T). Moreover, granulation on the side of septa is strong and granules are also found on the teeth tops. The typical morphologies of *H. australis*, *A. bowerbanki*, *A. hillae*, and *S. wilsoni* are characterized by thicker primary and secondary septa ornamented by elongated teeth being 1 to 2 mm in height (Figs. 7.8Z-AD). However, in *M. amakusensis* (both Indian Ocean and Pacific Ocean material), *A. lordhowensis*, *P. multipunctata*, and in cf *H. australis* the largest septal teeth are overall smaller than in the previous taxa attaining maximum height of 1 mm in all cases except in the latter where they can reach up to 1.5 mm. Moreover, while septal teeth size is smaller than in the previous group of species, septal sides granulation is stronger, with large and pronounced granules continuing until the tip of the teeth (Figs. 7.9U-Y). Interestingly, SEM examination of *A. hemprichii*, that belongs to the molecular clade E together with the genus type species *A. echinata* (Fig. 7.3), shows different micromorphology from the one described for *A. bowerbanki*, *A. hillae*, and *A. lordhowensis*. In fact, this species has remarkably less pronounced septal side granulation with granules embedded in thickening deposits, thus giving a smoother overall appearance (Figs. 7.8E, J, O, T, Y, AD). In all examined taxa the columella is trabecular and spongy (Figs. 7.8-9).

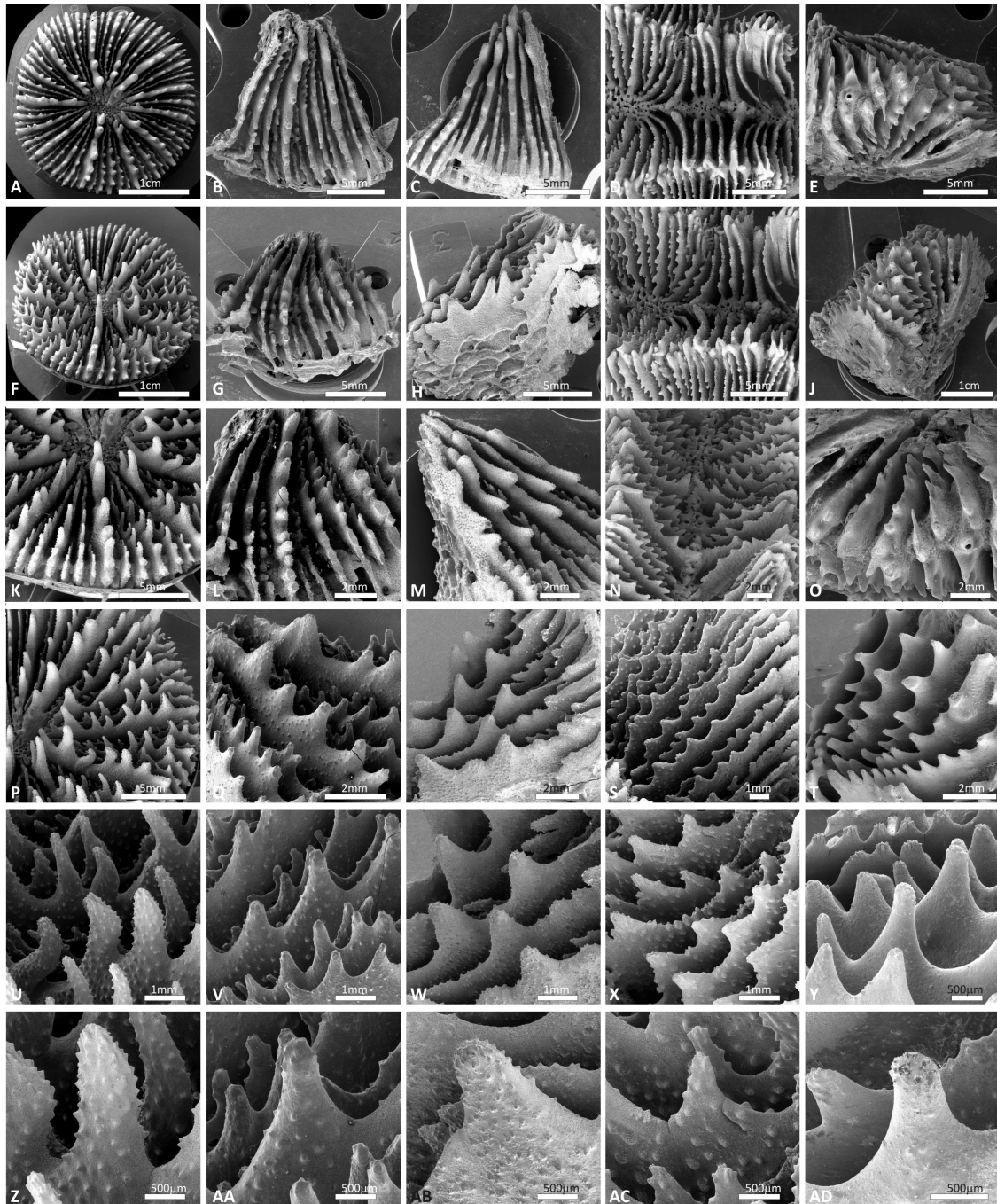


Figure 7.8. Scanning Electron Microscopy images of *Homophyllia australis* HS3311 with typical macro-morphology (A, F, K, P, U, Z), *Acanthastrea bowerbanki* 4629 (B, G, L, Q, V, AA), *Acanthastrea hillae* MH019 (C, H, M, R, W, AB), *Symphyllia wilsoni* WIL1 (D, I, N, S, X, AC), *Acanthastrea hemprichii* BA115 (E, J, O, T, Y, AD): **A-E)** top view of the examined fragments; **F-J)** side view of the examined fragments; **K-T)** view of septa size and ornamentation; **U-Y)** detail of septal teeth shape; **Z-AD)** granulation of the septal teeth.

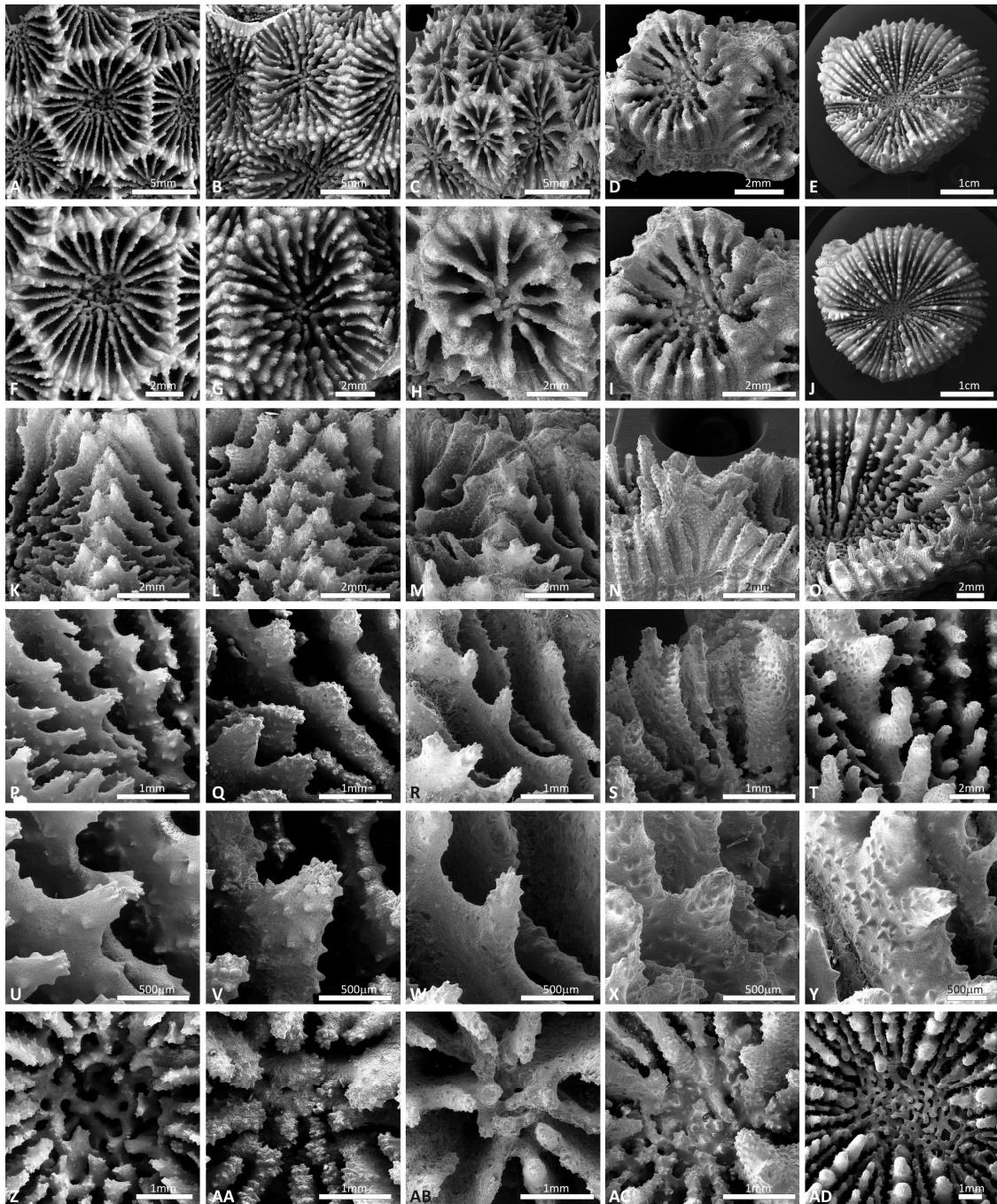


Figure 7.9. Scanning Electron Microscopy images of *Micromussa amakusensis* (A, F, K, P, U, Z) from Japan, *Acanthastrea lordhowensis* 1642 (B, G, L, Q, V, AA), *Micromussa amakusensis* from the Gulf of Aden, Yemen (C, H, M, R, W, AB), *Phymastrea multipunctata* (D, I, N, S, X, AC), cf *Homophyllia australis* (E, J, O, T, Y, AD). **A-E)** top view of the examined fragments; **F-J)** top view of corallites; **K-O)** side view of adjoining corallite walls; **P-T)** detail of septal teeth shape; **U-Y)** granulation of the septal teeth; **Z-AD)** structure of the columella.

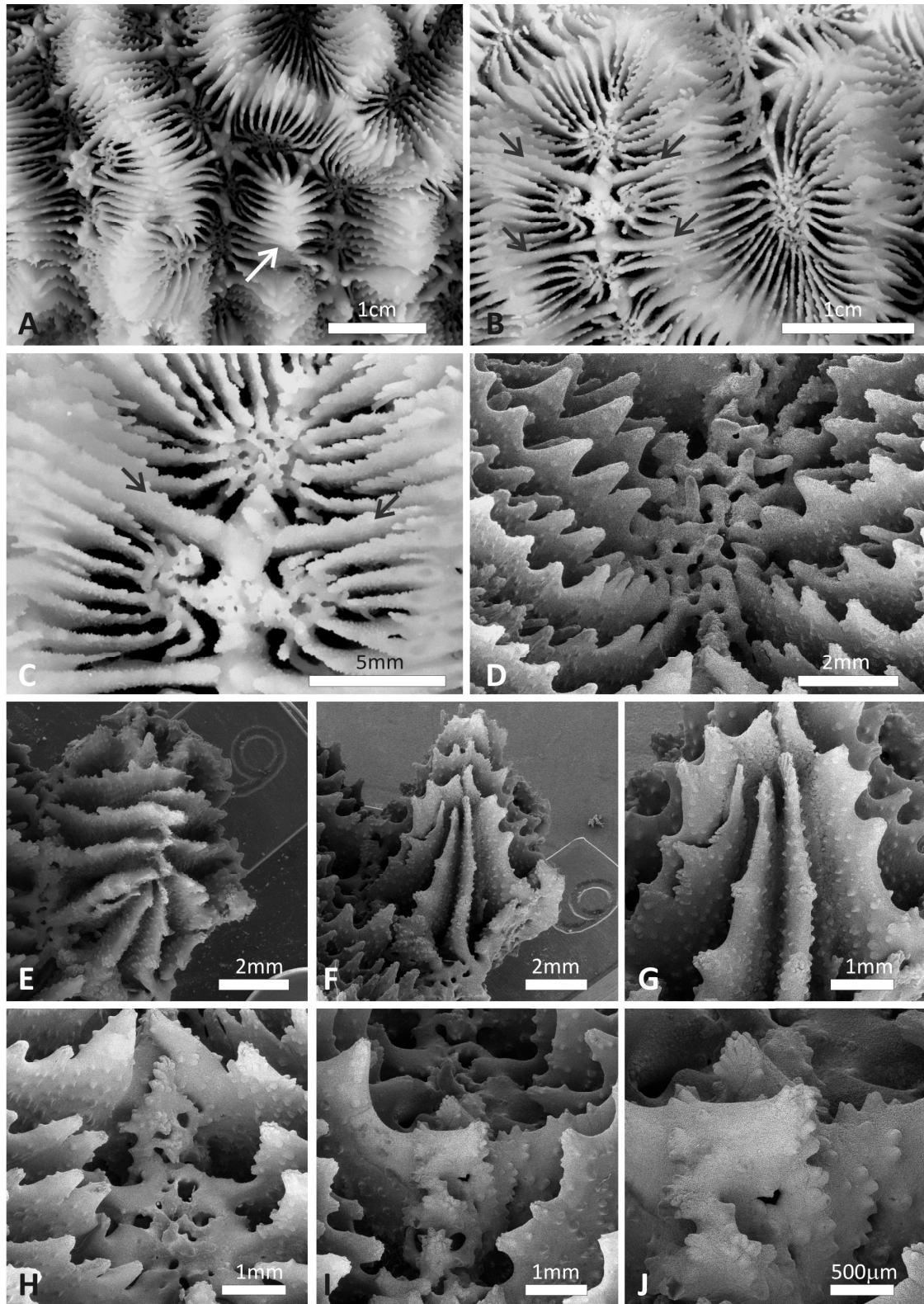


Figure 7.10. Morphology of *Symphyllia wilsoni*. **A)** meandering valleys and a hydnochoroid formation (white arrow) which can be found in this species; **B)** full sized corallite on the left hand side, side by side with a valley in which the centres have an unusual morphology and thicker septa (black arrows) seem to separate the columellae which are also almost split in two; **C)** a close up of the columellae shown in **B)**; **D)** SEM of the columella sitting deep in the valleys; **E)** SEM top view of an hydnochoroid formation; **F)** SEM side view of the

same hydnochoroid formation as in E; **G**) close up of F showing septal side granulation; **H**) in the foreground a columella and in the background behind it the thicker septa separating adjacent columellae indicated by the black arrows in B and C; **I**) a detail of the peculiar structure forming saddle-shaped structure on the two adjoining inner ends of the thicker septa separating adjacent columellae; **J**) granulation of the saddle-shaped structure shown in I.

7.5 Taxonomic account

7.5.1 Examined material

Homophyllia australis (Milne Edwards and Haime, 1849)

EXAMINED MATERIAL: **Australia** – 4631, Lord Howe Island, 19/03/2013, 1m, coll. A.H. Baird; **New Caledonia** – IRD HS3311, coll. F. Benzoni; IRD HS3441, coll. F. Benzoni; IRD HS3447, coll. F. Benzoni; IRD HS3470, coll. F. Benzoni; IRD HS3524, coll. F. Benzoni; IRD HS3525, coll. F. Benzoni; IRD HS3526, coll. F. Benzoni; IRD HS3544, coll. F. Benzoni; IRD HS3545, coll. F. Benzoni; IRD HS3469, coll. F. Benzoni.

cf *Homophyllia australis* (Milne Edwards and Haime, 1849)

EXAMINED MATERIAL: **French Polynesia, Gambier Islands** – UNIMIB GA130, coll. F. Benzoni; UNIMIB GA150, coll. F. Benzoni; UNIMIB GA186, coll. F. Benzoni; (International collection): MTQ G64026, Rapa, Tarakoi, French Polynesia; G64051, Rapa, Baie Aurei, French Polynesia; G64052, Rapa, Baie Aurei, French Polynesia; **New Caledonia** – IRD HS3202, coll. F. Benzoni; IRD HS3359, coll. F. Benzoni; IRD HS3471, coll. F. Benzoni; IRD HS3527, coll. F. Benzoni; IRD HS3528, coll. F. Benzoni; IRD HS3543, coll. F. Benzoni; IRD HS3327, coll. F. Benzoni; IRD HS3483, coll. F. Benzoni.

Acanthastrea bowerbanki Milne Edwards and Haime, 1857

EXAMINED MATERIAL: **Australia** – 4629, Lord Howe Island, 1m, 19/03/2013, coll. A.H. Baird; MH019, Lord Howe Island, Admiralty Islands, 19/03/2013, 14m, coll. M. Hoogenboom; (Moreton Bay collection, coll. C.C.

Wallace, I. Fellegara, P. Muir): MTQ G56536 Moreton Bay, Peel Island, QLD, 01/02/2002; QLD; MTQ G55343 Moreton Bay, Goat Island, QLD, 2m, 23/02/2005; MTQ G553 (AIMS monograph coral collection, Coll. M. Pichon and J.E.N. Veron): MTQ G58035 Heron Island, MTQ QLD, 10m; G58036 Lord Howe Island, NSW, 1m; **New Caledonia** – IRD HS3285, coll. F. Benzoni; IRD HS3286, coll. F. Benzoni; IRD HS3287, coll. F. Benzoni; IRD HS3288, coll. F. Benzoni; IRD HS3298, coll. F. Benzoni; IRD HS3525, coll. F. Benzoni; IRD HS3526, coll. F. Benzoni; IRD HS3446, coll. F. Benzoni; IRD HS3489, coll. F. Benzoni; **Indonesia** – (Snellius-II Expedition) RMNH Coel. 20004 Maisel Islands, 15m, 07/09/1984; RMNH Coel. 16306; **Japan** – AuB167, Coll. H. Fukami.

Acanthastrea hillae Wells, 1955

EXAMINED MATERIAL: **Australia** – MH043, Lord Howe Island, Admiralty Islands, 20/03/2013, 14m, coll. M. Hoogenboom; MH046, Lord Howe Island, Admiralty Islands, 20/03/2013, 14m, coll. M. Hoogenboom; (AIMS monograph coral collection, Coll. M. Pichon and J.E.N. Veron): MTQ G43111 Byron Bay, NSW, 1m; MTQ G43110 Dewar Island, QLD, 10m; MTQ G58034 Lord howe Island, QLD, 20m; MTQ G58033 Lord howe Island, QLD, 20m; MTQ G58032 Lord howe Island, QLD, 1m; (Moreton Bay collection, coll. C.C. Wallace, I. Fellegara, P. Muir): MTQ G58484 Moreton Bay, QLD, Stradbroke Island, 8m, 22/05/2005; MTQ G58486 Moreton Bay, Goat Island, QLD, 2m, 23/05/2005; RMNH Coel. 22400 Heron Island, GBR, 01/07/1973, Coll. M.B. Best; **New Caledonia** – IRD HS3066, coll. F. Benzoni; IRD HS3163, coll. F. Benzoni; IRD HS3169, coll. F. Benzoni; IRD HS3225, coll. F. Benzoni; IRD HS3438, coll. F. Benzoni; IRD HS3501, coll. F. Benzoni; IRD HS3531, coll. F. Benzoni; **Indonesia** – RMNH Coel. 15133 Sulawesi, Pajene-kang east side, 14.5m, 28/05/1980, Coll. H. Moll; **Japan** – R113, Coll. H. Fukami; CC72, Coll. H. Fukami; SSH12, Coll. H. Fukami.

Acanthastrea lordhowensis Veron and Pichon, 1982

EXAMINED MATERIAL: **Australia** – 1596, coll. A.H. Baird; 1597, Solitary

Island, Sandon Reef, 0.5m, 30/09/2012, coll. A.H. Baird; 1598, Solitary Island, Sandon Reef, 0.5m, 30/09/2012, coll. A.H. Baird; 1642, Solitary Island, Sandon Reef, 0.5m, 02/10/2012, coll. A.H. Baird; 5019, 5023, 5038, Solitary Island, Bubble Cave, 12m, 08/07/2014, coll. A.H. Baird; 5050, Solitary Island, Bubble Cave, 12m, 08/07/2014, coll. A.H. Baird; 5063, 5079, 5085, 5098, 5099G, 5099R, Solitary Island, Anemone Bay, 12m, 08/07/2014, coll. A.H. Baird; MH042, Lord Howe Island, Admiralty Islands, 20/03/2013, 14m, coll. M. Hoogenboom; (Moreton Bay collection, coll. C.C. Wallace, I. Fellegara, P. Muir): MTQ G56540 Moreton Bay, Peel Island, QLD, 1m, 01/12/2001; MTQ G.6628 Moreton Bay, QLD; (AIMS monograph coral collection, Coll. M. Pichon and J.E.N. Veron): MTQ G57483 (holotype) Lord Howe Island, NSW, 1m; MTQ G58513 Lord Howe Island, NSW; BM(NH).1983.9.27.12 Australia.

Micromussa amakusensis (Veron, 1990)

EXAMINED MATERIAL: **Japan** – AM65, coll. H. Fukami; 346, coll. H. Fukami; 359, coll. H. Fukami; 364, coll. H. Fukami; 368, coll. H. Fukami; G32485 (holotype) Amakusa Island, 10m, 1988, coll. J.E.N. Veron.

Micromussa cf amakusensis (Veron, 1990)

EXAMINED MATERIAL: **Gulf of Aden** – UNIMIB AD069, coll. F. Benzoni; UNIMIB BA117, coll. F. Benzoni; UNIMIB BU001, coll. F. Benzoni; UNIMIB FP, coll. F. Benzoni; UNIMIB MU185, coll. F. Benzoni; UNIMIB MU215, coll. F. Benzoni; **Socotra Islands** – UNIMIB SO071, coll. F. Benzoni; (International Collection): MTQ G57461 Ras Bidou, Socotra; **Kenya** – RMNH Coel. 17290 Watamu Marine National Reserve, Mayungu, 3m, 06/04/1983, coll. H. Moll.

Phymastrea multipunctata (Hodgson, 1985)

EXAMINED MATERIAL: **Malaysia** – RMNH Coel. 40070, station TMP20, Banggi Outer NE Reef, 9m, 14/09/2012, coll. B.W. Hoeksema; RMNH Coel. 40077, station TMP20, Banggi Outer NE Reef, 8m, 14/09/2012, coll. B.W.

Hoeksema; RMNH Coel. 40099, station TMP19, Outer Latoan Patch, 8m, 14/09/2012, coll. B.W. Hoeksema; **Philippines** – P131, coll. D. Huang.

Symphyllia wilsoni Veron, 1985

EXAMINED MATERIAL: **Western Australia** – WIL1, Hall Bank, 09/04/2013, 12m, coll. D. Thomson; WIL2, Hall Bank, 09/04/2013, 12m, coll. D. Thomson; WIL3, Hall Bank, 09/04/2013, 12m, coll. D. Thomson; WIL4, coll. D. Thomson; WIL5, coll. D. Thomson; RMNH Coel. 22399, West Australia, Abrolhos Islands, 2m, 03/04/1976; holotype (WAM 168-84), Rat Island, Houtman Abrolhos Islands, Western Australia, 8m, 1983, coll. J.E.N. Veron; paratype (WAM 169-84), Port Denison, Western Australia, 9m, 1982, J.E.N. Veron; paratype (WAM 170-84), Port Denison, Western Australia, 12m, 1982, J.E.N. Veron.

7.5.2 Taxonomy

On the basis of the molecular and morphologic results *Acanthastrea bowerbanki* and *Acanthastrea hillae* are to be moved in the genus *Homophyllia* and *Acanthastrea lordhowensis* and *Phymastrea multipunctata* in the genus *Micromussa*. Furthermore, we plan to describe *Micromussa pacifica* sp. nov (considered as cf *H. australis* in the previous paragraphs) and *Micromussa indiana* sp. nov. (considered as *M. amakusensis* from Yemen in the previous paragraphs) as new species, and establish the genus *Hydnophyllia* in order to accommodate *Symphyllia wilsoni*. These formal taxonomic actions will be effective only upon acceptance of this thesis chapter for publication in a peer-reviewed journal. However, for the discussion hereafter we refer to the new nomenclature proposed and provide hereafter the revised taxonomic framework currently in preparation with the list of examined material.

Order Scleractinia Bourne, 1900

Family Lobophylliidae Dai and Horng, 2009

Genus *Homophyllia* Brüggemann, 1877

TYPE SPECIES: *Homophyllia australis* (Milne Edwards and Haime, 1849)

SPECIES INCLUDED:

Homophyllia australis (Milne Edwards and Haime, 1849)

(Figs. 7.1F, 7.2F, 7.5, 7.8A, F, K, P, U, Z)

TYPE MATERIAL: *Caryophyllia australis* Milne Edwards and Haime, 1849a, vol. 11: 239, vol. 10, pl. 8: fig. 2; original designation Brüggemann, 1877: 310. Two syntypes (1840.11.30.77, 1840.11.30.79) are deposited at the NHMUK.

TYPE LOCALITY: South Australia.

DISTRIBUTION: Western Pacific, North-west to South-west Australia, New Caledonia.

REMARKS: Veron and Pichon (1980) record this species also “from the western Pacific east to the Marshall Islands and Fiji”. We did not examine material from this region and cannot ascertain if the mentioned record actually refers to this species or to *Micromussa pacifica* sp. nov., which has likely been confused with it in the literature so far (*i.e.* Veron and Pichon, 1980).

Homophyllia bowerbanki (Milne Edwards and Haime, 1857) comb. nov.

(Figs. 7.1G, 7.2G, 7.8 B, G, L, Q, V, AA)

TYPE MATERIAL: the holotype (scle850) is deposited at the MNHN.

TYPE LOCALITY: Australia.

DISTRIBUTION: Western Pacific with high latitudinal distribution in the north and in the south, North and Eastern Australia, New Caledonia.

Homophyllia hillae (Wells, 1955) comb. nov.

(Figs. 7.1H, 7.2H, 7.8 C, H, M, R, W, AB)

TYPE MATERIAL: the holotype (F17943) is deposited at the QM.

TYPE LOCALITY: Moreton Bay, Australia.

DISTRIBUTION: Western Pacific with high latitudinal distribution in the north and in the south, Western and Eastern Australia, New Caledonia.

Genus *Micromussa* Veron, 2000

TYPE SPECIES: *Micromussa amakusensis* (Veron, 1990)

DISTRIBUTION: from the Western Indian Ocean and Gulf of Aden to the central Pacific.

SPECIES INCLUDED:

Micromussa amakusensis (Veron, 1990)

(Figs. 7.1A, 7.2A, 7.9 A, F, K, P, U, Z)

TYPE MATERIAL: the holotype (G32485) is deposited at the MTQ.

TYPE LOCALITY: Amakusa Island, Japan.

DISTRIBUTION: Japan and the coral triangle. Previous records of this species in the Indian Ocean (Veron 2000) refer to *Micromussa indiana* sp.nov..

Micromussa lordhowensis (Veron and Pichon, 1982) comb. nov.

(Figs. 7.1B, 7.2B, 7.9 B, G, L, Q, V, AA)

TYPE MATERIAL: the holotype (G57483) is deposited at the MTQ.

TYPE LOCALITY: Lord Howe Island, Australia.

DISTRIBUTION: Western Australia and the coral triangle. Previous records of this species in the Indian Ocean (Veron 2000) refer to *Micromussa indiana* new sp..

Micromussa multipunctata (Hodgson, 1985) comb. nov.

(Figs. 7.1D, 7.2D, 7.9 D, I, N, S, X, AC)

TYPE MATERIAL: four syntypes (C-783, C-786, C-787, C-788) are deposited at the UP.

TYPE LOCALITY: Tambuli Reef, Mactan Island, Cebu, Philippines.

DISTRIBUTION: Japan, Philippines, the coral triangle, Vanuatu.

DISTRIBUTION: from the coral triangle to the northern central Pacific (Veron 2000).

Micromussa pacifica Benzoni and Arrigoni, 2015 sp. nov.

(Figs. 7.1E, 7.2E, 7.6, 7.9 E, J, O, T, Y, AD)

TYPE MATERIAL: holotype UNIMIB TO GA130. This specimen, designed as holotype is currently awaiting formal registration at the MNHN.

TYPE LOCALITY: Mangareva, Gambier Islands, French Polynesia.

DISTRIBUTION: the Gambier Islands and New Caledonia.

REMARKS: the formal description of this species is pending and it will be included in the final version of the paper for submission. Until formal acceptance of the paper the species name is *nomen nudum*.

Micromussa indiana Benzoni and Arrigoni, 2015 sp. nov.

(Figs. 7.1C, 7.2C, 7.7, 7.9C, H, M, R, W, AB)

TYPE MATERIAL: the holotype (IK-2012-14232) has been already deposited at MNHN.

TYPE LOCALITY: Al Mukallah, Yemen.

DISTRIBUTION: southern Red Sea, North-western Gulf of Aden, Socotra Island, Oman, Kenya.

REMARKS: the formal description of this species is pending and it will be included in the final version of the paper for submission. Until formal acceptance

of the paper the species name is *nomen nudum*.

Genus *Hydnophyllia* Arrigoni, Benzoni and Baird , 2015 gen. nov.

TYPE SPECIES: *Hydnophyllia wilsoni* (Veron, 1985) comb. nov.

DISTRIBUTION: South-western Australia

SPECIES INCLUDED:

Hydnophyllia wilsoni (Veron, 1985) comb. nov.

(Figs. 7.1J, 7.2J, 7.8D, I, N, S, X, AC, 7.10)

TYPE MATERIAL: the holotype (Z910) is deposited at the WAM. Two paratypes (Z911, Z912) are deposited at the WAM.

TYPE LOCALITY: Rat Island, Houtman Abrolhos Islands, Western Australia.

DISTRIBUTION: this species is restricted to South-western Australia and thrives in temperate conditions.

7.6 Discussion

A growing number of works dealing with taxonomy and systematics of scleractinian corals demonstrated that the integration of genetics and micromorphological analyses is the indispensable approach in order to understand and clarify the evolution of these invertebrates (Benzoni et al., 2007, 2010, 2012a; Budd et al., 2010, 2012; Gittenberger et al., 2011; Stolarski et al., 2011; Kitahara et al., 2012a, 2012b; Schmidt-Roach et al., 2014; Huang et al., 2014b; Terraneo et al., 2014; Arrigoni et al., 2014b, 2014d, 2015). In this study we combined robust molecular analyses based on multiple DNA regions with detailed observations of morphology at colony, corallite, and sub-corallite scales. As a result of such integrated morpho-molecular approach we transferred *P. multipunctata* and *A. lordhowensis* in the genus *Micromussa* and *A. bowerbanki* and *A. hillae* in

Homophyllia, providing a revised diagnosis for both two genera. Moreover, the two species *Micromussa pacifica* sp. nov. and *Micromussa indiana* sp. nov. are described. Finally, we establish the new genus *Hydnophyllia* gen. nov. to accommodate *S. wilsoni*, a species resulting closely related but distinct from *Micromussa* and *Homophyllia* based on our molecular trees and showing also unique morphological characters.

7.6.1 Phylogeny, taxonomy, and geographical distribution of *Homophyllia*

The genus *Homophyllia* was resurrected by Budd et al. (2012) following recent novel morphological observations on *H. australis* and *P. vitiensis* (Budd and Stolarski, 2009). The authors demonstrated that these two Pacific species are clearly unrelated looking at the septa granulation, the area between teeth, and the thickening deposits (Budd and Stolarski, 2009; Budd et al., 2012), as also shown in this study for *H. australis* (Figs. 7.8P, J, Z) and in Arrigoni et al. (2014b) for *P. vitiensis* (Arrigoni et al., 2015: Figs. 5.5C, D, 5.7). The phylogeny reconstruction proposed in this study indicates that *H. australis* belongs to the Lobophylliidae and it is not related to *P. vitiensis* (Fig. 7.3), providing enough genetic information to support taxonomic decisions proposed by Budd et al. (2012). These combined morpho-molecular data solved the old taxonomic riddle concerning the placement of these two species (Matthai, 1928; Vaughan and Wells, 1943; Wells, 1964; Veron and Pichon, 1980; Veron, 2000) and represent an excellent example of concordance between genetics and novel morphological characters (Stolarski and Roniewicz, 2001; Budd et al., 2010).

Furthermore, our molecular results show that *H. australis* belong to clade B and is sister to the group including *H. bowerbanki* and *H. hillae* (Fig. 7.3), two species previously ascribed to the genus *Acanthastrea*. As a result of the morphological and molecular investigations presented in this study, the once monospecific genus *Homophyllia* now includes three nominal species, *H. australis*, the type species predominantly solitary, and the colonial species *H. bowerbanki* and *H. hillae*. Although previous authors had remarked the pronounced septal sides granulation

of these species (Veron and Pichon, 1980), the strikingly different corallum shape has likely distracted them from considering this skeletal feature as phylogenetically informative, and solitary and colonial species were kept in different genera. A similar situation has been recently reported also for the lobophylliid genus *Sclerophyllia* that originally consisted of a monostomatous species (Klunzinger, 1879). The genus has been recently revised based on molecular and morphological evidence and now is composed by both solitary and colonial species based (Arrigoni et al., 2015). Despite superficial macromorphological similarities between *H. bowerbanki* and *H. hillae* and the species of *Acanthastrea*, mainly the size and arrangement of corallites and the number of septa (Veron and Pichon, 1980), consistent differences in septal teeth micro-structure were evidenced between these species (Figs. 7.8 Q, R, T, V, W, Y, AA, AB, AD; Budd and Stolarski, 2009; Arrigoni et al., 2015). Furthermore, a deep genetic divergence separates the clade including *H. bowerbanki* and *H. hillae* from the lineage leading to the species of *Acanthastrea* (Fig. 7.3; Arrigoni et al., 2014a, 2014b, 2015). Indeed, some large sized specimens of *Acanthastrea*, like the colonies of *A. hemprichii* included in molecular and morphological analyses of this study (Figs. 7.1I, 7.2I), can look similar to *H. bowerbanki* and *H. hillae* (Figs. 7.1G-H, 7.2G-H) and we therefore preliminarily identified as such in the field. However, none of the specimens collected in the Indian Ocean examined in this study which had been identified as *H. hillae* actually belong to this species. Thus, it is possible that the supposed presence of this species in the Indian Ocean (Veron, 2000) is actually derived from erroneous identifications of *A. hemprichii*. The author himself reports that “records from the Western Indian Ocean are doubtful” (Veron, 2000). If this was the case, the geographic distribution of the genus *Homophyllia* would be restricted to the western Pacific, encompassing tropical, sub-tropical, and temperate conditions. Moreover, all of the three species of *Homophyllia* show high latitudinal distribution and they are predominantly sub-tropical, being uncommon within their range but relatively frequent in sub-tropical localities, such as Japan, New Caledonia, and South-western Australia (Veron and Marsh, 1988; Veron, 1993,

2000; Wallace et al., 2009). For example, in Australia they are rare on the Great Barrier Reef and relatively common south to Moreton Bay (Veron and Pichon, 1980; Veron and Marsh, 1988; Wallace et al., 2009).

7.6.2 Phylogeny and taxonomy of *Micromussa*

The results presented in this study significantly increase the known species and macromorphologic diversity of *Micromussa*. The genus is now composed by a total of seven species of which five are investigated in this study, *i.e.* *M. amakusensis*, *M. indiana* sp. nov., *M. lordhowensis*, *M. multipunctata*, and *M. pacifica* sp. nov, while for the other two species, *M. diminuta* and *M. minuta* Moll and Best, 1984, no molecular and micromorphological are available and few dry specimens are deposited at museums.

The case of *M. indiana* sp. nov. is a remarkable example of how the morphologic variability of a species over a large geographic distribution range can actually hide previously undetected but significantly distinct lineages. This species from the Indian Ocean was previously identified as the genus type species *M. amakusensis* most likely due to *in situ* identification biased by a similar peculiar pattern of bright colouration occurring in both species (Fig. 7.2). The lack of direct comparison of skeletal morphology from Indian Ocean and Pacific Ocean material until this study (Veron 2000; Pichon et al., 2010) has perpetrated this error and underestimated, once more, the increasingly obvious peculiarities of the Indian Ocean coral fauna (Arrigoni et al., 2012; Obura, 2012). However, once type material and specimens collected from type locality and a large reference collection from Yemen were compared, the macromorphological differences became glaring. Recent works revealed several other cases of deep genetic divergence between Indian and Pacific populations in some species ascribed to other families, such as *Blastomussa merleti* (Arrigoni et al., 2012), *Coelastrea aspera* and *C. palauensis* (Huang et al., 2014b), *Favites halicora* (Arrigoni et al., 2012), *Goniopora somaliensis* (Kitano et al., 2014), *Pocillopora* spp. (Pinzon et al., 2013), *Stylophora pistillata* (Stefani et al., 2011; Keshawmurthy et al., 2011; Flot et al., 2011). These

evidence strongly argue against the concept of “geographic subspecies” proposed by Veron (1995) in order to explain the wide variety of geographic variations in some nominal species living both in the Indian and Pacific Ocean.

The other new species of *Micromussa* described in this study, *M. pacifica* sp. nov., represents a different case altogether. This solitary species has been confused for a long time with the largely sympatric *H. australis* (Veron and Pichon, 1980). The two species are indeed superficially impressively similar although a closer observation of the skeletal features allowed separating them effectively, a distinction fully confirmed by the molecular results.

Concerning the two existing nominal species previously assigned to different genera and here ascribed to *Micromussa*, *M. lordhowensis* and *M. multipunctata*, our integrated approach allows the formal revision of their placement. The former species represents one more case of *Acanthastrea* mis-assignment (Arrigoni et al., 2014a, 2015). As shown by Arrigoni et al. (2014a) this genus, as intended until Veron (2000), was the most polyphyletic in the family Lobophylliidae based on mitochondrial and nuclear phylogeny reconstructions. In the present study, these previous molecular findings were taken further, and the previously unstudied *M. lordhowensis* is transferred to *Micromussa* being unrelated to the genus type *A. echinata* (Fig. 7.3). Furthermore, our morphologic analyses confirmed that *M. lordhowensis* displays the septal size, shape, and granulation typical of all *Micromussa* species rather than the smoother septal sides ornamentation of *Acanthastrea* (see also Arrigoni et al., 2015). In the original description of *M. multipunctata*, Hodgson (1985) stated that, despite some characteristics shared with the other species of *Montastraea* (now exclusively an Atlantic genus, see Budd et al. (2012)), *M. multipunctata* is unusual on the basis of growth form, polyp shape, and notably septal dentations. Indeed this species is also different from all the others species examined in this study due to its plocoid corallite organization. Nevertheless the molecular results presented in this study show that *M. multipunctata* clearly belongs to the lineage composed by the other four *Micromussa* species (Fig. 7.3). Moreover a detailed examination of the

micromorphology of the skeleton has shown that this species shares with the other *Micromussa* species a similar septal teeth micromorphology, having for example the same type of strong septal sides and tips granulation (Fig. 7.9).

7.6.3 The strange case of *Hydnophyllia wilsoni*

The most unexpected result of this study is the recovery of *Hydnophyllia wilsoni* as a distinct lineage within the Lobophylliidae. The multi-locus phylogeny reconstruction and each of the three single gene topologies are concordant in supporting it although the best resolution is obtained using the concatenated data set (Fig. 7.3, Apps. 7.1, 7.2, 7.3). Considering the concatenated COI-Histone H3-ITS region data set, the inter-clade genetic distances between *H. wilsoni* and the other eight clades go from the smallest values with clade A ($3.2 \pm 0.4\%$) and clade B ($3 \pm 0.4\%$) to the largest one with clade G ($9.6 \pm 0.7\%$) (App.7.4), while all of the other distances vary between 5.6 and 6.2. These distances completely overlap with the pairwise interclade distances for the other clades, thus confirming the genetic distinctiveness of *H. wilsoni* within its family.

In the original description of *H. wilsoni*, Veron (1985) placed the species in the genus *Symphyllia* considering the massive or sub-massive flattened colony and a general resemblances of the meandroid corallite arrangement to that of this genus, although corallites are smaller than those of any other *Symphyllia* species (Veron, 2000). Despite a superficial appearance of the macromorphology of the colony to some merulinds genera, such as *Platygyra* and *Oulophyllia*, Veron (1985) included *H. wilsoni* within the Mussidae (now exclusively an Atlantic taxon, see Budd et al., 2012) because of the septal dentations size and the thick and fleshy aspect of living polyps. Our molecular analyses clearly demonstrate that the species belong to the Lobophylliidae but it is not closely related to any of the known lobophylliids genera, showing a sister relationship with a group composed by the genera *Micromussa* and *Homophyllia* (Fig. 7.3). These genetic findings are also supported by the examination of corallite and sub-corallite morphology, *i.e.* the columellar morphology, and by the presence, in particular, of hydnochoroid formations.

Another peculiarity of *H. wilsoni* is represented by its narrow geographic distribution. The species is actually restricted to the temperate waters of South-West Australia, being found as living colonies from Shark Bay to Geographe Bay along the coasts of Western Australia and thence east to Bremer Bay in the South Australia (Veron, 1985, 1993, 2000; Veron and Marsh, 1988). It is usually found in shallow water on kelp-dominated coastal exposed rock surfaces (Veron, 1985, 1993; Veron and Marsh, 1988). This peculiar distribution range mostly overlaps that of another distinctive species, *Coscinaraea marshae* Wells, 1962, and it is also similar to that of the south-eastern Australian species *Coscinaraea mcneilli* Wells, 1962, being otherwise unlike that of any other extant coral (Veron and Pichon, 1980; Veron and Marsh, 1988; Veron, 1993, 2000).

In conclusion, the present work increases the current knowledge of taxonomy and biodiversity of the family Lobophylliidae and, more in general, points out to the relevance of integrating genetics and morphology. However, despite it discloses how far we are from a comprehensive understanding of evolutionary relationships between reef corals. The inclusion of as many species as possible and from different localities, as done here for *M. amakusensis*, in a molecular phylogenetic framework continues to be a necessary step towards a comprehensive reconstruction of coral evolutionary history as an increasing number of previously unstudied taxa exhibit unexpected phylogenetic placements that have been misunderstood and ignored by traditional systematics (Fukami et al., 2004, 2008; Kitahara et al., 2010, 2012a, 201b; Stolarski et al., 2011; Huang et al., 2011, 2014b; Arrigoni et al., 2014a; Kitano et al., 2014). Finally, we strongly encouraged the examination of specimens from multiple localities, ideally including the entire geographic distribution range of a species and above all the type locality, in order to define the intra-specific morphological variation and evaluate the possible presence of cryptic or previously overlooked species.

General Discussion and Conclusions

8.1 Discussion

In the last decade, the increasing use of molecular tools and new morphological analyses have shed new light on the evolution and systematics of scleractinian corals (Fukami et al., 2004a, 2008; Wallace et al., 2007; Benzoni et al., 2007, 2010, 2011, 2012a, 2012b, 2014; Richards et al., 2008, 2013; Forsman et al., 2009; Budd and Stolarski, 2009, 2011; Kitahara et al., 2010, 2012a, 2012b; Stolarski et al., 2011; Stefani et al., 2011; Huang et al., 2011, 2014a, 2014b; Budd et al., 2012; Pinzon et al., 2013; Schmidt-Roach et al., 2013a, 2013b, 2014; Terraneo et al., 2014; Kitano et al., 2014; Arrigoni et al., 2014d). The reciprocal illumination between genetics and morphology has proven to be a successful and meaningful approach in order to formulate reliable hypothesis on coral evolutionary history and revolutionized the classical taxonomy at all systematic ranks (Stolarski and Janiszewska, 2001; Budd et al., 2010). This dissertation represents a notable effort in this direction, exploring the evolutionary relationships within the ecologically relevant reef coral family Lobophylliidae.

The first step of modern coral taxonomy is the definition of the molecular phylogenetic position of a known taxon in order to define its evolutionary relationships within the order Scleractinia. Despite the apparent simplicity of this sentence, the situation is far from to be definitive due to a host of problems, such as the rarity of a taxon or the complexity to collect stony corals in some regions (for example deep-water domain, remote localities, countries with political issues, and many others aspects). Considering the results reported in this dissertation, of the 52 extant species ascribed to the Lobophylliidae to date (Veron, 2000; Budd et al., 2012; Benzoni, 2013), 69% have been investigated from a molecular point of view and the percentage is higher if we consider the total number of analyzed genera (92%). In particular, in this dissertation we explored the phylogenetic position of a

total of 11 genera and 38 species ascribed to the Lobophylliidae, for an overall number of analyzed specimens of about 450 colonies. Approximately more than 600 sequences of lobophylliid representatives, plus the complete mitochondrial genome of *Acanthastrea maxima*, have been deposited on EMBL, and an higher number of sequences of lobophylliids is still unpublished and it will be used for future works, as described in the following paragraph of this dissertation. Taken all together, these figures provided a significant improvement in the knowledge of evolution of the Lobophylliidae and represented one the biggest efforts in the new era of “reverse taxonomy” of scleractinian corals.

We firstly provided a robust molecular phylogeny reconstruction of the Robust clade (Chapter 2), with a particular emphasis on the Lobophylliidae and the Merulinidae, two major families belonging to this group (Fukami et al., 2008; Kitahara et al., 2010), and some other taxa actually transferred to *incertae sedis* (Budd et al., 2012), such as *Leptastrea* Milne Edwards and Haime, 1848, *Blastomussa* Wells, 1968, and *Parasimplastrea* Sheppard, 1985. We demonstrated that *Blastomussa* does not belong to the Lobophylliidae despite it has been traditionally ascribed to the Mussidae (Veron and Pichon, 1980; Veron, 2000), providing the molecular basis for a formal revision of the genus later done by us (Benzoni et al., 2014) thanks to the inclusion of more species and colonies. Moreover, the entire biogeographic area of the Indian Ocean was largely unsampled until the study presented in Chapter 2 and we detected several cases of intraspecific divergences between Indian and Pacific Ocean populations. The latter aspect is critically important to better understand the real distribution patterns of scleractinian corals. Several molecular studies demonstrated that some widely distributed traditionally species are indeed complexes of distinct lineages, revealing high hidden species diversity (Flot et al., 2008, 2011; Keshavmurthy et al., 2013; Pinzon et al., 2013; Schmidt-Roach et al., 2013a, 2013b, 2014; Terraneo et al., in prep.). This confirms what other works revealed concerning intraspecific interoceanic divergences, suggesting that they could be caused by cryptic speciation or misidentification (Huang et al., 2011, 2014a; Kitano et al., 2014).

Also the case of *Micromussa amakusensis* and *Micromussa indiana* sp. nov. reported in Chapter 7 is another illuminating example of such unexpected situations. Widespread sampling of a species thought to live in the Indo-Pacific, *i.e.* *Micromussa amakusensis*, together with detailed molecular and morphological analyses revealed that Indian and Pacific populations belong to at least two species. These results glaringly demonstrate the need of widespread samplings and multi-localities approaches in order to detect possible evolutionary divergences between populations that live in distant geographic areas and to find possible new species.

In chapter 3 we supplied the most comprehensive molecular phylogeny reconstruction of the Lobophylliidae to date including several previously unstudied taxa. The monophyly of the family is now strongly supported and it is later supported in Chapters 5, 6, and 7 where we analyzed additional taxa, *i.e.* *Australomussa*, *Sclerophyllia*, *Homophyllia*, and *Hydnophyllia* gen. nov., using also another molecular locus, *i.e.* Histone H3, together with the previous markers COI and rDNA. The molecular phylogeny of the Lobophylliidae presented in Chapter 3 was further confirmed by phylogenetic trees proposed in Chapters 5, 6, and 7, indicating that the subdivision in nine major molecular clades is stable and reliable despite it is partially in conflict with traditionally taxonomy based on macromorphology (Vaughan and Wells, 1943; Veron, 2000). Chapter 3 greatly improved the knowledge of phylogenetic relationships within the Lobophylliidae that were previously mostly unknown, providing a broad-based molecular phylogeny of the entire family. Several works assessed evolutionary relationships within a family using molecular or morpho-molecular approaches, *i.e.* the Acroporidae (Wallace et al., 2007), the Mussidae (Nunes et al., 2008), the Fungiidae (Gittenberger et al., 2011), the Psammocoridae and the Coscinaraeidae (Benzoni et al., 2007, 2012a), the Merulinidae (Huang et al., 2011), the Poritidae (Kitano et al., 2014), and the Dendrophylliidae (Arrigoni et al., 2014d), and proved to be helpful for further taxonomic revisions (Wallace et al., 2007; Budd et al., 2012; Benzoni et al., 2012a, 2014; Huang et al., 2014a, in prep.; Kitano et al., 2014). Once a robust phylogenetic reconstruction of a family has been shown, the

most efficient way to obtain reliable evolutionary hypothesis is by analyzing one genus or molecular lineage at a time, including more specimens (Gittenberger et al., 2011; Huang et al., 2014b; Schmidt-Roach et al., 2013a, 2014; Kitano et al., 2013). Following this direction, in Chapters 5, 6, and 7 attention was focused on the taxonomy and phylogeny of two closely related genera, *i.e.* *Australomussa* and *Parascolymia* (Chapter 5), a genus, *i.e.* *Sclerophyllia* (Chapter 6), and two closely related molecular lineages, *i.e.* clades A and B *sensu* Arrigoni et al. (2014a) (Chapter 7), at a time. In these three Chapters we demonstrated the utility of a combined morpho-molecular approach for a better understanding of evolutionary relationships between corals and provided examples on how the “reverse taxonomy” is meaningful (Stolarski and Roniewicz, 2001; Budd et al., 2010). Solid molecular data are integrated with new micromorphological characters, such as the height, spacing, and shape of septal tooth, the distribution and shape of granules on septal face, and the structure of the interarea of teeth (for a definition see Budd and Stolarski (2009, 2011)), to generate diagnostic features for the taxonomic revision of the genera *Australomussa*, *Parascolymia*, *Sclerophyllia*, *Homophyllia*, and *Micromussa*. These micromorphological characters have been already effective at distinguishing molecular groups in other coral taxa at different systematic ranks and proved to be phylogenetically informative (Cuif et al., 2003; Benzoni et al., 2007, 2012a; Budd and Stolarski, 2009, 2011; Stolarski et al., 2011; Janiszewska et al., 2011; Budd et al., 2012; Kitahara et al., 2012a, 2012b; Huang et al., 2014a, 2014b; Schmidt-Roach et al., 2014). The inclusion of detailed micromorphological analyses will thus be necessary in order to clarify the evolutionary patterns between so far unstudied corals and to provide diagnostic characters that agree with molecular findings.

Furthermore, this dissertation contains significant information which will be of use for future strategies of reef corals biodiversity conservation. Huang and Roy (2013) recently showed that the loss of phylogenetic diversity in reef corals is dependent on the nature of extinction threats, especially bleaching, *i.e.* loss of dinoflagellate symbionts and/or symbiont pigmentation from the holobiont (Hoegh-

Guldberg and Smith, 1989; Brown, 1997), and diseases, *i.e.* impairment of vital functions from normal state of health caused by pathogens and/or environmental stressors (Harvell et al., 1999; Rosenberg and Loya, 2004), but also tree shape. Therefore, establishing evolutionary relationships between coral taxa and their evolutionary distinctiveness is essential for conservation strategies as the extinction of rare species can lead to larger loss of phylogenetic diversity due their old and unique lineages (Huang, 2012; Huang and Roy, 2013, 2015; Forest et al., 2015). In this context, the lobophylliid *Cynarina lacrymalis* (Milne Edwards and Haime, 1848) and *Moseleya latistellata* Quelch, 1884 are evolutionarily distinct lineages and they might therefore be, together with *Hydnophyllia wilsoni* (Veron, 1985) and the genus *Sclerophyllia* Klunzinger, 1879, priorities for future conservation actions.

8.2 Future perspectives

As a result of this PhD, several projects concerning the taxonomy and evolution of the Lobophylliidae are now in preparation. These works will cover three different levels: I) the inclusion of the still unstudied known lobophylliid species into the broad-based molecular phylogeny of the family proposed in Chapter 3; II) species-level phylogeny reconstructions of the other molecular clades of the Lobophylliidae that have not been analyzed in Chapter 5, 6 and 7; III) a formal revision of the entire family based on molecular results presented in this dissertation and novel rigorous and strict morphological (macromorphology, micromorphology, and microstructure) phylogenetic analyses and the detailed examination of relevant type materials.

I) Ideally, the inclusion of all taxa in a molecular phylogenetic scenario will be a necessary step towards a better understanding of evolutionary patterns of the Lobophylliidae. This dissertation and several studies showed that broad taxonomic samplings within families and/or genera have revealed several unexpected affinities and unforeseen evolutionary relationships (Cuif et al., 2003; Fukami et al., 2004a, 2008; Wallace et al., 2007; Huang et al., 2009, 2011, 2014b; Kitahara et al., 2010; 2012a, 2012b; Gittenberger et al., 2011; Benzoni et al., 2011, 2012a,

2012b, 2014; Terraneo et al., 2014; Kitano et al., 2013, 2014; Arrigoni et al., 2014d). Therefore, a particular effort will be made in order to include into a molecular context as many still unstudied lobophylliid species as possible.

II) Carrying on with the taxonomic revisions proposed in Chapters 5, 6, and 7, we will focus our attention also to the other molecular clades of the Lobophylliidae. In particular we will try to obtain species-level phylogenies of clades E, F, and G, integrating new molecular data with detailed macro- and micromorphological observations, as already done in Chapter 6 and 7. Firstly, some still unstudied known species will be included, such as *Echinophyllia taylorae* and *Oxypora convoluta*, while a greater number of coral samples coming from a wide geographic collection throughout the Red Sea, Indian and Pacific Ocean will be investigated for the other known species already included in Chapter 3. The phylogenetic relationships between species will be reconstructed using nuclear and mitochondrial DNA regions and detailed morphological analyses will be performed in order to define the morphological boundaries between the analyzed species. This kind of approach, proven to be illuminating in Chapters 5, 6 and 7, will allow us to revise the genera *Acanthastrea*, *Echinophyllia*, and *Oxypora*, and to formally introduce some undescribed species.

III) The families Mussidae and Merulinidae have been recently formally revised by integrating examinations of colony, corallite, and sub-corallite morphology with robust molecular data (Budd et al., 2012; Huang et al., 2014a). The authors proposed an exhaustive revision at genus level of these two taxa mapping several morphological characters (morphology, micromorphology, and microstructure) onto comprehensive molecular trees of the two families and tracing the evolution of these characters. They evaluated character state transformations and identified morphological traits that were diagnostic of monophyletic lineages, *i.e.* genus. The broad-based phylogeny reconstruction of the Lobophylliidae presented in Chapter 3, together with the inclusion of molecular data presented in Chapters 5, 6 and 7, will be used for a revised classification of this family. These molecular results will be integrated with detailed observations of macromorphology, micromorphology,

and microstructure and the examination of type materials. As a result of this integrated approach, a formal and rigorous revision of the Lobophylliidae at genus level will be carried out.

– ACKNOWLEDGMENTS –

First of all I'd like to thank Francesca, my supervisor, for these five wonderful years. Everything written here is thanks to Francesca. She guided me through this job with her invaluable comments, advices and enthusiasm, her incredible knowledge on the subjects exposed in this thesis and everything else. She stimulated me in explore whatever I want, and give me the outstanding chance to work with her numerous colleagues and go in so many different countries to increase my background. I am lucky and proud to have worked with her and I am enthusiastic to continue to collaborate with her also in my future job at Kaust. GRAZIE DI TUTTO!!!!

A particular thank to Paolo Galli for hosting me in his laboratory during these years, giving the chance to work with him and his group and to visit his amazing MaRHE Center in Maldives. I'm grateful also to Fabrizio for teaching me everything I know in laboratory and for his unique advices in all molecular aspects. Davide and Simone, what can I say? I'll miss you when I will be at Kaust. I enjoyed every single day of work with you in lab, you are always happy and positive, and you are always ready to give me suggestions and precious help. Avete trasformato questi anni di lavoro in un divertimento, grazie davvero. I'd like also to thank all the other several people I met and worked with in the lab, especially Giovanni Strona, so many laughs!

During these three years I had the chance to work with several Francesca's colleagues from all over the world and I am indebted to each of them. First of all, two really special thanks to Bert and Jarek!! I am honored for working with them, I learnt so many things from their huge knowledge and experience. We've been authors of several papers, they were always kind and enthusiastic in all our conversations and emails, and finally both of them supported my candidature to Kaust, GRAZIE! I am grateful to Mike for hosting me twice in his wonderful laboratory, giving the chance to live and work in an incredible place. I spent two magnificent months at Kaust and I can't wait to work with him! I also thank Hiro for our several collaborations in so many different projects and his illuminating comments and suggestions (I started to study corals reading his papers and I can't believe to work with him, a dream), Andrew for his enthusiastic working way and his precious Australian gifts, Danwei for his detailed and always perfect and correct comments and works.

Again, I am indebted to each of the co-authors of the papers presented in this thesis. So I really thank A.H. Baird (ARC), V. Barbe (Genoscope), M.L. Berumen (KAUST), J. Bouwmeester (KAUST), A.N. Budd (UIOWA) A. Caragnano

(UNIMIB), C.A. Chen (Academia Sinica), H. Fukami (Miyazaki University), P. Galli (UNIMIB), B.W. Hoeksema (Naturalis), M. Hoogenboom (JCU), D. Huang (UIOWA), Y. Kitano (Miyazaki University), M. Pichon (MTQ), Z.T. Richards (WAM), F. Stefani (IRSA-CNR), J. Stolarski (Polish Academy), T.I. Terraneo (KAUST), D. Thomson (CSIRO), B. Vacherie (Genoscope), Y. Zayasu (Kyoto University).

I acknowledge also to the financial support of the European Commission's Research Infrastructure Action via the Synthesys Program for my visit at Naturalis Biodiversity Center. I spent two beautiful weeks in the stimulating and fascinating Naturalis and I really want to thank the three guys Sancia E.T. van der Meij, Zarinah Waheed, and Bastian T. Reijnen (Naturalis) for their kindness and hospitality. I gratefully acknowledge the National Science Council of Taiwan (NSC) for my participation to Summer Program in Taiwan 2013 and Prof. C.A. Chen for allowing me to work in his laboratory for two months. It was really a productive period thanks to the help of several people from his laboratory, S. Keshawmurthy, G. Chai-Hsia, and S. De Palmas (Academia Sinica). A special thank to Silvia Fontana (Academia Sinica) for helping me in everything when I was there, grazie davvero!

All of the coral specimens analyzed in this study were collected by Francesca (grazie, grazie, e ancora grazie), with the exception of few but really fundamental samples (thank you very much also for this!!) collected by A.H Baird, H. Fukami, B.W. Hoeksema, M. Hoogenboom, Z.T. Richards, D. Thomson, Y. Zayasu, and we are thus grateful to all people, organizations, institutions, and countries that allowed her expeditions. We are grateful to E. Karsenti (EMBL) and É. Bourgois (Tara Expeditions) and the OCEANS consortium for samplings (Mayotte, Djibouti, and Gambier Island) during the Tara Oceans expedition. We thank the commitment of the following people and sponsors who made this singular expedition possible: CNRS, EMBL, Genoscope/CEA, VIB, Stazione Zoologica Anton Dohrn, UNIMIB, ANR (projects POSEIDON/ANR-09-BLAN-0348, BIOMARKS/ANR-08-BDVA-003, PROMETHEUS/ANR-09-GENM-031, and TARA-GIRUS/ ANR-09-PCS-GENM-218), EU FP7 (MicroB3/No.287589), FWO, BIO5, Biosphere 2, agnès b., the Veolia Environment Foundation, Region Bretagne, World Courier, Illumina, Cap L'Orient, the EDF Foundation EDF Diversiterre, FRB, the Prince Albert II de Monaco Foundation, Etienne Bourgois, the Tara schooner and its captain and crew. Tara Oceans would not exist without continuous support from 23 institutes (<http://oceans.taraexpeditions.org>). Samplings in New Caledonia were possible thanks to the kind help and support of C. Payri (IRD). We are grateful to G. Lasne, J.L. Menou, J. Butscher, E. Folcher, B. Dreyfus, A. Arnaud, and the R/V Alis Captain and crew for their valuable help and knowledge of the Neocaledonian

reefs during fieldwork. Samplings in Papua New Guinea were possible thanks to the "*Our Planet Reviewed*" Papua Niugini expedition organized by Muséum National d'Histoire Naturelle (MNHN), Pro Natura International (PNI), Institut de Recherche pour le Développement (IRD) and University of Papua New Guinea (UPNG), Principal Investigators P. Bouchet (MNHN), C. Payri (IRD), S. Samadi, and B. Dreyfus (IRD). The organizers of this expedition acknowledge funding from the Total Foundation, Prince Albert II of Monaco Foundation, Fondation EDF, Stavros Niarchos Foundation and Entrepose Contracting, and in-kind support from the Divine Word University (DWU). The expedition operated under a permit delivered by the Papua New Guinea Department of Environment and Conservation. For specimens from the Red Sea, a special acknowledgement goes to J.D. DiBattista, P. Saenz-Agudelo, J. Bouwmeester, M.A. Priest, T. Sinclair-Taylor, and E. Giles (KAUST), and A. Caragnano for their assistance at KAUST. Un grazie particolare a J.P.A. Hobbs (UWA) for collecting two samples of *S. margariticola* from 'the mood of the deep'. We also thank the crew of Dream Divers and the staff of the Coastal and Marine Resources Core Lab for field support in Saudi Arabia and A.R. Behzad (KAUST) for technical help with SEM imaging at KAUST. We are grateful to E. Dutrieux (CREOCEAN), C.H. Chaineau (Total SA), R. Hirst and M. AbdulAziz (YLNG) for allowing and supporting research in Yemen. We wish to thank M. Pichon, S. Basheen (Professional Divers Yemen), M.A. Ahmad, A. Suliman and F.N. Saeed (EPA Socotra), C. Riva, S. Montano, and A. Caragnano for their help in different parts of field work in Yemen. A special thank to P. Galli and Davide and Simone for samplings in Maldives at the magnificent MaRHE Center (Magoodhoo, Maldives). Concerning the work at UNIMIB we are grateful to P. Gentile (UNIMIB) for technical help with SEM specimen preparation, P. Galli for laboratory support during the entire period of my PhD, E. Reynaud (Adéquation & Développement) for part of the instruments for these studies, and Daniela, Andrea and Diego for their assistance with the Nanodrop 1000.

For chapter 3, I am indebted to D. Obura for his help with English editing. I gratefully acknowledge B.W. Hoeksema for samples of *M. multipunctata*, sampled during the Tun Mustapha Park Expedition (TMPE) 2012, which was jointly-organized by WWFMalaysia, Universiti Malaysia Sabah, Sabah Parks, Malaysia and Naturalis Biodiversity Center, and for stimulating discussion. For Chapter 4, the sequencing of mitogenome of *A. maxima* was performed at Genoscope by Prometheus (ANR-09-PCS-GENM-217) and France Genomique (ANR-10-INPS-09) grants. For chapter 5, a very special thank to Z.T. Richards for her great help and support, and for her enthusiasm in this work! I thank C.C. Wallace (MTQ) and B.W. Hoeksema for museum support. Z.T. Richards was supported in fieldwork and write-up phased by Woodside Energy and the Woodside Collection

(Kimberley) project. Coral collection by A.H. Baird was funded by the ARC Centre of Excellence for Coral Reef Studies. For Chapter 6, I am especially indebted to C. Leuter (ZMB) for his assistance in the search of type material of *S. margariticola*. I am grateful to A. Andouche (MNHN), K. Johnson (MNH), S. Cairns (USNM), and B.W. Hoeksema for their help in access to museum collection and to the NHM Imaging Resources Department for images of holotype of *A. maxima*. I thank A. Andouche (MNHN) for the assistance with illustrations of Gravier (1907). I really wish to thank A.H. Baird, H. Fukami and D. Huang (UIOWA) for their comments and suggestions during the first phase of analyses.

We are also really grateful to all anonymous reviewers of papers published during these three years for their help and constructive comments.

Infine i ringraziamenti più personali, in italiano.. Un enorme grazie a miei genitori per avermi dato la possibilità di continuare in questa strada lasciandomi totale libertà di scelta durante questi dieci anni di bicocca (e anche per i prossimi anni) e per sopportarmi tutti i giorni. Grazie anche a mia sorella Sara, Meo e alle due piccoline Maddalena e Annalisa per il vostro carattere solare e per essere sempre felici, sarà dura non vedere crescere le mie due nipotine nei prossimi anni. Un grazie speciale poi ai miei zii Francesca, Luigi e Dino, senza il vostro supporto non sarei qui a scrivere queste righe. Grazie poi a tutti i miei amici, Teo, Simo, Zio, e Fede su tutti, e ai miei compagni di squadra prima alla Pob e poi alla Barza per i tanti chilometri corsi e i pochi punti fatti.

E l'ultimo ringraziamento non poteva che andare al mio amore, Tullia.. amore mio ma anche collega.. Sei stata di aiuto fondamentale in laboratorio e fai parte di molti dei capitoli presentati in questa tesi. Abbiamo condiviso moltissime delle esperienze descritte in questa tesi vivendole sempre pienamente. È bellissimo essere al tuo fianco, mi dai tutto quello di cui ho bisogno e che desidero. E tra poco Kaust, pronti io e te per un nuovo capitolo della nostra vita, non vedo l'ora ☺

– REFERENCES –

- Alloiteau, J., 1952. Madreporaires post-paleozoïques. In: J. Piveteau (Ed.), *Traite de paleontologie*. Paris, Masson.
- Anisimova, M., Gascuel, O., 2006. Approximate likelihood ratio test for branches: A fast, accurate and powerful alternative. *Syst. Biol.* 55, 539-552.
- Arrigoni, R., Terraneo, T.I., Galli, P., Benzoni, F., 2014a. Lobophylliidae (Cnidaria, Scleractinia) reshuffled: pervasive non-monophyly at genus level. *Mol. Phylogenet. Evol.* 73, 60-64.
- Arrigoni, R., Vacherie, B., Benzoni, F., Barbe, V., 2014c. The complete mitochondrial genome of *Acanthastrea maxima* (Cnidaria, Scleractinia, Lobophylliidae). *Mitochondrial DNA*. doi:10.3109/19401736.2014.926489.
- Arrigoni, R., Stefani, F., Pichon, M., Galli, P., Benzoni, F., 2012. Molecular phylogeny of the Robust clade (Faviidae, Mussidae, Merulinidae, and Pectiniidae): An Indian Ocean perspective. *Mol. Phylogenet. Evol.* 65, 183-193.
- Arrigoni, R., Richards, Z.T., Chen, C.A., Baird, A.H., Benzoni, F., 2014b. Phylogenetic relationships and taxonomy of the coral genera *Australomussa* and *Parascalymia* (Scleractinia, Lobophylliidae). *Contrib. Zool.* 83, 195-215.
- Arrigoni, R., Berumen, M.L., Terraneo, T.I., Caragnano, A., Bouwmeester, J., Benzoni, F., 2015. Forgotten in the taxonomic literature: resurrection of the scleractinian coral genus *Sclerophyllia* (Scleractinia, Lobophylliidae) from the Arabian Peninsula and its phylogenetic relationships. *Syst. Biodivers.* DOI: 10.1080/14772000.2014.978915.
- Arrigoni, R., Kitano, Y.F., Stolarski, J., Hoeksema, B.W., Fukami, H., Stefani, F., Galli, P., Montano, S., Castoldi, E., Benzoni, F., 2014d. A phylogeny reconstruction of the Dendrophylliidae (Cnidaria, Scleractinia) based on molecular and micromorphological criteria, and its ecological implications. *Zool. Scr.* 43, 661-688.
- Baird, A.H., Guest, J.R., Willis, B.L., 2009. Systematic and biogeographical patterns in the reproductive biology of scleractinian corals. *Annu. Rev. Ecol. Evol. Syst.* 40, 551-571.
- Bandelt, H.J., Forster, P., Röhl, A., 1999. Median-joining networks for inferring intraspecific phylogenies. *Mol. Biol. Evol.* 16, 37-48.
- Barbeitos, M.S., Romano, S.L., Lasker, H.R., 2010. Repeated loss of coloniality and symbiosis in scleractinian corals. *Proc. Natl. Aca. Sci.* 107, 11877-11882.
- Benzoni, F., 2006. *Psammocora albopicta* sp. nov., a new species of scleractinian coral from the Indo-West Pacific (Scleractinia; Siderastreidae). *Zootaxa* 1358, 49-57.
- Benzoni, F., 2013. *Echinophyllia tarae* sp. n. (Cnidaria, Anthozoa, Scleractinia), a new reef coral species from the Gambier Islands, French Polynesia. *ZooKeys* 318, 59-79.
- Benzoni, F., Stefani, F., Pichon, M., Galli, P., 2010. The name game: morpho-molecular species boundaries in the genus *Psammocora* (Cnidaria, Scleractinia). *Zool. J. Linn. Soc.* 160, 421-456.
- Benzoni, F., Arrigoni, R., Stefani, F., Pichon, M., 2011. Phylogeny of the coral genus *Plesiastrea* (Cnidaria, Scleractinia). *Contrib. Zool.* 80, 231-249.
- Benzoni, F., Arrigoni, R., Stefani, F., Stolarski, J., 2012a. Systematics of the coral genus

Craterastrea (Cnidaria, Anthozoa, Scleractinia) and description of a new family through combined morphological and molecular analyses. *Syst. Biodiver.* 10, 417-433.

Benzoni, F., Arrigoni, R., Waheed, Z., Stefani, F., Hoeksema, B.W., 2014. Phylogenetic relationships and revision of the genus *Blastomussa* (Cnidaria: Anthozoa: Scleractinia) with description of a new species. *Raffles B. Zool.* 62, 358-378.

Benzoni, F., Stefani, F., Stolarski, J., Pichon, M., Mitta, G., Galli, P., 2007. Debating phylogenetic relationships of the scleractinian *Psammocora*: molecular and morphological evidences. *Contrib. Zool.* 76, 35-54.

Benzoni, F., Arrigoni, R., Stefani, F., Reijnen, B.T., Montano, S., Hoeksema, B.W., 2012b. Phylogenetic position and taxonomy of *Cycloseris explanulata* and *C. wellsi* (Scleractinia: Fungiidae): lost mushroom corals find their way home. *Contrib. Zool.* 81, 125-146.

Berumen, M.L., Hoey, A.S., Bass, W.H., Bouwmeester, J., Catania, D., Cochran, J.E.M., Saenz-Agudelo, P., 2013. The status of coral reef ecology research in the Red Sea. *Coral Reefs* 32, 737-748.

Best, M.B., Hoeksema, B.W., 1987. New observations on scleractinian corals from Indonesia: 1. Free-living species belonging to the Faviina. *Zool. Med. Leiden* 61, 387-403.

Bourne, G.C., 1887. On the anatomy of *Mussa* and *Euphyllia*, and the morphology of the madreporarian skeleton. *Q. J. Microsc. Sci.*, 28, 21-52.

Bowen, B.W., Rocha, L.A., Toonen, R.J., Karl, S.A., 2013. The origins of tropical marine biodiversity. *Trends Ecol. Evol.* 28, 359-366.

Brahmi, C., Meibom, A., Smith, D.C., Stolarski, J., Auzoux-Bordenave, S., Nouet, J., Doumenc, D., Djediat, C., Domart-Coulon, I., 2010. Skeletal growth, ultrastructure and composition of the azooxanthellate scleractinian coral *Balanophyllia regia*. *Coral Reefs* 29, 175-189.

Brown, B.E., 1997. Coral bleaching: causes and consequences. *Coral Reefs* 16, 129-138.

Brüggemann, F., 1877. Notes on stony corals in the British Museum. III. A revision of recent solitary Mussaceae. *Anna. Mag. Nat. Hist.* 4, 300-12.

Brugler, M.R., France, S.C., 2007. The complete mitochondrial genome of the black coral *Chrysopathes formosa* (Cnidaria:Anthozoa:Antipatharia) supports classification of antipatharians within the subclass Hexacorallia. *Mol. Phyl. Evol.* 42, 776-788.

Budd, A.F., 1990. Longterm patterns of morphological variation within and among species of reef-corals and their relationship to sexual reproduction. *Syst. Bot.* 15, 150-165.

Budd, A.F., 2009. Systematics and evolution of scleractinian corals. *Encyclopedia of Life Synthesis Meeting Report Smithsonian Institution, National Museum of Natural History.*

Budd, A.F., Klaus, J.S., 2001. The origin and early evolution of the *Montastraea annularis* species complex (Anthozoa: Scleractinia). *J. Paleontol.* 75, 527-545.

Budd, A.F., Stolarski, J., 2009. Searching for new morphological characters in the systematics of scleractinian reef corals: comparison of septal teeth and granules between Atlantic and Pacific Mussidae. *Acta Zool.* 90, 142-165.

Budd, A.F., Stolarski, J., 2011. Corallite wall and septal microstructure in scleractinian

reef corals: comparison of molecular clades within the family Faviidae. *J. Morphol.* 272, 66-88.

Budd, A.F., Romano, S.L., Smith, N.D., Barbeitos, M.S., 2010. Rethinking the phylogeny of Scleractinian corals: a review of morphological and molecular data. *Integr. Comp. Biol.* 50, 411-427.

Budd, A.F., Fukami, H., Smith, N., Knowlton, N., 2012. Taxonomic classification of the reef coral family Mussidae (Cnidaria: Anthozoa: Scleractinia). *Zool. J. Linn. Soc.* 166, 465-529.

Cadotte, M.W., Davies, J.T., 2010. Rarest of the rare: advances in combining evolutionary distinctiveness and scarcity to inform conservation at biogeographical scales. *Div. Distrib.* 16, 376-385.

Cairns, S.D., 1999. Cnidaria Anthozoa: deep-water azooxanthellate Scleractinia from Vanuatu, and Wallis and Futuna islands. *Mém. Mus. Natl. Hist. Nat.* 180, 31-167.

Cairns, S.D., 2001. A generic revision and phylogenetic analysis of the Dendrophylliidae (Cnidaria: Scleractinia). *Smithson. Contrib. Zool.* 615, 1-75.

Cairns, S.D., 2004. The azooxanthellate Scleractinia (Coelenterata: Anthozoa) of Australia. *Rec. Aus. Mus.* 56, 259-329.

Cairns, S.D., 2007. Deep-sea corals: An overview with special reference to diversity and distribution of deep-water scleractinian corals. *B. Mar. Sci.* 81, 311-322.

Cairns, S.D., Kitahara, M.V., 2012. An illustrated key to the genera and subgenera of the recent azooxanthellate scleractinia (Cnidaria: Anthozoa), with an attached glossary. *ZooKeys* 227, 1-47.

Carpenter, K.E., Harrison, P.L., Hodgson, G., Alsaffar, A.H., Ajhazeem, H., 1997. The corals and coral reefs of Kuwait. Kuwait Institute for Scientific Research, Kuwait.

Chen, C.A., Wallace, C.C., Wolstenholme, J.K., 2002. Analysis of the mitochondrial 12S rRNA gene supports a two-clade hypothesis of the evolutionary history of scleractinian corals. *Mol. Phylogenet. Evol.* 23, 137-149.

Chen, C.A., Chang, C.C., Wei, N.V., Chen, C.H., Lein, Y.T., Lin, H.E., Dai, C.F., Wallace, C.C., 2004. Secondary structure and phylogenetics utility of the ribosomal internal transcribed spacer 2 (ITS2) in scleractinian corals. *Zool. Stud.* 43, 759-771.

Chevalier, J.P., 1975. Les Scléactiniaux de la Mélanésie Française (Nouvelle-Calédonie, Iles Chesterfield, Iles Loyauté, Nouvelles Hébrides). *Expédition Française Sur les Récifs Coralliens de la Nouvelle-Calédonie*. Editions de la Fondation Singer-Polignac, Paris.

Chevalier, J.P., Beauvais, L. 1987. *Ordre des Scléactiniaux*. In: P.P. Grasse (Ed.), *Traite de Zoologie, Cnidaires, Anthozoaires*. Masson, Paris.

Claereboudt, M.R., 2006. *Coral Reefs and Reef Corals of the Gulf of Oman*. Al-Roya Publishing, Muscat.

Coles, S.L., 1996. *Corals of Oman*. Muscat printing press, North Yorkshire.

Colgan, D.J., Ponder, W.F., Eggle, P.E., 2000. Gastropod evolutionary rates and phylogenetic relationships assessed using partial 28S rDNA and histone H3 sequences. *Zool. Scr.* 29, 29-63.

Colgan, D.J., McLauchlan, A., Wilson, G.D.F., Livingston, S.P., Edgecombe, G.D.,

Macaranas, J., Gray, M.R., 1998. Histone H3 and U2 snRNA DNA sequences and arthropod molecular evolution. *Aus. J. Zool.* 46, 419-437.

Cowman, P.F., Bellwood, D.R., 2013. The historical biogeography of coral reef fishes: global patterns of origination and dispersal. *J. Biogeogr.* 40, 209-224.

Crossland, C., 1952. Madreporaria, Hydrocorallinae, *Heliopora* and *Tubipora*. Great Barrier Reef Exped. 1928-29. Catalogue of the Madreporarian Corals in the British Museum (Natural History) 6, 85-257.

Cuif, J.P., Sorauf, J.E. 2001. Biomineralization and diagenesis in Scleractinia: part I, biomineralization. *Bull. Tohoku Univer. Mus.* 1, 144-151.

Cuif, J.P., Lecointre, G., Perrin, C., Tillier, A., Tillier, S., 2003. Patterns of septal biomineralization in Scleractinia compared with their 28S rRNA phylogeny: a dual approach for a new taxonomic framework. *Zoo. Scr.* 5, 459-473.

Dai, C.F., Horng, S., 2009. Scleractinia fauna of Taiwan II. The robust group. National Taiwan University, Taipei.

Dana, J. D., 1846. Zoophytes. United States Exploring Expedition during the years 1838-1842, under the command of Charles Wilkes, U.S.N., vol. 7. C. Sherman, Philadelphia.

DeVantier, L., De'Ath, G., Klaus, R., Al-Moghrabi, S., Abdulaziz, M., Reinicke, G.B., Cheung, C., 2004. Reef-building corals and coral communities of the Socotra Archipelago, a zoogeographic 'crossroads' in the Arabian sea. *Fauna Arabia* 20, 117-168.

DiBattista, J.D., Berumen, M.L., Gaither, M.R., Rocha, L.A., Eble, J.A., Choat, J.H., Bowen, B.W., 2013. After continents divide: comparative phylogeography of reef fishes from the Red Sea and Indian Ocean. *J. Biogeogr.* 40, 1170-1181.

Diekmann, O.E., Bak, R.P.M., Stam, W.T., Olsen, J.L., 2001. Molecular genetic evidence for probable reticulate speciation in the coral genus *Madracis* from a Caribbean fringing reef slope. *Mar. Biol.* 139, 221-233.

Drummond, A.J., Rambaut, A., 2007. BEAST: bayesian evolutionary analysis by sampling trees. *BMC Evol. Biol.* 7, 214.

Faure, G. Pichon, M., 1978. Description de *Favites peresi*, nouvelle espece de Scleractiniaire hermatipique de l'Ocean Indien (Cnidaria, Anthozoa, Scleractinia). *Bull. Mus. Natn. Hist. Nat. Paris.* 513, 107-127.

Flot, J.F., Magalon, H., Cruaud, C., Couloux, A., Tillier, S., 2008. Patterns of genetic structure among Hawaiian corals of the genus *Pocillopora* yield clusters of individuals that are compatible with morphology. *Com. Ren. Biol.* 331, 239-247.

Flot, J.F., Blanchot, J., Charpy, L., Cruaud, C., Licuanan, W.Y., Nakano, Y., Payri, C., Tillier, S., 2011. Incongruence between morphotypes and genetically delimited species in the coral genus *Stylophora*: phenotypic plasticity, morphological convergence, morphological stasis or interspecific hybridization? *BMC Ecol.* 11, 22.

Forest, F., Crandall, K.A., Chase, M.W., Faith, D.P., 2015. Phylogeny, extinction and conservation: embracing uncertainties in a time of urgency. *Phil. Trans. R. Soc. B.* 370, 20140002.

Forsman, Z.H., Hunter, C.L., Fox, G.E., Wellington, G.M., 2006. Is the ITS region the solution to the "species problem" in corals? Intragenomic variation, and alignment

permutations in *Porites*, *Siderastrea* and outgroup taxa. Proc. 10th Int. Coral Reef Symp. 1, 14-23.

Forsman, Z.H., Barshis, D.J., Hunter, C.L., Toonen, R.J., 2009. Shapeshifting corals: molecular markers show morphology is evolutionary plastic in *Porites*. BMC Evol. Biol. 9, 45.

Fukami, H., Knowlton, N., 2005. Analysis of complete mitochondrial DNA sequences of three members of the *Montastraea annularis* coral species complex (Cnidaria, Anthozoa, Scleractinia). Coral Reefs 24, 410-417.

Fukami, H., Chen, C.A., Chiou, C.Y., Knowlton, N., 2007. Novel group I introns encoding a putative homing endonuclease in the mitochondrial *cox1* gene of scleractinian corals. J. Mol. Evol. 64, 591-600.

Fukami, H., Budd, A.F., Levitan, D.R., Jara, J., Kersanach, R., Knowlton, N., 2004b. Geographic differences in species boundaries among members of the *Montastraea annularis* complex based on molecular and morphological markers. Evolution 58, 324-337.

Fukami, H., Budd, A.F., Paulay, G., Sole-Cava, A., Chen, C.A., Iwao, K., Knowlton, N., 2004a. Conventional taxonomy obscures deep divergence between Pacific and Atlantic corals. Nature 427, 832-835.

Fukami, H., Chen, C.A., Budd, A.F., Collins, A., Wallace, C., Chuang, Y.Y., Chen, C., Dai, C.F., Iwao, K., Sheppard, C., Knowlton, N., 2008. Mitochondrial and nuclear genes suggest that stony corals are monophyletic but most families of stony corals are not (Order Scleractinia, Class Anthozoa, Phylum Cnidaria). PLoS ONE 3, e3222.

Gardiner, J.S., 1899. On the solitary corals, collected by Dr. A. Willey Zoological Results based on Material from New Britain, New Guinea, Loyalty Islands and Elsewhere 2, 161-180.

Gittenberger, A., Reijnen, B.T., Hoeksema, B.W., 2011. A molecularly based phylogeny reconstruction of mushroom corals (Scleractinia: Fungiidae) with taxonomic consequences and evolutionary implications for life history traits. Contrib. Zool. 80, 107-132.

Gravier, C.J., 1907. Note sur quelques coraux des récifs du Golfe de Tadjourah. Bull. Mus. Hist. Nat. 13, 339-43.

Gravier, C.J., 1911. Les récifs de coraux et les madréporaires de la baie de Tadjourah (Golfe d'Aden). Annales de l'Institut Oceanographique, Paris.

Guindon, S., Gascuel, O., 2003. A simple, fast, and accurate algorithm to estimate large phylogenies by maximum likelihood. Syst. Biol. 52, 696-704.

Hall, T.A., 1999. BioEdit: a user-friendly biological sequence alignment editor and analysis program for Windows 95/98/NT. Nucleic Acids Symp. Ser. 41, 95-98.

Harrison, P.L., Babcock, R.C., Bull, G.D., Oliver, J.K., Wallace, C.C., Willis, B.L., 1984. Mass spawning in tropical reef corals. Science 223, 1186-1189.

Harvell, C.D., Kim, K., Burkholder, J.M., Colwell, R.R., Epstein, P.R., Grimes, D.J., Hofmann, E.E., Lipp, E.K., Osterhaus, A.D.M.E., Overstreet, R.M., Porter, J.W., Smith, G.W., Vasta, G.R., 1999. Emerging marine diseases-climate links and anthropogenic factors. Science 285, 1505-1510.

Hellberg, M.E., 2006. No variation and low synonymous substitution rates in coral mtDNA despite high nuclear variation. BMC Evol. Biol. 6, 24.

- Hodgson, G., Carpenter, K., 1995. Scleractinian corals of Kuwait. *Pac. Science* 49, 227-246.
- Hoegh-Guldberg, O., Smith, G.J., 1989. The effect of sudden changes in temperature, irradiance and salinity on the population density and export of zooxanthellae from the reef corals *Stylophora pistillata* (Esper 1797) and *Seriatopora hystrix* (Dana 1846). *Exper. Mar. Biol. Ecol.* 129, 279-303.
- Hoeksema, B.W., 1989. Taxonomy, phylogeny and biogeography of mushroom corals (Scleractinia: Fungiidae). *Zool. Ver.* 254, 1-295.
- Hoeksema, B.W., 1991. Evolution of body size in mushroom corals (Scleractinia: Fungiidae) and its ecomorphological consequences. *Netherl. J. Zool.* 41, 122-139.
- Hoeksema, B.W., 1993. Phenotypic corallum variability in recent mobile reef corals. *Cour. Forsch.* 164, 263-272.
- Hoeksema, B.W., 2007. Delineation of the Indo-Malayan Centre of Maximum Marine Biodiversity: The Coral Triangle. In: W. Renema (Eds.), *Biogeography, Time and Place: Distributions, Barriers and Islands*. Springer, Berlin.
- Hoeksema, B.W., 2014. The “*Fungia patella* group” (Scleractinia, Fungiidae) revisited with a description of the mini mushroom coral *Cycloseris boschmai* sp. n. *ZooKeys* 371, 57-84.
- Hoeksema, B.W., Ofwegen, L.P. van, 2004. Reef corals of Indonesia and SE Asia: a generic overview. *World Biodiversity Database CD-ROM Series ETI*, Amsterdam.
- Hoeksema, B.W., Van der Land, J., Van der Meij, S.E.T., Van Ofwegen, L.P., Reijnen, B.T., Van Soest, R.W.M., De Voogd, N.J., 2011. Unforeseen importance of historical collections as baselines to determine biotic change of coral reefs: the Saba Bank case. *Mar. Ecol.* 32, 135-141.
- Huang, D., 2012. Threatened reef corals of the world. *PLoS ONE* 7, e34459.
- Huang, D., Roy, K., 2013. Anthropogenic extinction threats and future loss of evolutionary history in reef corals. *Ecol. Evol.* 3, 1184-1193.
- Huang, D., Roy, K., 2015. The future of evolutionary diversity in reef corals. *Phil. Trans. R. Soc. B.* 370, 20140010.
- Huang, D., Meier, R., Todd, P.A., Chou, L.M., 2008. Slow mitochondrial COI sequence evolution at the base of the metazoan tree and its implications for DNA barcoding. *J. Mol. Evol.* 66, 167-174.
- Huang, D., Meier, R., Todd, P.A., Chou, L.M., 2009. More evidence for pervasive paraphyly in scleractinian corals: systematic study of Southeast Asian Faviidae (Cnidaria; Scleractinia) based on molecular and morphological data. *Mol. Phylogen. Evol.* 50, 102-116.
- Huang, D., Licuanan, W.Y., Baird, A.H., Fukami, H., 2011. Cleaning up the “Bigmessidae”: molecular phylogeny of scleractinian corals from Faviidae, Merulinidae, Pectiniidae, and Trachyphylliidae. *BMC Evol. Biol.* 11, 37.
- Huang, D., Benzoni, F., Fukami, H., Knowlton, N., Smith, N.D., Budd, A.F., 2014a. Taxonomic classification of the reef coral families Merulinidae, Montastraeidae, and Diploastraeidae (Cnidaria: Anthozoa: Scleractinia). *Zool. J. Linn. Soc.* 171, 277-355.
- Huang, D., Benzoni, F., Arrigoni, R., Baird, A.H., Berumen, M.L., Bouwmeester, J.,

Chou, L.M., Fukami, H., Licuanan, W.Y., Lovell, E.R., Meier, R., Todd, P.A., Budd, A.F., 2014b. Towards a phylogenetic classification of reef corals: the Indo-Pacific genera *Merulina*, *Goniastrea* and *Scapophyllia* (Scleractinia, Merulinidae). *Zool. Scr.* 43, 531-548.

Huelsenbeck, J.P., Ronquist, F., 2001. MRBAYES: Bayesian inference of phylogenetic trees. *Bioinformatics* 17, 754-755.

Isomura, N., Iwao, K., Fukami, H., 2013. Possible Natural Hybridization of Two Morphologically Distinct Species of *Acropora* (Cnidaria, Scleractinia) in the Pacific: Fertilization and Larval Survival Rates. *PLoS ONE* 8, e56701.

Janiszewska, K., Jaroszewcz, J., Stolarski, J., 2013. Skeletal ontogeny in basal scleractinian micrabaciid corals. *J. Morphol.* 274, 243-257.

Janiszewska, K., Stolarski, J., Benzerara, K., Meibom, A., Mazur, M., Kitahara, M.V., Cairns, S.D., 2011. A unique skeletal microstructure of the deep-sea micrabaciid scleractinian corals. *J. Morphol.* 231, 191-203.

Janiszewska, K., Stolarski, J., Kitahara, M.V., Neuser, N.D., Mazur, M., 2015. Microstructural disparity between basal micrabaciids and other Scleractinia: new evidence from Neogene Stephanophyllia. *Lethaia*, DOI: 10.1111/let.12119.

Katoh, K., Standley, D.M., 2013. MAFFT multiple sequence alignment software version 7: improvements in performance and usability. *Mol. Biol. Evol.* 30, 772-780.

Katoh, K., Misawa, K., Kuma, K., Miyata, T., 2002. MAFFT: a novel method for rapid multiple sequence alignment based on fast Fourier transform. *Nucleic Acids Res.* 30, 3059-3066.

Kayal, E., Roure, B., Philippe, H., Collins, A.G., Lavrov, D.V., 2013. Cnidarian phylogenetic relationships as revealed by mitogenomics. *BMC Evol. Biol.* 13, 5.

Keshavmurthy, S., Yang, S.Y., Alamaru, A., Chuang, Y.Y., Pichon, M., Obura, D.O., Fontana, S., et al., 2013. DNA barcoding reveals the coral “laboratory-rat”, *Stylophora pistillata* encompasses multiple identities. *Sci. Rep.* 3, 1520.

Kitahara, M.V., Cairns, S.D., Stolarski, J., Miller, D.J., 2012a. Deltocyathiidae, an early-diverging family of Robust corals (Anthozoa, Scleractinia). *Zool. Scr.* 42, 201-212.

Kitahara, M.V., Cairns, S.D., Stolarski, J., Blair, D., Miller, D.J., 2010. A comprehensive phylogenetic analysis of the Scleractinia (Cnidaria, Anthozoa) based on mitochondrial CO1 sequence data. *PLoS ONE* 5, e11490.

Kitahara, M.V., Stolarski, J., Cairns, S.D., Benzoni, F., Stake, J.L., Miller, D.J., 2012b. The first modern solitary Agariciidae (Anthozoa, Scleractinia) revealed by molecular and microstructural analysis. *Invertebr. Syst.* 26, 303-315.

Kitahara, M.V., Lin, M.F., Foret, S., Huttley, G., Miller, D.J., Chen, C.A., 2014. The “naked coral” hypothesis revisited-evidence for and against scleractinian monophyly. *PLoS One* 9, e94774.

Kitano, Y.F., Obuchi, M., Uyeno, D., Miyazaki, K., Fukami, H., 2013. Phylogenetic and taxonomic status of the coral *Goniopora stokesi* and related species (Scleractinia: Poritidae) in Japan based on molecular and morphological data. *Zool. Stud.* 52, 1-16.

Kitano, Y.F., Benzoni, F., Arrigoni, R., Shirayama, Y., Wallace, C.C., Fukami, H., 2014. A phylogeny of the family Poritidae (Cnidaria, Scleractinia) based on molecular and morphological analyses. *PLoS ONE* 9, e98406.

- Klaus, J.S., Budd, A.F., Heikoop, J.M., Fouke, B.W., 2007. Environmental controls on corallite morphology in the reef coral *Montastraea annularis*. *Bull. Mar. Sci.* 80, 233-260.
- Klueter, A., Andreakis, N., 2013. Assessing genetic diversity in the scleractinian coral *Stylophora pistillata* (Esper 1797) from the Central Great Barrier Reef and the Coral Sea. *Syst. Biodiver.* 11, 67-76.
- Klunzinger, C.B., 1879. Die Korallenthiere des Rothen Meeres, 3. Theil: Die Steinkorallen. Zweiter Abschnitt, Die Asteraeaceen und Fungiaceen, Berlin.
- Knowlton, N., Fukami, H., Chen, C.A., Budd, A.F., 2008. Mitochondrial and nuclear genes suggest that stony corals are monophyletic but most families of stony corals are not. 11th Int. Coral Reef Symp. 251.
- Kongjandtre, N., Ridgway, T., Ward, S., Hoegh-Guldberg, O., 2010. Broadcast spawning patterns of *Favia* species on the inshore reefs of Thailand. *Coral Reefs* 29, 227-234.
- Kozub, D., Khmelik, V., Shapoval, J., Chentsov, V., Yatsenko, S., Litovchenko, B., Starikh, V., 2000-2012. Helicon Focus 5.3. Elicon Soft Ltd..
- Lasker, H.R., 1981. Phenotypic variation in the coral *Montastraea cavernosa* and its effects on the colony energetics. *Biol. Bull.* 160, 292-302.
- Lefebvre, C.T, Petit, A., Quartin-Dillon, L.R., Vignaud, A.R.A., Prévost, F., Guyard, S., Corbié, G., 1845. Voyage en Abyssinie: exécuté pendant les années 1839, 1840, 1841, 1842, 1843. Arthus Bertrand, Paris.
- Le Goff-Vitry, M.C., Rogers, A.D., Baglow, D., 2004. A deep-sea slant on the molecular phylogeny of the Scleractinia. *Mol. Phylogen. Evol.* 30, 167-177.
- Le Pichon, X.T., and Gaulier, J.M., 1988. The rotation of Arabia and the Levant fault system. *Tekstil.* 153, 271-294.
- Lin, M.F., Kitahara, M.V., Luo, H., Tracey, D., Geller, J., Fukami, H., Miller, D.J., Chen, C.A., 2014. Mitochondrial genome rearrangements in the Scleractinia/Corallimorpharia complex: implications for coral phylogeny. *Genome Biol. Evol.* 6, 1086-1095.
- Lin, M.F., Luzon, K.S., Licuanan, W.Y., Ablan-Lagman, M.C., Chen, C.A., 2011. Seventy-four universal primers for characterizing the complete mitochondrial genomes of scleractinian corals (Cnidaria; Anthozoa). *Zool. Stud.* 50, 513-524.
- Librado, P., Rozas, J., 2009. DnaSP v5: A software for comprehensive analysis of DNA polymorphism data. *Bioinformatics* 25, 1451-1452.
- Lyons-Weiler, J.L., Hoelzer, G.A., 1999. Null model selection, compositional bias, character state bias, and the limits of phylogenetic information. *Mol. Biol. Evol.* 16, 1400-1405.
- Maddison, W.P., Maddison, D.R., 2011. Mesquite: a modular system for evolutionary analysis. Version 2.75. Retrieved from <http://mesquiteproject.org>
- Marquez, L.M., Miller, D.J., MacKenzie, J.B., van Oppen, M.J.H., 2003. Pseudogenes contribute to the extremely diversity of nuclear ribosomal DNA in the hard coral *Acropora*. *Mol. Biol. Evol.* 20, 1077-1086.
- Matthai, G., 1928. A monograph of the Recent meandroid *Astraeidae*. Catalogue of Madreporarian Corals British Museum (Natural History) 7, 1-288.

- Maxmen, A.B., King, B.F., Cutler, E.B., Giribet, G., 2003. Evolutionary relationships within the protostome phylum Sipuncula: a molecular analysis of ribosomal genes and histone H3 sequence data. *Mol. Phylogen. Evol.* 27, 489-503.
- Maxson, R., Cohn, R., Kedes, L., Mohun, T., 1983. Expression and organization of histone genes. *Annu. Rev. Genet.* 17, 239-277.
- Medina, M., Collins, A.G., Takaoka, T.L., Kuehl, J.V., Boore, J.L., 2006. Naked corals: skeleton loss in Scleractinia. *Proc. Natl. Acad. Sci. USA.* 103, 96-100.
- Milne-Edwards, M., Haime, J., 1848. Recherches sur les polypiers; 4eme mémoire. Monographie des Astréides. *Ann. Sci. Nat.* 10, 209-320.
- Miller, K.J., 1992. Morphological variation in the scleractinian coral *Platygyra daedalea* (Ellis & Solander, 1786)-genetically or environmentally determined? *Proc. 7th Int. Coral Reef Symp.* 1, 550-556.
- Montanaro-Gattinelli, E., 1943. Coralli costruttori delle scogliere emerse di Massaua e Gibuti. Reale Accademia d'Italia, Roma.
- Moothien Pillay, R., Terashima, H., Venkatasami, A., Uchida, H., 2002. Field Guide to Corals of Mauritius. Albion Fisheries Research Center, Albion.
- Novo, M., Almodóvar, A., Fernández, R., Giribet, G., Díaz Cosín, D.J., 2011. Understanding the biogeography of a group of earthworms in the Mediterranean basin-The phylogenetic puzzle of Hormogastridae (Clitellata: Oligochaeta). *Mol. Phylogen. Evol.* 61, 125-135.
- Nunes, F., Fukami, H., Vollmer, S.V., Norris, R.D., Knowlton, N., 2008. Re-evaluation of the systematics of the endemic corals of Brazil by molecular data. *Coral Reefs* 27, 423-432.
- Nylander, J.A.A., 2004. MrModeltest v2. Program distributed by the author. Evolutionary Biology Centre, Uppsala University, Uppsala.
- Obura, D.O., 2012. The diversity and biogeography of Western Indian Ocean reef-building corals. *PLoS ONE* 7, e45013.
- Odorico, D.M., Miller, D.J., 1997. Variation in the ribosomal Internal Transcribed Spacers and 5.8S rDNA among five species of *Acropora* (Cnidaria; Scleractinia): patterns of variation consistent with reticulate evolution. *Mol. Biol. Evol.* 14, 465-473.
- Ogilvie, M.M., 1897. Korallen der Stramberger Schichten. *Palaeontogr. Supplement* 2, 73-282.
- Omar, G.I., Steckler, M.S., 1995. Fission track evidence on the initial rifting of the Red Sea: two pulses, no propagation. *Science* 270, 1341-1344.
- Pichon, M., Benzoni, F., Chaineu, C.H., Dutriex, E., 2010. Field Guide to the hard corals of the southern coast of Yemen. Biotope Parthenope, Paris.
- Pinzón, J.H., Sampayo, E., Cox, E., Chauka, L.J., Chen, C.A., Voolstra, C.R., LaJeunesse, T.C., 2013. Blind to morphology: genetics identifies several widespread ecologically common species and few endemics among Indo-Pacific cauliflower corals (*Pocillopora*, Scleractinia). *J. Biogeogr.* 40, 1595-1608.
- Pola, M., Gosliner, T.M., 2010. The first molecular phylogeny of cladobranchian opisthobranchs (Mollusca, Gastropoda, Nudibranchia). *Mol. Phylogen. Evol.* 56, 931-941.
- Posada, N., Crandall, K.A., 1998. Modeltest: testing the model of DNA substitution.

Bioinf. 14, 817-818.

Rambaut, A., Drummond, A.J., 2007. Tracer v1.4. Retrieved from <http://beast.bio.ed.ac.uk/Tracer>

Reijnen, B.T., McFadden, C.S., Hermanlimianto, Y.T., aVan Ofwegen, L.P., 2014. A molecular and morphological exploration of the generic boundaries in the family Melithaeidae (Coelenterata: Octocorallia) and its taxonomic consequences. *Mol. Phylogen. Evol.* 70, 383-401.

Richards, Z.T., Wallace, C.C., Miller, D.J., 2013. Molecular phylogenetics of geographically restricted *Acropora* species: Implications for conservation. *Mol. Phylogen. Evol.* 69, 837-851.

Richards, Z.T., van Oppen, M.J.H., Wallace, C.C., Willis, B.L., Miller, D.J., 2008. Some rare Indo-Pacific coral species are probable hybrids. *PLoS ONE* 3, e3240.

Rocha, L.A., Aleixo, A., Allen, G., Almeda, F., Baldwin, C.C., Barclay, M.V., Witt, C.C., et al., 2014. Specimen collection: An essential tool. *Science* 344, 815-816.

Roberts, C.M., McClean, C.J., Veron, J.E.N., Hawkins, J.P., Allen, G.R., McAllister, D.E., Werner, T.B., 2002. Marine biodiversity hotspots and conservation priorities for tropical reefs. *Science* 295, 1280-1284.

Romano, S.L., Palumbi, S.R., 1996. Evolution of scleractinian corals inferred from molecular systematics. *Science* 271, 640-642.

Romano, S.L., Palumbi, S.R., 1997. Molecular evolution of a portion of the mitochondrial 16S ribosomal gene region in scleractinian corals. *J. Mol. Evol.* 45, 397-411.

Romano, S.L., Cairns, S.D., 2000. Molecular phylogenetic hypotheses for the evolution of scleractinian corals. *Bull. Mar. Sci.* 67, 1043-1068.

Ronquist, F., Huelsenbeck, J.P., 2003. MrBayes 3: Bayesian phylogenetic inference under mixed models. *Bioinf.* 19, 1572-1574.

Rosenberg, E., Loya, Y., 2004. *Coral health and disease*. Springer, Berlin.

Sargent, T.D., Jamrich, M., Dawid, I.B., 1986. Cell interactions and the control of gene activity during early development of *Xenopus laevis*. *Dev. Biol.* 114, 238-246.

Scheer, G., Pillai, C.S.G., 1983. Report on the stony corals from the Red Sea. *Zoologica* 133, 1-198.

Schmidt-Roach, S., Miller, K.J., Andreakis, N., 2013b. *Pocillopora aliciae*: a new species of scleractinian coral (Scleractinia, Pocilloporidae) from subtropical Eastern Australia. *Zootaxa* 3626, 576-582.

Schmidt-Roach, S., Miller, K.J., Lundgren, P., Andreakis, N., 2014. With eyes wide open: a revision of species within and closely related to the *Pocillopora damicornis* species complex (Scleractinia; Pocilloporidae) using morphology and genetics. *Zool. J. Linn. Soc.* 170, 1-33.

Schmidt-Roach, S., Lundgren, P., Miller, K.J., Gerlach, G., Noreen, A., Andreakis, N., 2013a. Assessing hidden species diversity in the coral *Pocillopora damicornis* from Eastern Australia. *Coral Reefs* 32, 1-12.

Shearer, T.L., Coffroth, M.A., 2008. Barcoding corals: limited by interspecific divergence, not intraspecific variation. *Mol. Ecol. Res.* 8, 247-255.

Shearer, T.L., Van Oppen, M.J.H., Romano, S.L., Worheide, G., 2002. Slow

mitochondrial DNA sequence evolution in the Anthozoa (Cnidaria). *Mol. Ecol.* 11, 2475-2487.

Sheppard, C.R.C., 1985. Reefs and coral assemblages of Saudi Arabia 2. Fringing reefs in the southern region, Jeddah to Jizan. *Fauna Arabia* 7, 37-58.

Sheppard, C.R.C., Salm, R.V., 1988. Reef and coral communities of Oman, with a description of a new coral species (Order Scleractinia, genus *Acanthastrea*). *J. Nat. Hist.* 22, 263-279.

Sheppard, C.R.C., Sheppard, A.L.S., 1991. Corals and coral communities of Saudi Arabia. *Fauna Arabia* 12, 1-170.

Shimodaira, H., Hasegawa, M., 1999. Multiple comparisons of log-likelihoods with applications to phylogenetic inference. *Mol. Biol. Evol.* 16, 1114-1116.

Siddal, M., Rohling, E.J., Almogi-Labin, A., Hemleben, C., Meischner, D., Schmelzer, I., Smeed, D.A., 2003. Sea level fluctuations during the last glacial cycle. *Nature* 423, 853-858.

Souter, P., 2010. Hidden genetic diversity in a key model species of coral. *Mar. Biol.* 157, 875-885.

Stanley, G.D., Fautin, D.G., 2001. The origin of modern corals. *Science* 291, 1913-1914.

Stefani, F., Benzoni, F., Pichon, M., Cancelliere, C., Galli, P., 2007. A multidisciplinary approach to the definition of species boundaries in branching species of the coral genus *Psammocora* (Cnidaria, Scleractinia). *Zool. Scr.* 37, 71-91.

Stefani, F., Benzoni, F., Yang, S.Y., Pichon, M., Galli, P., Chen, C.A., 2011. Comparison of morphological and genetic analyses reveals cryptic divergence and morphological plasticity in *Stylophora* (Cnidaria, Scleractinia). *Coral Reefs* 30, 1033-1049.

Stolarski, J., 2003. 3-Dimensional micro- and nanostructural characteristics of the scleractinian corals skeleton: a biocalcification proxy. *Acta Palaeontol. Pol.* 48, 497-530.

Stolarski, J., Roniewicz, E., 2001. Towards a new synthesis of evolutionary relationships and classification of Scleractinia. *J. Paleo.* 75, 1090-1108.

Stolarski, J., Kitahara, M.V., Miller, D.J., Cairns, S.D., Mazur, M., Meibom, A., 2011. An ancient evolutionary origin of Scleractinia revealed by azooxanthellate corals. *BMC Evol. Biol.* 11, 316.

Swofford, D.L., 2003. PAUP*. Phylogenetic Analysis Using Parsimony (*and other methods). Version 4. Sinauer Associates, Sunderland.

Takabayashi, M., Carter, D.A., Loh, W.K.T., Hoegh-Guldberg, O., 1998. A coral-specific primer for PCR amplification of the internal transcribed spacer region in ribosomal DNA. *Mol. Ecol.* 7, 925-931.

Tamura, K., Peterson, D., Peterson, N., Stecher, G., Nei, M., Kumar, S., 2011. MEGA5: molecular evolutionary genetics analysis using Maximum Likelihood, Evolutionary Distance, and Maximum Parsimony method. *Mol. Biol. Evol.* 28, 2731-2739.

Thompson, J.D., Gibson, T.J., Plewniak, F., Jeanmougin, F., Higgins, D.G., 1997. The ClustalX windows interface: flexible strategies for multiple sequence alignment aided by quality analysis tools. *Nucleic Acids Res.* 25, 4876-4882.

Todd, P.A., 2008. Morphological plasticity in scleractinian corals. *Biol. Rev.* 83, 315-

337.

Todd, P.A., Sanderson, P.G., Chou, L.M., 2001. Morphological variation in the polyps of the scleractinian coral *Favia speciosa* (Dana) around Singapore. *Hydrob.* 444, 227-235.

Todd, P.A., Ladle, R.J., Lewin-Koh, N.J.I., Chou, L.M., 2004. Flesh or Bone? Quantifying small-scale coral morphology using with-tissue and without-tissue techniques. *Mar. Biol.* 145, 323-328.

Turak, E., Sheppard, C., Wood, E., 2008. *Acanthastrea maxima*. In: IUCN 2013. IUCN Red List of Threatened Species. Version 2013. Retrieved from: <http://www.iucnredlist.org/details/133490/0>

van Oppen, M.J.H., McDonald, B.J., Willis, B.L., Miller, D.J., 2001. The evolutionary history of the coral genus *Acropora* (Scleractinia, Cnidaria) based on a mitochondrial and a nuclear marker: reticulation, incomplete lineage sorting or morphological convergence? *Mol. Biol. Evol.* 18, 1315-29.

van Oppen, M.J.H., Willis, B.L., van Rheede, T., Miller, D.J., 2002a. Spawning times, reproductive compatibilities and genetic structuring in the *Acropora aspera* group: evidence for natural hybridization and semipermeable species boundaries in corals. *Mol. Ecol.* 11, 1363-76.

van Oppen, M.J.H., Catmull, J., McDonald, B.J., Hislop, N.R., Hagerman, P.J., Miller, D.J., 2002b. The mitochondrial genome of *Acropora tenuis* (Cnidaria: Scleractinia) contains a large group I intron and a candidate control region. *J. Mol. Evol.* 55, 1-13.

Vaughan, T.W., 1907. Some madreporarian corals from French Somaliland, East Africa. *Proc. Nat. Mus.* 32, 249-266.

Vaughan, T.W., Wells, J.W., 1943. Revision of the Sub-orders, Families and Genera of the Scleractinia. *Geol. Soc. Am.* 44, 1-363.

Veron, J.E.N., 1985. New Scleractinia from Australian coral reefs. *Rec. West. Aus. Mus.* 12, 147-183.

Veron, J.E.N., 1986. Corals of Australia and the Indo-Pacific. Angus and Robertson, North Ryde.

Veron, J.E.N., 1992. Hermatypic corals of Japan. *Aust. Inst. Mar. Sci. Monogr. Ser.* 9, 1-234.

Veron, J.E.N., 1993. A biogeographic database of hermatypic corals. *Aust. Inst. Mar. Sci. Monogr. Ser.* 10, 1-433.

Veron, J.E.N., 1995. Corals in space and time: the biogeography and evolution of the Scleractinia. Cornell University Press, New York.

Veron, J.E.N., 2000. Corals of the World. Australian Institute of Marine Science, Townsville.

Veron, J.E.N., 2002. New species described in "Corals of the world". *Aust. Inst. Mar. Sci. Monogr. Ser.* 11, 1-206.

Veron, J.E.N., Pichon, M., 1976. Scleractinia of Eastern Australia. I Families Thamnasteriidae, Astrocoeniidae, Pocilloporidae. *Aust. Inst. Mar. Sci. Monogr. Ser.* 1, 1-86.

Veron, J.E.N., Pichon, M., 1980. Scleractinia of Eastern Australia, III: Families Agariciidae, Siderastreidae, Fungiidae, Oculinidae, Merulinidae, Mussidae, Pectiniidae,

Caryophylliidae, Dendrophylliidae. Aust. Inst. Mar. Sci. Monogr. Ser. 4, 1-433.

Veron, J.E.N., Pichon, M., 1982. Scleractinia of Eastern Australia. IV Family Porindae. Aust. Inst. Mar. Sci. Monogr. Ser. 5, 1-159.

Veron, J.E.N., Wallace, C.C., 1984. Scleractinia of Eastern Australia. V Family Acroporidae. Aust. Inst. Mar. Sci. Monogr. Ser. 9, 1-485.

Veron, J.E.N., Pichon, M., Wijsman-Best, M., 1977. Scleractinia of Eastern Australia. Part II. Families Faviidae, Trachyphylliidae. Aust. Inst. Mar. Sci. Monogr. Ser. 3, 1-233.

Veron, J.E.N., Devantier, L.M., Turak, E., Green, A.L., Kininmonth, S., Stafford-Smith, M., Peterson, N., 2009. Delineating the Coral Triangle. *Galaxea, J. Cor. Reef Stud.* 11, 91-100.

Volmer, S.V., Palumbi, S.R., 2002. Hybridization and the evolution of reef coral diversity. *Science* 296, 2023-2025.

Vollmer, S.V., Palumbi, S.R., 2004. Testing the utility of internally transcribed spacer sequences in coral phylogenetics. *Mol. Ecol.* 13, 2763-2772.

Wallace, C.C., 1999. Staghorn corals of the world: a revision of the genus *Acropora*. CSIRO Publication, Melbourne.

Wallace, C.C., Willis, B.L. 1994. Systematics of the coral genus *Acropora*: implications of new biological findings for species concepts. *Annu. Rev. Ecol. Syst.* 25, 237-262

Wallace, C.C., Done, B.J., Muir, P.R., 2012. Revision and catalogue of worldwide staghorn corals *Acropora* and *Isopora* (Scleractinia: Acroporidae) in the museum of Tropical Queensland. Queensland Museum, Townsville.

Wallace, C.C., Chen, C.A., Fukami, H., Muir, P.R., 2007. Recognition of separate genera within *Acropora* based on new morphological, reproductive and genetic evidence from *Acropora togianensis*, and elevation of the subgenus *Isopora* Studer, 1878 to genus (Scleractinia: Astrocoeniidae; Acroporidae). *Coral Reefs* 26, 231-239.

Wang, M., Sun, J., Li, J., Qiu, J.W., 2013. Complete mitochondrial genome of the brain coral *Platygyra carnosus*. *Mitochondrial DNA* 24, 194-195.

Wei, N.W.V., Wallace, C.C., Dai, C.F., Moothien Pillay, K.R., Chen, C.A., 2006. Analyses of the ribosomal internal transcribed spacers (ITS) and the 5.8S gene indicate that extremely high rDNA heterogeneity is a unique feature in the scleractinian coral genus *Acropora* (Scleractinia; Acroporidae). *Zool. Stud.* 45, 404-418.

Wells, J.W., 1937. Coral studies, Pt. 2. Five new genera of the Madreporaria. *Bull. Am. Paleontol.* 79, 8-15.

Wells, J.W., 1956. Scleractinia. In: R.C. Moore (Ed.), *Treatise on Invertebrate Paleontology, Part F: Coelenterata*. University of Kansas Press, Lawrence.

Wells, J.W., 1964. The recent solitary mussid scleractinian corals. *Zool. Med. Leiden* 39, 375-384.

Wells, J.W., 1968. Notes on Indo-Pacific scleractinian corals. V. A new species of *Alveopora* from New Caledonia. VI. Further notes on *Bantamia merletti* Wells. *Pac. Sci.* 22, 274-276.

White, T.J., Bruns, T., Lee, S., Taylor, J., 1990. Amplification and direct sequencing of fungal ribosomal RNA genes for phylogenetics. In: M.A. Innis, D.H. Gelfand, J.J. Sninsky, and T.J. White (Eds.), *PCR Protocols: A Guide to Methods and Application*. Academic

Press, San Diego.

Willis, B.L., van Oppen, M.J.H., Miller, D.J., Vollmer, S.V., Ayre, D.J., 2006. The role of hybridization in the evolution of reef corals. *Annu. Rev. Ecol. Evol. Syst.* 37, 489-517.

Willis, B.L., Babcock, R.C., Harrison, P.L., Oliver, J.K., 1985. Patterns in the mass spawning of corals on the Great Barrier Reef from 1981 to 1984. *Proc. 5th. Int. Coral Reef Symp.* 4, 343-48

Wijsman-Best, M., 1976. Biological results of the Snellius Expedition. XXVII. Faviidae collected by the Snellius expedition. II. The genera *Favites*, *Goniastrea*, *Platygyra*, *Oulophyllia*, *Leptoria*, *Hydnophora* and *Caulastrea*. *Zool. Meded.* 50, 45- 63.

Wijsman-Best, M., 1977. Indo-Pacific coral species belonging to the subfamily Montastreinae Vaughan & Wells, 1943 (Scleractinia-Coelenterata) Part I. The genera *Montastrea* and *Plesiastrea*. *Zool. Meded.* 52, 81-97.

Zlatarski, V.N., Estalella, N.M., 1982. Les Sclèractiniaires de Cuba. Academie Bulgare des Sciences, Sofia.

– ANNEXES –

ANNEX I

List of publications arising from this PhD Thesis

At the time of thesis submission, three papers describing the research results of Chapters 2, 3, and 5, were published, two paper describing the research results of Chapters 4 and 6 in press, one paper describing the research results of Chapter / is in preparation and will be submitted by the end of February 2015, and other manuscripts are currently/will be in preparation. Among these works, a complete taxonomic revision of the family Lobophylliidae is currently in preparation for submission to *Zoologica Journal of the Linnean Society*. Details of each manuscript and talks presented during my PhD candidature are provided below:

Published manuscripts

- **Arrigoni, R.**, Stefani, F., Pichon, M., Galli, P., Benzoni, F., 2012. Molecular phylogeny of the Robust clade (Faviidae, Mussidae, Merulinidae, and Pectiniidae): An Indian Ocean perspective. *Mol. Phylogenet. Evol.* 65, 183–193.
- **Arrigoni, R.**, Richards, Z.T., Chen, C.A., Baird, A.H., Benzoni, F., 2014. Phylogenetic relationships and taxonomy of the coral genera *Australomussa* and *Parascalymia* (Scleractinia, Lobophylliidae). *Contrib. Zool.* 83, 195–215.
- **Arrigoni, R.**, Terraneo, T.I., Galli, P., Benzoni, F., 2014. Lobophylliidae (Cnidaria, Scleractinia) reshuffled: pervasive non-monophyly at genus level. *Mol. Phylogenet. Evol.* 73, 60–64.
- **Arrigoni, R.**, Vacherie, B., Benzoni, F., Barbe, V., in press. The complete mitochondrial genome of *Acanthastrea maxima* (Cnidaria, Scleractinia, Lobophylliidae). Mitochondrial DNA. DOI: 10.3109/19401736.2014.926489.

- **Arrigoni, R.,** Berumen, M.L., Terraneo, T.I., Caragnano, A., Bouwmeester, J., Benzoni, F., in press. Forgotten in the taxonomic literature: resurrection of the scleractinian coral genus *Sclerophyllia* (Scleractinia, Lobophylliidae) from the Arabian Peninsula and its phylogenetics relationships. Syst. Biodiver. DOI: 10.1080/14772000.2014.978915.

Presentations at congresses and symposia

- **Arrigoni, R.,** 2012. The biogeographic perspective: Intraspecific divergences between Indian and Pacific Oceans. Presented at *Scleractinian Systematics Working Group meeting*, SSWG 2012, July 6-8, Townsville, Queensland, Australia.
- **Arrigoni, R.,** Benzoni, F., 2013. Evolution of the scleractinian coral genera *Echinophyllia* and *Oxypora* explained by genetic analyses. Presented at *International Conference on Coelenterate Biology*, ICCB 2013, December 1-5, Eilat, Israel.

ANNEX II

Publications arising during my PhD Candidature not directly related to Thesis

During his PhD candidature, the candidate co-authored 9 papers in peer-reviewed international journals and was first author for one of these:

Published manuscripts

- **Arrigoni, R.**, Kitano, Y.F., Stolarski, J., Hoeksema, B.W., Fukami, H., Stefani, F., Galli, P., Montano, S., Castoldi, E., Benzoni, F., 2014. A phylogeny reconstruction of the Dendrophylliidae (Cnidaria, Scleractinia) based on molecular and micromorphological criteria, and its ecological implications. *Zool. Scr.* 43, 661-688.
- Benzoni, F., **Arrigoni, R.**, Stefani, F., Stolarski, J., 2012. Systematics of the coral genus *Craterastrea* (Cnidaria, Anthozoa, Scleractinia) and description of a new family through combined morphological and molecular analyses. *Syst. Biodiver.* 10, 417-433.
- Benzoni, F., **Arrigoni, R.**, Waheed, Z., Stefani, F., Hoeksema, B.W., 2014. Phylogenetic relationships and revision of the genus *Blastomussa* (Cnidaria: Anthozoa: Scleractinia) with description of a new species. *Raffles B. Zool.* 62, 358-378.
- Montano, S., **Arrigoni, R.**, Pica, D., Maggioni, D., Puce, S., 2015. New insights into the symbiosis between *Zanclaea* (Cnidaria, Hydrozoa) and scleractinians. *Zool. Scr.* 44, 92-105.
- Benzoni, F., **Arrigoni, R.**, Stefani, F., Reijnen, B.T., Montano, S., Hoeksema, B.W., 2012. Phylogenetic position and taxonomy of *Cycloseris explanulata* and *C. wellsi* (Scleractinia: Fungiidae): lost mushroom corals find their way home. *Contrib. Zool.* 81, 125-146.
- Kitano, Y.F., Benzoni, F., **Arrigoni, R.**, Shirayama, Y., Wallace, C.C., Fukami, H., 2014. A phylogeny of the family Poritidae (Cnidaria,

Scleractinia) based on molecular and morphological analyses. PLoS ONE 9, e98406.

- Terraneo, T.I., Berumen, M.L., **Arrigoni, R.**, Waheed, Z., Bouwmeester, J., Caragnano, A., Stefani, F., Benzoni, F., 2014. *Pachyseris inattesa* sp. n. (Cnidaria, Anthozoa, Scleractinia): a new reef coral species from the Red Sea and its phylogenetic relationships. Zookeys 433, 1-30.
- Huang, D., Benzoni, F., **Arrigoni, R.**, Baird, A.H., Berumen, M.L., Bouwmeester, J., Chou, L.M., Fukami, H., Licuanan, W.Y., Lovell, E.R., Meier, R., Todd, P.A., Budd, A.F., 2014. Towards a phylogenetic classification of reef corals: the Indo-Pacific genera *Merulina*, *Goniastrea* and *Scapophyllia* (Scleractinia, Merulinidae). Zool. Scr. 43, 531-548.
- Montano, S., Seveso, D., Strona, G., **Arrigoni, R.**, Galli, P., 2012. *Acropora muricata* mortality associated with extensive growth of *Caulerpa racemosa* in Magoodhoo island, Republic of Maldives. Coral Reefs 31, 793.

Presentations at congresses and symposia

- **Arrigoni, R.**, Benzoni, F., Stefani, F., Galli, P., Montano, S., 2012. Evolutionary relationships within the family Dendrophylliidae based on morpho-molecular evidence. Presented at *12th International Coral Reef Symposium*, ICRS 2012, July 9-13, Cairns, Queensland, Australia.
- Benzoni, F., **Arrigoni, R.**, Stefani, F., 2012. Once were Faviidae: unexpected robust coral clades explained by morphology. Presented at *12th International Coral Reef Symposium*, ICRS 2012, July 9-13, Cairns, Queensland, Australia.
- Montano, S., Seveso, D., Strona, G., **Arrigoni, R.**, Galli, P., 2012. Coral diseases in the central Republic of Maldives. Presented at *12th International Coral Reef Symposium*, ICRS 2012, July 9-13, Cairns, Queensland, Australia.

ANNEX III

Grants and Internships during the PhD candidature

During my PhD candidature, I was awarded two grants that let me to work abroad for three months in 2013, the SYNTHESYS research grant from European Union and the Summer Program in Taiwan from National Science Council of Taiwan. Moreover, I was hosted for a three months period at the King Abdullah University of Science and Technology (Thuwal, Kingdom of Saudi Arabia) in 2013. Details and a brief description of the work conducted in the frame of each grant and internship are provided below:

- **February 2013:** SYNTHESYS research grant (NL-TAF-3235) from the European Commission's FPVII programme, at **Naturalis Biodiversity Center** (Leiden, the Netherlands), under the supervision of **Dr. Bert W Hoeksema**, Head of the department of Marine Zoology. Project title: *“Molecular phylogeny of the coral family Lobophylliidae (Cnidaria, Scleractinia) explained by morphological analyses of museum collections”*.

I worked on the Coelenterata collection of the museum where I could study and image approximately 150 specimens ascribed to the family Lobophylliidae in order to gain first hand experience of the variability of traditional macromorphological structures within and between lobophylliid species. Moreover, I observed and analyzed numerous rapresentatives of the closely related families Merulinidae and Mussidae. Finally I learnt from fruitful discussions with BW Hoekesema and each of the other his dutch colleagues every day during my visit at Naturalis Biodiversity Center.

- **July – August 2013:** Summer Program in Taiwan 2013 for Italian Graduate Students from the National Science Council of Taiwan, at **Biodiversity Research Center, Academia Sinica** (Taipei, Taiwan), under

the supervision of Prof. **Chaolun Allen Chen**. Project title: “*Exploring phylogenetic relationships within the Lobophylliidae*”.

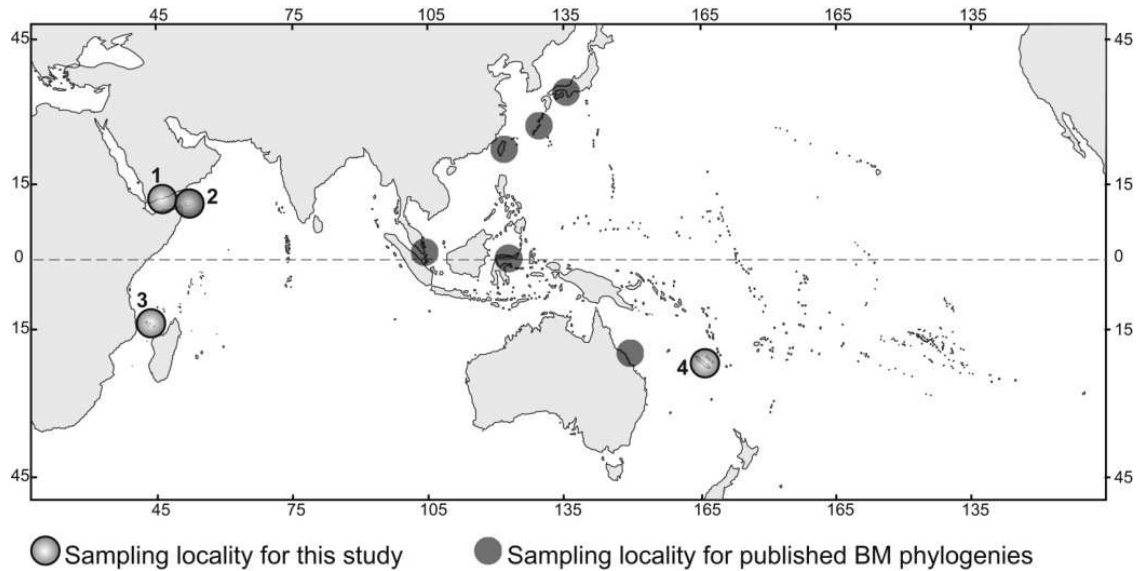
During July and August 2013 I’ve been at Biodiversity Research Center of Academia Sinica in Taipei (Taiwan) thank to the Summer Program in Taiwan 2013 for Italian Graduate Students from the National Science Council of Taiwan. Under the supervision of Prof. Chaolun Allen Chen, I worked in his hi-tech laboratory with the help of several people of his group, such as Silvia, Shashank, Chai-Hsia, Stephane, Vianney, and many others. I had the opportunity to investigate many molecular aspects of the family Lobophylliidae, analyzing several molecular markers in order to explore the phylogenetic relationships between species within each molecular clades of the Lobophylliidae.

- **March 2013 and October - November 2013:** internship at **Red Sea Research Center, King Abdullah University of Science and Technology** (Thuwal, Kingdom of Saudi Arabia) in the frame of “Biodiversity in the Saudi Arabian Red Sea” project, under the supervision of **Prof. Michael L Berumen**. Project title: “*Biodiversity of the Lobophylliidae in the Saudi Arabian Red Sea*”.

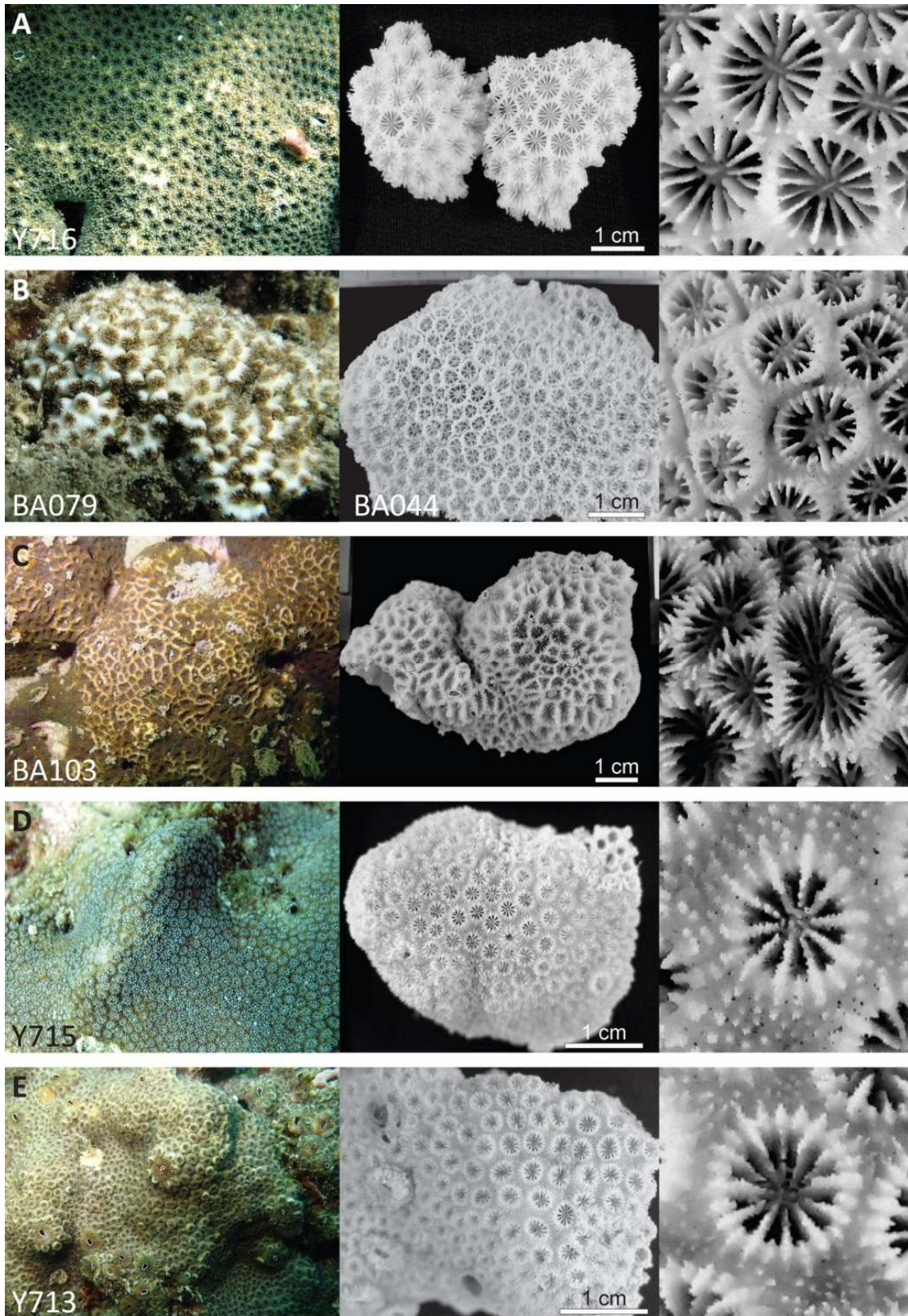
During March 2013 and October – November 2013 I visited two times the Red Sea Research Center of King Abdullah University of Science and Technology in Thuwal (Kingdom of Saudi Arabia). In the frame of “Biodiversity in the Saudi Arabian Red Sea” project organized by Prof. Michael L Berumen with University of Milano-Bicocca as scientific partner, I worked at Reef Ecology Lab of Prof. ML Berumen focusing my attention on the scleractinian corals collection sampled by my supervisor, Dr. Francesca Benzoni, along the coast of the Saudi Arabian Red Sea. I had the opportunity to molecularly analyzed the interesting and poor-studied corals fauna of this biogeographic region using the outstanding facilities of King Abdullah University of Science and Technology.

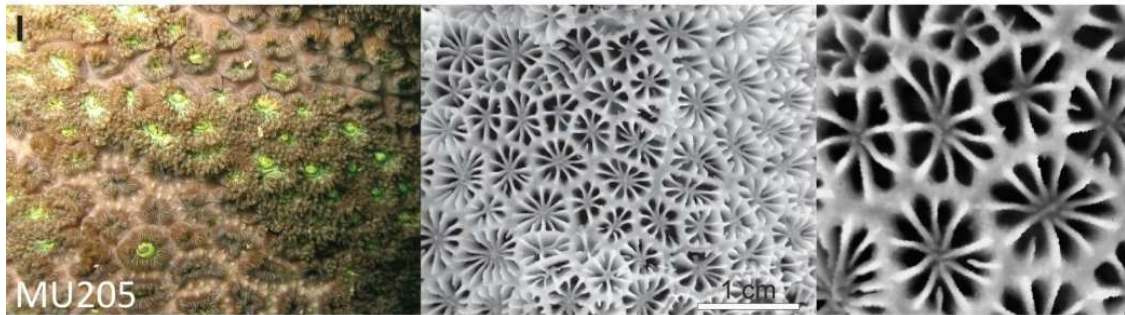
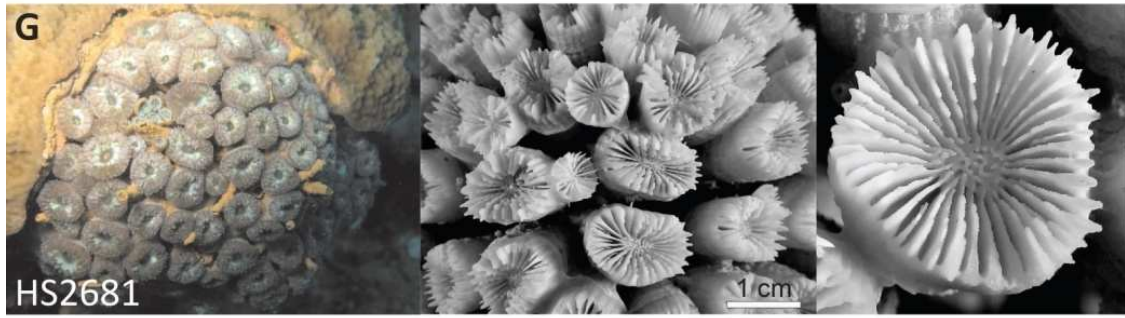
ANNEX IV

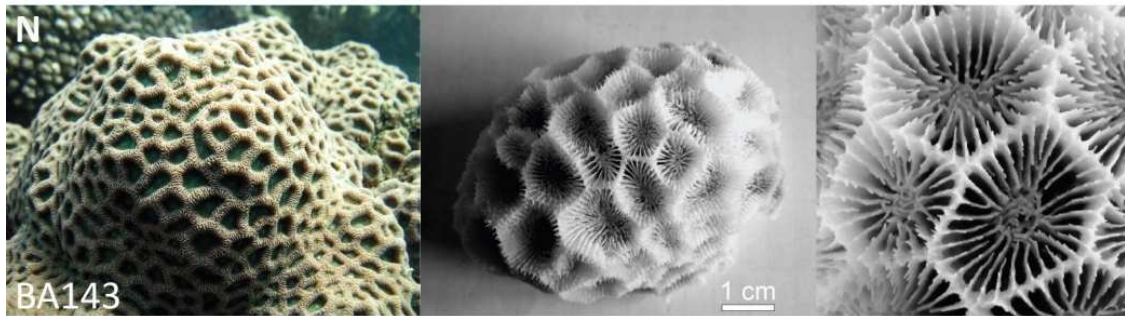
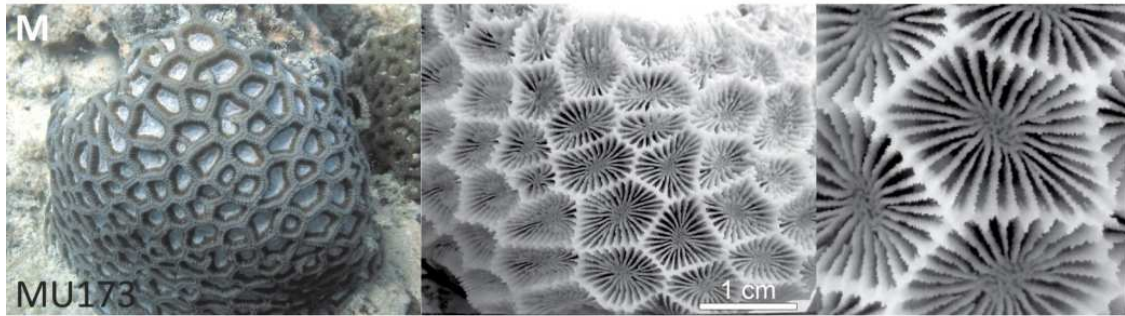
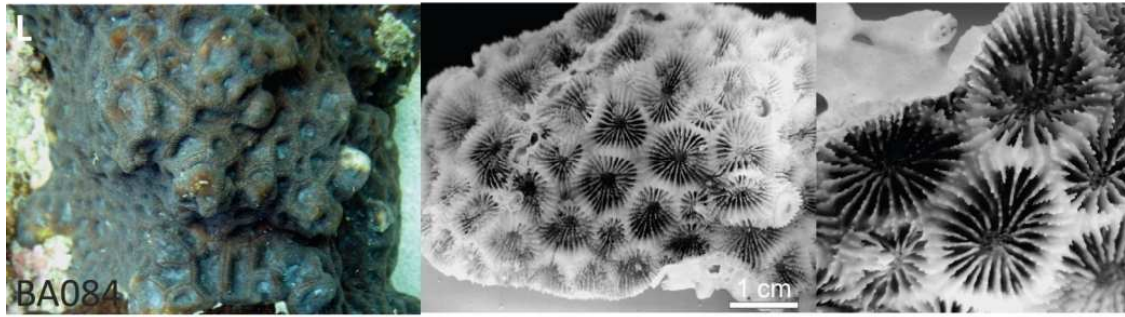
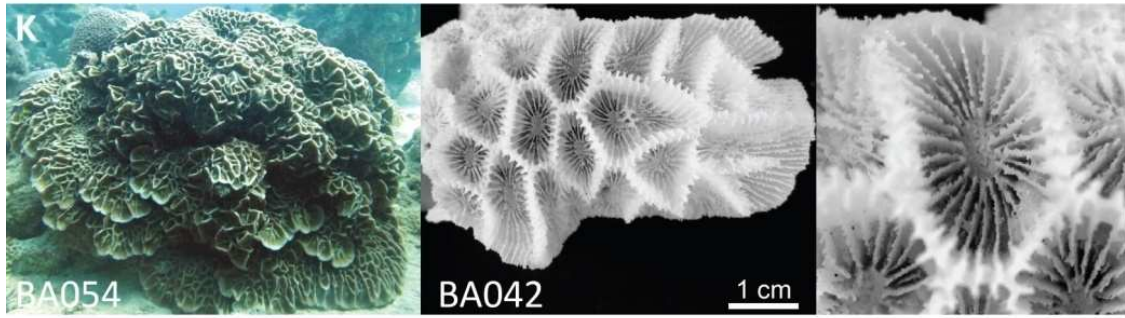
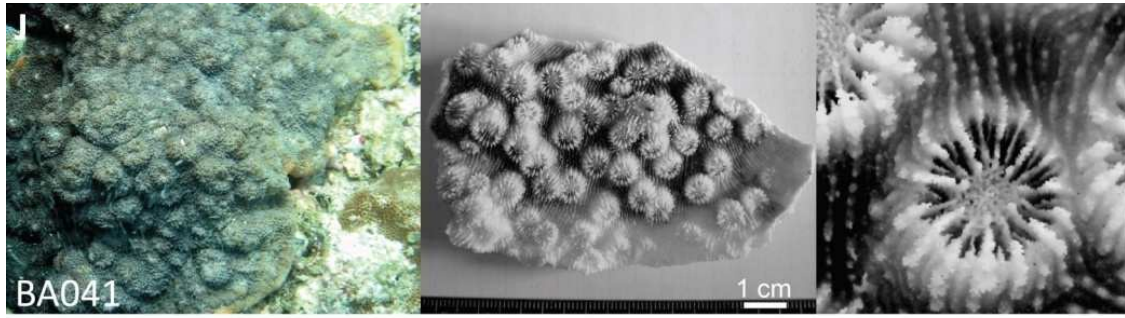
List of Appendices

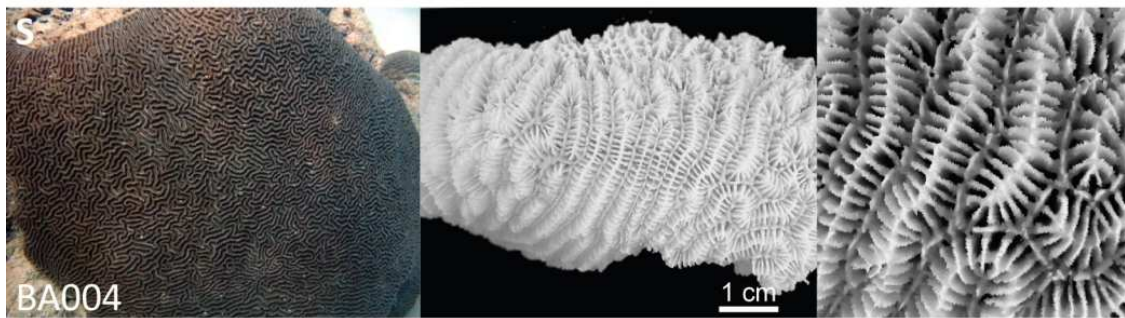
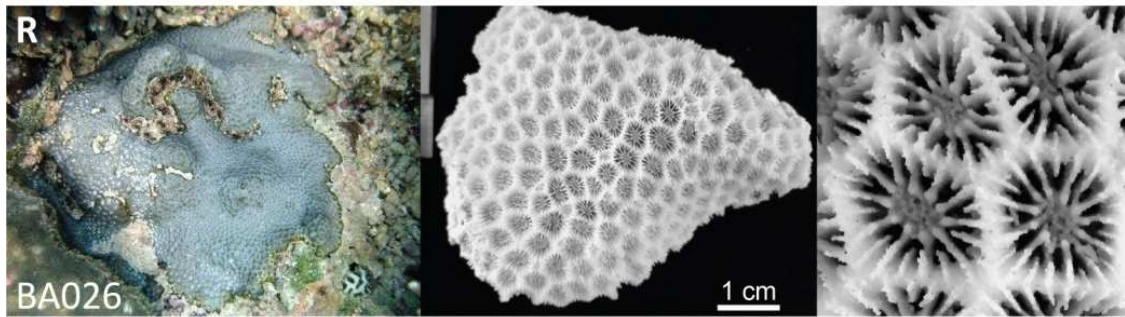
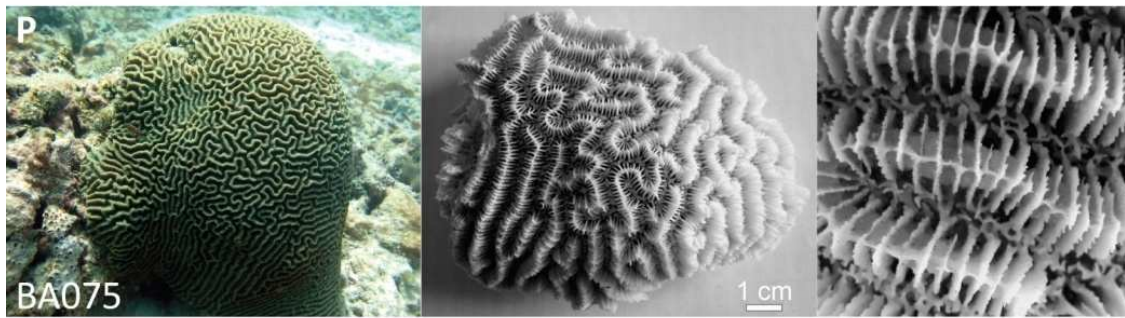
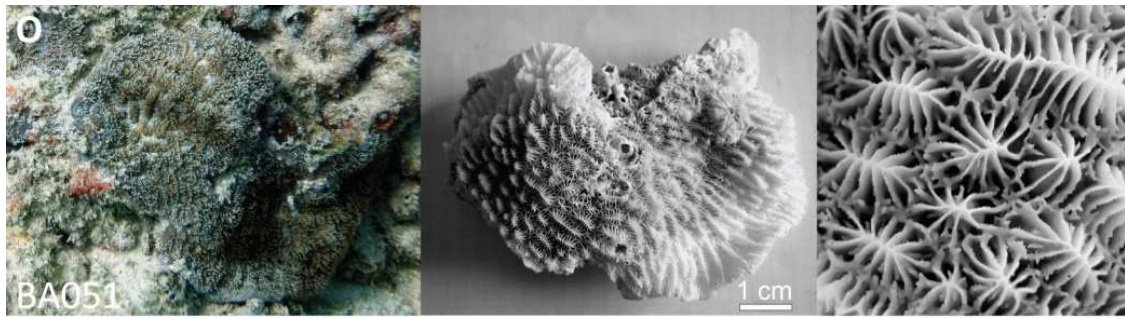


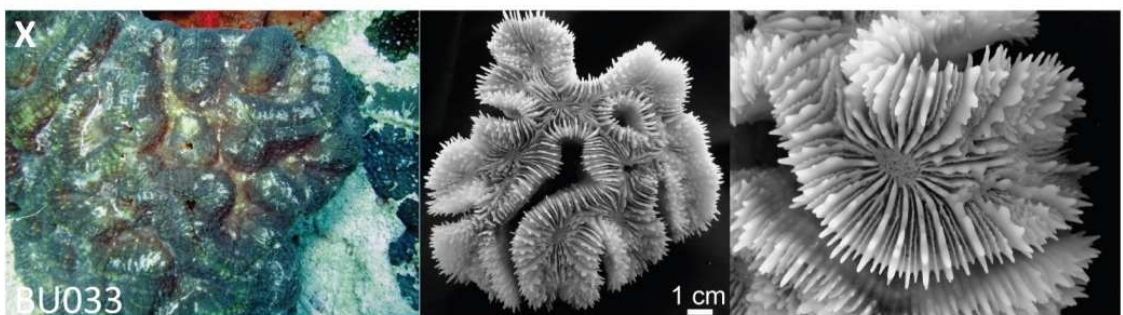
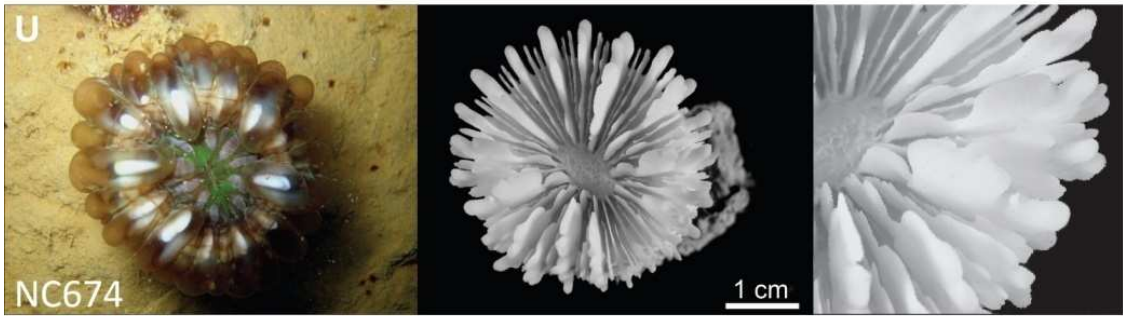
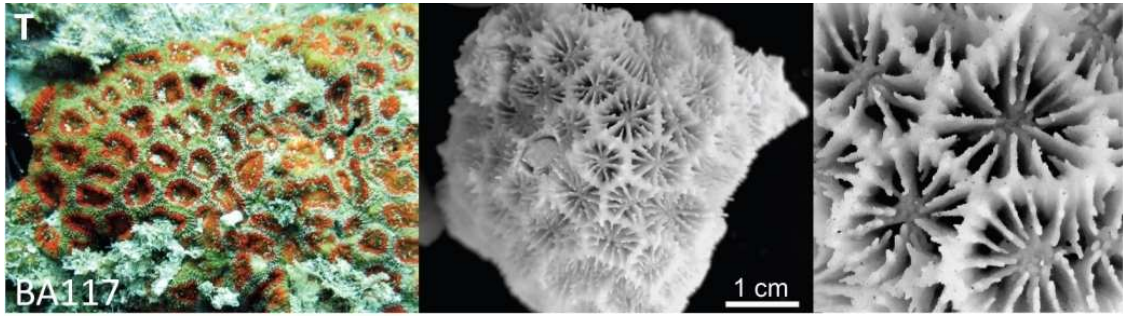
Appendix 2.1. Map of the Indo-Pacific showing sampling localities for this study (numbered from 1 to 4) and sampling localities of the “Bigmessidae” samples included in published phylogenies (Fukami et al., 2008; Huang et al., 2009; Kitahara et al., 2010; Huang et al., 2011; Benzoni et al., 2011). 1 = Yemen, north-western Gulf of Aden coast, 2 = Socotra Island; 3 = Mayotte Island; 4 = New Caledonia. Geographical coordinates: Kamaran (Lat. 15°22.82' N, Long. 42°36.27' E), Aden (Lat. 12°46.60' N, Long. 44°56.28' E), Balhaf (Lat. 13°58.12' N, Long. 48°10.66' E), Bir Ali (Lat. 13°59.48' N, Long. 48°19.67' E), Burum (Lat. 14°18.76' N, Long. 48°59.84' E), Al Mukallah (Lat. 14°30.52' N, Long. 49°09.82' E), Socotra (Lat. 12°40.35' N, Long. 54°11.75' E), Mayotte Island (Lat. 12°38.48' S, Long. 45°02.74' E), Côte Oubliée (Lat. 21°55.78 S, Long. 166°41.11' E).

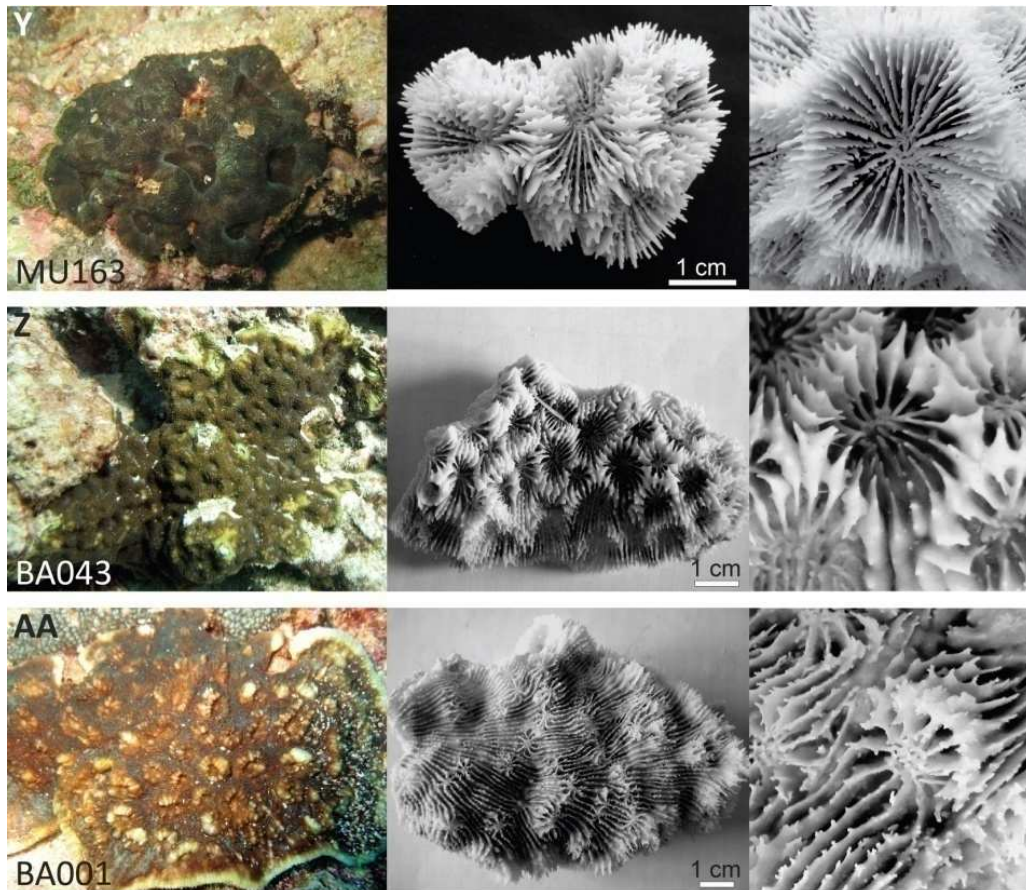




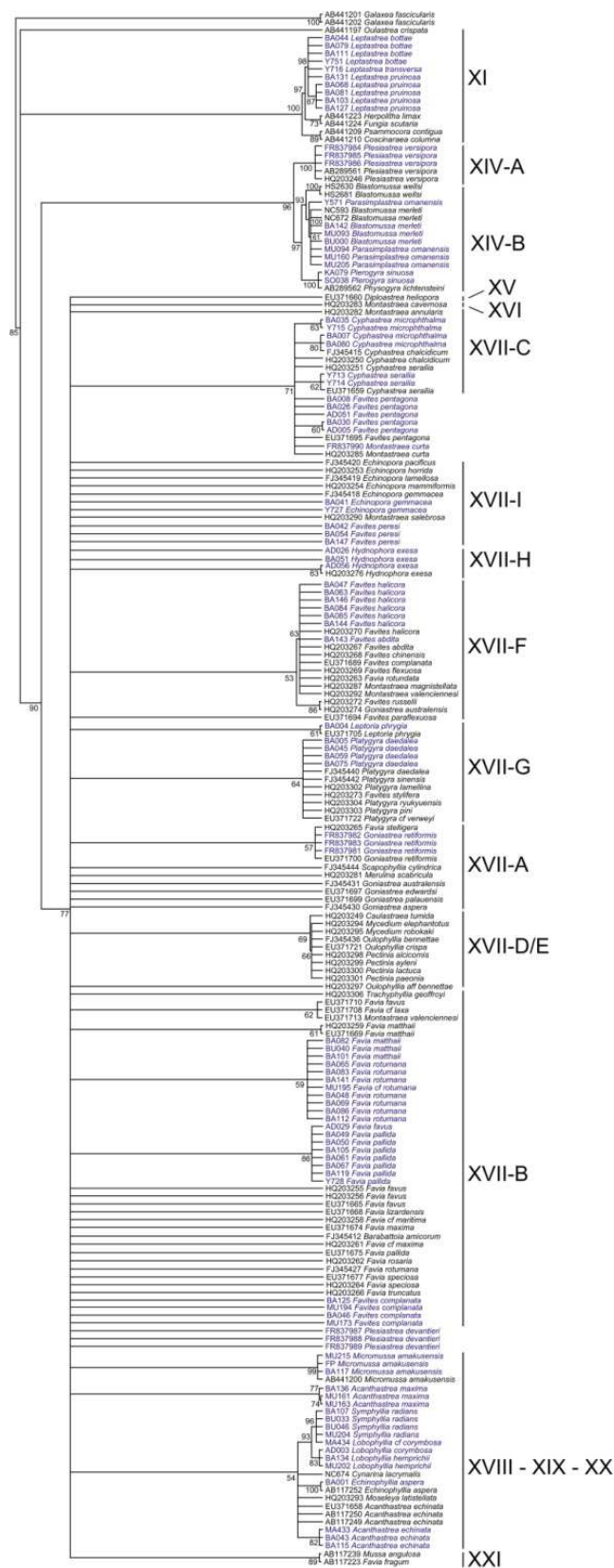




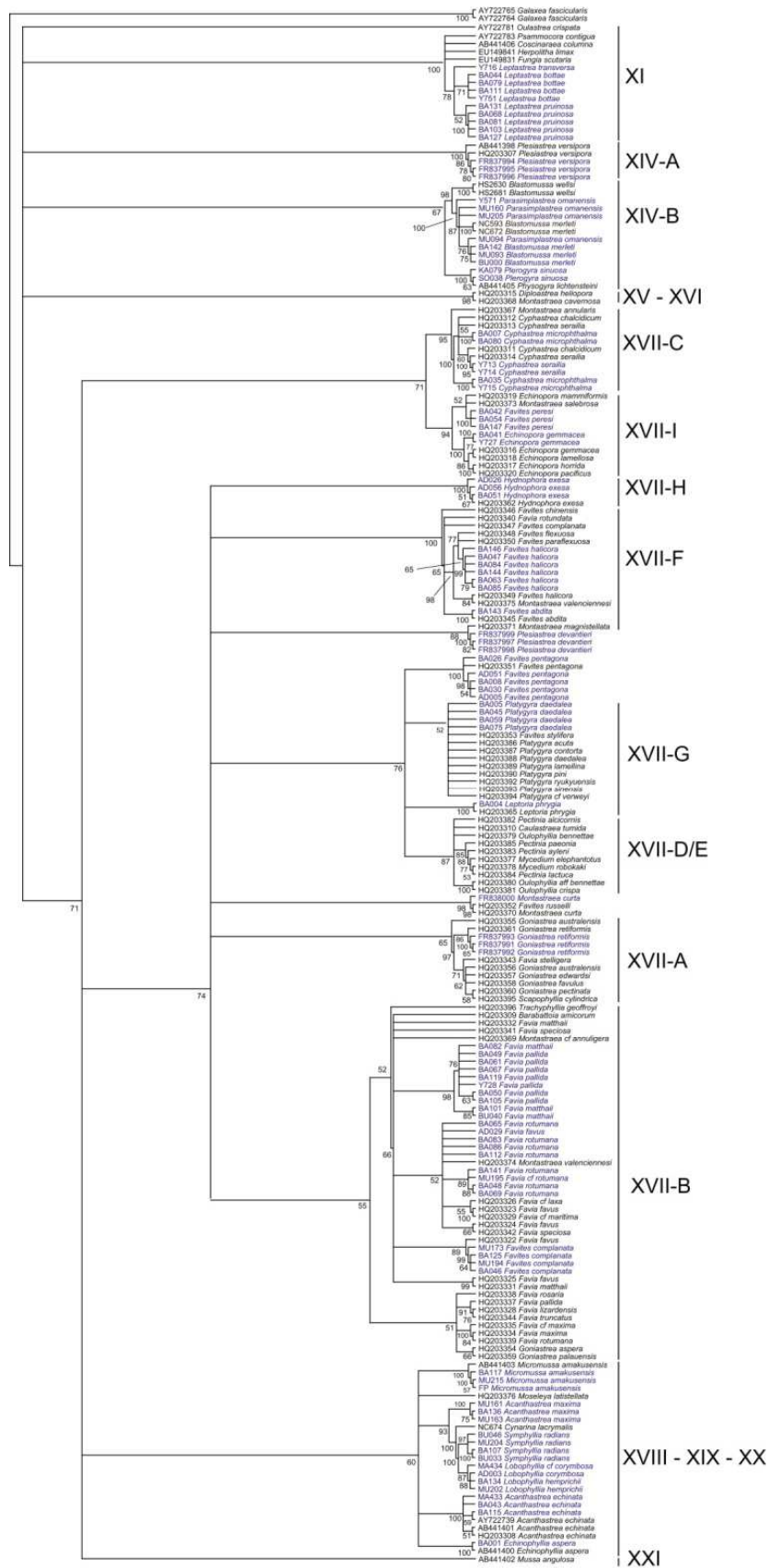




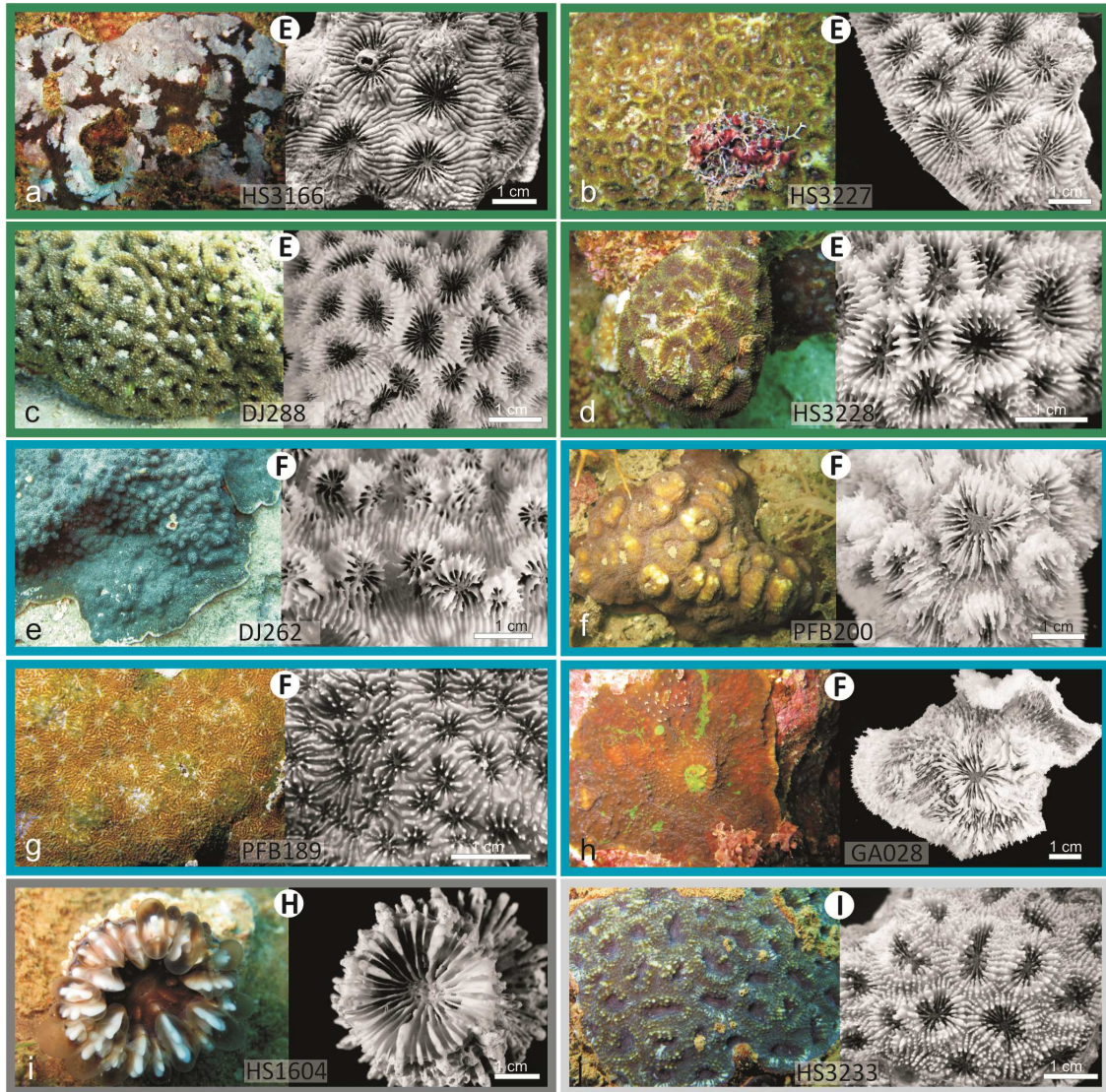
Appendix 2.2. *In-vivo*, corallum, and detail of corallites morphology of the species with Indian Ocean (IO) or Indo-Pacific (IP) analyzed in this study. A) *Leptastrea transversa* (IP); B) *L. bottae* (IP); C) *L. pruinosa* (IP); D) *Cyphastrea microphthalma* (IP); E) *C. serailia* (IP); F) *Plerogyra sinuosa* (IP); G) *Blastomussa wellsii* (IP); H) *B. merleti* (IP); I) *Parasimplastrea omanensis* (IO); J) *Echinopora gemmacea* (IP); K) *Favites peresi* (IO); L) *Favites halicora* (IP); M) *F. complanata* (IP); N) *F. abdita* (IP); O) *Hydnophora exesa* (IP); P) *Platygyra daedalea* (IP); Q) *Favia favius* (IP); R) *Favites pentagona* (IP); S) *Leptoria phrygia* (IP); T) *Micromussa amakusensis* (IP); U) *Cynarina lacrymalis* (IP); V) *Lobophyllia hemprichii* (IP); W) *Lobophyllia corymbosa* (IP); X) *Symphyllia radians* (IP); Y) *Acanthastrea maxima* (IO); Z) *A. echinata* (IP); AA) *Echinophyllia aspera* (IP). Please refer to Veron et al. (1977) and Veron (2000) for the diagnostic morphologic characters that correspond with each of these species. When all images refer to the same specimen its code is shown on the bottom left corner of the *in situ* image. In case images refer to different specimens this is indicated. Corallite detail on the right hand side always refer to the corallum shown in the centre image. For images of *Favia pallida* (IP), *F. rotumana* (IP), and *F. matthaii* (IP) refer to Fig. 2. For images of *Goniastrea retiformis* (IP) and *Plesiastrea versipora* (IP) refer to Benzoni et al. (2011). Sampling localities: Y = Balhaf (Gulf of Aden, Yemen); BA = Bir Ali (Gulf of Aden, Yemen); AD= Aden (Gulf of Aden, Yemen); BU = Burum (Gulf of Aden, Yemen); MU and FP = Al Mukallah (Gulf of Aden, Yemen); SO = Socotra Island (Indian Ocean, Yemen); MA = Mayotte Island (Indian Ocean, France); KA = Kamaran Island (Red Sea, Yemen); SO = Socotra Island (Gulf of Aden Yemen); NC and HS = Côte Oubliée (New Caledonia).



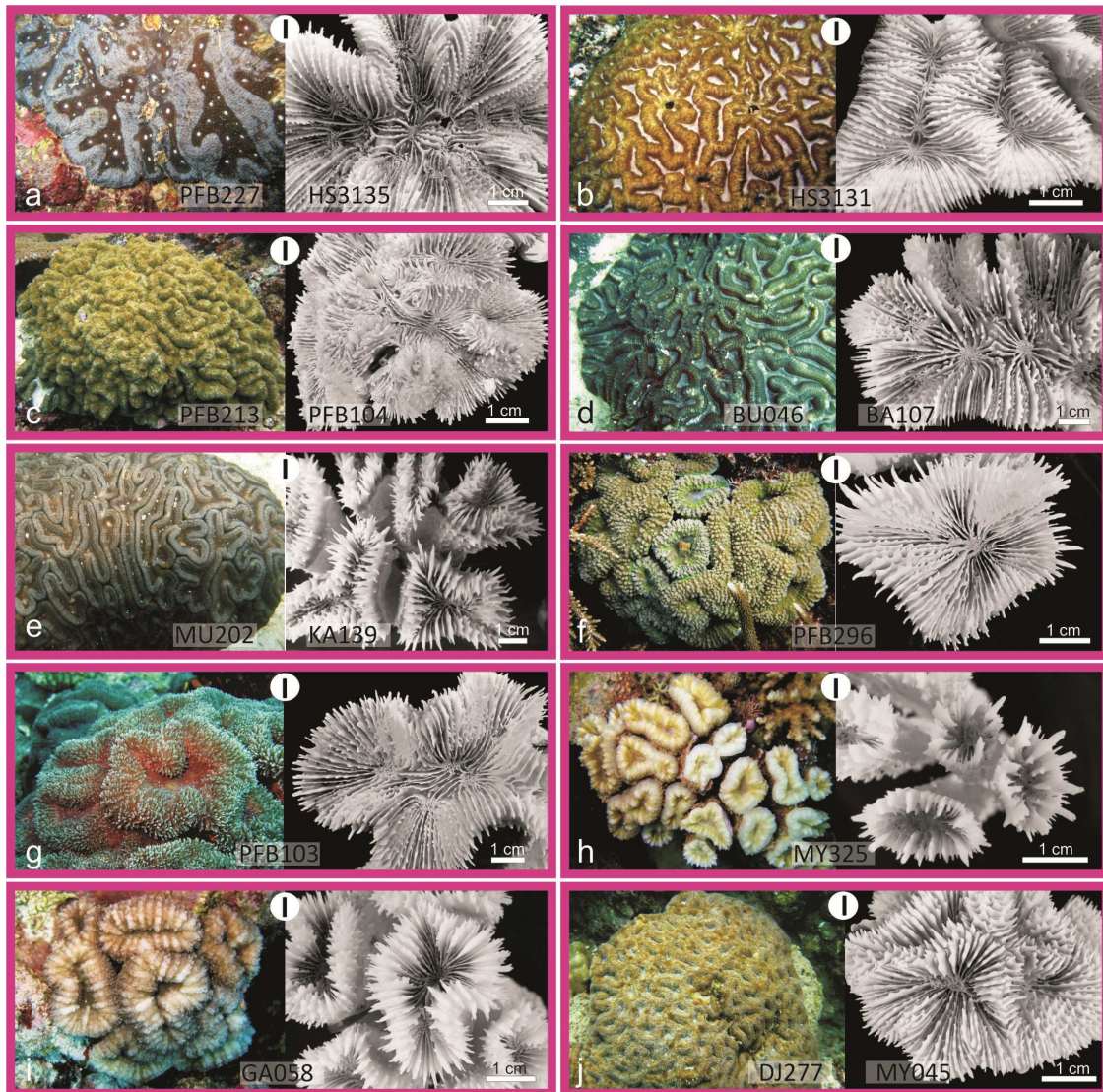
Appendix 2.3. Maximum Parsimony tree based on COI dataset. Numbers are bootstrap values. Clade numbers and sub-clade codes are the same ones reported respectively by Fukami et al. (2008) and Huang et al. (2011). Values <50% are not shown. IO samples are evidenced in blue and PO samples in black.



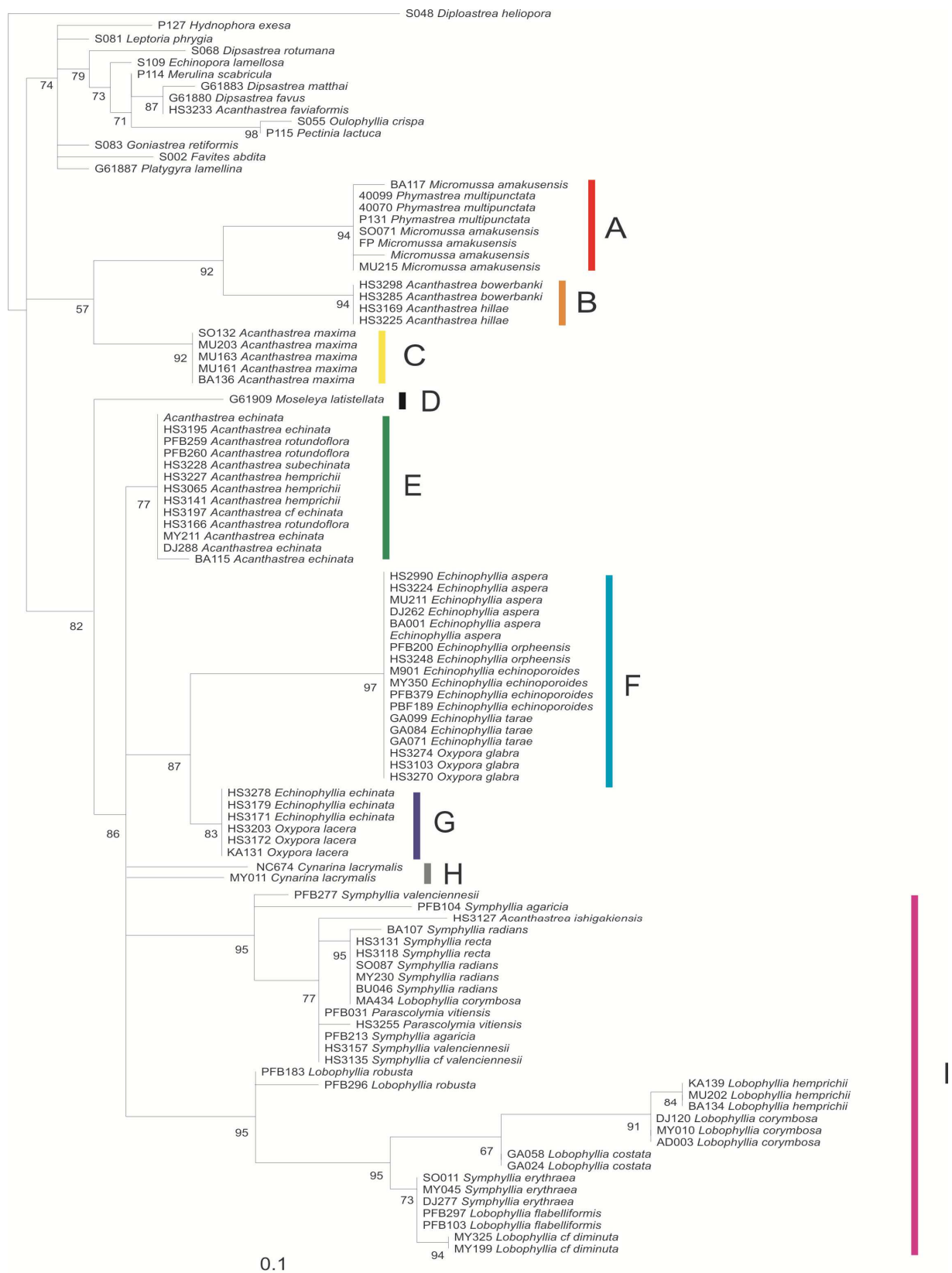
Appendix 2.4. Maximum Parsimony tree based on rDNA dataset. Numbers are bootstrap values. Clade numbers and sub-clade codes are the same ones reported respectively by Fukami et al. (2008) and Huang et al. (2011). Values <50% are not shown. IO samples are evidenced in blue and PO samples in black.



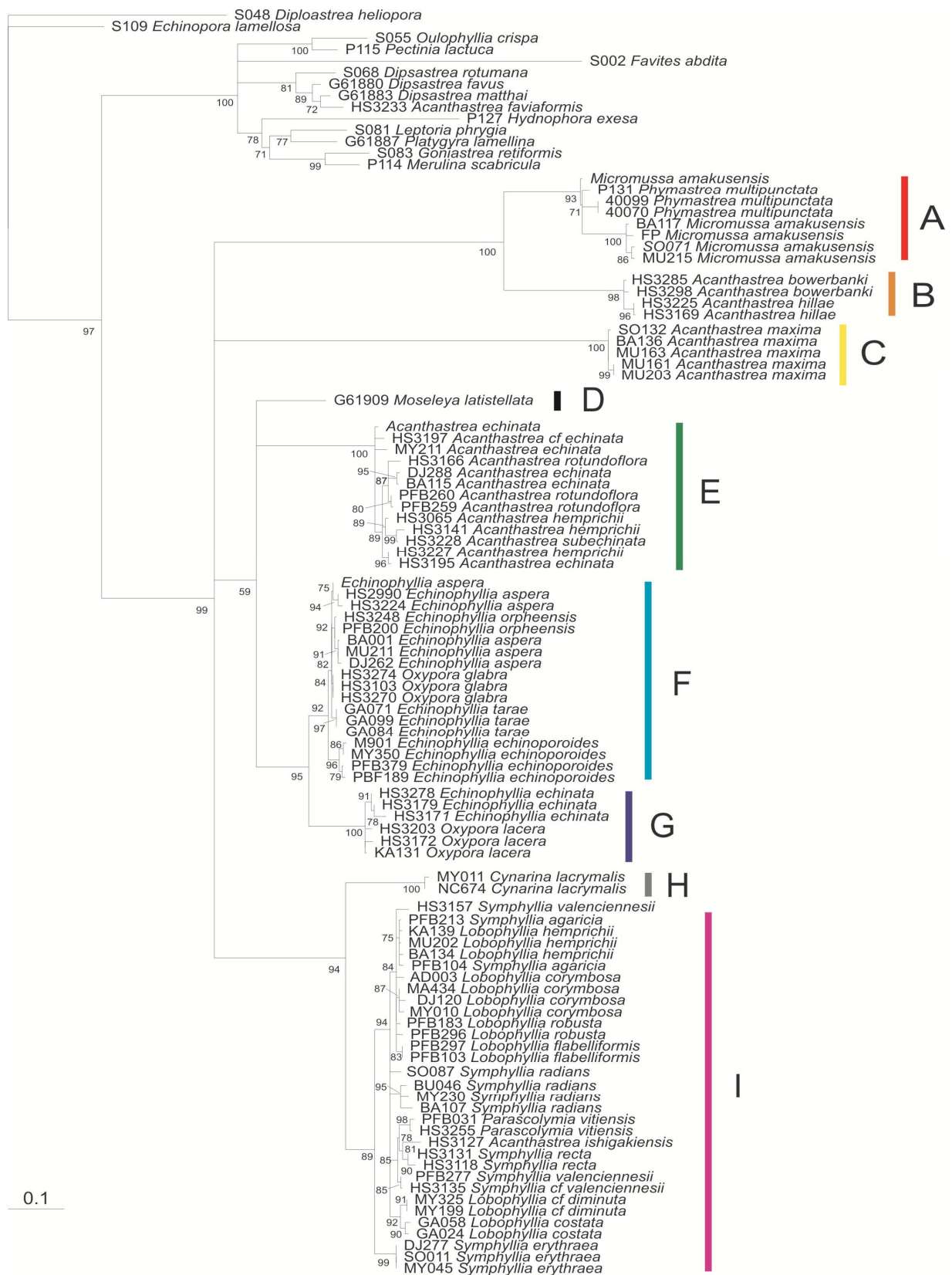
Appendix 3.1. *In situ* and corallum of species examined in this study: a) *Acanthastrea rotundoflora* from type locality (New Caledonia); b) *A. hemprichi*; c) *A. echinata*; d) *A. subechinata*; e) *Echinophyllia aspera* from the Indian Ocean; f) *E. orpheensis*; g) *E. echinoporoides*; h) *E. tarae*; i) *Cynarina lacrymalis*; j) *A. faviaformis*. Colour codes and capital letters in white circles refer to clades in Fig. 3.1. Specimen code on the images.



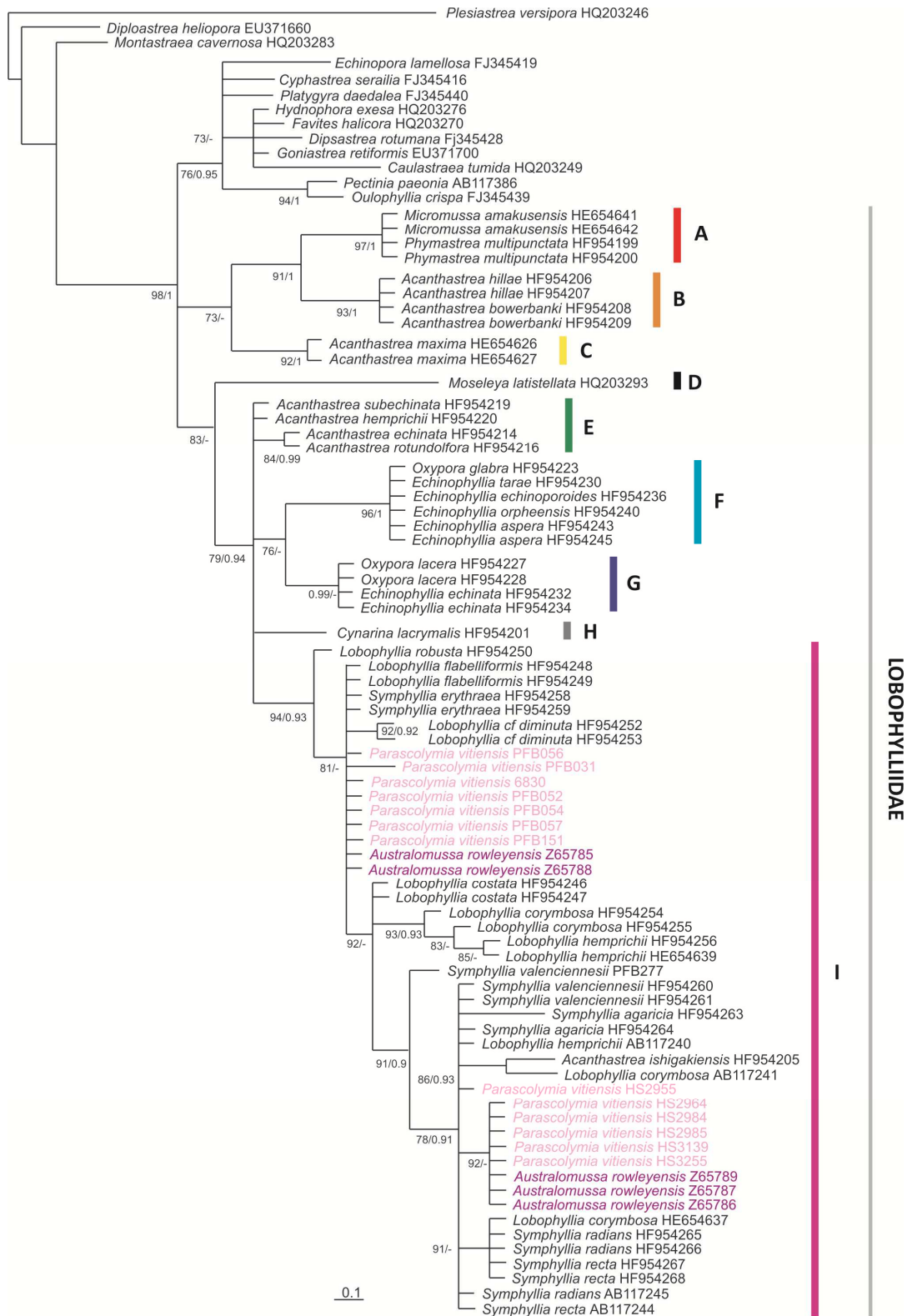
Appendix 3.2. *In situ* and corallum of species examined in this study: a) *Symphyllia valenciennesi*; b) *S. recta*; c) *S. agaricia*; d) *S. radians*; e) *Lobophyllia hemprichii*; f) *L. robusta*; g) *L. flabelliformis*; h) *L. cf. diminuta*; i) *L. costata*; j) *S. erythraea*. Colour codes and capital letters in white circles refer to clades in Fig. 3.1. Specimen code on the image.



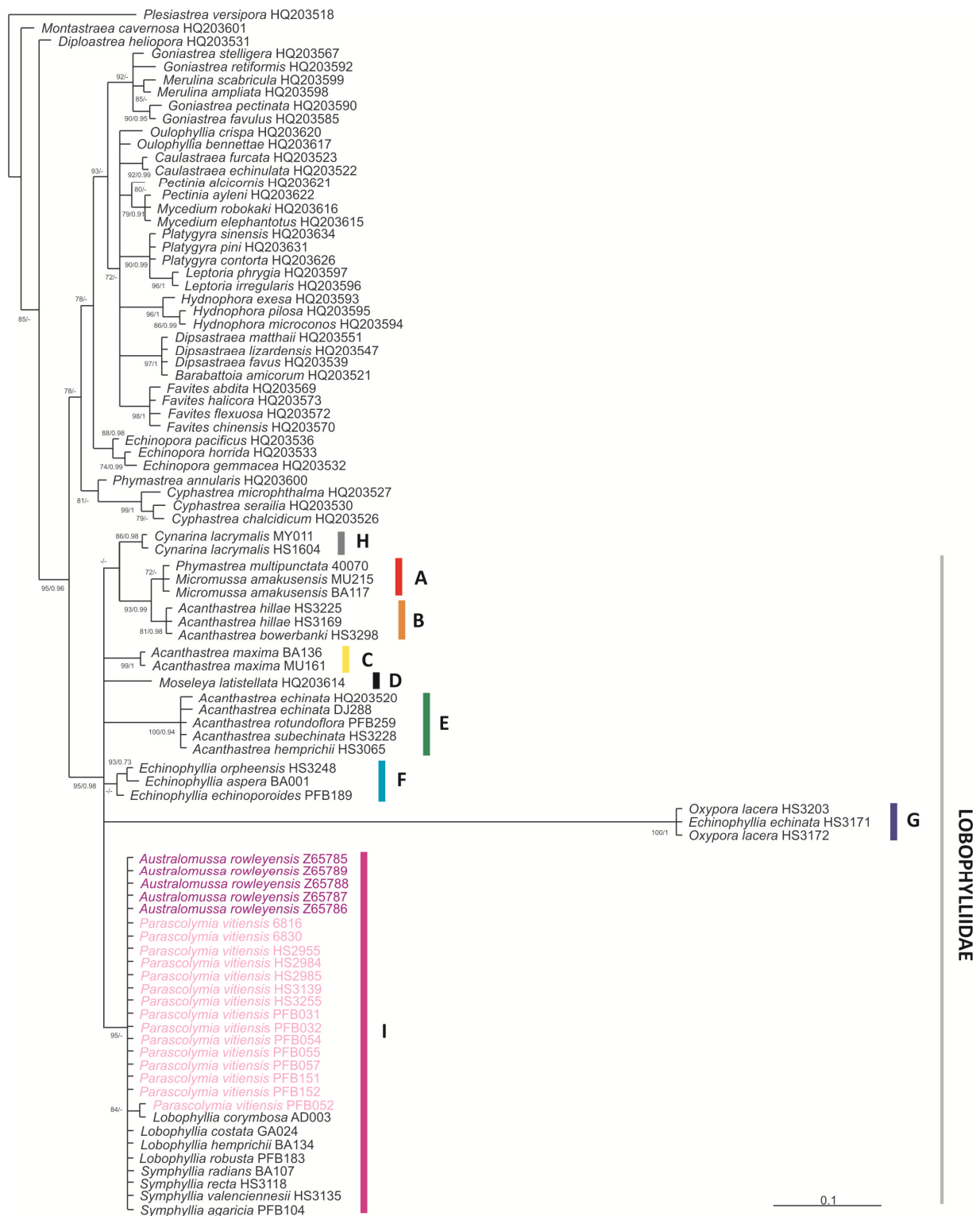
Appendix 3.3. ML tree based on COI dataset. Node values are ML SH-like support (> 70%).



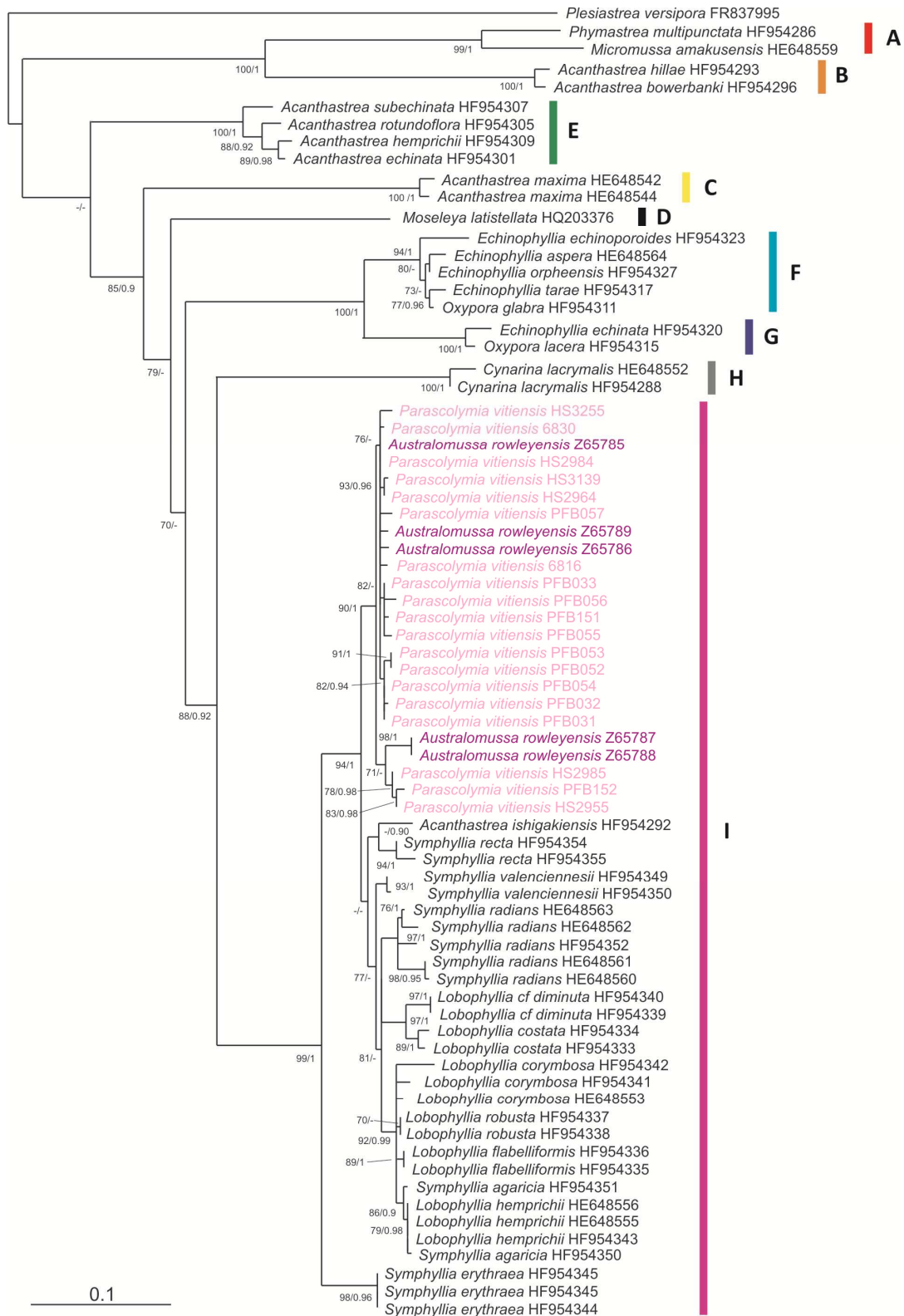
Appendix 3.4. ML tree based on rDNA dataset. Node values are ML SH-like support (>70%).



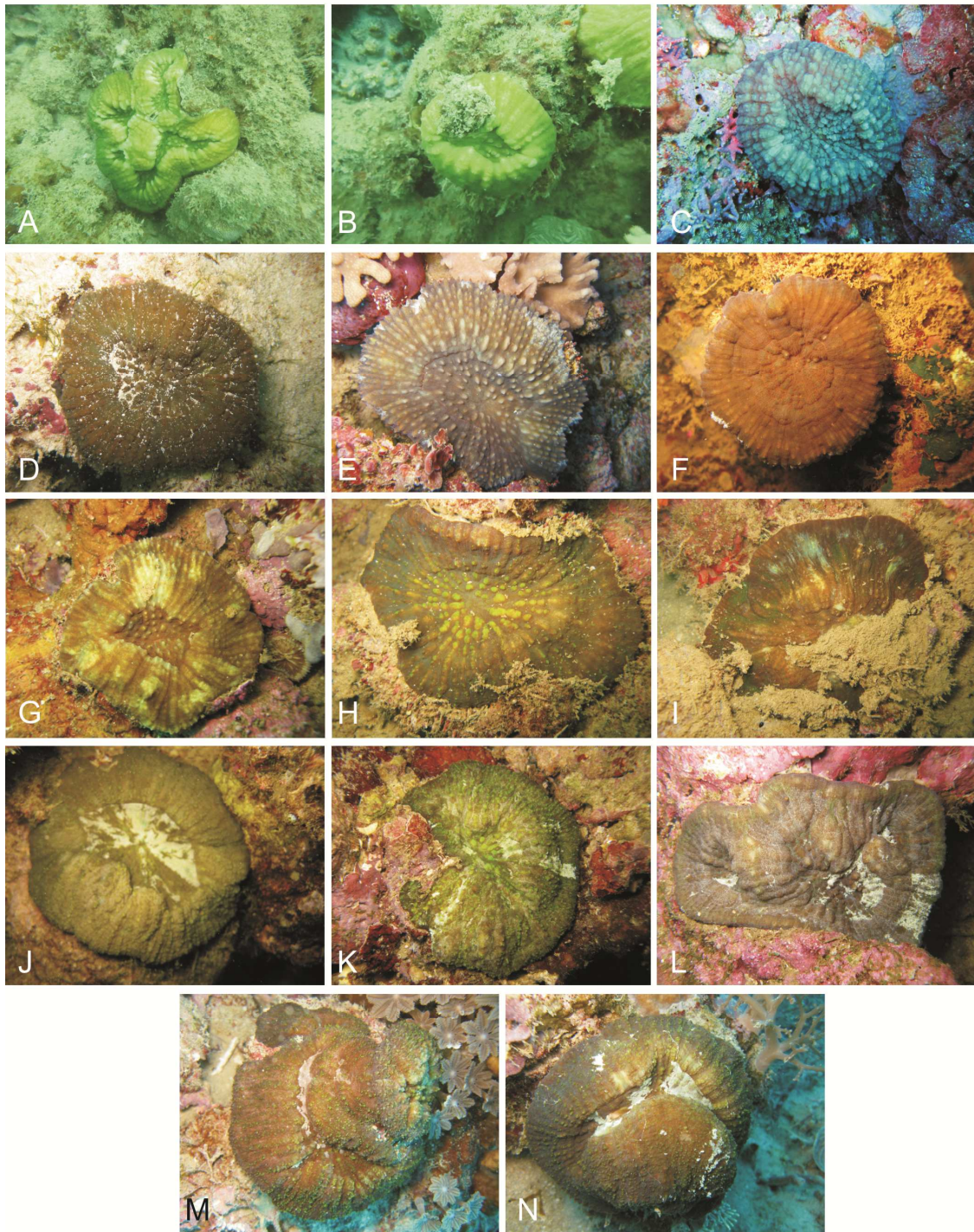
Appendix 5.1. Phylogenetic position of *Parascolymia vitiensis* and *P. rowleyensis* (previously *Australomussa*) within the family Lobophylliidae based on partial mitochondrial COI gene. Bayesian topology is shown. Numbers associated with branches indicate Maximum Likelihood bootstrap (>70%) support (left) and Bayesian posterior probabilities (>0.9) (right). Clades within Lobophylliidae are coloured and labelled A to I according to Arrigoni et al. (2014a).



Appendix 5.2. Phylogenetic position of *Parascolymia vitiensis* and *P. rowleyensis* (previously *Australomussa*) within the family Lobophylliidae based on nuclear histone H3. Bayesian topology is shown. Numbers associated with branches indicate Maximum Likelihood bootstrap (>70%) support (left) and Bayesian posterior probabilities (>0.9) (right). Clades within Lobophylliidae are coloured and labelled A to I according to Arrigoni et al. (2014a).



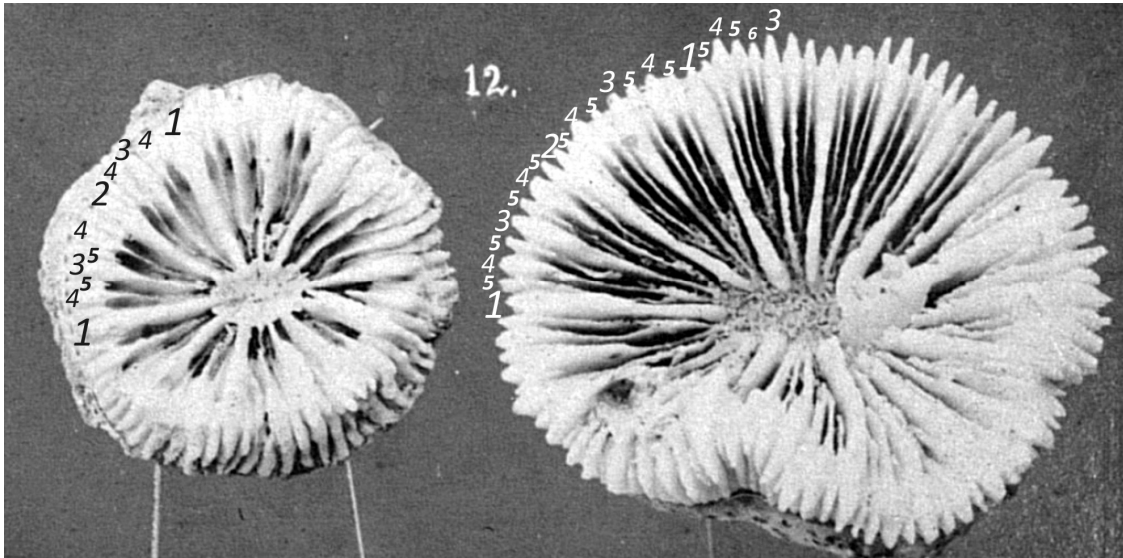
Appendix 5.3. Phylogenetic relationships between *Parascalomyia vitiensis* and *P. rowleyensis* (previously *Australomussa*) within the family Lobophylliidae based on nuclear ITS region. Bayesian topology is shown. Numbers associated with branches indicate Maximum Likelihood bootstrap (>70%) support (left) and Bayesian posterior probabilities (>0.9) (right). Clades within Lobophylliidae are coloured and labelled A to I according to Arrigoni et al. (2014a).



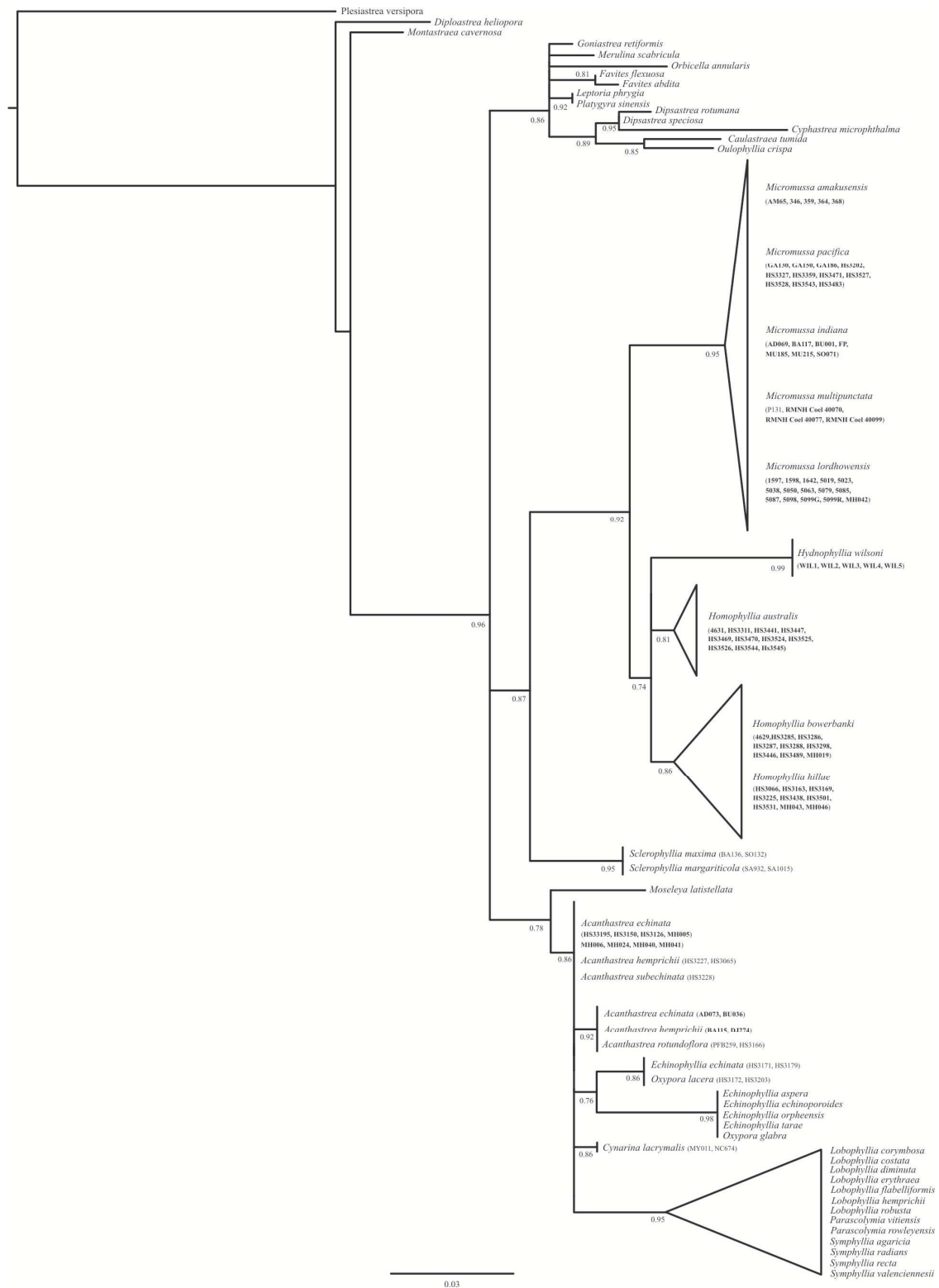
Appendix 5.4. *In situ* photos of the specimens of *Parascolymlia vitiensis* analyzed in this study: A) 6816, B) 6830; C) IRD HS2955; D) IRD HS2964; E) IRD HS2985, F) IRD HS3255; G) UNIMIB PFB031; H) UNIMIB PFB032; I) UNIMIB PFB033; J) UNIMIB PFB052; K) UNIMIB PFB053; L) UNIMIB PFB055; M) UNIMIB PFB151; N) UNIMIB PFB152.

Appendix 6.1. List of sequences of COI, Histone H3, and rDNA used for the Ancestral character state reconstruction.

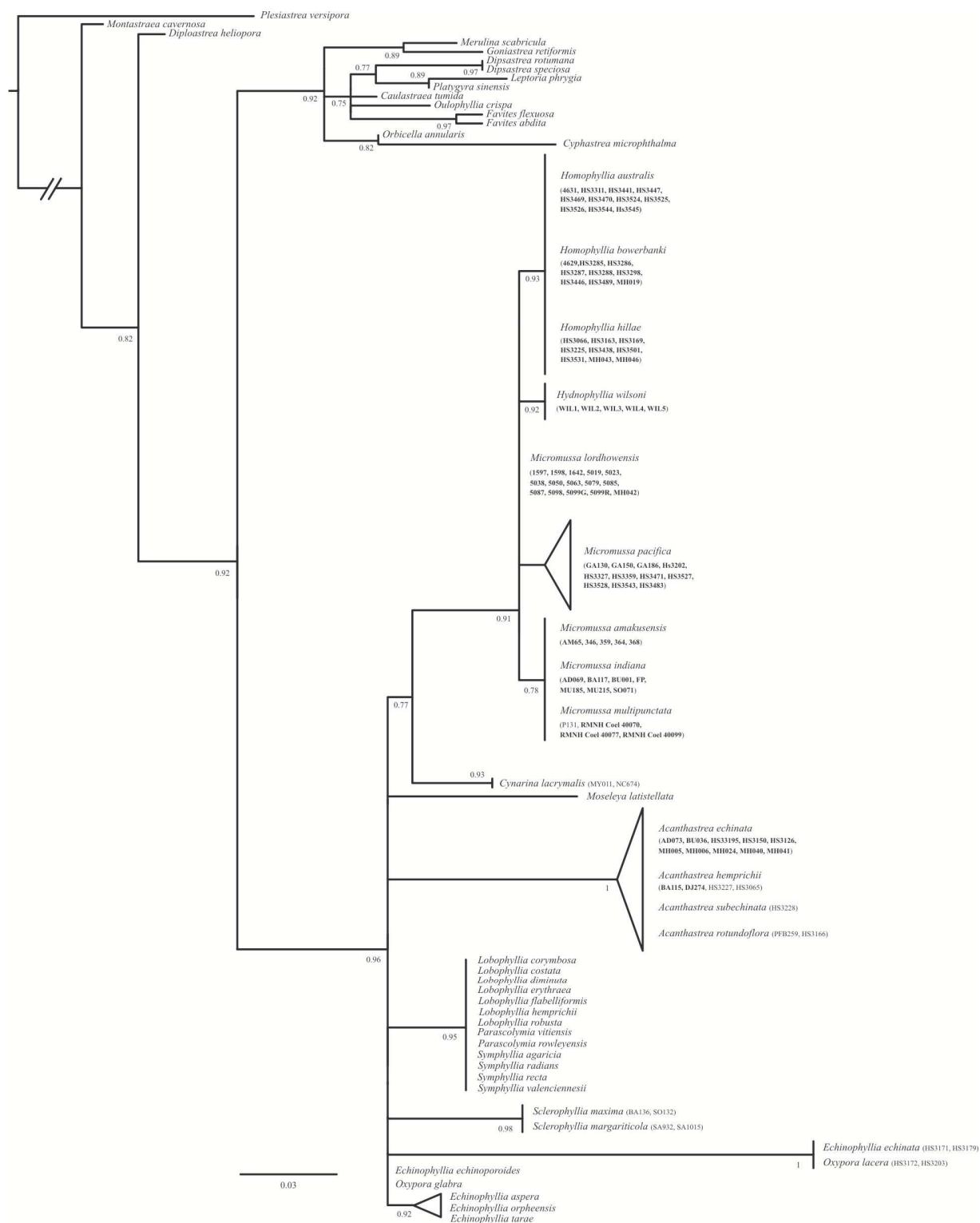
Specie	COI	Histone H3	rDNA
<i>Plesiastrea versipora</i>	HQ203246	HQ203518	HQ203307
<i>Diploastrea heliopora</i>	EU371660	HQ203531	HQ203315
<i>Montastraea cavernosa</i>	HQ203283	HQ203601	HQ203368
<i>Acanthastrea echinata</i>	HF954214	LK022408	HF954301
<i>Acanthastrea rotundoflora</i>	HF954218	LK022410	HF954305
<i>Acanthastrea subechinata</i>	HF954219	LK022409	HF954307
<i>Acanthastrea hemprichii</i>	HF954221	LK022411	HF954309
<i>Sclerophyllia margariticola</i>	LM993330	LM993308	LM993347
<i>Sclerophyllia maxima</i>	LM993329	LM993310	LM993346
<i>Acanthastrea hillae</i>	HF954206	LK022403	HF954293
<i>Acanthastrea bowerbanki</i>	HF954209	LK022405	HF954296
<i>Phymastrea multipunctata</i>	HQ203289	HQ203608	HQ203372
<i>Micromussa amakusensis</i>	HE654643	LK022400	HE648559
<i>Moseleya latistellata</i>	HQ203293	HQ203614	HQ203376
<i>Echinophyllia echinata</i>	HF954232	LK022415	HF954320
<i>Oxypora lacera</i>	HF954227	LK022416	HF954315
<i>Echinophyllia echinoporoides</i>	HF954235	LK022413	HF954323
<i>Echinophyllia orpheensis</i>	HF954240	LK022414	HF954327
<i>Echinophyllia aspera</i>	HE654648	LK022412	HE648564
<i>Cynarina lacrymalis</i>	HF954201	LK022418	HF954288
<i>Lobophyllia hemprichii</i>	HE654639	LK022422	HE648555
<i>Lobophyllia corymbosa</i>	HE654638	LK022420	HE648554
<i>Lobophyllia robusta</i>	HF954250	LK022423	HF954337
<i>Symphyllia radians</i>	HE654644	LK022425	HE648560
<i>Lobophyllia costata</i>	HF954246	LK022421	HF954333
<i>Symphyllia agaricia</i>	HF954263	LK022424	HF954350
<i>Symphyllia recta</i>	HF954267	LK022426	HF954354
<i>Symphyllia valenciennesii</i>	HF954260	LK022427	HF954347
<i>Parascolymia vitiensis</i>	LK022350	LK022387	LK022366
<i>Parascolymia rowleyensis</i>	LK022344	LK022380	LK022359



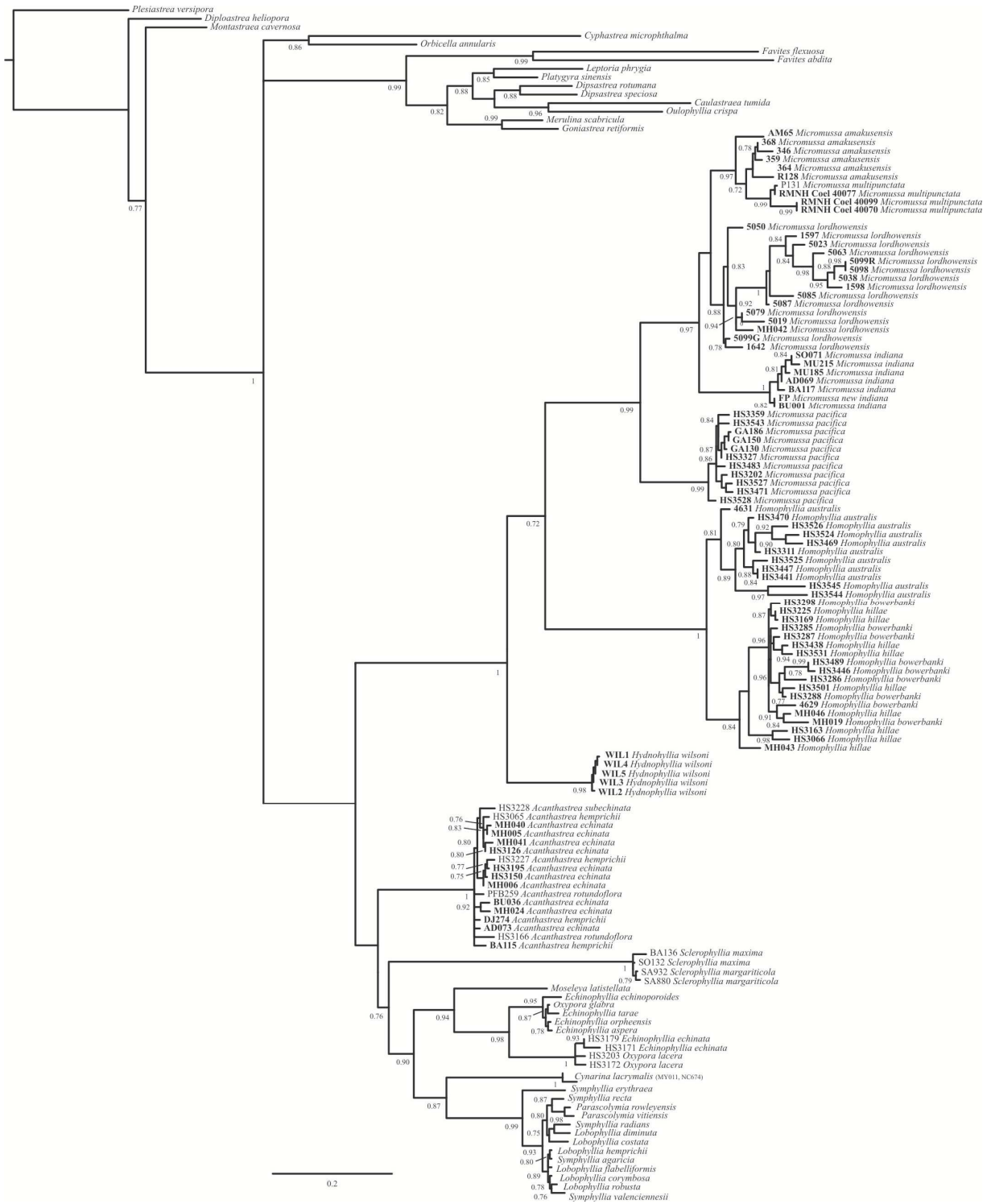
Appendix 6.2. Original illustration of *S. margariticola* by Klunzinger (1879). Arabic numerals at the outer end of the septa indicate the cycle number (from 1 to 5).



Appendix 7.1. Maximum Likelihood tree based on partial mitochondrial COI gene. Numbers associated with branches indicate SH-like supports (> 0.7). Samples analyzed in this study are in bold.



Appendix 7.2. Maximum Likelihood tree based on nuclear Histone H3 gene. Numbers associated with branches indicate SH-like supports (> 0.7). Samples analyzed in this study are in bold.



Appendix 7.3. Maximum Likelihood tree based on nuclear ITS region. Numbers associated with branches indicate SH-like supports (> 0.7). Samples analyzed in this study are in bold.

Appendix 7.3. Pairwise genetic distance values within and between clades of the Lobophylliidae using the combined COI-Histone H3-ITS regions data set. Standard deviations are listed on the upper right hand portions for each set of comparisons.

	A	B	C	D	E	F	G	H	I	J
A	0.0127 (0.0019)	0.0041	0.0060	0.0060	0.0057	0.0056	0.0073	0.0058	0.0059	0.0042
B	0.0359	0.0091 (0.0014)	0.0061	0.0059	0.0059	0.0056	0.0068	0.0056	0.0057	0.0042
C	0.0616	0.0620	0	0.0053	0.0052	0.0052	0.0069	0.0047	0.0051	0.0057
D	0.0586	0.0556	0.0398	-	0.0048	0.0044	0.0064	0.0044	0.0044	0.0059
E	0.0598	0.0603	0.0471	0.0379	0.0031 (0.0007)	0.0044	0.0064	0.0041	0.0044	0.0058
F	0.0617	0.0610	0.0437	0.0278	0.0348	0.0029 (0.0001)	0.0056	0.0045	0.0044	0.0053
G	0.0969	0.0960	0.0818	0.0639	0.0662	0.0592	0.0051 (0.0013)	0.0062	0.0063	0.0068
H	0.0606	0.0567	0.0388	0.0332	0.0355	0.0336	0.0704	0.0007 (0.0007)	0.0035	0.0057
I	0.0624	0.0590	0.0409	0.0303	0.0375	0.0286	0.0694	0.0234	0.0091 (0.0015)	0.0057
J	0.0324	0.0302	0.0545	0.0510	0.0573	0.0548	0.0908	0.0535	0.0547	0.0004 (0.0004)

"The future is unwritten"

(Joe Strummer)